Molecular characterization of the SNF1 signaling pathway in *Candida albicans*

Austin Mottola

Julius-Maximilians-Universität
Würzburg, 2021

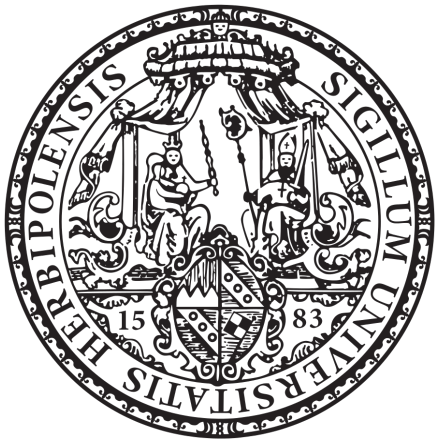

Molecular characterization of the SNF1 signaling pathway in *Candida albicans*

Molekulare Charakterisierung des SNF1-Signalweges von *Candida albicans*

Doctoral thesis for a doctoral degree
at the Graduate School of Life Sciences,
Julius-Maximilians-Univsersität Würzburg,
Section Infection and Immunity

submitted by

Austin Mottola

from

New York, USA

Würzburg 2021

Submitted on:

Members of the *Promotionskomitee*:

Chairperson: Prof. Dr. Thomas Dandekar

Primary Supervisor: Prof. Dr. Joachim Morschhäuser

Supervisor (Second): Dr. J. Christian Pérez

Supervisor (Third): Prof. Dr. Bernhard Hube

Date of Public Defense:

Date of Receipt of Certificates:

Affidavit

I hereby confirm that my thesis entitled "Molecular characterization of the SNF1 signaling pathway in *Candida albicans*" is the result of my own work. I did not receive any help or support from commercial consultants. All sources and / or materials applied are listed and specified in the thesis.

Furthermore, I confirm that this thesis has not yet been submitted as part of another examination process neither in identical nor in similar form.

Würzburg, March 2021
Place, Date Signature

Eidesstattliche Erklärung

Hiermit erkläre ich an Eides statt, die Dissertation "Molekulare Charakterisierung des SNF1-Signalweges von *Candida albicans*" eigenständig, d.h. insbesondere selbständig und ohne Hilfe eines kommerziellen Promotionsberaters, angefertigt und keine anderen als die von mir angegebenen Quellen und Hilfsmittel verwendet zu haben.

Ich erkläre außerdem, dass die Dissertation weder in gleicher noch in Ähnlicher Form bereits in einem anderen Prüfungsverfahren vorgelegen hat.

Würzburg, März 2021
Ort, Datum Unterschrift

Contents

Summary

The fungus *Candida albicans* is a typical member of the human microbiota, where it usually behaves as a commensal. It can also become pathogenic; often causing minor superficial infections in healthy people, but also potentially fatal invasive systemic infections in immunocompromised people. Unfortunately, there is only a fairly limited set of antifungal drugs, and evolution of drug resistance threatens their efficacy. Greater understanding of the mechanisms that *C. albicans* uses to survive in and infect the host can uncover candidate targets for novel antifungals. Protein kinases are central to a vast array of signaling pathways which govern practically all aspects of life, and furthermore are relatively straightforward to design drugs against. As such, investigation and characterization of protein kinases in *C. albicans* as well as their target proteins and the pathways they govern are important targets for research.

AMP-activated kinases are well conserved proteins which respond to energy stress; they are represented in yeasts by the heterotrimeric SNF1 complex, which responds primarily to the absence of glucose. SNF1 has been well characterized in baker's yeast, *Saccharomyces cerevisiae*, but much less so in *C. albicans*. Prior work has shown that SNF1 in this organism is still a regulator of carbon source utilization, and also is essential for *in vivo* fitness. It has also suggested notable differences in the pathway; some observations suggested that major targets are not conserved. Additionally, unlike in *S. cerevisiae*, the catalytic subunit of SNF1 seemed to be an essential gene in *C. albicans*. In this work, the SNF1 pathway was investigated with two primary goals: identify novel targets of this protein kinase and elucidate why SNF1 is essential. Also, the homologs of major targets of *S. cerevisiae* SNF1, transcriptional repressors Mig1 and Mig2, were investigated with the goal of determining whether they continued to function within this pathway, because they lack a consensus SNF1 recognition site.

Investigation of Mig1 and Mig2 determined that they continued to function downstream of SNF1 as repressors of growth on alternative carbon sources. Surprisingly, both Mig1 and Mig2 are phosphorylated dependent on SNF1 activity; in *S. cerevisiae*, Mig2 is regulated indirectly by SNF1, rather than by direct phosphorylation. Also surprising was that Mig1 is apparently regulated at the level of protein accumulation, in contrast with *S. cerevisiae*, where it is regulated by changing subcellular localization. Mig1 and Mig2 also appear to have largely overlapping functions, as both must be deleted to significantly suppress phenotypes of reduced SNF1 activity. These results therefore confirmed that Mig1 and Mig2 are targets of SNF1, but the mechanism by which SNF1 regulates them is distinct from the homologous

pathway in baker's yeast.

Two approaches were used to identify novel targets of SNF1. In one, suppressor mutants were evolved from a strain in which SNF1 activity is reduced, which exhibits defects in carbon source utilization and cell wall integrity. This revealed a suppressor mutation within *SNF1* itself, coding for the catalytic subunit of the complex – $SNF1^{\Delta 311\text{-}316}$. This mutation rendered the kinase active even in the absence of the regulatory Snf4 subunit. Most interestingly, the mutation, an in-frame deletion of six codons, occurred via recombination at a repeated sequence within the open reading frame, suggesting that this mutation was not entirely random, but rather a preprogrammed event.

The second approach screened a library of artificially activated zinc cluster transcription factors, identifying Czf1 as one such transcription factor which, upon artificial activation, restored resistance to cell wall stress in a mutant of the SNF1 pathway. Czf1, generally recognized as a regulator not of cell wall integrity, but rather morphogenesis, was not shown to be a target of SNF1, but activation of it overcame cell wall defects of many tested kinase mutants, and it was found to be phosphorylated, though the responsible kinase is unknown. RNA sequencing revealed that Czf1 regulates genes related to the cell wall, and transmission electron microscopy showed that its artificial activation affects cell wall architecture; mutants lacking *CZF1* also exhibit altered profiles in susceptibility to chemicals that affect the cell wall.

Finally, a, inducible gene deletion system revealed that *SNF1* is not an essential gene. Mutants were capable of weak growth in rich media containing glucose, which improved at 37°C. The inability of past published attempts to delete it likely are a result of growth of transformants on commonly used media, temperature, and incubation time which also happened to be inappropriate considering the phenotypes of the null mutant. Using this knowledge, *SNF1* was then successfully deleted using a modified but otherwise standard gene deletion approach which had previously failed. In summary, the work presented here ultimately expands the knowledge of the SNF1 signaling pathway in *C. albicans*.

Zusammenfassung

Der Pilz *Candida albicans* ist ein typisches Mitglied der menschlichen Mikrobiota, wo er sich normalerweise als Kommensale verhält. Als fakultativ pathogener Erreger kann er jedoch auch leichte, oberflächliche Infektionen bei gesunden Menschen verursachen, sowie potenziell tödliche, invasive systemische Infektionen bei immungeschwächten Menschen. Leider gibt es nur eine recht begrenzte Anzahl von Antimykotika, und die Entwicklung von Resistenzen bedroht deren Wirksamkeit. Ein besseres Verständnis der Mechanismen, die *C. albicans* nutzt, um im Wirt zu überleben und ihn zu infizieren, kann mögliche Angriffspunkte für neue Antimykotika aufdecken. Proteinkinasen sind von zentraler Bedeutung für eine Vielzahl von Signalwegen, die praktisch alle Aspekte des Lebens steuern und gegen die sich zudem relativ einfach Medikamente entwickeln lassen. Daher ist die Untersuchung und Charakterisierung von Proteinkinasen in *C. albicans* sowie ihrer Zielproteine und der von ihnen gesteuerten Signalwege ein wichtiges Ziel für die Forschung.

AMP-aktivierte Kinasen sind hoch konservierte Proteine, die auf Energiestress reagieren; sie sind in Hefen durch den heterotrimeren SNF1-Komplex vertreten, der vor allem auf das Fehlen von Glukose reagiert. SNF1 ist zwar in der Bäckerhefe, *Saccharomyces cerevisiae*, gut charakterisiert worden, jedoch kaum in *C. albicans*. Frühere Arbeiten haben gezeigt, dass SNF1 in diesem Organismus ebenfalls die Verwertung von Kohlenstoffquellen reguliert und auch für *in vivo* Fitness essentiell ist. Es wurden allerdings auch bemerkenswerte Unterschiede im Stoffwechselweg festgestellt. Einige Beobachtungen deuten darauf hin, dass wichtige Zielproteine nicht konserviert sind. Außerdem schien die katalytische Untereinheit von SNF1 in *C. albicans* im Gegensatz zu SNF1 in *S. cerevisiae* ein essentielles Gen zu sein. In dieser Arbeit wurde der SNF1-Signalweg mit zwei primären Zielen untersucht: die Identifizierung neuer Zielproteine dieser Proteinkinase und die Klärung der Frage, warum SNF1 essentiell ist. Außerdem wurden die Homologe der wichtigsten Zielproteine des *S. cerevisiae* SNF1-Komplexes, die transkriptionellen Repressoren Mig1 und Mig2, untersucht, um festzustellen, ob sie trotz eines fehlenden SNF1-Bindemotivs weiterhin innerhalb dieses Signalweges agieren.

Die Untersuchung von Mig1 und Mig2 ergab, dass sie von SNF1 reguliert, als Repressoren des Wachstums auf alternativen Kohlenstoffquellen funktionieren. Überraschenderweise werden sowohl Mig1 als auch Mig2 über die Phosphorylierung durch SNF1 reguliert; in *S. cerevisiae* hingegen, wird Mig2 nur indirekt durch SNF1 reguliert und nicht durch direkte Phosphorylierung. Überraschend war auch, dass Mig1 offenbar durch Steuerung der Proteinakkumulation reguliert wird, im Gegensatz zu *S. cerevisiae*, wo die

Regulation von Mig1 durch Änderung der subzellulären Lokalisation stattfindet. Mig1 und Mig2 scheinen außerdem weitgehend überlappende Funktionen zu haben, da beide deletiert werden müssen, um die Phänotypen einer reduzierten SNF1-Aktivität signifikant zu unterdrücken. Diese Ergebnisse bestätigen also, dass Mig1 und Mig2 zwar Zielproteine von SNF1 sind, aber der Mechanismus, der Regulation selbst nicht konserviert ist.

Für die Identifikation neuer Zielproteine von SNF1 wurden zwei Ansätze verwendet. Zum einen wurde ein Stamm mit reduzierter SNF1-Aktivität, für die Entwicklung von Suppressor-Mutanten verwendet, die einen Defekte bei der Verwertung von Kohlenstoffquellen und eine eingeschränkte Zellwandintegrität aufweisen. Dabei wurde eine Suppressormutation in *SNF1* selbst entdeckt, die für die katalytische Untereinheit des Komplexes - $SNF1^{\Delta 311\text{-}316}$ - kodiert. Diese Mutation führte zu einer Aktivierung der Kinase, trotz Abwesenheit der regulatorischen Snf4-Untereinheit. Interessanterweise trat die Mutation, eine in-frame Deletion von sechs Codons, durch Rekombination an einer repetitiven Sequenz innerhalb des offenen Leserahmens auf. Dies deutet darauf hin, dass diese Mutation nicht völlig zufällig auftrat, sondern eher ein vorprogrammiertes Ereignis war.

Für den zweite Ansatz wurde eine Bibliothek von künstlich aktivierten Zink-Cluster-Transkriptionsfaktoren untersucht. Dies führte zur Identifikation von Czf1 als einen solchen Transkriptionsfaktor, der nach künstlicher Aktivierung die Resistenz gegen Zellwandstress in einer Mutante des SNF1-Signalweges wiederherstellte. Czf1 gilt allgemein als Regulator nicht der Zellwandintegrität, sondern der Morphogenese. Obwohl sich Czf1 nicht als Zielprotein von SNF1 erwies, überwand dessen Aktivierung die Zellwanddefekte vieler getesteter Kinase-Mutanten. Außerdem wurde eine Phosphorylierung des Proteins festgestellt, obwohl die verantwortliche Kinase unbekannt ist. Eine RNA-Sequenzierung ergab, dass Czf1 Zellwand assoziierte Gene reguliert. Dies konnte durch Transmissionselektronenmikroskopie bestätigt werden, da eine künstliche Aktivierung von Czf1 die Zellwandarchitektur beeinflusste. Mutanten, denen *CZF1* fehlt, zeigten außerdem eine veränderte Anfälligkeit gegenüber Chemikalien, die auf die Zellwand wirken.

Schließlich zeigte ein induzierbares Gendeletionssystem, dass *SNF1* kein essentielles Gen ist. Die Mutanten waren zu einem schwachen Wachstum in reichhaltigen, mit Glukose versetzten Medien fähig, das sich bei 37°C verbesserte. Dass die Deletion des Gens in früheren Publikationen nicht erfolgreich war, ist wahrscheinlich auf das Wachstum der Transformanten auf den üblichen Medien, die Temperatur und die Inkubationszeit zurückzuführen, die sich ebenfalls als ungeeignet erwiesen, wenn man die Phänotypen der Null-Mutanten betrachtet. Mit diesem Wissen konnte *SNF1* dann erfolgreich mit einem modifizierten, aber ansonsten standardmäßigen Ansatz deletiert

werden, der zuvor fehlgeschlagen war. Zusammenfassend lässt sich sagen, dass durch die hier vorgestellte Arbeit das Wissen über den SNF1-Signalweg in *C. albicans* erweitert werden konnte.

1. Introduction

1.1 Fungi and their ecological, cultural, and medical importance

The kingdom Fungi is extraordinarily diverse. Conservative estimates of the global number of fungal species approach 1.5 million (Hawksworth and Lücking 2017), while in all likelihood the actual number is much higher. This compares favorably, for example, to estimates of the total species richness of plants, which trends toward about a quarter million species (Wilson *et al.* 2012). Unsurprisingly, the phenotypic diversity of the kingdom is also immense, ranging from microscopic yeasts to networks of mushrooms which are likely the largest individual organisms on Earth (Ferguson *et al.* 2003). This diversity naturally extends to lifestyle - fungi can be found in nearly every environmental niche, from deep-sea hydrothermal vents (Calvez *et al.* 2009) to soil (Tedersoo *et al.* 2014) to the human body (Seed 2015) and more. Across these niches, fungi have influenced practically all forms of life. Fossil evidence suggests for example that mycorrhizal fungus-plant mutualism appeared simultaneously with and perhaps facilitated the appearance of terrestrial plant life (Remy *et al.* 1994) – and the evolution of saprophytic fungi capable of digesting the remains of the resulting woody plants facilitated the recycling of the carbon contained within (Floudas *et al.* 2012) – drastically changing the environment that terrestrial animals, and eventually humans, encountered.

While these roles are naturally essential to humankind as it now exists, fungi have served humans in more direct ways. Besides the obvious culinary uses of macroscopic fungi like mushrooms, domesticated yeast species like *Kluyveromyces lactis* and *Saccharomyces cerevisiae* have been intertwined with human civilization for essentially as long as civilizations have existed – archaeological evidence of yeasts being used to ferment beverages, leaven bread, and make cheeses date back thousands of years (Varela *et al.* 2019; Mcgovern *et al.* 2004; Trivedi *et al.* 1986). More recently, the discovery

that *Penicillium chrysogenum* mold inhibits the growth of certain bacteria, and the ensuing antibiotic revolution, leaves fungi to be thanked for saving tens of millions of lives over the last century (Fleming 1980; Kardos and Demain 2011). Beyond its usage as a fermenter, *Saccharomyces cerevisiae* has long been used as a model organism for efficient and ethical studies of the cellular function of eukaryotic organisms; its scientific value is reflected by the fact that it was the first eukaryotic organism to have its genome fully sequenced (Goffeau *et al.* 1996). It and other fungal species have adopted increasingly important economic and industrial roles, as well. Fungi have figuratively sunk their mycelia into industries as diverse as forestry, waste disposal, biofuel production, and cosmetics (Hyde *et al.* 2019).

Fungi also interact with humans much more intimately. While far from a majority (less than 0.1% by genus (Qin *et al.* 2010)), the human microbiome includes a number of fungi, most prominently members of the genus *Candida* in the gastrointestinal tract and vagina (Hallen-Adams and Suhr 2017; Jo *et al.* 2017) and *Malassezia* on the skin (Bradford and Ravel 2017). Unfortunately, these commensals are not always benign – infections by these opportunistic pathogens as well as by other non-commensals cause superficial infections including skin and nail infections that affect up to 25% of the global population (Havlickova *et al.* 2008) and vulvovaginal candidiasis affecting upwards of 75% of women at some point in their lives (Sobel 2007). Unsurprisingly, the human immune system has evolved to detect and act against fungi. The innate immune system relies on a number of receptors that recognize fungal pathogen-associated molecular patterns (PAMPs), including complement receptors, Toll-like receptors (TLRs), and C-type lectin receptors (CLRs) (Romani 2011). Detection by various immune cell types leads to complex downstream responses dependent on cell type, including induction of phagocytosis by phagocytes or maturation of T helper cells leading to an adaptive immune response (Romani 2011). These activities are suppressed, however, at the mucosa; here, host and microbe exist in a careful balance which allows commensal microbiota to stably colonize (Mowat 2003). Indeed, this colonization seems to benefit the host as well, as treatment of mice with antifungal drugs was found to exacerbate diseases of overactive immune systems like colitis or development of allergies in models of these conditions (Wheeler *et al.* 2016).

Should the host defenses falter, however (for example due to treatment with immunosuppressants or contraction of AIDS) or be bypassed (for example during abdominal surgeries), the host is at risk of invasive, opportunistic infections by both noncommensal fungi, such as *Aspergillus* or *Cryptococcus* spp., or commensal fungi such as *Candida* spp., which are the cause of nearly half of fungal bloodstream infections (BSIs) (Yapar 2014; Pfaller *et al.* 2006).

Indeed, *Candida* spp. account for upwards of 22% of all healthcare-associated BSIs in the United States, and such an infection, known as candidaemia, is detected in 1-2% of all patients in intensive care (Pappas *et al.* 2018). Such infections are not trivial – while mortality is difficult to estimate, conservative judgments suggest that around 20% of patients suffering from candidaemia will not survive due to this infection (Pappas *et al.* 2018). Furthermore, BSI allows the fungus to traverse the body, invading various organs. Investigation of the actual cause of death in a commonly used mouse model of disseminated candidiasis was a combination of sepsis and kidney failure which correlated with renal fungal burden (Spellberg *et al.* 2005).

Treatment of fungal infections poses unique challenges due to the eukaryotic nature of fungi. The evolutionary closeness between fungi and humans limits the breadth of targets of antifungal molecules, and as a result there are currently only four classes of drugs used to treat systemic fungal infections. The oldest, polyenes, are primarily represented by the cyclic heptaene amphotericin B (AMB). AMB leads to cell death by binding to ergosterol, an important component of the fungal cell membrane (Gray *et al.* 2012). Additionally, when taken up by the cell, AMB induces oxidative stress (Mesa-Arango *et al.* 2012). Flucytosine (5-FC), a synthetic cytosine analogue, exists in a class all its own. Fungal cells – unlike human cells – express cytosine deaminase, which acts upon 5-FC and lead to further conversion to two toxic compounds: 5-fluorouridine triphosphate, which incorporates into RNA and inhibits protein synthesis, and 5-fluorodeoxyuridine, which inhibits a major thymidine biosynthesis pathway, thus inhibiting DNA synthesis (Waldorf and Polak 1983). Azoles, most prominently the triazole class exemplified by fluconazole, are popular as front-line treatments and prophylactics, and act via inhibition of lanosterol 14-α-demethylase (Watson *et al.* 1989). This prevents production of ergosterol, an essential fungal membrane sterol analogous in function to animal cholesterol, and causes an accumulation of toxic sterol byproducts (Bossche *et al.* 1995). The newest class, echinocandins, disrupt the integrity of the fungal cell wall and elicit cell lysis by inhibition of β-(1,3)-D-glucan synthase, preventing production of an important component of the fungal cell wall (Gordee *et al.* 1988; Sawistowska-Schröder *et al.* 1984).

The evolution of drug resistant *C. albicans* strains, as well as the emergence of intrinsically resistant non-*albicans Candida* (NAC) species, poses a threat to the current repertoire of antifungals. Resistance to fluconazole, one of the most commonly used antifungal drugs, is particularly noteworthy. The SENTRY Antifungal Surveillance Program has investigated the occurrence of infections from various *Candida* species, as well as trends in resistance to various antifungal agents, over time. Between 1996 and 2016, resistance to fluconazole in *C. albicans* remained low, ranging from 0.1 to 0.4% of tested

isolates (Pfaller *et al.* 2019). However, the NAC species *C. parapsilosis*, *C. glabrata*, and *C. tropicalis* exhibited fluconazole resistance rates between 2.0 and 10.1%, and *C. glabrata* also has a similarly high rate of resistance to echinocandins, which are typically frontline treatments for hospitalized patient (Pfaller *et al.* 2019; Pappas *et al.* 2015). Notably, the distribution of species isolated from patients (of which *C. albicans* is predominant) has revealed a relative increase over time of *C. glabrata* and *C. parapsilosis* (Pfaller *et al.* 2019). Furthermore, in the past decade, the discovery and global spread of *C. auris* infections has alarmed physicians and researchers in large part due to its high resistance to several antifungal classes (Cortegiani *et al.* 2018). These trends towards infections by multiple drug resistant *Candida* species therefore demand the development of novel antifungal classes and targets. While screening methods can help identify potentially effective drug candidates, it is also essential to study the unique biology of *Candida* species and how they are able to colonize and infect their host, in order to suggest potential targets for antimycotic drugs.

1.2 Regulation of carbon source utilization in yeasts

The acquisition and metabolism of nutrients as sources of energy and as building blocks for biological macromolecules is an essential feature of life. One of the most basic needs for all cells is a source of carbon. However, not all sources of carbon are created equal. Some are more energetically efficient to utilize, others less so. Different molecular machinery is often required to metabolize different molecules, and the production of this machinery adds to the energetic costs. Therefore, carbon metabolism tends to be managed by networks of regulators such as sensor proteins, signal transducing kinases, and transcription factors, among others. In the context of yeasts, regulation of carbon metabolism has been most extensively studied in the model organism *S. cerevisiae*. Glucose is generally speaking the ideal source of energy, and can be processed either by fermentation or respiration. *S. cerevisiae* readily and preferentially uses this carbon source – enzymes involved in the utilization of other potential carbon sources are significantly less abundant when cells are grown in the presence of glucose (Gancedo 1992) – until available glucose is rare, upon which it will then begin to metabolize other carbon sources. To achieve this so-called glucose repression, *S. cerevisiae* employs several pathways involved in sensing available glucose and repressing the expression genes required for the utilization of non-glucose carbon sources (also called

alternative carbon sources). Glucose sensing and signaling pathways are therefore major mediators of carbon source utilization more broadly.

The niche(s) that *S. cerevisiae* typically occupy, however, are markedly different than those occupied by commensal yeasts such as *C. albicans*. This difference extends to the types and concentrations of nutrients available, including sources of carbon. A common niche for *S. cerevisiae*, for example, is on fruits, which contain high concentrations of simple sugars including glucose. In contrast, sugar concentrations within the gastrointestinal tract vary depending on sugar consumption and there is a high degree of competition with the host a well as other members of the microbiome. In other niches that *C. albicans* may occupy as either commensal or pathogen, the abundance of glucose remains low - around 0.1% in the bloodstream, vagina, or skin (Van Ende *et al.* 2019). This requires additional metabolic flexibility. The pathways involved in glucose sensing and signaling are typically very well characterized in *S. cerevisiae*, and much less so in *C. albicans*. Unsurprisingly due to the notable differences in niches, investigations into these same pathways in *C. albicans* have revealed notable differences. Two important pathways will be discussed here in detail as they relate to *S. cerevisiae*, while highlighting notable differences in *C. albicans* – the Sugar Receptor Repressor (SRR) pathway and the glucose repression (or SNF1) pathway. In many cases, homologous genes/proteins have the same name in both organisms; for clarity, they will be given prefixes of Sc (*S. cerevisiae*) or Ca (*C. albicans*) where necessary.

1.2.1 The Sugar Receptor Repressor pathway

Yeasts express a number of hexose transporters which import glucose and other six-carbon sugars into the cell in order to be metabolized. *S. cerevisiae* and *C. albicans* express 17 and 20 such members of the hexose transporter (HXT) gene family, respectively, which exhibit varying affinities for glucose (Wieczorke *et al.* 1999; Fan *et al.* 2002). The major regulatory mechanism which senses differing concentrations of glucose and determines which transporters must be expressed is the Sugar Receptor Repressor pathway, which is summarized in Figure 1.1.

In the absence of glucose, the transcriptional repressor ScRgt1 prevents expression of its target HXT genes (Özcan *et al.* 1996a). This repression is dependent on the association of ScRgt1 with two additional corepressors, ScMth1 and ScStd1 (Lakshmanan *et al.* 2003). When glucose is present, repression is relieved, leading to the expression of HXT genes. The hexose transporter-like membrane proteins ScSnf3 and ScRgt2 are responsive to low or high concentrations of glucose, respectively, but cannot themselves

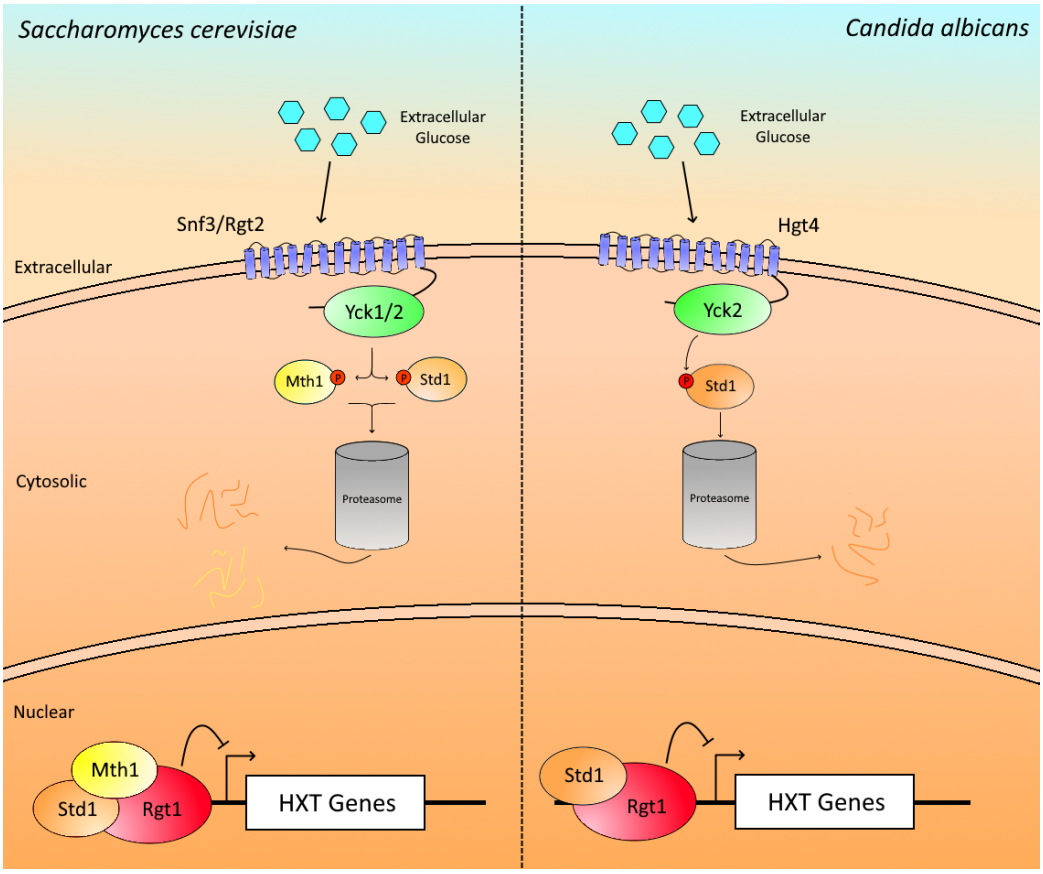

.

Figure 1.1: The Sugar Receptor Repressor pathways in *S. cerevisiae* and *C. albicans*. Expression of HXT genes is repressed by Rgt1 when it is bound by corepressor transcription factor Std1 and, in *S. cerevisiae*, Mth1. Sensing of extracellular glucose by the hexose transporter-like proteins Snf3 or Rgt2 in *S. cerevisiae* or Hgt4 in *C. albicans* leads to nuclear export of these corepressors, paired with phosphorylation which is dependent on Yck2 and, additionally, Yck1 in *S. cerevisiae*. This phosphorylation leads to degradation by the proteasome and derepression of HXT genes in the presence of glucose. Figure inspired by figures from Van Ende *et al.* 2019

transport hexoses (Sabire Özcan and Johnston 1998; Özcan *et al.* 1996b). Upon sensing of glucose, ScMth1 and ScStd1 are recruited to the long intracellular tail of ScSnf3/ScRgt2 along with the membrane-bound protein kinase ScYck1 or its paralog ScYck2, which phosphorylates the corepressors (Moriya and Johnston 2004). Phosphorylation of ScMth1 and ScStd1 trigger Grr1-dependent degradation by the proteasome and dissociation of ScRgt1 from its target promoters, leading to derepression of HXT genes (Moriya and Johnston 2004; Flick *et al.* 2003).

The pathway is largely analogous in *C. albicans*, indeed in a somewhat streamlined fashion, because several components in *S. serevisiae* have par-

alogs derived from the whole-genome duplication event which did not occur in the evolutionary lineage of *C. albicans*. The transporter-like membrane protein Hgt4 is homologous to ScSnf3/ScRgt2 and is essential for expression of HXT genes and important for hexose metabolism (Brown *et al.* 2006). Similarly, Std1 fulfills the responsibilities of ScMth1 and ScStd1; deletion of this gene phenocopies both strains expressing a constitutively active Hgt4 and strains which are deleted for Rgt1, which is functionally conserved in *C. albicans* (Sexton *et al.* 2007; Brown *et al.* 2009). The role of Yck2, homologous to ScYck1/ScYck2, has not been experimentally tied to the pathway in *C. albicans*, though important functional regions, including a C-terminal palmitoylation motif (Cys–Cys) which is required for ScYck1/ScYck2-mediated HXT gene expression in *S. cerevisiae* (Moriya and Johnston 2004), are conserved.

Molecular crosstalk between regulatory pathways is common and allows an increased degree of precision in responding to extracellular signals, and this naturally extends to carbon source signaling pathways. The SRR pathway interacts with a second major regulatory pathway, the SNF1 pathway in a number of ways. The SNF1 pathway, which regulates the expression of genes requires to utilize alternative (non-glucose) carbon sources, will be clarified in detail in the following section. However, evidence indicates that inactivation of the SNF1 pathway is required for proteasome degradation of ScMth1 and ScStd1; SNF1 activity may prevent nuclear export of these corepressors (Pasula *et al.* 2007). Furthermore, expression of ScSnf3 and ScMth1 is regulated by the transcriptional repressor ScMig1, which as will be discussed is an important element of the SNF1 pathway (Kaniak *et al.* 2004). In contrast with the SRR pathway, which is activated upon sensing of glucose, the SNF1 pathway responds to the absence of glucose.

1.2.2 The SNF1 pathway

As previously mentioned, it is important that the cell conserves energy where possible. Therefore, regulatory pathways often control the expression of genes so that they are only expressed when there is a need for the proteins which they encode. AMP-activated kinases (AMPKs) are a highly conserved family of protein kinases in eukaryotes which broadly respond to energy stress. Indeed, the amino acid sequence of the catalytic subunit of the *S. cerevisiae* AMPK, Snf1, is 41% identical to its human homolog, AMPKα. AMPKs are functionally similar, if not identical, as well. Whereas mammalian AMPK responds to high levels of AMP (Carling *et al.* 1989), fungal SNF1 responds to glucose starvation; early reports identified it as necessary for growth on alternative carbon sources in the absence of glucose (Zimmermann *et al.* 1977;

Carlson *et al.* 1981; Celenza and Carlson 1986). Indeed, while it is accepted that the major role of SNF1 is as a regulator of glucose repression, it also is necessary for proper response to a number of other environmental stresses, including heat shock, alkaline pH, and reactive oxygen species, among others (Hsu *et al.* 2015; Hong and Carlson 2007). For clarity, the entire protein complex which mediates the pathway will be called SNF1, where the catalytic kinase subunit will be called Snf1. Major components of the pathway as they exist in *S. cerevisiae* and *C. albicans* are illustrated in Figure 1.2.

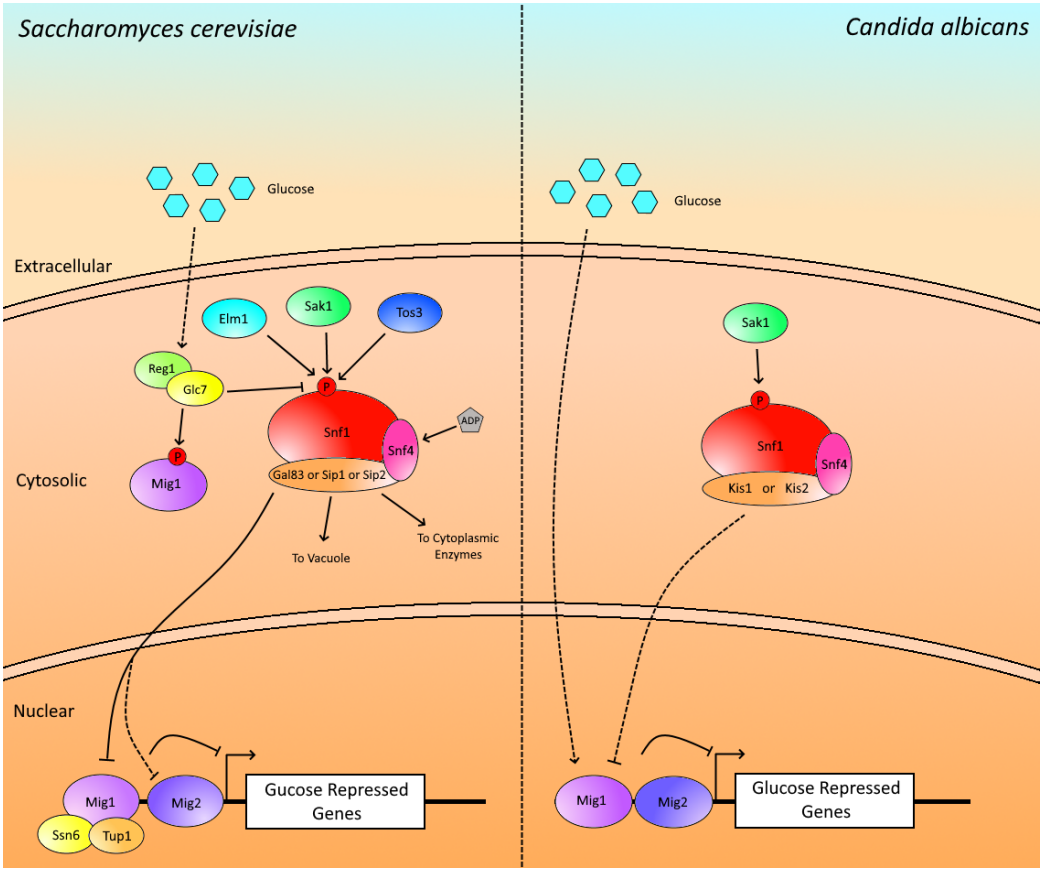

Figure 1.2: The SNF1 pathways in *S. cerevisiae* and *C. albicans*. In *S. cerevisiae*, three upstream kinases, Sak1, Elm1, and Tos3, phosphorylate Snf1. When glucose is present, Reg1-Glc7 dephosphorylates Snf1 to deactivate it (and dephosphorylates Mig1 induce nuclear localization), and Ssn6-Tup1-Mig1 and Mig2 repress glucose repressed genes. Under glucose starvation, Snf1 is protected from dephosphorylation dependent on ADP binding to Snf4. Active SNF1 complexes localize to differing areas of the cell depending on whether they include Gal83, Sip1, or Sip2. $SNF1^{Gal83}$ enters the nucleus and phosphorylates Mig1, causing it to be removed from the nucleus, and indirectly deactivates Mig2, allowing glucose repressed genes to be expressed. In *C. albicans*, much less is known. Dashed lines indicate indirect activation or deactivation.

SNF1 in *S. cerevisiae*

Since its original identification, the SNF1 pathway has been heavily investigated in *S. cerevisiae*, including the components of the core SNF1 kinase complex, its targets both direct and indirect, and its regulators. SNF1 is a heterotrimeric complex, composed of the Snf1 α-subunit, the Snf4 γ-subunit, and Sip1/Sip2/Gal83, three β-subunits which bind depending on activating conditions. Activation is mediated by three upstream kinases – Sak1, Elm1, and Tos3, which are each able to phosphorylate the α-subunit at Thr-210 in a largely redundant manner, though Sak1 is apparently the major activating kinase (Wilson *et al.* 1996; Hong *et al.* 2003; Nath *et al.* 2003; Sutherland *et al.* 2003). However, it is still unclear exactly how, or indeed whether at all, these upstream kinases are themselves regulated.

In the presence of glucose, SNF1 is deactivated, a process mediated by a complex of the yeast type 1 protein phosphatase Glc7 in complex with the targeting subunit Reg1 (Sanz *et al.* 2000; Tu and Carlson 1994; Tu and Carlson 1995). Additionally, the phosphatases Ptc1 and Sit4 negatively regulate SNF1, though they appear to have more minor roles (Ruiz *et al.* 2011; Ruiz *et al.* 2013)). Evidence suggests that it is from this perspective that SNF1 activity is regulated: glucose availability affects the rate of dephosphorylation, but not phosphorylation, of SNF1 (Rubenstein *et al.* 2008). Glucose-dependent exposure of Thr-210 to dephosphorylation is regulated by binding of ADP in low glucose conditions to the γ-subunit Snf4, indicating that SNF1 senses and responds to intracellular glucose availability at least in part by using ADP as a proxy (Chandrashekarappa *et al.* 2011; Mayer *et al.* 2011).

In order to fully understand the SNF1 pathway, the individual components must be dissected. The core of the complex, the α subunit Snf1, is a 633 amino acid serine/threonine protein kinase. It exhibits two significant functional domains – the kinase domain and an autoinhibitory domain, with a number of smaller notable features. Crystal structures of the kinase domain reveal conserved protein kinase features. The ATP-binding P loop includes a highly conserved lysine residue (Lys-84) which is essential for catalytic activity and proper response to glucose starvation (Celenza and Carlson 1989; Estruch *et al.* 1992; Nayak *et al.* 2006). Additionally, mutation of any of several residues surrounding the catalytic Asp-177 residue have also been shown to confer an artificially active state, including Tyr-167, Leu-183, Lys-192, and Ile-241 (Leech *et al.* 2003). The previously mentioned Thr-210, residing in the activation loop, is also essential for SNF1 activity; replacement of the phoshorylatable threonine with alanine results in an inactive kinase (Estruch *et al.* 1992). Additional modes of regulation other than phosphorylation by activating kinases largely occur however at the autoinhibitory domain. A

relatively recent example of this is the discovery that when cells are grown in glucose, Snf1 is modified with the small ubiquitin-like modifier SUMO at Lys-549, which negatively regulates SNF1 activity both by interaction between the SUMOylated residue and a SUMO-interacting motif in the kinase domain and by targeting Snf1 for degradation (Simpson-Lavy and Johnston 2013). Another is the identification of a ubiquitin-associated domain in this region which negatively regulates SNF1 activity (Wilson *et al.* 2011; Jiao *et al.* 2015). Most important, however is the association of the autoinhibitory domain with Snf4.

Early investigations of Snf1 revealed that deletion of *SNF4* led to reduced SNF1 function, and this dependence on Snf4 could be circumvented by a C-terminal truncation of Snf1 (Celenza and Carlson 1989; Jiang and Carlson 1996). A portion of the C-terminus evidently serves an autoinhibitory function, and glucose-dependent association of Snf4 relieves this (Jiang and Carlson 1996). A crystal structure of the heterotrimer core of SNF1 indicates that Snf4 is in direct contact with residues 465-495 (Amodeo *et al.* 2007). Thus Snf4 is a positive regulator of SNF1 activity; in conjunction with glucose-dependent association of Snf4 with Snf1, Snf4 additionally binds ADP resulting in the previously described protection from phosphatase activity which leads to SNF1 activation. In addition to Snf4, the complex additionally comprises either Sip1, Sip2, or Gal83, which each contain a conserved C-terminal domain which associates with both Snf1 and Snf4 (Yang *et al.* 1992; Yang *et al.* 1994; Amodeo *et al.* 2007). Association of a β-subunit is essential for SNF1 function, but there is apparently some redundancy in the function of these subunits - deletion of all three results in inactive SNF1, but deletion of any two of the three generally does not have an impact on growth in alternative carbon sources (Schmidt and McCartney 2000). Indeed it seems that the primary function of these subunits is to guide SNF1 to different regions of the cell – while SNF1 in cells grown in glucose remains largely in the cytoplasm, when growth is shifted to an alternative carbon source, $SNF1^{Sip1}$ primarily localized to the vacuole, $SNF1^{Sip2}$ remained in the cytoplasm, and $SNF1^{Gal83}$ (the dominant form) moved to the nucleus (Vincent *et al.* 2001).

The different localizations of the SNF1 complex in response to activating conditions reveal the variety of targets upon which the kinase acts. One of the earliest identified targets of SNF1 is acetyl-CoA carboxylase, an important enzyme in the fatty acid biosynthesis pathway which is deactivated upon glucose starvation (Woods *et al.* 1994). High-throughput experiments also have suggested Fox2, an enzyme in the fatty acid β-oxidation pathway, is activated by SNF1 phosphorylation. Additionally, localization of the hexokinase Hxk2 is likely regulated by SNF1 phosphorylation (Fernández-García

et al. 2012). A significant portion of SNF1's targets relate to the control of gene expression. SNF1 regulates histone acetylation by phosphorylating and activating the histone acetyltransferase Gcn5 and even potentially by directly phosphorylating histone H3 (Liu *et al.* 2010b; Lo *et al.* 2001). It has also been shown to phosphorylate RNA-polymerase II and stimulate transcription, while also regulating the rate of mRNA decay by acting upon the exoribonuclease Xrn1 (Kuchin *et al.* 2000; Young *et al.* 2012; Braun *et al.* 2014). Most notably, however, SNF1 regulates the expression of over 400 genes (Young *et al.* 2003) via (de)activation and of a number of transcription factors.

Among these transcription factors are transcriptional activators Sip4 and Cat8, which are activated by phosphorylation which is dependent on SNF1 activity and regulate the expression of a number of genes (Vincent and Carlson 1999; Lesage *et al.* 1996; Hedges *et al.* 1995; Randez-Gil *et al.* 1997; Vincent and Carlson 1998). These transcription factors, particularly Cat8, bind to carbon source responsive elements (CRSEs) which are found upstream of genes coding for elements of gluconeogenesis, the glyoxylate cycle, and utilization of alternative carbon sources (Vincent and Carlson 1998; Tachibana *et al.* 2005). The most significant target of SNF1, however, is the transcriptional repressor Mig1.

Mig1 was first identified simultaneously as a gene which, when mutated, conferred constitutive derepression of invertase, maltase, and cytochrome c even in the absence of Snf1, and as a transcriptional repressor of *GAL* genes, which are required for the metabolism of galactose (Schüller and Entian 1991; Nehlin *et al.* 1991; Johnston *et al.* 1994; Vallier and Carlson 1994). This repression is achieved in part by recruiting the repressor complex of Ssn6 and Tup1 to target genes (Treitel and Carlson 1995; Tzamarias and Struhl 1995). Later microarray experiments investigating the transcriptional roles of Mig1 and the similar Mig2, which will be discussed shortly, found a largely redundant set of nearly 200 genes which are regulated by one or both of these transcription factors, including many genes associated with hexose transport and carbohydrate metabolism (Westholm *et al.* 2008). It was also shown that Mig1 was differentially phosphorylated in response to glucose, and furthermore, localization of Mig1 changes from the nucleus to the cytoplasm in response to glucose (Treitel and Carlson 1995; De Vit *et al.* 1997). SNF1 is responsible for phosphorylation of Mig1, and this phosphorylation is necessary for derepression of target genes (Treitel *et al.* 1998; Smith *et al.* 1999). Phosphorylation mediates two steps in derepression of Mig1 target genes; disassociation of Mig1 from Ssn6-Tup1, and Msn5-dependent nuclear export (DeVit and Johnston 1999; Papamichos-Chronakis *et al.* 2004). Conversely, when glucose is depleted and SNF1 is deactivated, Mig1 is also de-

phosphorylated by Reg1-Glc7, and returned to the nucleus (De Vit *et al.* 1997; Shashkova *et al.* 2017).

In addition to Mig1, Mig2 also regulates many of the same genes in a redundant manner. This transcriptional repressor has a similar zinc-finger DNA binding domain to Mig1, and deletion of both is required, for example, for complete derepression of invertase in the presence of glucose (Lutfiyya *et al.* 1998). Mig2 is apparently not, however, directly regulated by SNF1 (Lutfiyya *et al.* 1998). Mig2 expression is induced by glucose via the SRR pathway, in an additional example of crosstalk between regulatory pathways, complementary to the previously discussed role of Mig1 in the SRR pathway (Kaniak *et al.* 2004). In the absence of glucose, Mig2 is negatively regulated by SNF1-dependent ubiquitination and subsequent degradation (Lim *et al.* 2011).

While SNF1 is a major regulator of carbon metabolism, it also plays roles in other processes which are affected by nutrient stress. Two examples which are particularly relevant for this work are filamentous growth and cell wall integrity. A number of yeasts are also capable of adopting an elongated, multicellular/multinucleate filamentous form as either hyphae or pseudohyphae, often in response to certain stresses. *S. cerevisiae* adopts a pseudohyphal form under nutrient starvation, among which is glucose starvation (Cullen and Sprague 2000). In this form, filaments are capable of invading agar, which is dependent both on the expression of the flocculin Flo11 and on SNF1 activity (Cullen and Sprague 2000; Lo and Dranginis 1998). Expression of *FLO11* is in fact regulated in part by $SNF1^{Gal83}$ through two of its targets, the transcriptional repressors Nrg1 and Nrg2, which are also repressors of certain genes important for response to glucose starvation (Vyas *et al.* 2001; Kuchin *et al.* 2002; Vyas *et al.* 2003). Independent of *FLO11* regulation, $SNF1^{Gal83}$ and $SNF1^{Sip2}$ also influence invasive growth in a less well characterized way (Vyas *et al.* 2003).

In relation to the cell wall, a number of large-scale mutant screening experiments have reported that deletion of *SNF1* results in increased susceptibility to chemicals which interfere with the cell wall (Kapitzky *et al.* 2010; Dudley *et al.* 2005; García *et al.* 2015). While the fungal cell wall will be discussed in greater detail in section 1.3, it is worth noting that many important components of the wall are polysaccharides; a logical connection may be made between maintenance of the cell wall and ability to metabolize carbon sources. More directly, it was shown that deletion of various components of the SNF1 pathway leads to increased susceptibility to a variety of cell wall perturbing chemicals and to a reduced thickness of the glucan layer of the cell wall, and that SNF1 influences the cell wall independent of the cell wall integrity pathway (Backhaus *et al.* 2013).

SNF1 in *C. albicans*

While many important components of the SNF1 pathway are conserved between *S. cerevisiae* and *C. albicans*, there are a number of important distinctions. CaSnf1 is 65% identical to ScSnf1 in terms of amino acid sequence, and was found to co-precipitate with three additional proteins - CaSnf4 (68% identity to ScSnf4), and two further proteins, one of which strongly resembles both ScGal83 and ScSip2 (54% and 53% identity respectively), and another which only shares homology at domains which are associated with the α- and γ-subunits; these were named Kis1 and Kis2, respectively (Corvey *et al.* 2005). Snf1 is phosphorylated at Thr-208 (corresponding with Thr210 in *S. cerevisiae*) by only one upstream kinase, Sak1 (Ramírez-Zavala *et al.* 2017; Mottola 2016). Before the work presented here, very little work investigated the β- and γ-subunits of *C. albicans* SNF1.

One surprising observation was the apparently essential nature of *SNF1*. Over the years, several published attempts to delete *SNF1* reported failures to obtain null mutants, on stark contrast with observations to the contrary in *S. cerevisiae* (Petter *et al.* 1997; Enloe *et al.* 2000; Ramírez-Zavala *et al.* 2017). Additionally, a system using a glucose-repressible *SNF1* allele failed to produce viable colonies under repressing conditions (Vyas *et al.* 2015). Complementary to these observations, it has been reported that Snf1 is phosphorylated at Thr-208 even in cells grown in glucose, which could indicate a degree of activity even in glucose-repressing conditions (Orlova *et al.* 2008; Ramírez-Zavala *et al.* 2017; Mottola 2016). Interestingly, it has been shown that while RNA transcripts of some genes required to utilize alternative carbon sources are regulated by glucose availability, their protein products remain stable even in cells grown in glucose; this appears to be the product of evolutionary rewiring of ubiquitination targets (Sandai *et al.* 2012).

Evolutionary rewiring of regulatory pathways, in which conserved regulators act on novel targets, is well documented when comparing *S. cerevisiae*, where pathways are often first characterized, and *C. albicans*. In addition to the aforementioned rewiring of targets of ubiquitination, transcription factors have been shown in many cases to have gained new targets in *C. albicans*, either having dual functions or losing their ancestral targets altogether (reviewed in Nocedal and Johnson 2015). This rewiring has been observed in the regulation of a number of metabolic pathways (Martchenko *et al.* 2007; Tebung *et al.* 2016; Tebung *et al.* 2017; Dalal *et al.* 2016). In relation to SNF1 targets, the ScSNF1 target Cat8, which as previously mentioned binds to CRSEs and is essential for grown on nonfermentable carbon sources in that organism, is dispensable for growth on such carbon sources in *C. albicans*, and

SIP4 lacks a clear homolog in *C. albicans* (Hedges *et al.* 1995; Ramírez and Lorenz 2009). Interestingly, the closest match to *ScMIG1* in *C. albicans* has a very similar DNA binding domain, but is otherwise largely different. Most importantly, it lacks an apparent SNF1 phosphorylation site, though there is evidence of post-translational modification dependent on carbon source (Zaragoza *et al.* 2000; Lagree *et al.* 2020). These data could suggest rewiring within the SNF1 pathway.

Transcript profiling of *mig1* deletion mutants indicates that Mig1 primarily acts as a repressor of genes involved in the utilization of alternative carbon sources, and growth of cells on maltose increases the susceptibility of cells to weak organic acids, an effect associated with *mig1* deletion, suggesting that Mig1 has a conserved role and its function is regulated by carbon source (Murad *et al.* 2001; Cottier *et al.* 2015; Lagree *et al.* 2020). Additionally, deletion of the SNF1 activating kinase *SAK1* leads to reduced expression of a number of genes required for utilization of alternative carbon sources as well as a number of glucose transporters (Ramírez-Zavala *et al.* 2017). Thus, while it may be the case that the exact connections between members of the SNF1 pathway have changed, the core function has been conserved, an effect that has been observed in other regulatory circuits (Homann *et al.* 2009). Mig1 and Mig2 exhibit additional differences from their homologs in *S. cerevisiae*. While Mig1 is apparently the dominant repressor in *S. cerevisiae* (Lutfiyya *et al.* 1998; Westholm *et al.* 2008), the pair largely regulate the same set of genes in *C. albicans* (Lagree *et al.* 2020). In regard to the regulation of Mig1 and Mig2 themselves, neither are apparently regulated by carbon source at the RNA level (Lagree *et al.* 2020). Surprisingly, unlike in *S. cerevisiae*, Mig1 protein levels are notably reduced in alternative carbon sources, suggesting a mode of regulation more akin to that of ScMig2 than ScMig1 (Lagree *et al.* 2020).

As mentioned previously, SNF1 has been implicated in morphogenesis and maintenance of cell wall integrity in *S. cerevisiae*. Similarly, in *C. albicans*, Mutants lacking *SNF4* or *SAK1* have exhibited reduced response to filamentation inducing conditions, and increased susceptibility to chemicals which perturb the cell wall (Noble *et al.* 2010; Ramírez-Zavala *et al.* 2017; Mottola 2016). Deletion of *mig1* and *mig2* was also shown, perhaps paradoxically, to lead to abnormal filamentation and reduced biofilm formation (Lagree *et al.* 2020). Metabolic flexibility has also been shown to be important for both colonization and infection within the host (Sandai *et al.* 2012; Childers *et al.* 2016), and in line with this, *sak1* deletion prevents successful gastrointestinal colonization in a mouse model (Ramírez-Zavala *et al.* 2017).

1.3 Regulation of the *C. albicans* cell wall

C. albicans cells are encapsulated in a cell wall which serves to protect the cell from its surroundings and also serves as the interface at which the fungus interacts with other cells, be they from the host, other members of the microbiome, or indeed other *Candida* cells. The cell wall is characterized by several layers, each distinct in their molecular composition, which varies depending on whether cells are in the yeast or hyphal morphology. The *C. albicans* cell wall comprises essentially three components – chitin, glucan, and mannoprotein. In yeast cells, the dry-weight distribution is normally 1-2% chitin, 20% β(1,6)-linked glucan, 40% β(1,3)-linked glucan, and 35-40% mannoprotein (Brown and Catley 1992; Kapteyn *et al.* 2000; Klis *et al.* 2001). Hyphae exhibit an increased chitin content, upwards of 10% by dry weight (Braun and Calderone 1978; Nather and Munro 2008). In terms of spacial organization, chitin forms a basal layer to which β(1,3)-glucan is covalently linked – β(1,6)-glucan is linked to this, and the three form the inner cell wall (Chaffin *et al.* 1998; Ruiz-Herrera *et al.* 2006; Kapteyn *et al.* 2000). The outer cell wall comprises numerous cell wall proteins which are bound to glucan. These proteins are heavily modified with long, branching mannan polysaccharides (Chaffin *et al.* 1998; Klis *et al.* 2001).

The importance of the fungal cell wall is apparent in the phenotypes of mutants which are unable to create particular components of the cell wall and in the effect of chemicals that disrupt the cell wall. Despite its relatively low presence in terms of dry weight, chitin synthesis is essential for growth of *C. albicans* (Munro *et al.* 2001). Chemicals which interfere with chitin assembly, such as calcofluor white or Congo red, also reduce growth (Ram and Klis 2006). Chitin is also important for virulence – strains lacking *CHS3*, which codes for one of four chitin synthases, grown normally in culture, but are avirulent in a mouse model (Bulawa *et al.* 1995). Synthesis of β(1,3)-glucan is essential for growth of *S. cerevisiae* (Mazur *et al.* 1995), and as mentioned in section 1.1, the echinocandin class of antifungal drug inhibits this activity. In regard to mannoprotein (also referred to as mannan), two specific forms of mannosylation exist – simple mannose chains (*O*-mannosylation), and complex branching *N*-mannosylation. Disruption of the formation of either results in reduced virulence and increased susceptibility to cell wall stresses (Prill *et al.* 2005; Munro *et al.* 2005; Hall *et al.* 2013). Interestingly, decreasing the amount of one component of the cell wall results in compensatory increases in other components. Reduced *N*-mannan leads to thickened inner cell walls with increased glucan and chitin (Bates *et al.* 2006), and reduction of β-glucan levels results in increased chitin and mannan (Fonzi 1999; Douglas *et al.* 1997; Kapteyn *et al.* 2000; Moreno *et al.*

2010). These observations make clear the interconnected regulation of cell wall maintenance.

Cell wall damage elicits a rapid response via signal transduction pathways mediated by protein kinases which attempt to compensate for deficiencies to retain integrity of the cell wall. Central to this response is the cell wall integrity (CWI) pathway, which has largely been dissected in *S.cerevisiae* and is generally believed to be conserved in *C. albicans*. In *S. cerevisiae*, it has been shown that cell wall damage is sensed by membrane-bound ScWsc1, ScWsc2, and ScDfi1, which have large extracellular domains which detect mechanical stresses that occur when the cell wall is weakened (Heinisch *et al.* 2010). This activates protein kinase C via the guanosine-nucleotide exchange factor ScRom2 and Rho GTPase ScRho1 (Philip and Levin 2001; Kamada *et al.* 1996; Ozaki *et al.* 1996). Protein kinase C activates a mitogen-activated protein kinase (MAPK) pathway comprising the MAPKKK ScBck1, the MAPKK ScMkk2, and ultimately the MAPK ScMpk1; these kinases are required for resistance to a number of stresses including cell wall stress (Levin 2011). This kinase cascade leads to activation of the transcription factor ScRlm1 (Jung *et al.* 2002). ScRlm1 regulates a number of genes directly and indirectly related to the cell wall, and Ca*RLM1* deletion, unlike deletion of its *S. cerevisiae* counterpart, results in significant alterations to the cell wall and hypersusceptibility to cell wall stress (Levin 2011; Lenardon *et al.* 2009; Delgado-Silva *et al.* 2014). This pathway is conserved in *C. albicans* (Dichtl *et al.* 2016). The CWI pathway is not alone however in its regulation of cell wall integrity.

Other MAPK pathways, the high osmolarity glycerol (HOG) pathway and Cek1 pathway, are regulators of the cell wall. While the canonical role of the MAPK Hog1 is to respond to osmotic stress, *hog1* deletion also results in an increased resistance to cell wall stress in *C. albicans* (Alonso-Monge *et al.* 1999). This resistance is connected with hyperactivation of the Cek1 MAPK, which influences cell wall mannosylation (Eisman *et al.* 2006; Cantero and Ernst 2011; Román *et al.* 2016). Additionally, the HOG pathway coordinates with the CWI pathway as well as the Ca^{2+}/calcineurin signaling pathway to regulate chitin synthesis (Munro *et al.* 2007). The HOG pathway and CWI pathway are also entwined in the regulation of their target transcription factors. Rlm1 has been shown to regulate the expression of *SKO1*, which encodes a transcription factor which is a major target of Hog1, and the two transcription factors bind many of the same promoter sequences in response to exposure to the echinocandin caspofungin (Heredia *et al.* 2020).

Outside of MAPK pathways, an additional transcription factor, Cas5, has been identified as a major regulator of cell wall integrity which lacks a clear homolog in *S. cerevisiae* (Bruno *et al.* 2006). Cas5 is activated by

Glc7-dependent dephosphorylation, which leads to nuclear localization and differential expression of a set of genes which include cell wall biogenesis and organization genes (Xie *et al.* 2017). Interestingly, the DNA-binding domain of Cas5 shares some similarity with those of Mig1 and Mig2, which are also required for resistance to cell wall stress, and *CAS5* deletion affects the expression of genes involved in metabolic pathways (Lagree *et al.* 2020; Xie *et al.* 2017). Additionally, a major morphological regulator, the transcription factor Efg1 (which promotes hyphal growth and expression of hyphae-specific wall proteins (Sohn *et al.* 2003)), associates with Cas5 and co-regulates a set of cell wall related genes (Xiong *et al.* 2020) and its expression is directly regulated by Sko1 (Heredia *et al.* 2020); these observations showcase the complex interconnectedness of cell wall organization with other major cellular functions such as morphogenesis and metabolism.

The cell wall is also the point of contact between *C. albicans* cells and those of the host. While all components of the fungal cell wall are recognized by host immune receptors (Gow and Hube 2012), it is apparent that β-glucan is particularly immunogenic, and recognition by the CLR Dectin-1 is an important component of the overall response to fungal infection (Brown and Gordon 2005; Dennehy and Brown 2007). Typically, most β-glucan is obscured from the immune system by the outer cell wall; exposure of this glucan through chemical or mutational methods results in a strong proinflammatory response (Wheeler and Fink 2006). Mannan in the outer cell wall therefore acts as a protective barrier against immune response. In line with this reasoning, perturbation of cell wall mannosylation affects immune response and strains which are defective in mannosylation exhibit reduced virulence (Mora-Montes *et al.* 2010; Hall *et al.* 2013; Davis *et al.* 2014; Hasim *et al.* 2017). Glucan masking appears to be regulated via more than one regulatory pathway. The Cek1 MAPK pathway apparently is important for maintenance of glucan masking, although whether the pathway positively or negatively regulates it is debated (Chen *et al.* 2019b; Galán-Díez *et al.* 2010; Chen *et al.* 2019a; Li *et al.* 2015).

A number of physiologically relevant environmental conditions have been shown to induce masking via different signaling pathways. When lactate is present in growth medium, glucan masking increases, dependent on activity of the transcription factor Crz1, but not on its canonical regulator, the calcineurin pathway (Ballou *et al.* 2016). Iron starvation and hypoxia additionally induce masking, though this signaling occurs via the cAMP-dependent protein kinase A pathway (Pradhan *et al.* 2018; Pradhan *et al.* 2019). Interestingly, acidic pH like what is encountered in the vagina, one niche of *C. albicans*, was shown to have the opposite effect of exposing β-glucan, though this effect is short-lasting, and glucan is remasked in response to the quorum

sensing signal molecule farnesol (Sherrington *et al.* 2017; Cottier *et al.* 2019).

1.4 Goals of this study

Fungi are often overlooked as causes of illness. This neglect belies the impact that fungi, and especially *Candida* spp., have on public health. Fungal infections kill around one and a half million people per year – a toll rivaling that of tuberculosis or malaria; estimates place the number of life threatening infections by *C. albicans* higher than 400,000 (Brown *et al.* 2012). However, as discussed in section 1.1, the available arsenal of antifungal drugs is limited, and their efficacy is threatened by the evolution of drug resistance. Thus, thorough investigation of the biology of fungal pathogens like *C. albicans* and detailed delineation of the differences in these organisms compared to better-studied but nonpathogenic model organisms like *S. cerevisiae* is vital to the development of novel antifungal drugs. In the past several decades, protein kinases have become one of the most popular drug targets because they are ubiquitous, critical for practically all signaling pathways, and are relatively simple to design inhibitors for (Cohen 2002; Ferguson and Gray 2018).

Protein kinases in *C. albicans*, naturally, have been included in consideration as potential antifungal targets (Bastidas *et al.* 2008). Previous and continuing work in this lab has included the construction of a comprehensive library of deletion mutants of all known and putative protein kinases in *C. albicans* and phenotypic investigation of these mutants (Ramírez-Zavala *et al.* 2017). The identification of the previously uncharacterized orf19.3840 as the Snf1-activating kinase Sak1 highlighted the SNF1 pathway as a relatively untouched subject in this organism. As mentioned in section 1.2.2, this work revealed SNF1 as a regulator of *in vivo* fitness, an important trait for a potential drug target. And, while Snf1 is conserved in mammals, Sak1 is not. This, plus the myriad differences between the SNF1 pathways in *S. cerevisiae* and *C. albicans* as well as the absence of confirmed targets of CaSNF1 (as illustrated in Fig. 1.2), suggested that SNF1 was ripe for investigation in *C. albicans*. Two major goals, spurred by earlier work (Ramírez-Zavala *et al.* 2017; Mottola 2016), were pursued: the identification of direct or indirect targets of regulation by SNF1, and the related goal of understanding the apparent essentiality of Snf1, which has been discussed in section 1.2.2. While these were the original goals of the work presented here, they gave way to several unexpected discoveries.

2. Results

2.1 Regulation of Mig1 and Mig2 activity by the SNF1 pathway

As described in section 1.2.2, a number of observed differences between aspects of the SNF1 pathway in *S. cerevisiae* and *C. albicans* spurred interest in investigating novel targets of SNF1 in *C. albicans*. However, it also raised questions about the conservation of known targets. The most significant target of ScSNF1 is the transcriptional repressor Mig1, which functions alongside Mig2, which is indirectly regulated in part by SNF1, to repress a set of target genes. Surprisingly, while the DNA-binding domains of these transcription factors are well conserved between these two organisms as well as related yeasts, the rest of the protein is poorly conserved. Figure 2.1 illustrates the conservation (and lack thereof) of Mig1 protein sequence between *S. cerevisiae*, *C. albicans*, and two additional pathogenic yeasts: *Candida glabrata*, which is more closely related to *S. cerevisiae*, and *Candida dubliniensis*, which is more closely related to *C. albicans*. Outside of the DNA binding domain, there are stark differences between the two clades. A recognition motif for ScSNF1 is known: ΦXRXXSXXXΦ, where Φ represents a hydrophobic residue (M, V, L, I, or F; Dale *et al.* 1995). Three such sites on Mig1 are known to be phosphorylated *in vivo* in *S. cerevisiae* (Smith *et al.* 1999). In *C. albicans*, two of the three phosphorylated serines are conserved, but the recognition motif is absent. Similarly, an alignment of Mig2 amino acid sequences (or closest match in the genomes of *C. glabrata* and *C. dubliniensis*) shows a conserved DNA-binding domain but otherwise significant differences between the two clades (Figure 2.2). This observation raised the question of whether or not Mig1 and Mig2 are regulated by SNF1, and if so, whether the effect is direct or indirect. It should be noted additionally that much of the work presented in this section was produced contemporaneously with similar results which have been published by Lagree *et al.* 2020.

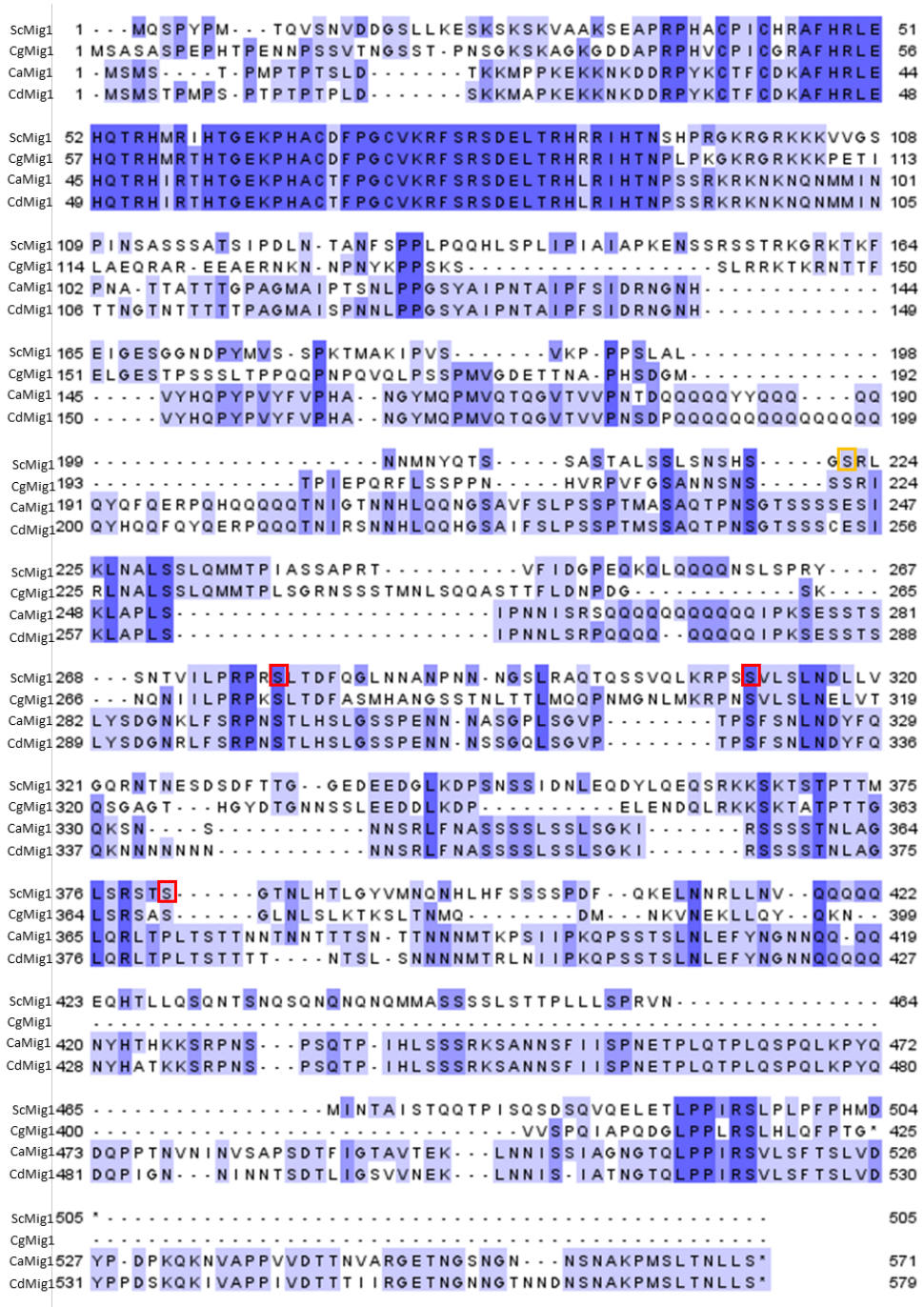

Figure 2.1: Mig1 sequence is poorly conserved. Multiple sequence alignment of Mig1 proteins from *S. cerevisiae, C. glabrata, C. albicans,* and *C. dubliniensis* was produced using Clustal Omega and visualized in Jalview version 2 (Sievers *et al.* 2011; Waterhouse *et al.* 2009). Color denotes conservation where the lightest shade is conserved among two of the four species, and the darkest is conserved among all four species. Serine residues which are phosphorylated by ScSnf1 *in vitro* are highlighted; those which sit in a recognition motif in red, and one which lacks the recognition motif in orange (Dale *et al.* 1995; Smith *et al.* 1999).

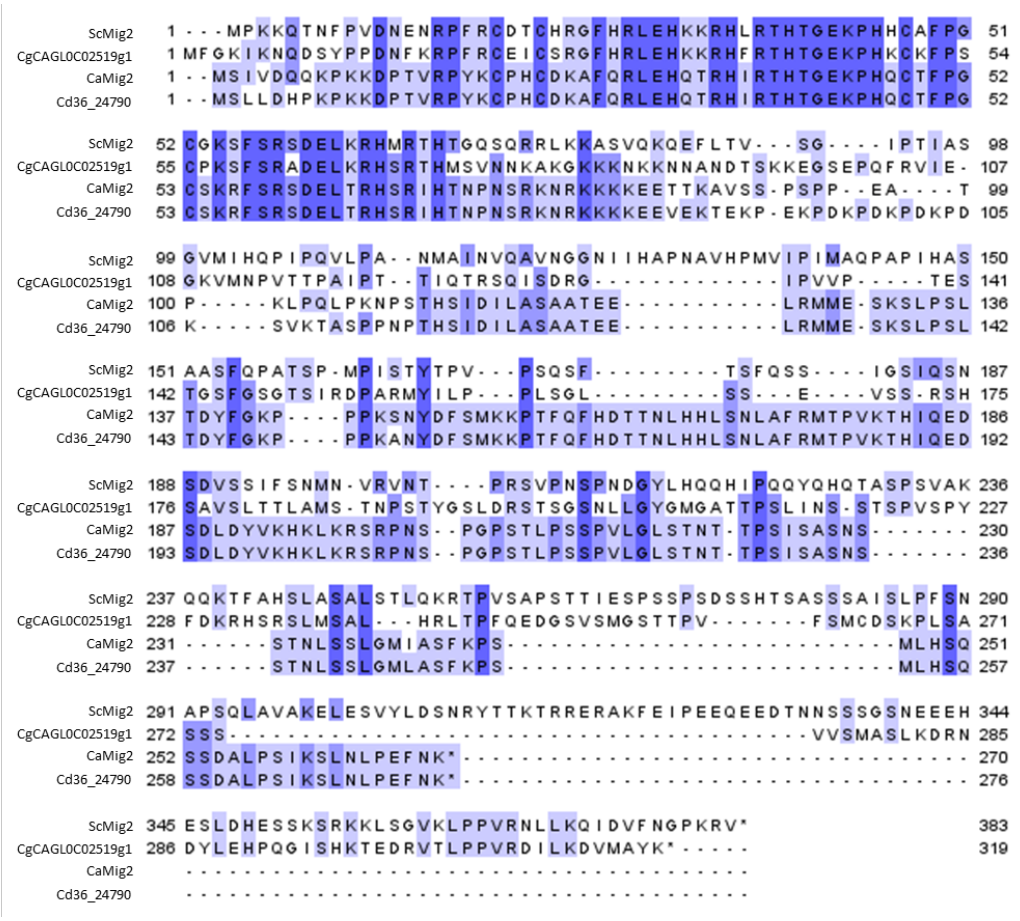

Figure 2.2: Mig2 sequence is poorly conserved. Multiple sequence alignment of Mig2 proteins from *S. cerevisiae* and *C. albicans* as well as the most similar uncharacterized proteins from *C. glabrata* and *C. dubliniensis* was produced using Clustal Omega and visualized in Jalview version 2 (Sievers *et al.* 2011; Waterhouse *et al.* 2009). Color denotes conservation where the lightest shade is conserved among two of the four species, and the darkest is conserved among all four species.

2.1.1 Mig1 and Mig2 negatively regulate growth on alternative carbon sources

While the DNA-binding domains of Mig1 and Mig2 are conserved, it is conceivable that the binding sites of targets within the genome could have changed over time, resulting in the gain and/or loss of targets. A possible consequence of this would be change in biological role for these transcription factors. To determine whether Mig1 and Mig2 are functionally conserved, growth assays were conducted to examine whether or not deletion of Mig1 and Mig2 could restore growth on alternative carbon sources in an *snf4*Δ mutant (Figure 2.3). Deletion of *SNF4* is used here as a proxy for *SNF1* inactivation, as *SNF1* was believed to be essential (see section 1.2.2).

As has been previously described (see section 1.2.2), deletion of *SNF4* results in an inability to grow when glucose is not available as a carbon source, and even results in reduced growth when glucose is the sole carbon source in minimal medium. Figure 2.3 shows that when strains were grown at 30°C, deletion of *MIG1* restored growth partially or completely to wild type levels in rich media and minimal medium where glucose was the carbon source, but had very little effect in other minimal media or in Spider medium, where mannitol is the carbon source. At 37°C, *snf4*Δ mutants had an exaggerated growth defect, and the effect of *mig1* deletion was reduced, but still apparent. Subsequent deletion of *MIG2* further restored growth in rich media at both temperatures. Additionally at both temperatures deletion of both repressors restored the ability to grow on minimal media containing sucrose as the carbon source, but this growth was extremely poor. Interestingly, deletion of both *MIG1* and *MIG2* significantly improved growth on Spider medium at both temperatures. These deletions did not however appear to restore growth on minimal media where glycerol was the carbon source. These results indicate that Mig1 and Mig2 do repress activities that are required for the utilization of alternative carbon sources, but their deletion is insufficient to fully overcome the defects of an *snf4*Δ mutant. Nonetheless, they also suggest that Mig1 and Mig2 may continue to function within the SNF1 pathway.

Inability to grow in alternative carbon sources is one prominent phenotype of reduced SNF1 function. An additional phenotype is increased susceptibility to cell wall and membrane stresses. One hypothesis to explain this is that dysfunction in carbohydrate metabolism interferes with proper construction of the cell wall, which as described in section 1.3 is primarily composed of carbohydrates. In this case, restoration of carbon metabolism should also result in restoration of cell wall integrity in *snf4*Δ mutants. Figure 2.4 compares the susceptibility of the wild type and *snf4*Δ mutant to chemicals which

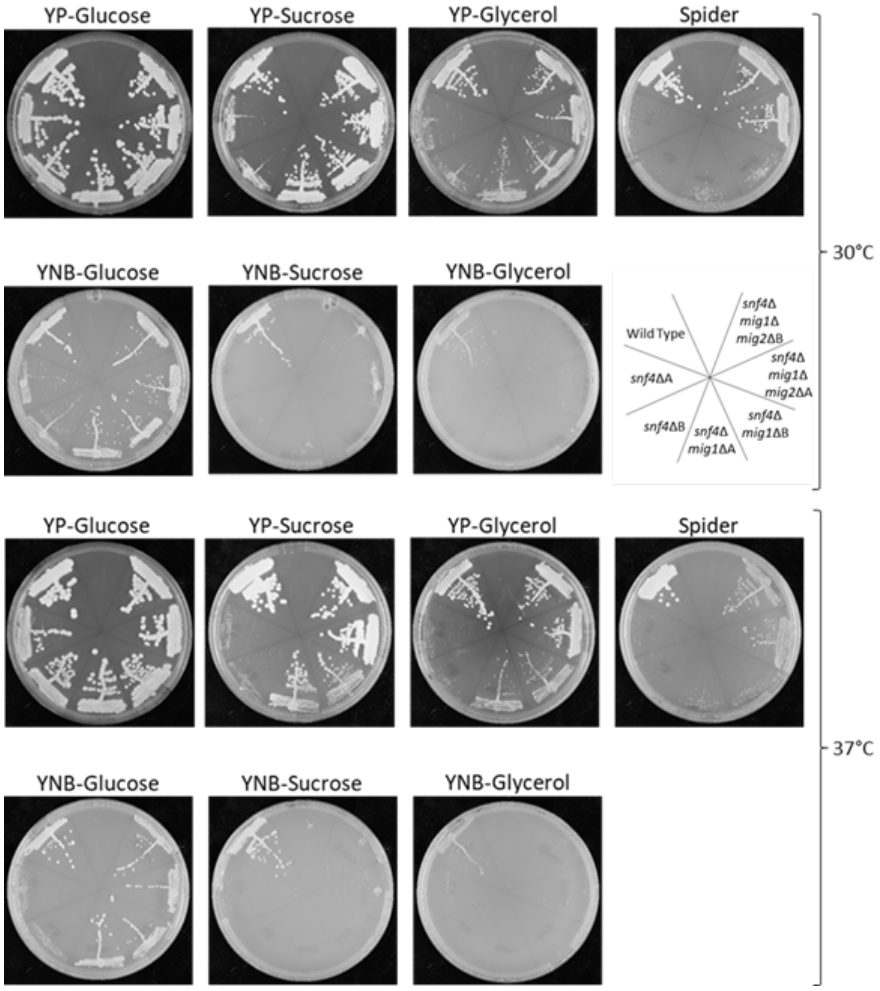

Figure 2.3: Deletion of *MIG1* and *MIG2* partially restores growth on alternative carbon sources in *snf4*Δ mutants. The wild type, *snf4*Δ, *snf4*Δ*mig1*Δ double mutants, and *snf4*Δ*mig1*Δ*mig2*Δ triple mutants were grown overnight in YPD before being diluted to an OD 600 of 2.0. 3µL were streaked on the shown media and grown for two days at 30° or 37°C. For each mutant, two independently constructed strains are shown.

induce cell wall and membrane stress, and the effect of subsequent deletion of *MIG1* and *MIG2*. The *snf4*Δ mutant was hypersusceptible to all tested chemicals. Deletion of *MIG1* resulted in a strong improvement in growth on the antifungal fluconazole; this strain grew nearly as well as the wild type.

The effect was more modest in Congo red and calcofluor white, but the wild type was also highly susceptible at the tested concentrations. Subsequent deletion of *MIG2* enhanced this effect. The triple mutant (*snf4*Δ *mig1*Δ *mig2*Δ) grew as well or even better than the wild type in fluconazole and calcofluor white. Surprisingly, deletion of *MIG1* in cells lacking *SNF4* exacerbated the already increased susceptibility to the antifungal caspofungin, and the triple mutant was entirely unable to grow at the tested concentration. These results appear to conflict; in some cases, deletion of *MIG1* and *MIG2* seemed to alleviate the defects of the *snf4*Δ mutant in cell wall integrity, but they appeared to exacerbate this defect in the presence of caspofungin. To some degree however, derepression of Mig1 and Mig2 target genes appears to improve resistance to cell wall and membrane stress.

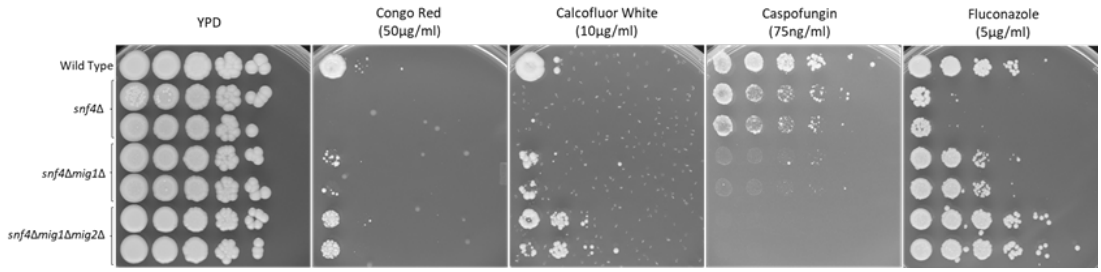

Figure 2.4: Deletion of *MIG1* and *MIG2* partially affects cell wall integrity in *snf4*Δ mutants. The wild type, *snf4*Δ, *snf4*Δ*mig1*Δ double mutants, and *snf4*Δ*mig1*Δ*mig2*Δ triple mutants were grown overnight in YPD before being diluted to an OD 600 of 2.0, serially diluted, and spotted on the shown media. Plates were incubated for three days at 30°C. For each mutant, two independently constructed strains are shown.

2.1.2 Mig1 and Mig2 are phosphorylated dependent on SNF1 activity

The ability of *MIG1* and *MIG2* deletion to rescue several defects of *snf4*Δ mutants suggested that Mig1 and Mig2 are to some degree functionally conserved with their *S. cerevisiae* homologs, and that they may continue to operate within the SNF1 pathway. This raised the question of how these transcription factors are regulated. As has been discussed in section 1.2.2, ScSNF1 negatively regulates ScMig1 by phosphorylation, which induces nuclear export. To determine whether Mig1 is also phoshorylated and whether this phosphorylation is dependent on carbon source in *C. albicans*, western

blotting was performed using a C-terminally HA-tagged form of Mig1. To avoid any competition between tagged and untagged Mig1, a heterozygous *MIG1* mutant with only one remaining *MIG1* allele was mutated to add the epitope tag, so that the tagged form was the only expressed form of the protein. Figure 2.5 shows an unexpected result. If Mig1 were phosphorylated in response to growth on an alternative carbon source, here sucrose, a more slowly migrating band would be expected. Treatment of cell extracts with phosphatase would lead to identical mobility in both carbon sources. This is not the case. Instead, the amount of Mig1 protein was lower when sucrose was the carbon source. The amount of Mig1 detected overall also was reduced following phosphatase treatment, though the reason for this is unclear. This suggested an alternate mode of Mig1 regulation.

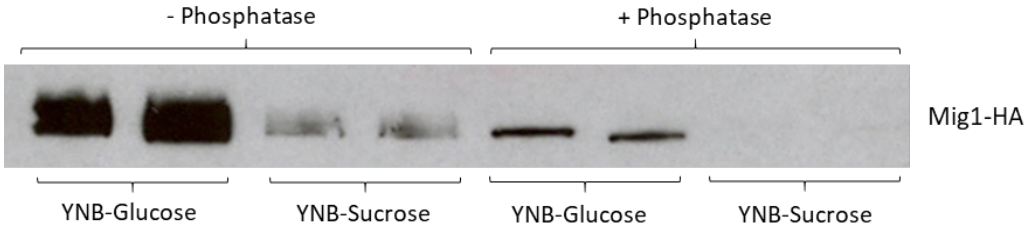

Figure 2.5: Mig1 protein levels respond to carbon source. Strains containing only one copy of Mig1 which was tagged with the HA epitope were grown to mid log phase in YNB-Glucose and resuspended in either YNB-Glucose or YNB-Sucrose and grown for a further two hours. For phosphatase treatment, cell extracts were washed using centrifugal filters and treated with λ-phosphatase. Immunodetection was done with an antibody specific to the HA epitope. For each mutant, two independently constructed strains are shown.

These results were soon supported by the publication of Lagree *et al.* 2020, which presented similar data showing that shifting growth medium from YP-Glucose to YP-Glycerol resulted in a reduction of Mig1 levels, but not a band shift. However, they did note that growth in Spider medium resulted in the appearance of a second, more slowly migrating band, suggesting that in certain conditions, Mig1 is in fact modified. They did not, however, confirm that this modification was phosphorylation. In the Bachelor's thesis of Weber 2020, this was investigated further. Using rich (YP) media like in Lagree *et al.* 2020 rather than minimal media as used in Figure 2.5, this work showed that, in addition to the previously observed reduction in Mig1 levels, growth in YP-Sucrose also resulted in a band shift suggesting posttranslational modification; furthermore, deletion of *SNF4* abolished this shift.

In an attempt to reproduce the detection of modification reported by these works, it was also tested whether such a shift could be detected when glycerol was the carbon source; this was not detected by Lagree *et al.* 2020, but here was successful (Figure 2.6). In this particular experiment, it was

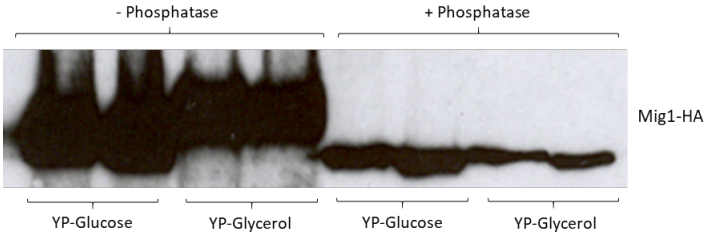

Figure 2.6: Mig1 is phosphorylated in response to carbon source. Strains containing only one copy of Mig1 which was tagged with the HA epitope were grown to mid log phase in YP-Glucose and resuspended in either YP-Glucose or YP-Glycerol and grown for a further two hours. For phosphatase treatment, cell extracts were washed fugal filters and treated with λ-phosphatase. Immunodetection was done with an antibody specific to the HA epitope. For each mutant, two independently constructed strains are shown.

difficult however to determine if Mig1 protein amount decreased; because phosphatase treatment seemed to reduce the amount of Mig1 protein in Figure 2.5, a greater amount of protein (30µg) was used in this experiment than is typically loaded. Treatment of cell extracts with phosphatase abolish this change in mobility, indicating that Mig1 was phosphorylated in response to glycerol, as had been shown by Weber 2020 to be the case in sucrose. It is worth noting that the apparent amount of detected protein following phosphatase treatment was reduced (see Figures 2.5 and 2.6), although total protein loading was equal as determined by Ponceau S staining. Furthermore, this phosphorylation was dependent on SNF1 activity. Figure 2.7 shows both a change in mobility and reduction in Mig1 protein level in response to glycerol. Both of these responses were affected in strains lacking *SNF4*. The degree of reduction in protein amount was strongly limited, and while a slower migrating form seems to still be present, the fastest form is dominant, suggesting that SNF1 activity is required for regulation of Mig1 in glycerol.

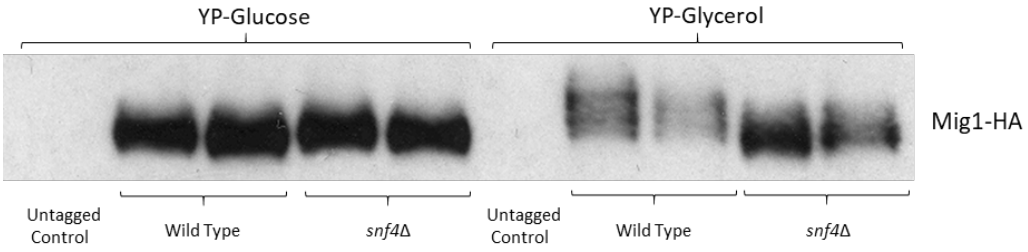

Figure 2.7: Carbon source-dependent Mig1 phosphorylation requires *SNF4*. Strains containing only one copy of Mig1 which was tagged with the HA epitope in either the wild type or *snf4*Δ mutants were grown to mid log phase in YP-Glucose and resuspended in either YP-Glucose or YP-Glycerol and grown for a further two hours. Immunodetection was done with an antibody specific to the HA epitope. For each mutant, two independently constructed strains are shown.

Lagree and colleagues reported that they were unable to detect HA-tagged Mig2 protein, and therefore could not observe any carbon source-dependent modification of this protein. In contrast, HA-tagged Mig2 was successfully detected by Weber in several electrophoretic forms; the relative amounts of these forms depending on carbon source and SNF1 activity. Mig2 is ubiquitinated in an SNF1-dependent manner in *S. cerevisiae* (Lim *et al.* 2011), but it was unclear from this work whether overall Mig2 protein levels are affected by carbon source. The nature of this modification was investigated further.

Figure 2.3 indicates that growth of an *snf4*Δ mutant on Spider medium was only normal when both *MIG1* and *MIG2* are deleted; Weber 2020 showed that deletion of *MIG2* had a greater effect on growth than deletion of*MIG1*. This was the only observed medium where Mig2 appeared to have a greater role than Mig1. Therefore, to further investigate carbon source-dependent regulation of Mig2, Spider medium was used. In the wild type, three electrophoretically distinct forms were again observed when grown in YP-Glucose medium, where the smallest form appears to be dominant. Changing medium to Spider resulted in a significant reduction of protein amount. Additionally, only the largest band was detectable, suggesting that in this medium, it is the dominant form (Figure 2.8A). Upon treatment of cell extracts with phosphatase, only the smallest form was visible regardless of medium, though there was still protein observed in Spider medium. This indicates that all

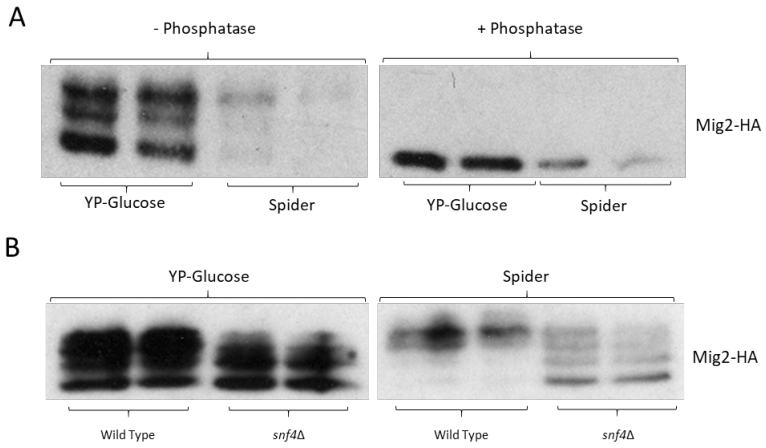

Figure 2.8: Mig2 is phosphorylated in response to carbon source in an *SNF4*-dependent manner. (A) The change in Mig2 electrophoretic mobility is due to phosphorylation. (B) Carbon source-dependent modification partly depends on *SNF4*. Strains containing only one copy of Mig2 which was tagged with the HA epitope in either the wild type of *snf4*Δ mutants were grown to mid log phase in YP-Glucose and resuspended in either YP-Glucose or Spider and grown for a further two hours. For phosphatase treatment, cell extracts were washed using centrifugal filters and treated with λ-phosphatase. Immunodetection was done with an antibody specific to the HA epitope. Left and right panels from (A) or (B) are from the same blot, with an intervening lane removed for clarity in presentation. For each mutant, two independently constructed strains are shown.

of the distinct forms of Mig2 represent differently phoshorylated forms of the protein. In Figure 2.8B, four distinct forms of Mig2 can be seen; the largest two potentially overlapping in previous blots due to the intensity of the bands and their relative proximity. Additionally, deletion of *SNF4* resulted in a reduced intensity of the largest bands and increased intensity of the smallest, unphosphorylated form in YP-Glucose. As in Figure 2.8A, shifting to Spider medium resulted in loss of the smaller bands. This was partially, but not fully, reversed by deletion of *SNF4*; in these mutants, the smallest band was most prominent even in Spider medium. These results provide evidence that Mig2 is regulated in response to carbon source by SNF1 via phosphorylation, differing notably from the mode of regulation of ScMig2.

2.2 Generation and analysis of SNF1 mutant suppressors

One approach that was used to attempt to identify novel targets of SNF1 was to generate suppressor mutants which were able to overcome defects of the *snf4*Δ mutant. Strains which lack *SNF4* but are able to grow on alternative carbon sources, tolerate cell wall stresses, or filament normally will exhibit genomic alterations which result in some degree of independence from SNF1 regulation; these mutants can be sequenced, and if the mutation responsible for the phenotypic effect can be identified, it should give us some insight into downstream elements of SNF1 or alternative pathways which are able to compensate for reduced SNF1 activity. Ideally, such mutations would even be in direct targets which have mutated to be SNF1-independent. To generate suppressors, an *snf4*Δ mutant was passaged over several days in YPD medium. Previous work has shown that this mutant grows worse than the wild type in this medium (Ramírez-Zavala *et al.* 2017; Mottola 2016). Over time, as random mutation occurs, selection should enrich mutants which grow more quickly than the parent strain. Aliquots of each passage were plated on media where the *snf4*Δ strain typically cannot grow – either an alternative carbon source (YNB-Sucrose) or in the presence of cell wall stress (50µg/mL Congo red). Through this approach, over two days of passaging, three colonies were identified: *snf4*ΔSupA (identified on Congo red from the second day passage), *snf4*ΔSupB (identified on YNB-Sucrose from the first day passage), and *snf4*ΔSupC (identified on YNB-Sucrose from the second day passage).

Spot assays were conducted to determine the ability of these suppressors

to utilize several alternative carbon sources, as well as their susceptibility to cell wall stresses. Figure 2.9 shows that the suppressor mutants did not all behave alike. Suppressor A, identified on Congo red, stood out mainly in its increased resistance to Congo red and calcofluor white. This suppressor was not only much more resistant than the parental *snf4*Δ strain, but is also more resistant than even the wild type. In contrast, however, it was even more susceptible to caffeine than the parental strain. In carbon utilization, this suppressor had no appreciable effect on growth using glucose or glycerol, but modestly restored growth on sucrose and acetate, though not to wild type levels. Suppressors B and C behaved similarly. Both were identified on sucrose, and indeed both notably restored growth on sucrose and acetate, though not to wild type levels. Additionally, they fully reverted the glucose slow-growth phenotype. However, no effect was observed on glycerol. The effect of these suppressors in resistance to cell wall stress was much more muted. Both modestly increased resistance to Congo red and calcofluor white, though not to the degree of the wild type. No effect was observed in resistance to caffeine.

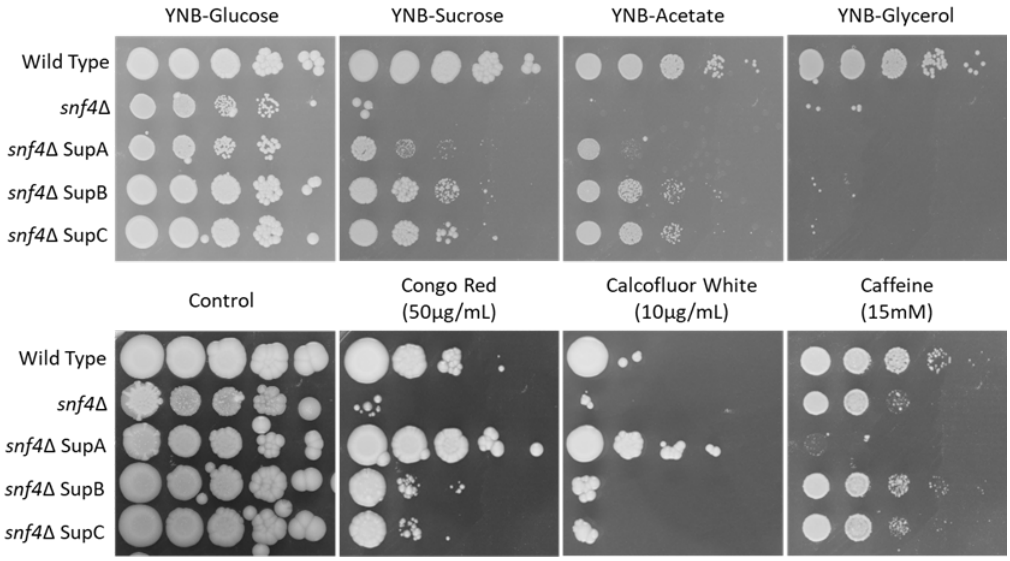

Figure 2.9: *SNF4* suppressors have varied phenotypes. The wild type, *snf4*Δ, and derived suppressors (SupA/B/C) were grown overnight in YPD before being diluted to an OD 600 of 2.0, serially diluted, and spotted on the shown media. Plates were incubated for three days at 30°C.

2.2.1 Suppressor B contains an in-frame deletion in *SNF1*

The primary goal of this experiment was to generate suppressors in targets of SNF1 which have not been previously identified. Prior to devoting resources to whole genome sequencing to search for genetic differences with the parental *snf4*Δ strain, *MIG1*, *MIG2*, and *SNF1* were individually sequenced to rule out mutations in these genes. *MIG1* and *MIG2* regulate likely targets of SNF1 (see section 2.1) and a number of mutations have previously been identified in Sc*SNF1* which confer independence from regulation by Snf4 (Celenza and Carlson 1989; Estruch *et al.* 1992; Leech *et al.* 2003). In all three suppressor mutants, *MIG1* and *MIG2* remained wild type. Interestingly, suppressor B exhibited a heterozygous mutation wherein allele A (which can be distinguished from allele B due to a shortened polyhistidine tract in the N-terminus and silent polymorphisms at base positions 1443, 1620, and 1809) contained an internal, in-frame deletion of six codons in a region situated between the N-terminal kinase domain and C-terminal regulatory domain – *SNF1*$^{\Delta 311\text{-}316}$ (Figure 2.10).

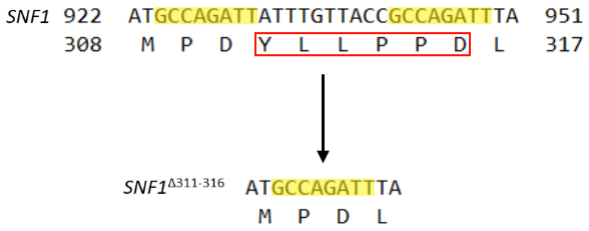

Figure 2.10: The *SNF1*$^{\Delta 311\text{-}316}$ mutation is an in-frame deletion of six codons. An excerpt of the *SNF1* coding sequence and translated amino acids from the wild type allele A (top) and mutated form identified in *snf4*ΔSupB (bottom) Highlighted in yellow is an eight-nucleotide sequence which is repeated in the wild type; one repeat and the intervening nucleotides are lost in the mutation. Amino acids marked by the red box are lost as a result.

2.2.2 Snf1$^{\Delta 311\text{-}316}$ rescues some *snf4*Δ growth defects

In order to confirm that this mutation within *SNF1* was responsible for the observed phenotype of the strain, one allele of *SNF1* in the *snf4*Δ strain was replaced with *SNF1*$^{\Delta 311\text{-}316}$. The effect of this mutation on the ability of the *snf4*Δ mutant to utilize various carbon sources was compared with several other *SNF1* mutations (Figure 2.11). *SNF1*$^{\text{L181I}}$ was chosen because the homologous mutation in *S. cerevisiae* was shown to render ScSNF1 independent from regulation by ScSnf4, and in *C. albicans* it improves growth of *sak1*Δ mutants (Leech *et al.* 2003; Ramírez-Zavala *et al.* 2017;

Mottola 2016). The location of the internal deletion is reminiscent of a previously identified *snf4*Δ suppressor mutation – a C-terminal truncation of ScSnf1 after amino acid 309, corresponding with residue 311 in *C. albicans*. An analogous truncation was also investigated, in addition to a previously characterized C-terminal truncation which ends at residue 340 which was shown to confer γ-subunit independence in a mammalian cell line, but only moderately affected *C. albicans* cells, allowing *snf4*Δ mutants to filament under certain conditions (Crute *et al.* 1998; Mottola 2016). Interestingly, both *SNF1*$^{\mathrm{L181I}}$ and *SNF1*$^{\Delta 311\text{-}316}$ exhibited essentially identical effects on the ability of *snf4*Δ mutants to utilize different carbon sources. The effects were modest, however. Figure 2.11 shows that growth on glucose and sucrose reverted to wild type levels, but this was largely the limit. Both mutations allowed growth on acetate, but at a much lower level than the wild type. Neither had an apparent effect on the ability to grow on glycerol. In contrast, both C-terminal truncations had no appreciable effect on growth.

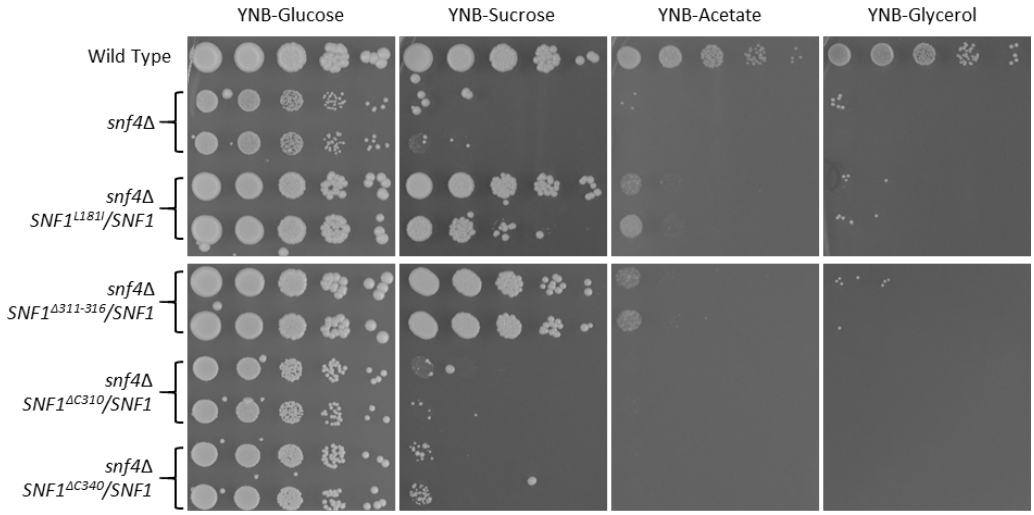

Figure 2.11: Influence of mutations in *SNF1* on growth of *snf4*Δ mutants in different carbon sources. The wild type, *snf4*Δ mutants, and derived strains in which one allele of *SNF1* was replaced with *SNF1*$^{\mathrm{L181I}}$, *SNF1*$^{\Delta 311\text{-}316}$, *SNF1*$^{\Delta \mathrm{C}310}$ or *SNF1*$^{\Delta \mathrm{C}340}$ were grown overnight in YPD before being diluted to an OD 600 of 2.0, serially diluted, and spotted on the shown media. Plates were incubated for four days at 30°C. Strains plated on a single medium were plated on a single plate, with pictures rearranged for clarity in presentation. For each mutant, two independently constructed strains are shown.

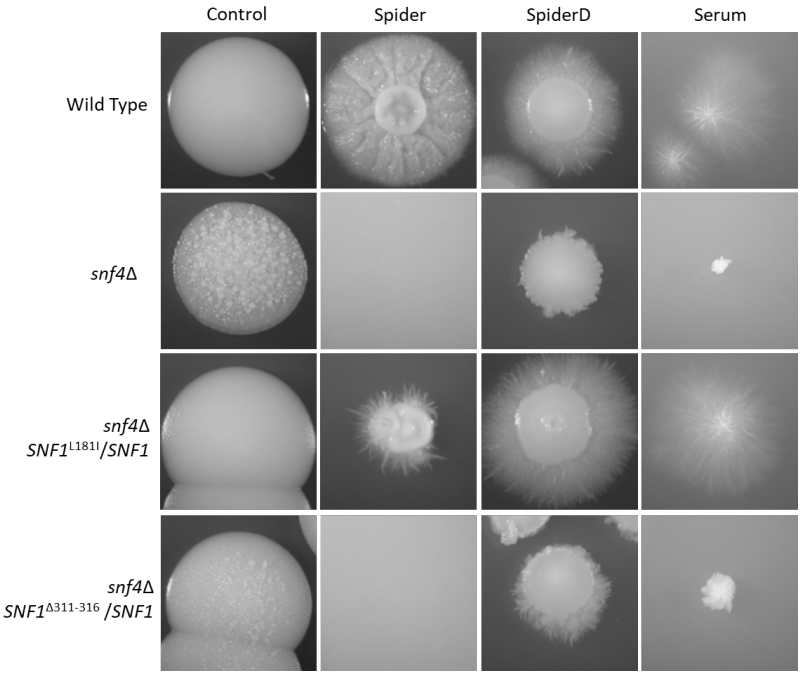

Figure 2.12: Influence of mutations in *SNF1* on colony morphology of *snf4*Δ mutants on different hyphae inducing media. The wild type, *snf4*Δ mutants, and derived strains in which one allele of *SNF1* was replaced with $SNF1^{\mathrm{L181I}}$ or $SNF1^{\Delta 311\text{-}316}$ were grown overnight in YPD before being diluted and plated on the shown media. Plates were incubated for seven days at 30°C (Control) or 37°C (all others). Images are representative of two independently constructed mutants of each genotype.

The effect of the $SNF1^{\Delta 311\text{-}316}$ mutation in comparison with that of the $SNF1^{\mathrm{L181I}}$ mutation on *snf4*Δ phenotypes was also investigated in relation to filamentous growth. Previous work has shown that *snf4*Δ mutants exhibit diminished filamentous growth in conditions which typically activate this morphological change (Ramírez-Zavala *et al.* 2017; Mottola 2016). While the phenotypes of *snf4*Δ mutants expressing one copy of the two mutations were essentially identical in growth on alternative carbon sources, a striking difference was observable in Figure 2.12. The $SNF1^{\Delta 311\text{-}316}$ mutation modestly restored filamentous growth in SpiderD medium, in which the carbon source is glucose. Additionally, it partially reverted the rough colony morphology of the strain when grown in control conditions which do not induce filamentous growth. However, the $SNF1^{\mathrm{L181I}}$ mutation had a much stronger effect. It fully restored filamentous growth on SpiderD and serum agar, and additionally allowed cells to grow on Spider medium, which contains mannitol as a carbon source, and filament to a limited degree. These observations suggest that these two mutations have overlapping, but distinct effects on activity of SNF1.

Gene dosage is known to affect phenotype (reviewed in Liang and Bennett

2019); a number of genes in *C. albicans* have been found to be haploinsufficient for example, while expression of two copies of mutant alleles which confer drug resistance rather than one can result in even higher resistance. Therefore, it was investigated whether replacing not only one, but both copies of *SNF1* with either $SNF1^{\mathrm{L181I}}$ or $SNF1^{\Delta 311\text{-}316}$ would have a greater impact on carbon source utilization and/or resistance to cell wall stress. As previously observed, one copy of either of the suppressor mutations was sufficient to fully restore growth on glucose or sucrose (Figure 2.13A) and partially

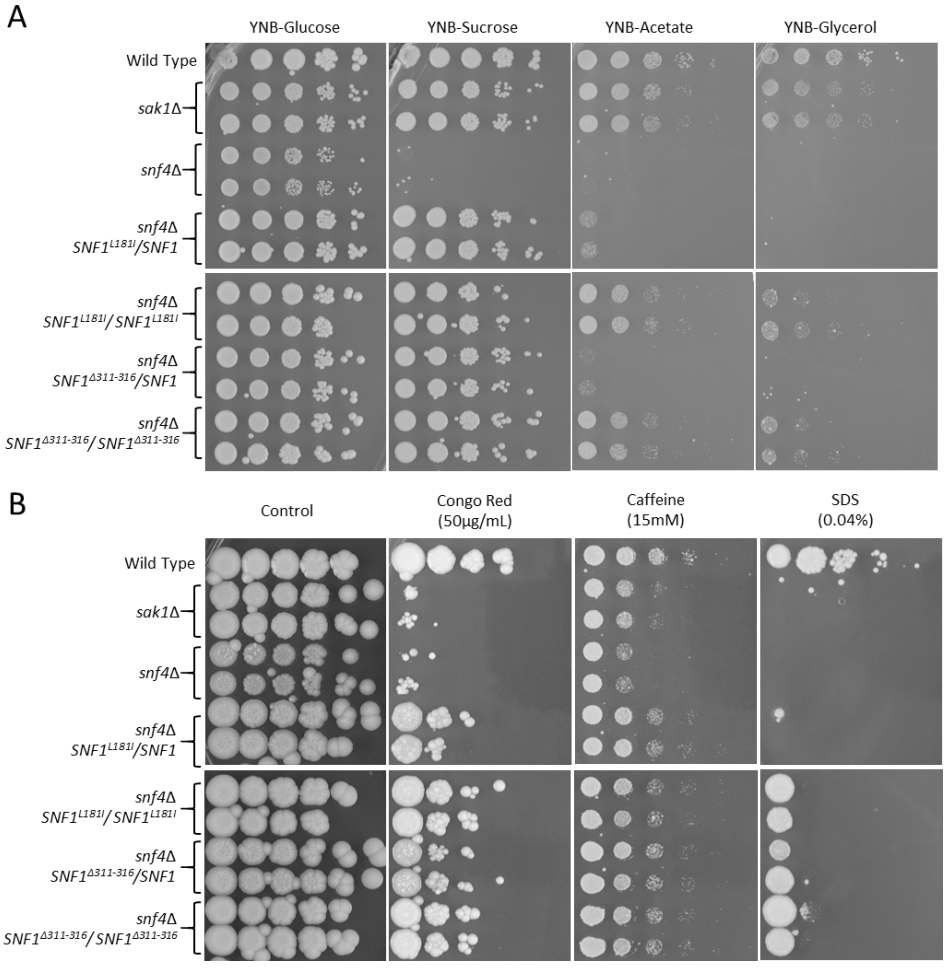

Figure 2.13: Influence of homozygous mutations in *SNF1* on growth of *snf4*Δ mutants in different carbon sources (A) or cell wall stresses (B). The wild type, *snf4*Δ mutants, and derived strains in which one or both alleles of *SNF1* was replaced with $SNF1^{\mathrm{L181I}}$ or $SNF1^{\Delta 311\text{-}316}$ were grown overnight in YPD before being diluted to an OD 600 of 2.0, serially diluted, and spotted on the shown media. Plates were incubated for four days at 30°C. Strains plated on a single medium were plated on a single plate, with pictures rearranged for clarity in presentation. For each mutant, two independently constructed strains are shown.

restore growth on acetate. Replacement of the second allele did not increase growth further in glucose or sucrose, but led to a much stronger growth in acetate and allowed a small amount of growth on glycerol. Interestingly, the phenotypes of the homozygous suppressor mutants in the *snf4*Δ background strongly resembled the phenotype of the *sak1*Δ mutant, which has milder growth defects than the *snf4*Δ mutant. In contrast, replacement of the second allele of *SNF1* with either suppressor had little to no effect on resistance to cell wall stress (Figure 2.13B). In these conditions, the homozygous mutants exhibited the same resistance as heterozygous mutants, which somewhat resemble the phenotype of the *sak1*Δ mutant, with notable differences in Congo red and SDS. However, there was an observable effect of the homozygous mutations in terms of color and morphology of colonies, which more closely resembled the wild type than the heterozygous mutants.

2.2.3 Effects of *SNF1*$^{\Delta 311\text{-}316}$ on expression of target genes

Transcript profiling of a mutant lacking the Snf1 activating kinase *SAK1* revealed a number of genes that are differentially expressed in this strain compared to the wild type in rich media, including numerous genes related to utilization of alternative carbon sources (Ramírez-Zavala *et al.* 2017). Sak1 presumably mediates their expression via activity of the SNF1 pathway. Northern blotting of two of these genes (*HGT10* and *ICL1*), plus an additional gene which did not appear in the profiling results but is likely essential for sucrose utilization (*MAL2*), probed at whether expression of these genes is indeed dependent on SNF1 activity, and whether suppressor mutations restore proper expression (Figure 2.14). Somewhat unexpectedly, *HGT10* and *ICL1* were expressed at similar levels whether cells were grown in glucose or an alternative carbon source, which would be expected to activate SNF1. *MAL2* expression, in contrast, was specifically induced in response to growth on sucrose, but not other carbon sources.

Disruption of the SNF1 pathway via *snf4* deletion significantly reduced expression of all three genes, though expression of *HGT10* and *ICL1* was not completely abolished in all carbon sources. Homozygous replacement of *SNF1* with either the *SNF1*$^{\text{L181I}}$ or *SNF1*$^{\Delta 311\text{-}316}$ suppressor alleles was able to strongly, if not completely, restore expression of *HGT10* in all tested carbon sources. *ICL1* expression was restored by these mutations in cells grown in glucose and acetate, and to a lesser degree in glycerol. Only *SNF1*$^{\Delta 311\text{-}316}$

however rescued expression of *ICL1* in sucrose. Sucrose-dependent expression of *MAL2* was partially restored by *SNF1*$^{\Delta 311\text{-}316}$, but *SNF1*^{L181I} was apparently insufficient for this. These results provide evidence beyond the resolution of growth phenotypes that there are notable differences in the effect these suppressor mutations have on SNF1 activity.

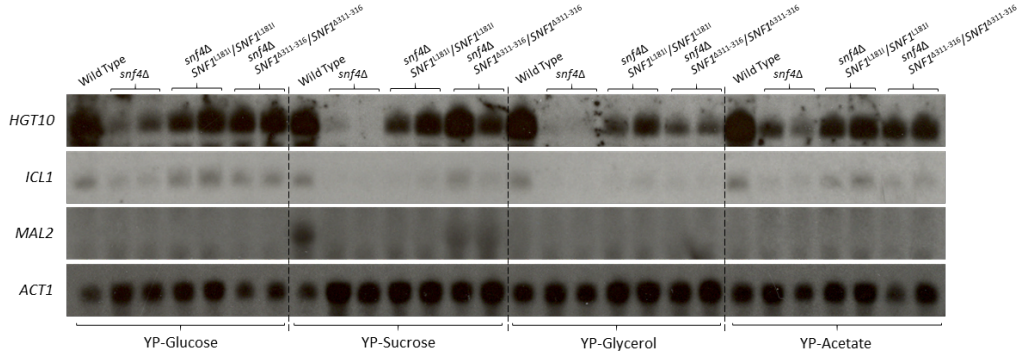

Figure 2.14: Snf4-dependent expression of carbon source utilization genes is partially restored in *snf4*-independent *SNF1* mutants. Overnight cultures of the wild type, *snf4*Δ mutants, and derived strains in which both alleles of *SNF1* was replaced with *SNF1*^{L181I} or *SNF1*$^{\Delta 311\text{-}316}$ were diluted in YP-Glucose and grown for 3 hours at 30°C before being washed in water and resuspended in the labeled medium and incubated for a further hour before RNA was harvested and northern blotting performed. Probes binding to the coding sequence of *HGT10*, *ICL1*, *MAL2*, and *ACT1* as a loading control were successively hybridized to detect expression of these transcripts. For each mutant, two independently constructed strains are shown.

2.2.4 Snf1$^{\Delta 311\text{-}316}$ is not hyperphosphorylated at Thr-208

Because *SNF1*$^{\Delta 311\text{-}316}$ was identified as a suppressor of a *snf4*Δ mutant, the parsimonious mechanistic explanation for its effect is that it alters the three-dimensional structure of Snf1 such that it is no longer autoinhibited in the absence of Snf4. An alternative explanation, however, relates to phosphorylation of Snf1 at the activating Thr-208 residue. Replacement of this threonine with a nonphosphorylatable alanine results in severe growth defects even in rich, stress-free medium, and deletion of the kinase responsible for this phosphorylation, Sak1, also results in growth defects in alternative carbon sources and cell wall stress (Ramírez-Zavala *et al.* 2017; Mottola 2016). The *snf4*Δ mutant exhibits reduced Snf1-T208 phosphorylation as well (Ramírez-Zavala *et al.* 2017). To investigate the possibility that *SNF1*^{L181I} or *SNF1*$^{\Delta 311\text{-}316}$ suppresses *snf4*Δ phenotypes by restoring normal phosphorylation of Snf1-T208, western blots were performed using an antibody which is specific to the phosphorylated form of Snf1 (Figure 2.15). As has been previously observed,

the *sak1*Δ mutant exhibited no Snf1-T208 phosphorylation, and the *snf4*Δ mutant exhibited reduced phosphorylation in all tested carbon sources. Neither mutations of *SNF1* resulted in increased Snf1-T208 phosphorylation, indicating that their mechanism of action is unrelated to Snf1 phosphorylation.

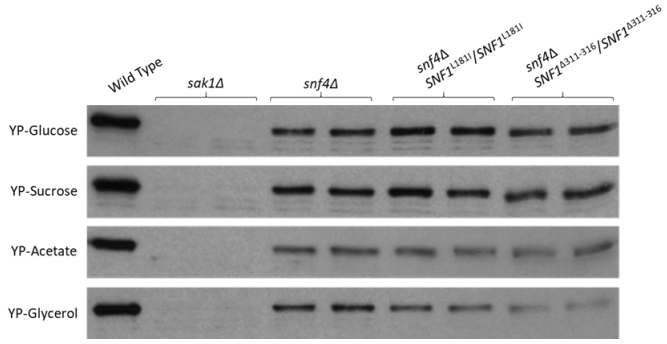

Figure 2.15: *SNF4*-independent *SNF1* mutants do not affect phosphorylation of Snf1 at Thr-208. Overnight cultures of the wild type, *snf4*Δ mutants, and derived strains in which both alleles of *SNF1* was replaced with $SNF1^{L181I}$ or $SNF1^{\Delta 311\text{-}316}$ were diluted in YP-glucose and grown for one hour at 30°C before being washed and grown for an additional two hours at 30°C in the labeled medium before cell extracts were prepared. Equal amounts of protein were separated and probed with an antibody against phosphorylated Snf1-T208. For each mutant, two independently constructed strains are shown.

2.2.5 $\text{Snf1}^{\Delta 311\text{-}316}$ does not suppress *kis1*Δ phenotypes

As mentioned in section 1.2.2, ScSNF1 is nonfunctional in the absence of a β-subunit. In the course of this work, attempts to create a double deletion of both *KIS1* and *KIS2* were unsuccessful, suggesting that the same is true in *C. albicans*. The inability of C-terminally truncated Snf1 to revert growth defects of an *snf4*Δ mutant seen in Figure 2.11 may be because, while the autoinhibitory domain is removed, so is the interaction site for the β-subunits. The $SNF1^{\Delta 311\text{-}316}$ mutation has above been shown to allow Snf1 activity independent of regulation by Snf4; it was also investigated whether this mutant allele additionally confers independence from the β-subunits.

Previous work has revealed that deletion of either *KIS1* or *KIS2* result in disparate phenotypes suggesting that they direct SNF1 toward distinct functional outcomes, much as the β-subunits of *S. cerevisiae* (Ramírez-Zavala *et al.* 2017). Deletion of *KIS1* resulted in moderate defects in utilization of alternative carbon sources and cell wall integrity (Figure 2.16), whereas *kis2*Δ mutants exhibit filamentation defects (Ramírez-Zavala, unpublished data). Replacement of one or both *SNF1* alleles with the Δ311-316 mutant had only very minor effects on the phenotype of *kis1*Δ mutants, in which

replacement of one allele was sufficient to very slightly improve growth on acetate and glycerol, with no effect on other tested carbon sources nor in the presence of cell wall stresses. These results suggest that the *SNF1*$^{\Delta 311\text{-}316}$ mutation does not render Snf1 independent of β-subunit regulation.

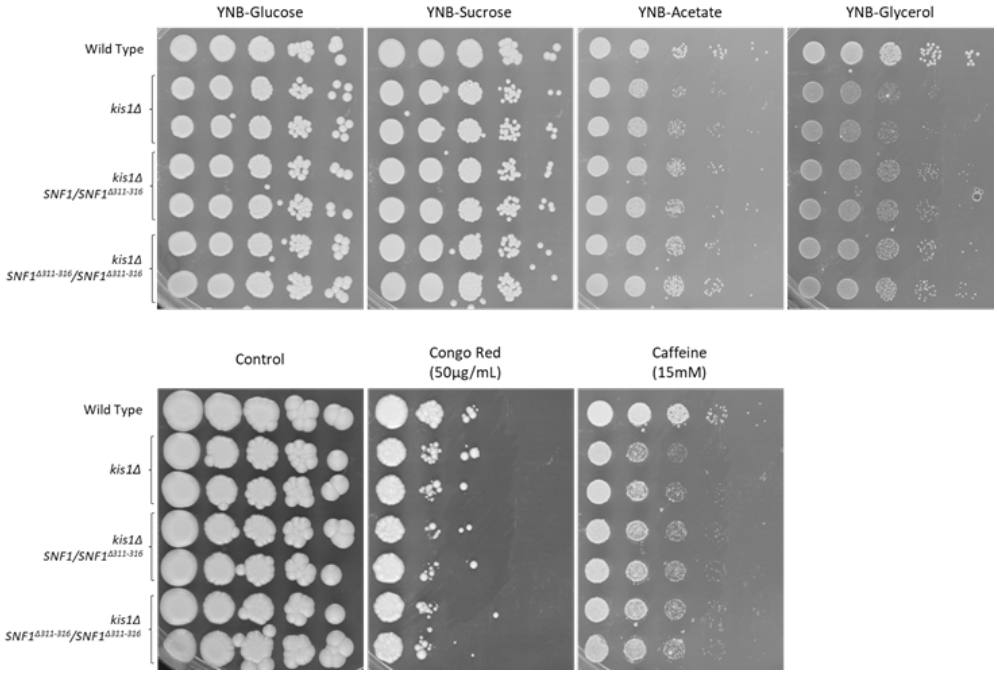

Figure 2.16: Influence of heterozygous and homozygous *SNF1*$^{\Delta 311\text{-}316}$ mutation on growth of *kis1*Δ mutants in different carbon sources or cell wall stresses. The wild type, *kis1*Δ mutants, and derived strains in which one or both alleles of *SNF1* was replaced with *SNF1*$^{\Delta 311\text{-}316}$ were grown overnight in YPD before being diluted to an OD 600 of 2.0, serially diluted, and spotted on the shown media. Plates were incubated for four days at 30°C. For each mutant, two independently constructed strains are shown.

2.2.6 Snf1$^{\Delta 311\text{-}316}$ is not hyperactive

An interesting possibility regarding the *SNF1*$^{\Delta 311\text{-}316}$ mutation is that, on one hand, it may simply reduce dependence of Snf1 on Snf4 regulation, but on the other hand, it may in fact confer hyperactivity of Snf1 which is partly able to compensate for *snf4*Δ defects. To test this, the mutant allele was introduced into the wild type background to examine whether it would grow better than the wild type on different carbon sources or cell wall stresses. As seen in Figure 2.17A, there was no observable effect of the mutation on growth on different carbon sources. Nor was there an increased resistance to cell wall stresses (Figure 2.17B). Interestingly, there was a slightly increased susceptibility of the homozygous mutant to Congo red. A further possibility is that the mutant allele may have equal capability as the wild

type to utilize different carbon sources, it may be able to adapt to use them more quickly, resulting in a higher fitness in an often changing environment. To examine this, growth curves were produced (Figure 2.17C). All tested strains grew equally, and adapted to growth on sucrose at the same speed. The *SNF1*$^{\Delta 311\text{-}316}$ allele is apparently not hyperactive, and functions as well as wild type *SNF1*.

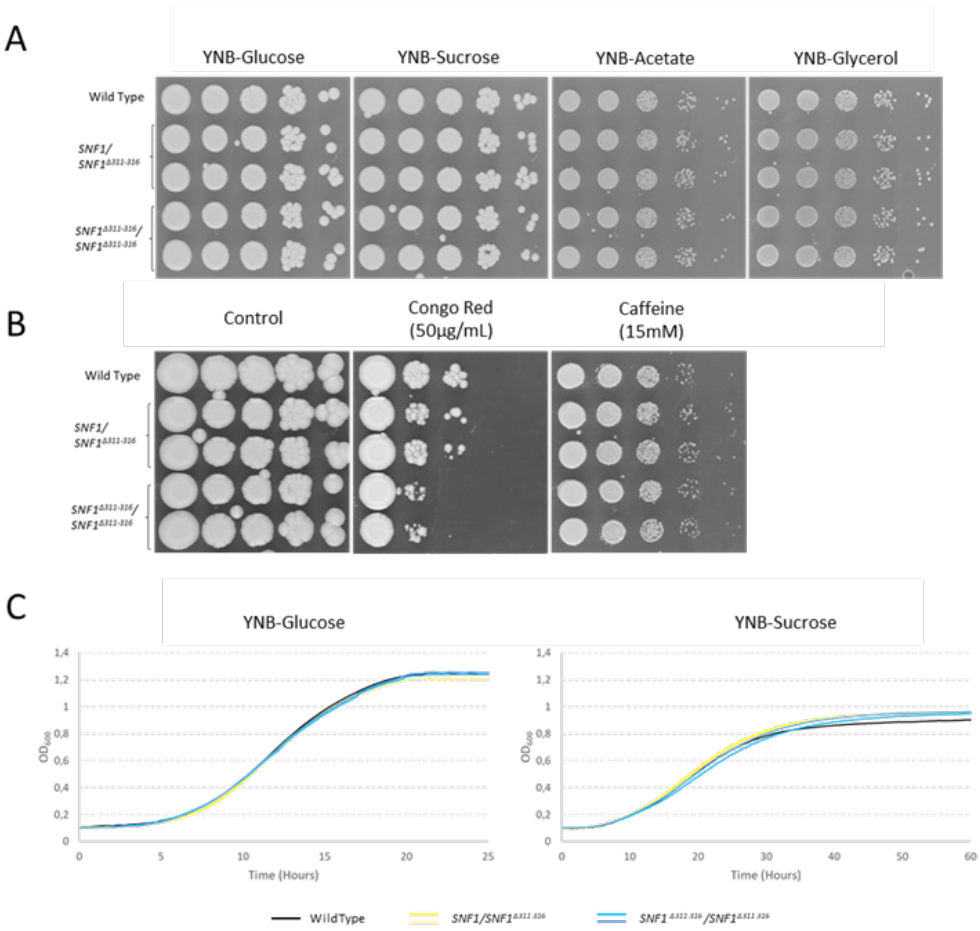

Figure 2.17: Snf1$^{\Delta 311\text{-}316}$ is not a hyperactive mutant. Growth of the wild type as well as strains in which one or both *SNF1* alleles were replaced with *SNF1*$^{\Delta 311\text{-}316}$ on carbon sources (A) or cell wall stress (B) as well as growth curves in liquid media containing different carbon sources (C) were examined. For spot assays, strains were grown overnight in YPD before being diluted to an OD 600 of 2.0, serially diluted, and spotted on the shown media. Plates were incubated for four days at 30°C. For growth curves, strains were grown in triplicate overnight in YNB-Glucose, washed in water, and diluted to an OD_{600} of 0.1 in either YNB-Glucose or -Sucrose in a 96-well plate and incubated at 30°C. OD_{600} values were measured every 10 minutes in a Tecan Infinite F200 PRO plate reader, with curves representing the average of the three replicates. For each mutant, two independently constructed strains are shown, represented by different shades of the same color.

2.3 Searching for SNF1 targets in a fungal-specific transcription factor family

Many of the targets of ScSNF1, as mentioned in section 1.2.2, are transcription factors. Previous work has shown that deletion of the Snf1 activating kinase *SAK1* results in altered expression of a number of genes which are involved in the utilization of alternative carbon sources, suggesting that SNF1 activity influences transcription in *C. albicans* (Ramírez-Zavala *et al.* 2017). When this work began, Mig1 and Mig2 had not yet been confirmed to be components of the *C. albicans* SNF1 pathway, and as mentioned previously, evidence suggested they may not have been targets of SNF1. In order to identify novel transcription factor targets of SNF1, a previously constructed library of artificially activated zinc cluster transcription factors (ZCFs) was utilized. Zinc cluster transcription factors are the largest class of transcription factor in *C. albicans*; 82 known and putative transcription factors include a conserved ZCF DNA-binding domain. C-terminal fusion of the ScGal4 activation domain (GAD) with many of these ZCFs (ZCF-GAD) has been shown to result in hyperactivity or otherwise artificial activation in the absence of inducing signals, and a library in which all 82 ZCFs are fused with the GAD and expressed under control of the constitutively active *ADH1* promoter has been constructed (Schillig and Morschhäuser 2013). In the case that one of these transcription factors is a downstream target of SNF1 whose activity is normally regulated by the kinase, and whose loss of function in mutants of the SNF1 pathway is the cause for defects in carbon source utilization, cell wall integrity, or filamentation, artificial activation may suppress the mutant phenotype.

2.3.1 Artificial activation of Czf1 rescues *snf4*Δ cell wall defects

To search for SNF1 targets among the set of ZCFs, all 82 artificially activated ZCFs were introduced to the *snf4*Δ mutant and screened for growth on YNB-Sucrose, Congo red, or filamentation on Spider medium (described in detail in section 4.9). Through this screen, artificial activation of Czf1 was shown to restore growth of the *snf4*Δ mutant on Congo red (Figure 2.18), and in fact strains expressing this form of Czf1 were able to grow even better than the wild type in caffeine.

This was surprising, because the Czf1's characterized roles are in morphogenesis, where it has been shown to regulate white-opaque switching and filamentous growth in certain conditions (Vinces and Kumamoto 2007; Brown

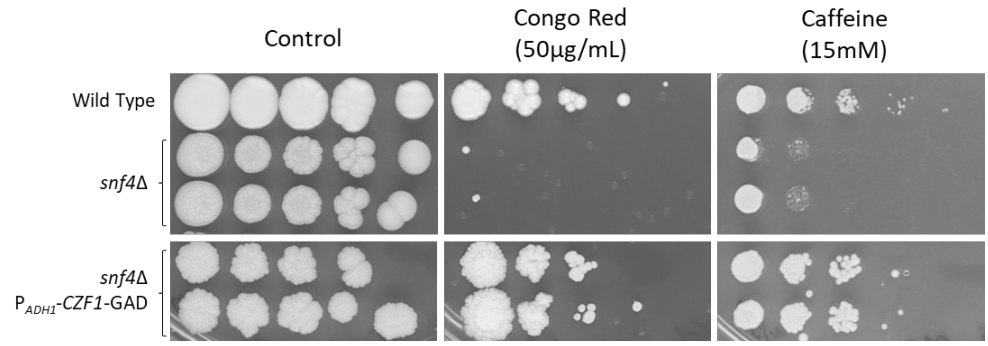

Figure 2.18: Artificial activation of Czf1 rescues cell wall defects of SNF1 pathway mutants. The wild type, *snf4*Δ and deletion mutants expressing the artificially activated Czf1 were grown overnight in YPD before being diluted to an OD 600 of 2.0, serially diluted, and spotted on the shown media. Plates were incubated for four days at 30°C. Per medium, strains were spotted on the same plates, with pictures rearranged for clarity in presentation. For each mutant, two independently constructed strains are shown.

et al. 1999). The effect of artificial activation of Czf1 on other *snf4*Δ phenotypes was also investigated to see if these too were affected. Artificial activation of Czf1 had a slight positive impact on the ability of the *snf4*Δ mutant to grow on carbon sources, most notably on glucose, but also on sucrose and acetate, but these effects were vanishingly small (Figure 2.19A). Nor did it have any observable effect on the ability of the mutant to respond to filamentation inducing conditions (Figure 2.19B). A notable observation, however, was that despite the inability to restore filamentation on media which typically do induce it, artificial activation of Czf1 resulted in a hyperfilamentous phenotype in non-inducing media (most visible in Figure 2.19B, but also visible in Figure 2.18).

This suggested the possibility of a connection between hyperfilamentous growth and resistance to cell wall stress. To examine whether filamentation was responsible for the effect of the artificially activated Czf1 on cell wall integrity, or whether these effects were unrelated, a *UME6*-GAD fusion was also introduced to the *snf4*Δ mutant to see if it too could improve cell wall integrity. *UME6* encodes a major activator of filamentous growth, and artificial activation leads to constitutive filamentation (Banerjee *et al.* 2008; Schillig and Morschhäuser 2013). As a ZCF, it was one of the genes that was screened as mentioned above, but did not appear as a candidate suppressor. It was possible though that the pooling method used to screen the library could have allowed for false negative results. As seen in Figure 2.20, artificial activation of Ume6 had no effect on cell wall integrity of the *snf4*Δ mutant, suggesting that these two effects of Czf1 activation are not related.

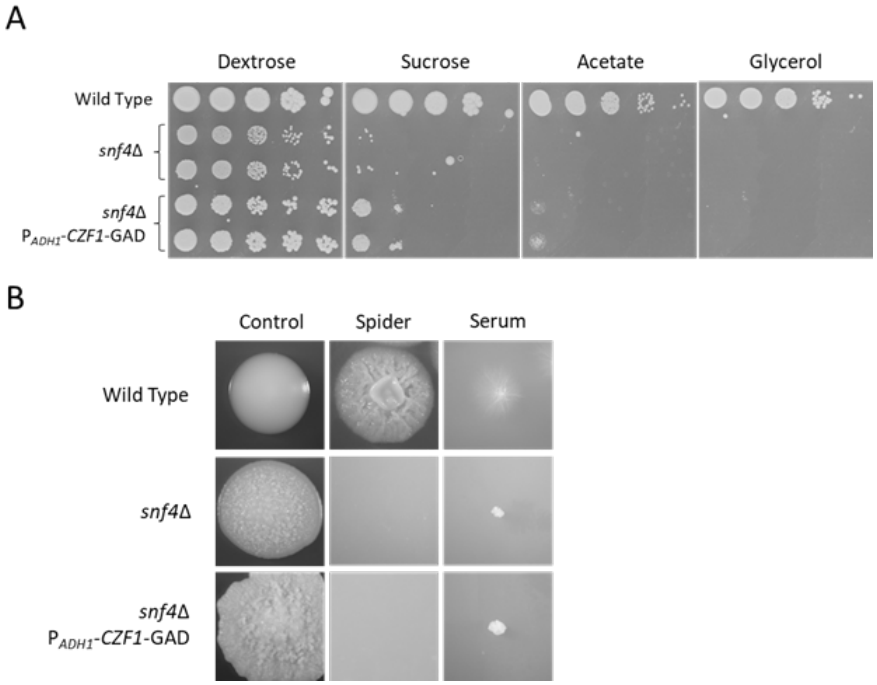

Figure 2.19: Artificial activation of Czf1 does not revert carbon utilization or filamentation defects of the *snf4*Δ mutant. (A) The wild type, *snf4*Δ and deletion mutants expressing artificially activated Czf1 were grown overnight in YPD before being diluted to an OD 600 of 2.0, serially diluted, and spotted on the shown media. Plates were incubated for four days at 30°C. (B)The same strains were grown overnight in YPD before being diluted and plated on the shown media. Plates were incubated for seven days at 30°C (Control) or 37°C (all others). Colony images are representative of two independently constructed mutants of each genotype.

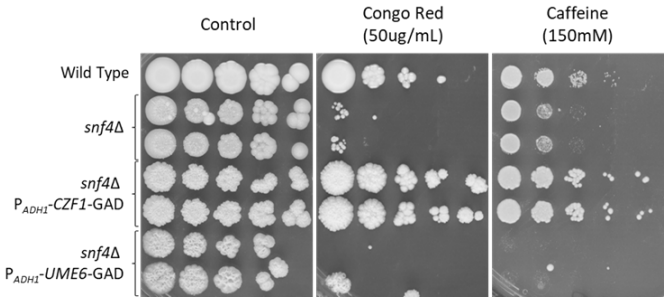

Figure 2.20: Artificial activation of Ume6 does not rescue cell wall defects of the *snf4*Δ mutant. The wild type, the *snf4*Δ mutants, and the deletion mutants expressing the artificially activated Czf1 or Ume6 were grown overnight in YPD before being diluted to an OD 600 of 2.0, serially diluted, and spotted on the shown media. Plates were incubated for four days at 30°C. For each mutant, two independently constructed strains are shown.

2.3.2 Activation of Czf1 is required to rescue *snf4*Δ cell wall integrity

The artificially activated form of *CZF1* used in this investigation is expressed under the control of the constitutively active *ADH1* promoter, which is highly active. A possible reason that the construct improved growth in cell wall stresses was not in fact that Czf1 was artificially activated, but rather simply that it was overexpressed. To confront this possibility, wild type *CZF1* was placed under the control of the *ADH1* promoter. Northern blot analysis of the *CZF1* transcript (Figure 2.21C) showed the expected long and short isoforms in the wild type, where the long isoform was dominant (Vinces *et al.* 2006). All detected bands corresponded with *CZF1* transcript, as all signal was abolished in the *czf1*Δ mutant. In the *snf4*Δ background, overexpression of wild type *CZF1* resulted in a significant increase in the short isoform of *CZF1*, which lacks a long 3' UTR and matches the form expressed at the *ADH1* promoter. Expression of the artificially activated *CZF1* resulted in the appearance of a slightly larger transcript which is likely the overexpressed *CZF1*-GAD, which is expressed at a similar level as the overexpressed wild type. Interestingly, An additional band appeared as well at a similar intensity but at a size larger than 4000nt, of which the identity is uncertain. An additional oddity is the apparent reversal in the dominant form of the endogenously expressed *CZF1*; here, the small isoform was dominant compared to the large isoform.

Overexpression of wild type *CZF1* had only minor effects on cell wall integrity in the *snf4*Δ mutant (Figure 2.21A), including very slight improvements in growth on Congo red, calcofluor white, and caffeine, while no effect was observed on SDS. This supported the idea that the activation of Czf1 was responsible for cell wall stress resistance. Because the relationship between *CZF1* and cell wall integrity is largely unexplored, phenotypes of *CZF1* deletion, overexpression, and artificial activation were also explored in a wild type background (Figure 2.21B). In these assays, deletion of *CZF1* had only a small impact on cell wall stress resistance; a slight hypersensitivity to caffeine was observed, as well as a very minor increase in resistance, unexpected, to Congo red. Thus it seemed unlikely that the cell wall defects associated with the *snf4*Δ mutant were due (solely) to lack Czf1 activity. The most notable effect of overexpression of wild type *CZF1* was a hyperresistance to SDS, but a similarly small increase in resistance to Congo red was also observed. Interestingly, this mutant was apparently not hyperfilamentous (as seen on the control plate), in contrast with the artificially activated Czf1. Artificial activation resulted increased resistance to caffeine and Congo red, but also in hypersusceptibility to SDS.

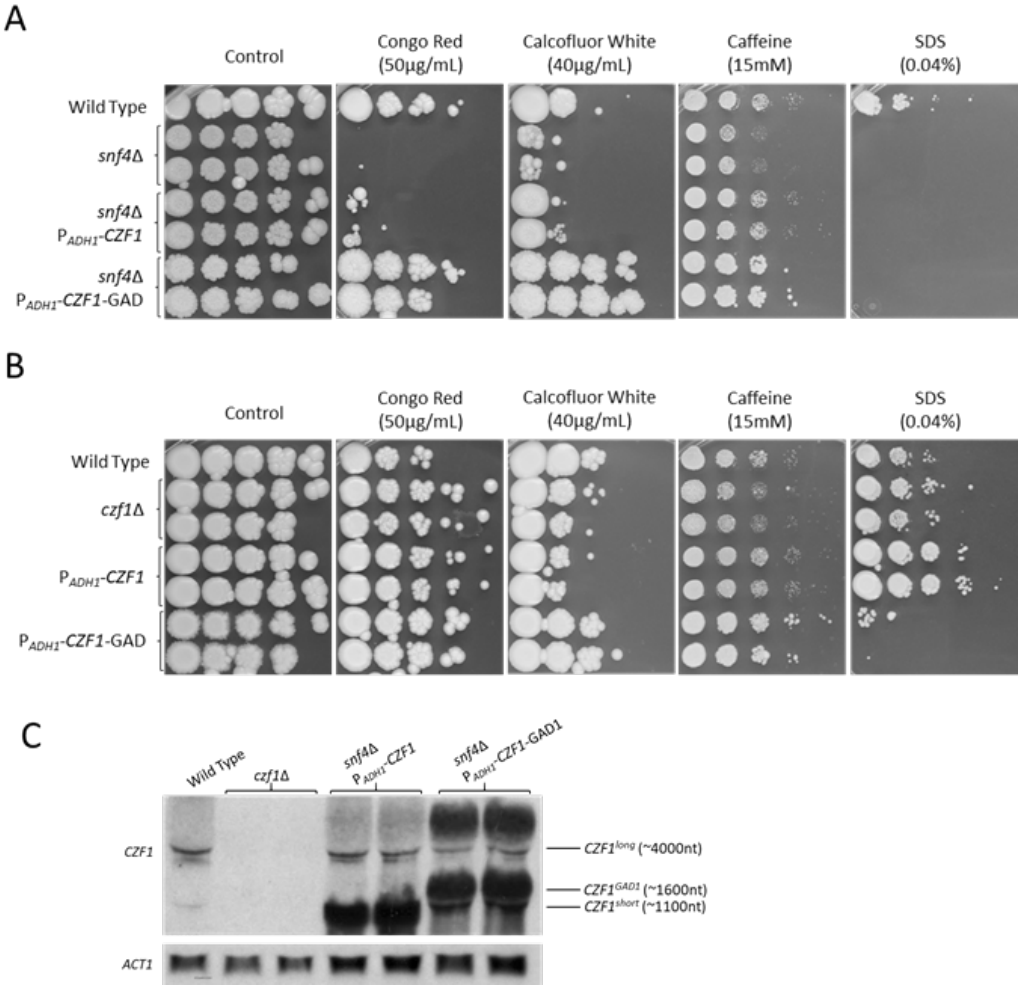

Figure 2.21: Activation of Czf1 is required to increase resistance to cell wall stresses. The wild type as well as derived strains expressing *CZF1* or *CZF1*-GAD under control of the *ADH1* promoter in the *snf4*Δ (A) or wild type (B) background were grown overnight in YPD before being diluted to an OD 600 of 2.0, serially diluted, and spotted on the shown media. Plates were incubated for four days at 30°C. (C) Overnight cultures of the wild type, *czf1*Δ mutants, and *snf4*Δ derived mutants expressing either *CZF1* or *CZF1*-GAD were diluted in YPD and grown for 3 hours at 30°C before RNA was harvested and northern blotting performed. Probes binding to the coding sequence of *CZF1* and *ACT1* as a loading control were successively hybridized to detect expression of these transcripts. For each mutant, two independently constructed strains are shown.

2.3.3 Investigating Czf1 phosphorylation

If Czf1 is a target of SNF1, it would be expected to exhibit phosphorylation which is dependent on SNF1 activity (see the examples of Mig1 and Mig2 in section 2.1). This phosphorylation may also be dependent on the presence of cell wall stress, the condition in which artificial activation of Czf1 was able to suppress *snf4*Δ defects. To examine this, Czf1 was tagged with the HA

epitope in the wild type and *snf4*Δ backgrounds and grown in the absence or presence of cell wall stress, followed by western blotting (Figure 2.22A). No change in electrophoretic mobility suggestive of a posttranslational modification such as phosphorylation could be detected which depended on either SNF1 activity, cell wall stress, or both. A slight reduction of Czf1 protein levels were however observed in the *snf4*Δ mutant after exposure to Congo red. To determine if Czf1 is phosphorylated at all, cell extracts from the wild type grown in the absence of cell wall stress were treated with phosphatase and probed for the tagged Czf1 (Figure 2.22B). After phosphatase treatment, Czf1 exhibited a faster mobility, indicating that in fact Czf1 is phosphorylated, though SNF1 is either not responsible or not solely responsible for this.

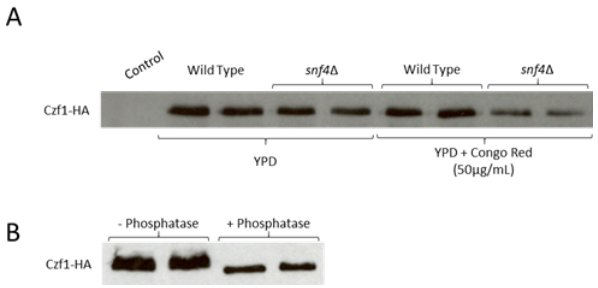

Figure 2.22: Czf1 is phosphorylated, but it does not depend on cell wall stress or SNF1 activity. (A) Overnight cultures of the wild type as well as wild type and *snf4*Δ mutants expressing 3xHA-tagged Czf1 were diluted in YPD and grown for one hour at 30°C, then grown for an additional two hours at 30°C in the absence or presence of Congo red (50µg/mL) before cell extracts were prepared. (B) Cell extracts from the wild type expressing Czf1-HA were washed using centrifugal filters and treated with λ-phosphatase. Equal amounts of protein were separated and probed with an antibody against the HA tag. For each mutant, two independently constructed strains are shown.

2.3.4 Artificial activation of Czf1 rescues cell wall defects of other kinase mutants

The above described results indicate that artificial activation of Czf1 has a positive effect on cell wall integrity, and that Czf1 is normally phosphorylated, but deletion of *SNF4* is insufficient to result in an observable loss of phosphorylation. Therefore Czf1 may not in fact be a target of SNF1, but its effect on cell wall integrity is able to overcome the unspecified defects related to the cell wall of an *snf4*Δ mutant. To determine if this effect is specific or also applies to other mutants which exhibit cell wall defects, the artificially activated form of Czf1 was introduced into several protein kinase deletion mutants with cell wall defects (Ramírez-Zavala *et al.* 2017 and unpublished results). In about half (five of eleven) of the tested kinase mutants, artificial

activation of Czf1 at least partially restored cell wall integrity in all tested cell wall stresses (Figure 2.23). In the *cla4*Δ mutant, growth on Congo red and calcofluor white was largely restored, and growth on caffeine was slightly improved. In the *mck1*Δ mutant, growth on Congo red was slightly improved, while growth on calcofluor white exceeded even that of the wild type, as did growth on caffeine to a lesser degree. Artificial activation of Czf1 in the *nik1*Δ mutant resulted in resistance beyond that even of the wild type to Congo red, calcofluor white, and caffeine. In the *pan3*Δ mutant, growth was restored to wild type levels in Congo red, whereas it exceeded the wild type in calcofluor white and caffeine. Finally, resistance to Congo red in the *sak1*Δ mutant was fully restored, and resistance to calcofluor white and caffeine was increased beyond the wild type. In all of these mutants, growth defects on SDS, which disrupts the cell membrane instead of the cell wall, were not restored; much like what was observed in the *snf4*Δ mutant and wild type backgrounds, growth was abolished.

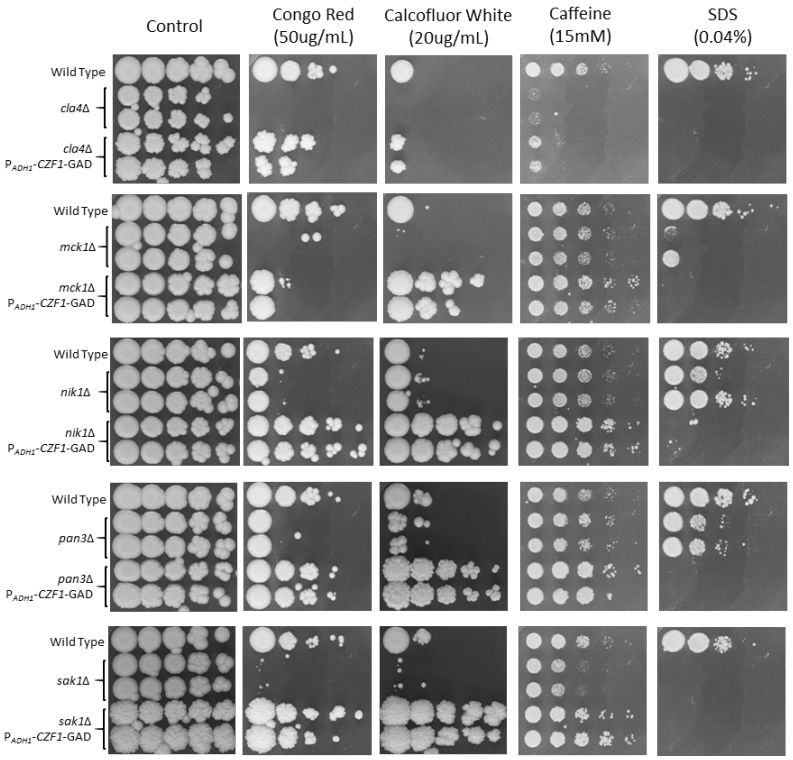

Figure 2.23: Artificial activation of Czf1 strongly improves cell wall integrity of some kinase mutants. The indicated kinase deletion mutants and derived strains expressing *CZF1*-GAD were grown overnight in YPD before being diluted to an OD 600 of 2.0, serially diluted, and spotted on the shown media. Plates were incubated for four days at 30°C. For each mutant, two independently constructed strains are shown.

In four further kinase mutants, certain cell wall defects were reverted or partially improved by artificial activation of Czf1 (Figure 2.24A). Growth on calcofluor white was restored to wild type levels in the *mkc1* and *mkk2* deletion mutants, but resistance to Congo red was unaffected and resistance to caffeine was slightly improved. In the *kin2*Δ mutant only resistance to caffeine improved, while Congo red susceptibility in the *ssn3*Δ mutant returned to wild type levels and calcofluor white resistance exceeded that of the wild type, but caffeine resistance was unaffected. Surprisingly, while in all other tested backgrounds artificial activation of Czf1 resulted in hypersusceptibility to SDS, there were two notable exceptions in this set of mutants. In the *kin2*Δ mutant, growth on SDS was restored to wild type levels, while in the *ssn3*Δ mutant, the growth defect was not exacerbated.

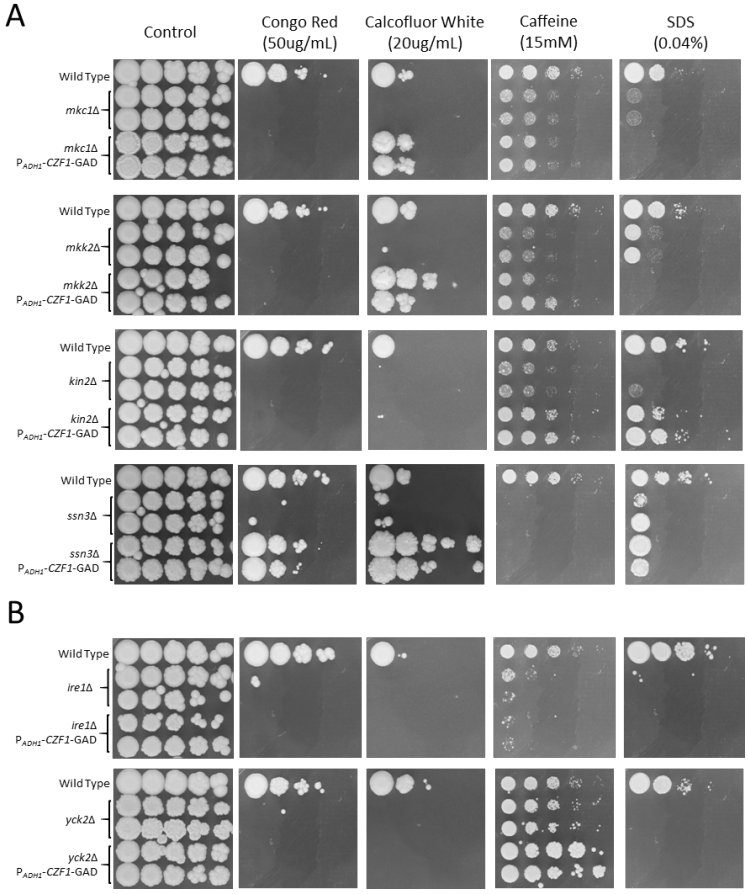

Figure 2.24: Artificial activation of Czf1 (A) partially improves or (B) does not improve cell wall integrity of some kinase mutants. The indicated kinase deletion mutants and derived strains expressing *CZF1*-GAD were grown overnight in YPD before being diluted to an OD 600 of 2.0, serially diluted, and spotted on the shown media. Plates were incubated for four days at 30°C. For each mutant, two independently constructed strains are shown.

Artificial activation of Czf1 was insufficient to suppress the cell wall defects of two final tested kinase mutants (Figure 2.24B). The *ire1*Δ mutant remained hypersusceptible to Congo red, calcofluor white, and caffeine. The susceptibility of the *yck2*Δ mutant to Congo red and calcofluor white was unaffected, but artificial activation of Czf1 led to hyperresistance to caffeine, where the mutant showed no growth defect. Resistance to SDS was unaffected in either background.

In order to examine whether any of these tested kinases was responsible for the observed phosphorylation of Czf1, western blots were performed against HA-tagged Czf1 which was introduced into the kinase mutants (Figure 2.25). In no case was deletion of one of the tested kinases sufficient to cause a shift in mobility indicative of loss of phosphorylation. This, however, cannot discount the possibility that multiple kinases (either from the tested set or not) act upon Czf1 in a redundant manner. Interestingly, Czf1 protein levels were reduced in a large number of the tested mutants. Czf1 protein was reduced in the *cla4*, *ire1*, *kin2*, *mkc1*, *mkk2*, and *ssn3* deletion mutants. No Czf1 protein was detectable at all in the *yck2*Δ mutant. No change was observed in the *mck1*, *nik1*, or *pan3* deletion mutants.

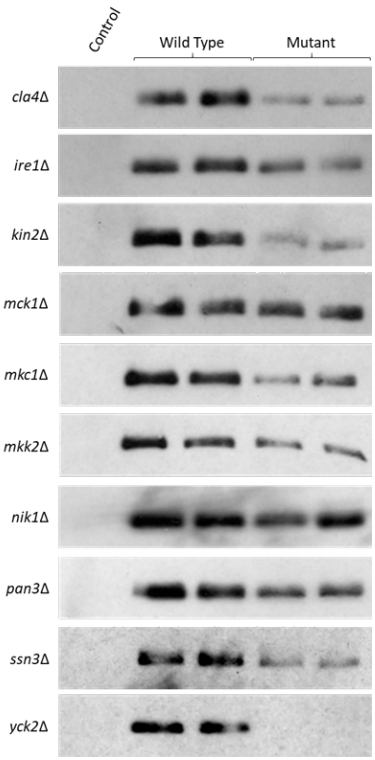

Figure 2.25: Kinase mutants affect Czf1 protein levels, but not phosphorylation state. Overnight cultures of the wild type as well as wild type and labeled kinase mutants expressing 3xHA-tagged Czf1 were diluted in YPD and grown for three hours at 30°C before cell extracts were prepared. Equal amounts of protein were separated and probed with an antibody against the HA tag. For each mutant, two independently constructed strains are shown.

2.3.5 Artificial activation of Czf1 causes changes in the structure of the cell wall

The effects of artificial activation of Czf1 on cell wall integrity across numerous different mutants was striking, because as mentioned above there is little evidence from other works to suggest that Czf1 is a regulator of cell wall integrity. In order to better understand the underlying cause for the observed phenotypes of the artificial activation of this transcription factor, RNA sequencing was performed, comparing gene expression in strains expressing *CZF1*-GAD in the wild type background to the wild type. A list of all genes which were significantly differentially expressed ($p<0.01$) compared to the wild type can be found in supplemental table 4.7. Artificial activation of Czf1 primarily resulted in gene activation; the expression of 211 genes is increased by at least fourfold. In comparison, only 19 genes exhibited expression which was reduced by at least the same threshold. The expression of a further 725 genes was affected in a statistically significant manner, but did not meet the selected threshold for genes of interest in terms of fold-change. Analysis of significantly enriched gene ontology (GO) terms in the set of activated genes is detailed in supplemental Figures 4.1, 4.2, and 4.3, which analyze cellular process, function, and compartment terms respectively.

In brief, all GO cellular compartment terms that were significantly enriched related to the cell wall, surface, and membrane. For instance, 16% of activated genes had the GO term "cell surface," compared to 3.1% of the total genome – an enrichment of more than fivefold ($p=5.52e^{-14}$). Relatedly, enriched cellular process and function GO terms generally involved activities that occur at the cell wall, such as "cell adhesion" (4.7-fold enriched) or processes which are inherently related to cell wall construction, such as "hydrolase activity" or "carbohydrate metabolic process;" many of the activated genes which have these GO terms affect cell wall carbohydrates (examples include *XOG1*, *CHT2*, *CRH11* among others). Notably, several known and putative mannosyltransferases were differentially expressed – *BMT7*, *MNN22*, *MNN45*, and *MNN46* are activated (*MNN46* lies very slightly below the fourfold activation threshold mentioned above), while *MNN14* was repressed. Additionally, a number of genes related to hyphal growth were identified, such as *HWP1*, *BRG1*, *UME6*, and *ECE1* among others, reflecting the role of Czf1 as a regulator of filamentous growth as well as the filamentous phenotype of this mutant. Altogether these results clearly support a role for Czf1 in regulation of cell wall integrity.

Dhamgaye *et al.* 2012 suggested a potential role for Czf1 in cell wall integrity in which it was found that *czf1*Δ mutants expressed increased levels of the β-glucan synthase subunit *GSL1* transcript, which in that work was

not detected in the wild type, and in another work was shown to be induced by caspofungin treatment (Dhamgaye *et al.* 2012; Watamoto *et al.* 2011). Northern blot analysis investigating the expression of *GSL1* in the wild type, *czf1*Δ, complemented mutant, and the strain expressing artificially activated Czf1 grown either in the absence or presence of caspofungin was performed to examine *GSL1* expression, additionally examining *MNN45* to compare with the above described results (Figure 2.26). As indicated by RNA sequencing, *MNN45* was strongly induced by artificial activation of Czf1 – though it did not appear to be activated by caspofungin treatment, nor was transcript detectable in other strains, making it impossible to determine whether the *czf1*Δ mutant expressed less *MNN45*. *GSL1* expression was confirmed to be induced by caspofungin, though in this experiment *czf1* deletion did not result in heightened expression in the absence of caspofungin. Interestingly, artificial activation seemed to have a slight positive effect on *GSL1* expression.

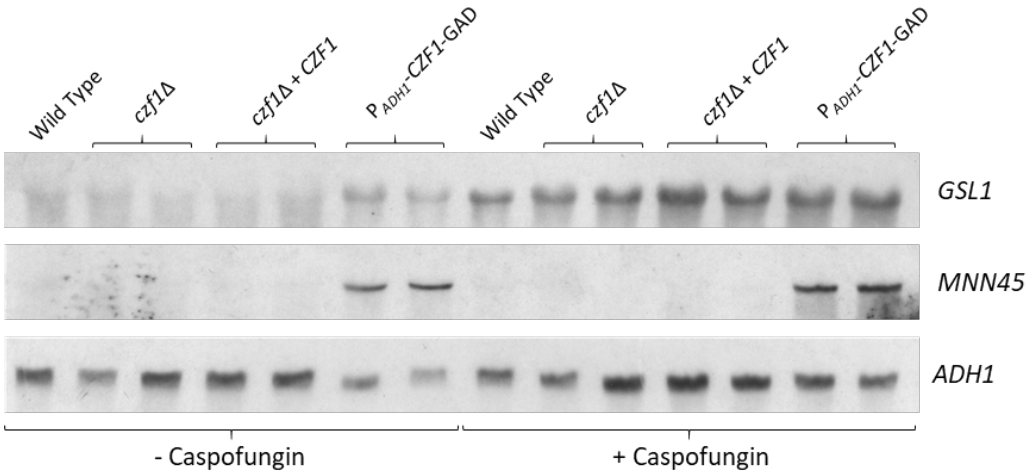

Figure 2.26: *GSL1* expression is not dependent on Czf1. The wild type, *czf1*Δ mutants and derived complemented strains, and strains expressing artificially activated Czf1 were diluted in YPD and grown for 3 hours at 30°C, at which time cultures to be treated with caspofungin were given caspofungin at a final concentration of 125ng/mL, and all cultures were incubated for a further hour before RNA was harvested and northern blotting performed. Probes binding to the coding sequence of *GSL1*, *MNN45*, and *ACT1* as a loading control were successively hybridized to detect expression of these transcripts. For each mutant, two independently constructed strains are shown.

The effects of artificial activation of Czf1 on growth phenotypes and gene expression suggested that Czf1 affects the structure of the cell wall. The fact that several mannosyltransferases were differentially expressed in the *CZF1*-GAD mutant suggested the possibility that Czf1 regulated mannosylation of the cell wall. Fluorescence microscopy was performed, staining either chitin or mannan, to determine if the the *snf4*Δ mutant (as an example of a mutant

with cell wall defects which could be rescued by activation of Czf1) exhibited altered mannosylation and whether activation of Czf1 influenced mannosylation. As seen in Figure 2.27, analysis was complicated by the filamentous nature of cells expressing *CZF1*-GAD. Nevertheless, no visibly appreciable change in chitin was observed in any of the tested strains. Additionally, the *snf4*Δ mutant did not exhibit any significant loss of mannan signal. Artificial activation of Czf1 in the wild type may have led to a somewhat brighter signal but it did not seem to have an effect in the *snf4*Δ mutant. Previous work investigating cell wall mannosylation has shown that significant reduction in mannan is required to detect changes via ConA staining of the cell wall (Hall *et al.* 2013), so these results did not preclude the possibility that changes in mannosylation did occur, but were simply not detectable using this method.

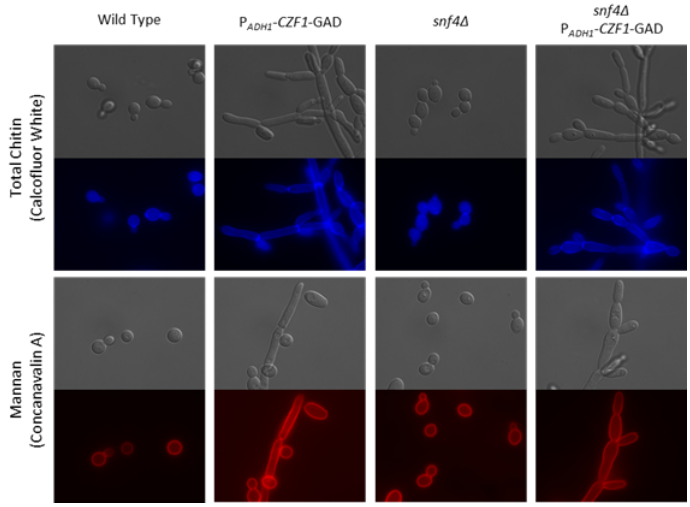

Figure 2.27: Fluorescent staining of chitin and mannan. The wild type, *snf4*Δ mutants, strains expressing *CZF1*-GAD in both backgrounds were grown to mid-log phase, fixed in formaldehyde, and stained in either calcofluor white (to stain chitin) or ConA-Texas Red (to stain mannan) and visualized under a fluorescent microscope. Images are representative of two independently constructed mutants per genotype.

To observe the effects of the various kinase mutants described above and of the artificial activation of Czf1 on the structure of the cell wall, transmission electron microscopy (TEM) was performed. Representative images are shown in Figure 2.28, while measurements of the inner and outer cell wall and statistical comparisons are detailed in Figure 2.29. All tested mutants exhibited statistically significant changes in the thickness of either the inner (*kin2*Δ and *ssn3*Δ), outer (*mkc1*Δ and *mkk2*Δ), or both (all others) cell wall compared to the wild type, with the exception of the *snf4*Δ mutant, which did not differ significantly from the wild type. These differences were

not however unidirectional; some mutants exhibited thickened inner or outer cell walls, some exhibited thinner inner/outer cell walls, despite all mutants having similar, if not identical, profiles in susceptibility to tested chemicals.

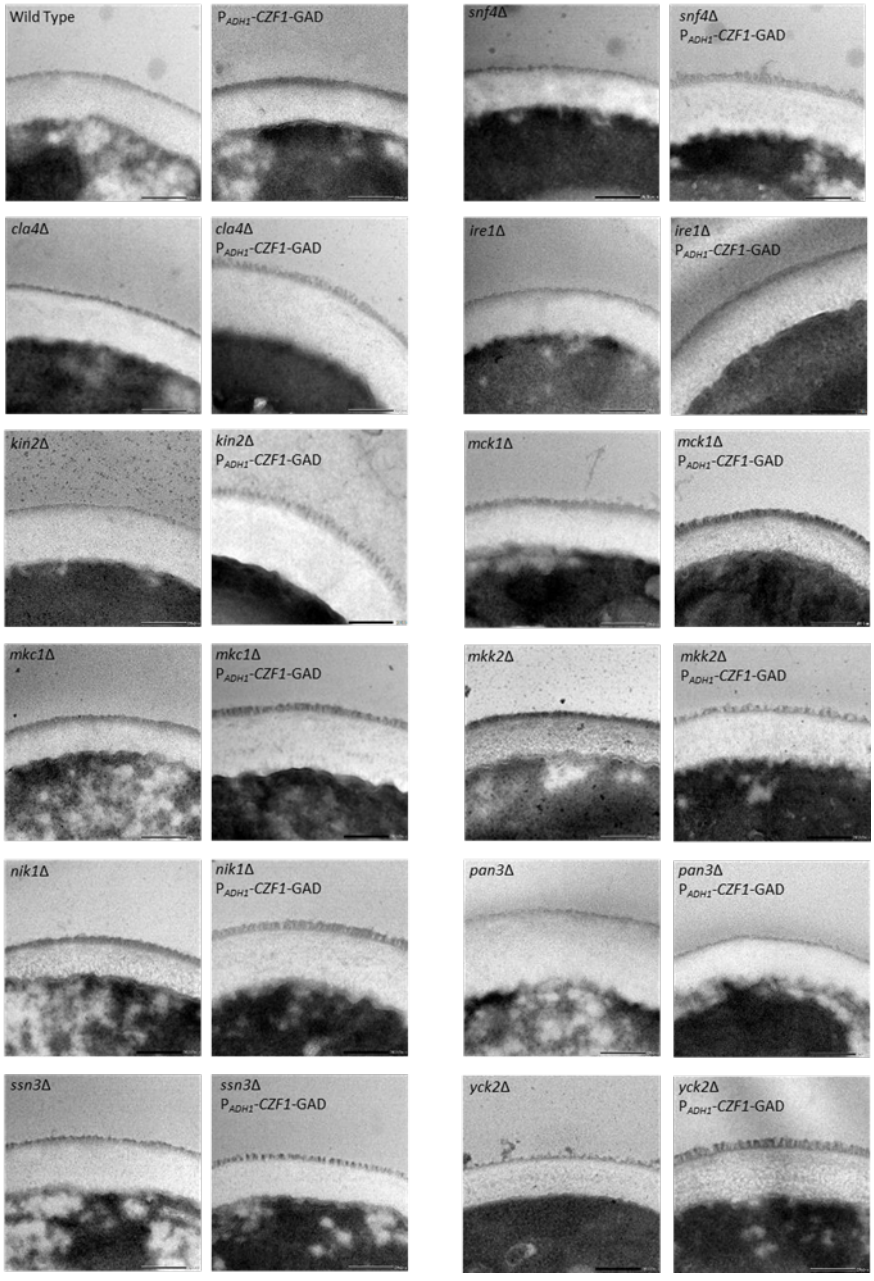

Figure 2.28: Transmission electron micrographs of the cell wall of the wild type, kinase deletion mutants, and derived strains expressing *CZF1*-GAD. Scale bars represent 200nm. Pictures are representative of the average characteristics of cells from two independently constructed mutants of each genotype.

Generally, artificial activation of Czf1 resulted in thickening of the outer cell wall, which was observed in all backgrounds except the *mck1*Δ mutant, in which no change was observed, and the *mkk2*Δ and *pan3*Δ mutants, where this resulted in a thinner outer cell wall. The effect on the inner cell wall was less uniform. Expression of *CZF1*-GAD had no effect on the thickness of the inner cell wall in the wild type, nor in the *ire1*Δ mutant. It resulted in thickening of the inner cell wall in the *snf4*Δ, *cla4*Δ, *kin2*Δ, *mkc1*Δ, *nik1*Δ and *yck2*Δ mutants, and thinning of the inner cell wall in the *mck1*Δ, *pan3*Δ, and *ssn3*Δ mutants. The most striking effect however is visible in the images of the cell wall (Figure 2.28). In many of the strains expressing *CZF1*-GAD, the outer cell wall took on a more fibrous appearance, even when the actual thickness of the layer was unaffected. This clearly suggests alterations to cell wall mannan, which is the principle component of this layer (see section 1.3).

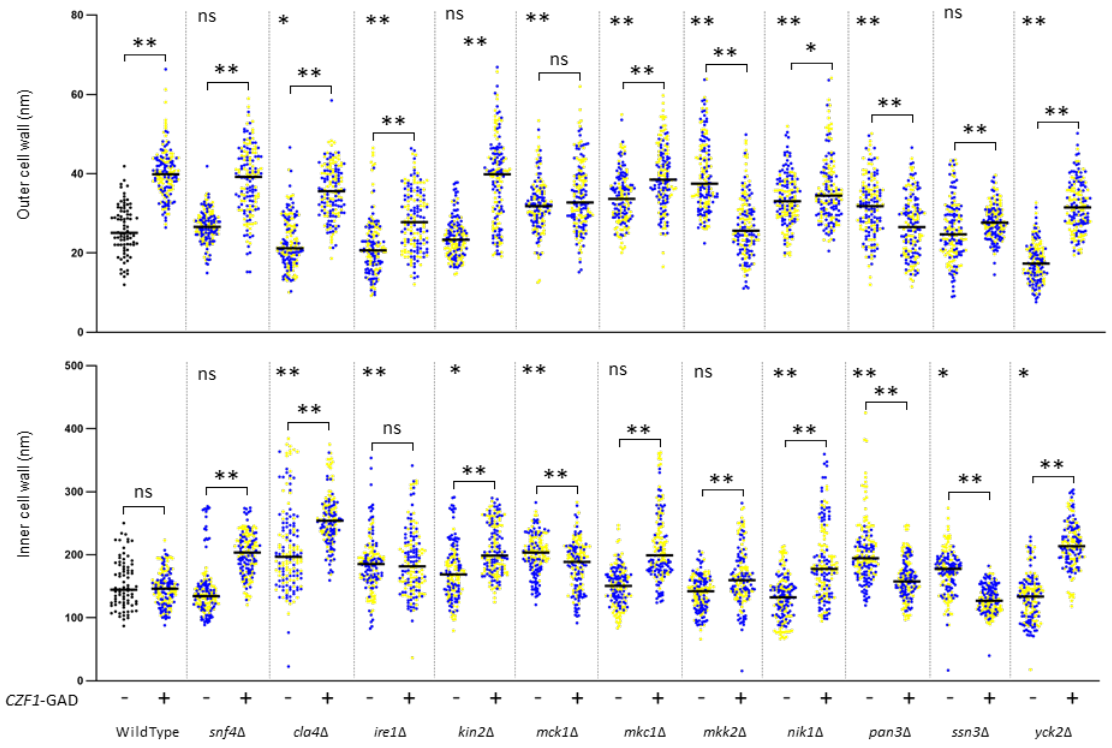

Figure 2.29: Quantification of transmission electron microscopy. The thickness of the outer and inner cell wall of ten cells were measured at eight locations per cell per strain, of which all strains except the wild type include two independently constructed mutants. Measurements from the two independently constructed mutants are colored blue or yellow. Measurements were combined because they resembled one another and the average of all measurements within a given genotype is marked by a black bar. Statistically significant differences in thickness comparing the wild type to a kinase mutant as well as between a kinase mutant (or the wild type) and derived stain expressing *CZF1*-GAD are marked as stars, where * is $p<0.01$, ** is $p<0.001$, and ns $p>0.01$ (not significant).

2.3.6 Specific susceptibility of *czf1*Δ mutants to cell wall stress

The above described experiments find strong evidence that Czf1 is a regulator of cell wall integrity. However, as seen in Figure 2.21, *CZF1* appeared to be largely dispensable for resistance to the tested conditions. Therefore, additional chemicals and concentrations were tested to identify cell wall defects in a *czf1*Δ mutant. Additionally, nutrient composition was probed, as Childers *et al.* 2020 recently reported that Czf1 plays a role in lactate-induced β-glucan masking. This is shown in Figure 2.30. Plates were also incubated for only three days rather than four, to detect differences that may be overgrown at later time points. Here, deletion of *CZF1* was found to result in increased resistance to calcofluor white and Congo red. Most striking was that *czf1*Δ mutants exhibited hypersusceptibility to the antifungal caspofungin, which disrupts glucan synthesis. The addition of lactate to plates containing Congo red resulted in two notable effects – the resistant phenotype of the *czf1*Δ mutant was lost, and all strains grew better than on plates without lactate.

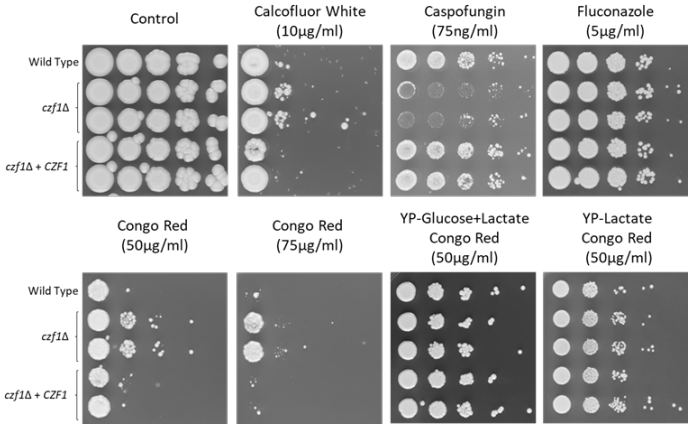

Figure 2.30: Deletion of *CZF1* results in altered cell wall integrity. The wild type, *czf1*Δ mutants, and complemented strains were grown overnight in YPD before being diluted to an OD 600 of 2.0, serially diluted, and spotted on the shown media. Plates were incubated for three days at 30°C. For each mutant, two independently constructed strains are shown.

2.4 Probing the essentiality of *SNF1*

Perhaps the biggest mystery regarding SNF1 in *C. albicans* has long been its essential nature. Numerous attempts have reported no success in generating *snf1* null mutants (Petter *et al.* 1997; Enloe *et al.* 2000; Ramírez-Zavala *et al.* 2017) Furthermore, conditional repression of *SNF1* expression was reported to result in nonviable cells (Vyas *et al.* 2015). This stands in stark contrast with *SNF1* in *S. cerevisiae*, where it is not an essential gene when cells are grown in the presence of glucose. Very recent work showed that *SNF1* could be deleted in cells lacking *MIG1*; Lagree *et al.* 2020 proposed that absence of *SNF1* leads to hyperrepression of glucose transporters and thus cell death. Concurrently with that work, we sought to investigate the essentiality of *SNF1* through inducible deletion.

Investigation of essential genes is naturally challenging. One approach to understand the roles that an essential gene plays is to generate strains in which the gene of interest can be conditionally deleted – following deletion, the effects on the cell prior to death can be observed (Michel *et al.* 2002). Such a system was used to investigate *SNF1*. Figure 2.31 provides a schematic of this process. In brief: beginning with the wild type (Figure 2.31A) one allele of *SNF1* was deleted through standard methods (see section 4.10.1, Figure 2.31B). Subsequently, a functional *SNF1* copy was inserted into an ectopic locus (Figure 2.31C), in this case *ADH1*, flanked by FLP recombination sites. Then, the remaining wild-type allele was deleted (Figure 2.31D). Finally, the *FLP*-recombinase gene was inserted under the control of an inducible promoter (Figure 2.31E). Thus, the remaining copy of *SNF1* could be efficiently removed by growth in an inducing medium (Figure 2.31F). Respectively, strains at each step of this process were named SCSNF1M2, SCSNF1M3, SCSNF1M5, SCSNF1M6, and SCSNF1M8. Additional control strains were constructed in which only one wild type *SNF1* allele was deleted; prior to excision of the ectopic *SNF1* allele this strain was named SCSNF1M7, after which it was called SCSNF1M9. Construction of these strains was conducted by Julia Haubenreißer (SCSNF1M2) and Sonja Schwanfelder (rest).

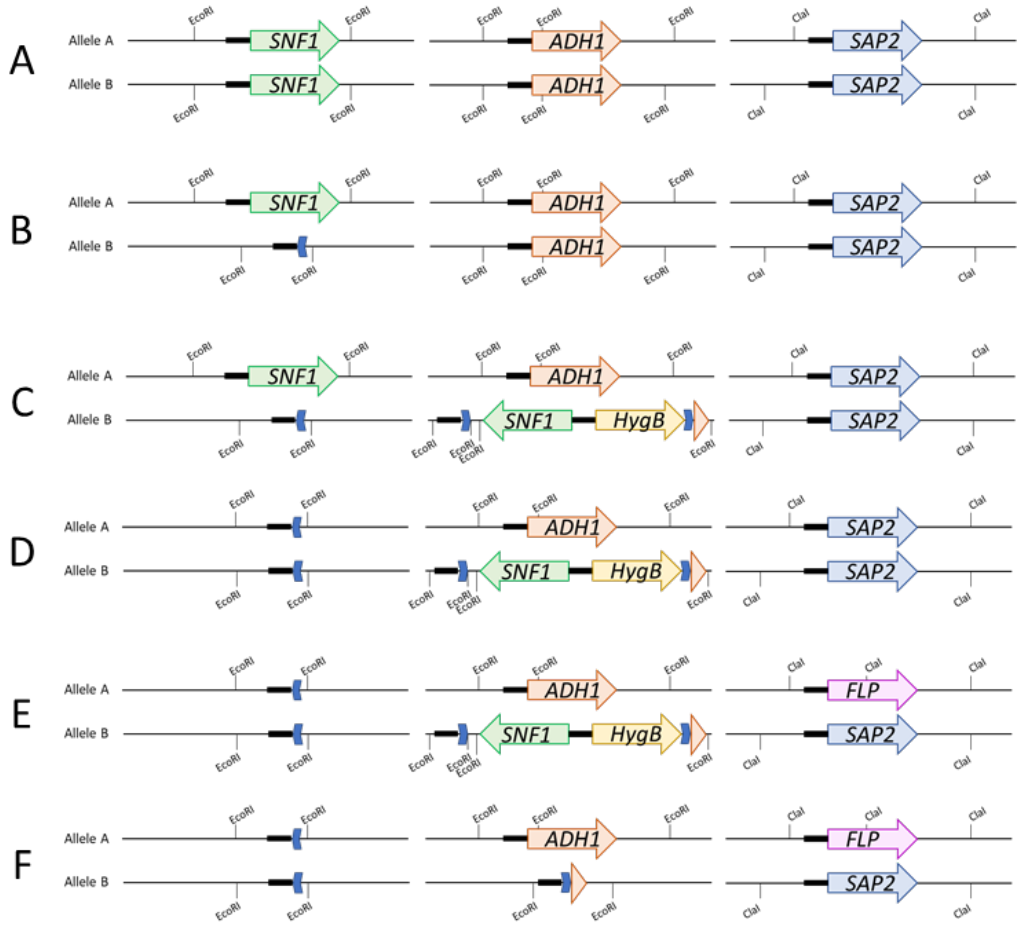

Figure 2.31: Stepwise schematic for inducible deletion of *SNF1* with strain names. (A) wild type *SNF1*, *ADH1*, and *SAP2* loci. (B) One *SNF1* allele is deleted, leaving behind an FRT scar; SCSNF1M2. (C) An ectopic *SNF1* copy is introduced at the *ADH1* locus with a different selectable marker (all other transformations use *SAT1*); SNF1M3. (D) The remaining wild type copy of *SNF1* is deleted; SNF1M5. (E) FLP-recombinase is placed under control of the inducible *SAP2* promoter; SNF1M6. (F) Induced expression of FLP-recombinase results in excision of the remaining *SNF1* allele and selectable marker; SNF1M8. Black bars represent DNA probes used for Southern blot analysis. Blue chevrons represent minimal FRT recognition sites. Labeled restriction sites relate to the enzyme used for Southern blot analysis of that locus. Sizes are not to scale. Intermediate steps involving replacement of a gene with the recyclable marker described in section 4.10.1 are omitted for simplicity.

2.4.1 Conditional deletion of *SNF1* yields viable cells

In order to determine the efficiency of the inducible deletion, cells grown overnight in inducing medium, in this case YCB-BSA-YE (defined in table 4.2) medium to induce the *SAP2* promoter, were diluted and plated on YPD plates and grown for two days (Figure 2.32A). After two days of growth at 30°C, colonies from the control strain grew normally, in contrast to those of the test strain, where only a few large colonies at low dilution grew normally. This showed that the efficiency of deletion was high. Surprisingly, however, there was a background of extremely small colonies visible in the test strain which continued to grow over longer incubation periods. Hypothesizing that growth may be faster at 37°C, these colonies grew notably better than at 30°C. Genetic analysis of these small colonies showed that the ectopic *SNF1* allele was successfully excised, and in the test strain, no *SNF1* coding sequence was observable, indicating that they were in fact *snf1* null mutants (Figure 2.32B).

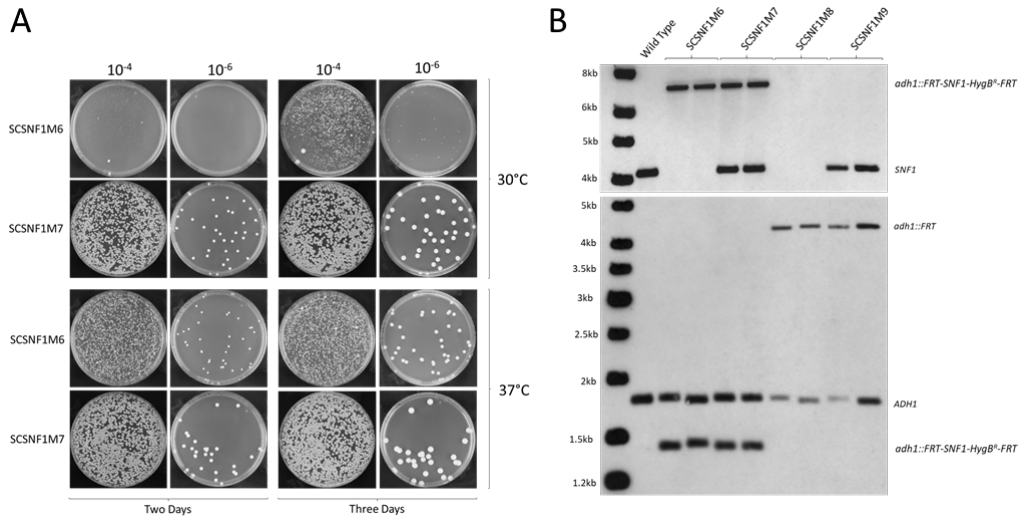

Figure 2.32: Inducible deletion of *SNF1* yields viable colonies. (A) SCSNF1M6 and SCSNF1M7 were grown overnight in YCB-BSA-YE, serially diluted, and plated on YPD. Plates were incubated for three days at either 30°C or 37°C, and pictures were taken after two and three days of growth. Plates are representative of two independently constructed strains per genotype. (B) Southern blot analysis shows successful deletion of *SNF1* in SCSNF1M8. EcoRI digested genomic DNA from the wild type, SCSNF1M6, SCSNF1M7, SCSNFM8, and SCSNF1M9 was hybridized with probes binding to the *SNF1* coding sequence (top) or *ADH1* 5' sequence (bottom). DNA size marker is shown on the left, and the genotype represented by bands is labeled on the right.

This raised the obvious question of why previous attempts to delete *SNF1* were unsuccessful. The poor growth of the colonies following induced *SNF1* excision suggested that transformants were previously not identified because they were simply unable to grow in the medium on which they were selected. The strategies employed by both Petter *et al.* 1997 and Enloe *et al.* 2000 required transformants to be plated on minimal media. Ramírez-Zavala *et al.* 2017, in contrast, selected for transformants by plating on YPD supplemented with 200µg/mL nourseothricin, incubating plates for two days at 30°C. Following induced deletion of *SNF1* as described above, overnight cultures of SCSNF1M6 and SCSNF1M7 were plated additionally on YNB-Glucose and YPD+Nourseothricin (200µg/mL) and grown for two days (Figure 2.33). No colonies were visible on plates from SCSNF1M6 overnight cultures after three days, suggesting that either the *snf1* null mutant cannot grow in this condition, or it grows slowly enough that more time is required to detect it. After two days of growth on YPD+Nourseothricin, some large colonies which likely still contain *SNF1* were observable and there were some extremely small

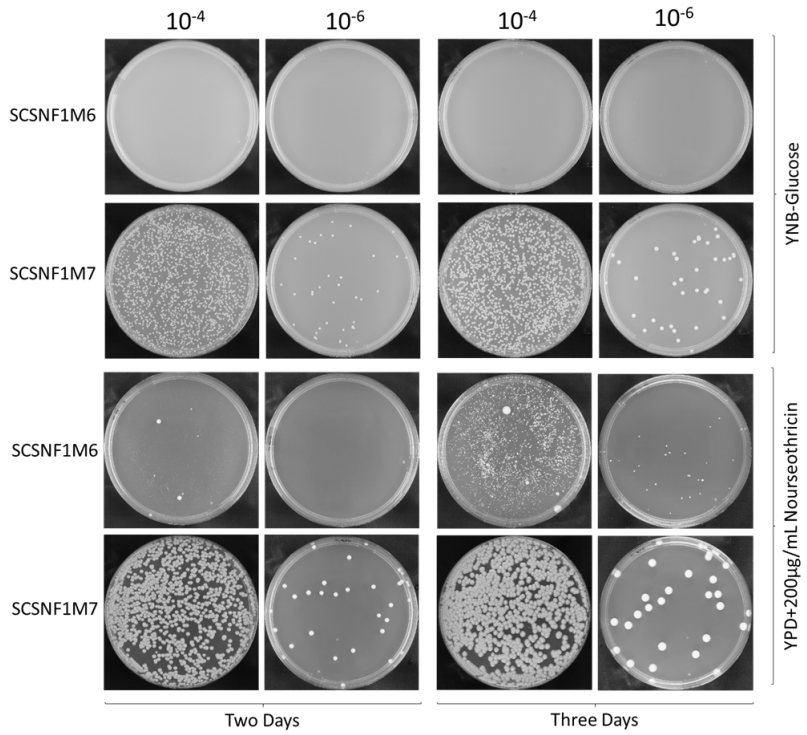

Figure 2.33: Growth of *snf1*Δ mutants plated on common selection media. SCSNF1M6 and SCSNF1M7 were grown overnight in YCB-BSA-YE, serially diluted, and plated on YNB-Glucose (top) or YPD+Nourseothricin (200µg/mL). Plates were incubated for three days at 30°C, and pictures were taken after two and three days. Plates are representative of two independently constructed strains per genotype.

colonies visible. These became more apparent at three days of growth, but were still very small, resembling "background" colonies which appear when transformants are plated on such medium and have spontaneously developed a degree of resistance to nourseothricin. Thus *snf1*Δ transformants were not likely to be found in previous deletion attempts due to drawbacks in the methodology.

2.4.2 Phenotypic analysis of *snf1*Δ mutants

The generation of viable *snf1*Δ mutants was an unexpected but intriguing outcome of an experiment which had initially intended to investigate phenotypes of conditional *snf1* knockouts prior to cell death. Viable *snf1*Δ mutants naturally allow for simpler phenotypic assays. The ability of the *snf1*Δ mutants to grow on various carbon sources in either rich or minimal media at either 30°C or 37°C was compared to that of *snf4*Δ mutants, which as seen here and elsewhere have been used as a proxy for Snf1 inactivation in the absence of such strains. As seen in Figure 2.34, deletion of *SNF1* led to severe growth defects, including a complete absence of growth when glucose was not included in the medium. Furthermore, SCSNF1M8 exhibited extremely poor growth on minimal (YNB) media. As seen in Figure 2.32A, these mutants did however grow better at 37°C than 30°C (in conditions where growth was indeed observed at all). In contrast, SCSNF1M6, which contains only the ectopic *SNF1* allele, grew normally, reflecting previous results which indicated that *SNF1* is haplosufficient for growth on alternative carbon source (Ramírez-Zavala *et al.* 2017) and that this allele was expressed normally. In comparison with the *snf4*Δ mutant, SCSNF1M8 grew worse under all tested conditions, but growth phenotypes overlapped; in conditions where *snf4*Δ grew poorly, so did SCSNF1M8. There was one interesting disparity between the two mutants, however. Figure 2.3 showed that the growth defect of *snf4*Δ mutants is exaggerated at higher temperatures, while as mentioned above, the opposite is true of SCSNF1M8. This is put in stark relief in Figure 2.34, which directly compares the two genotypes.

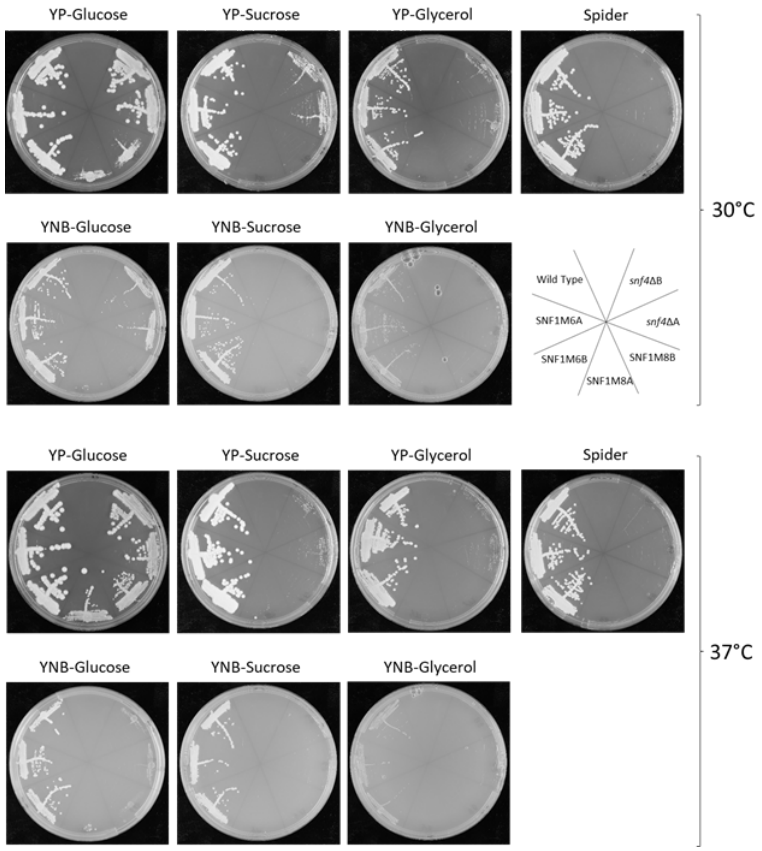

Figure 2.34: Growth of *snf1*Δ and *snf4*Δ mutants in various carbon sources. The wild type, SCSNFM6, SCSNFM8 (*snf1*Δ) and *snf4*Δ mutants were grown overnight in YPD before being diluted to an OD 600 of 2.0. 3µL were streaked on the shown media and grown for two days at 30° or 37°C. For each mutant, two independently constructed strains are shown.

2.4.3 Snf1 catalytic activity is required for function

In addition to aforementioned work which was unsuccessful in generating *snf1*Δ mutants through transformation techniques, Vyas *et al.* 2015 reported that strains expressing *SNF1* under the control of the glucose-repressible *MAL2* promoter were unable to grow in repressing conditions, supporting the belief that *SNF1* was an essential gene. They also reported, however, that a catalytically nonfunctional Snf1^{K81R} mutant, in which a conserved lysine residue in the ATP-binding pocket is mutated to arginine, is viable but grows very poorly unless grown in rich, glucose containing media at 37°C. This suggested that kinase activity of Snf1 was not responsible for the essentiality of *SNF1*.

The work described here has shown that *SNF1* is not in fact essential. This allowed a phenotypic comparison of *snf1*Δ mutants to those expressing a single copy of Snf1^{K82R} as the only remaining *SNF1* allele (the two alleles of *SNF1* differ by one amino acid residue in a polyhistidine tract near the N-terminus; the Snf1^{K81R} mutant used in the mentioned work is equivalent to Snf1^{K82R}). This mutant was generated in a similar manner to SCSNF1M8, but instead of deletion of the second wild type allele, it was replaced with *SNF1*^{K82R}, named here SCSNF1M13. As seen in Figure 2.35A, the phenotypes of SCSNF1M8 and SCSNF1M13 in all tested conditions were identical. Western blot analysis confirmed that the Snf1^{K82R} protein was expressed in comparable amounts to that of SCSNF1M9, which expresses one wild type copy of *SNF1*, and that phosphorylation of Snf1-T208 was unaffected. These results indicate that in fact Snf1 kinase activity is required for Snf1 function, as mutants lacking kinase activity resemble those lacking Snf1 altogether.

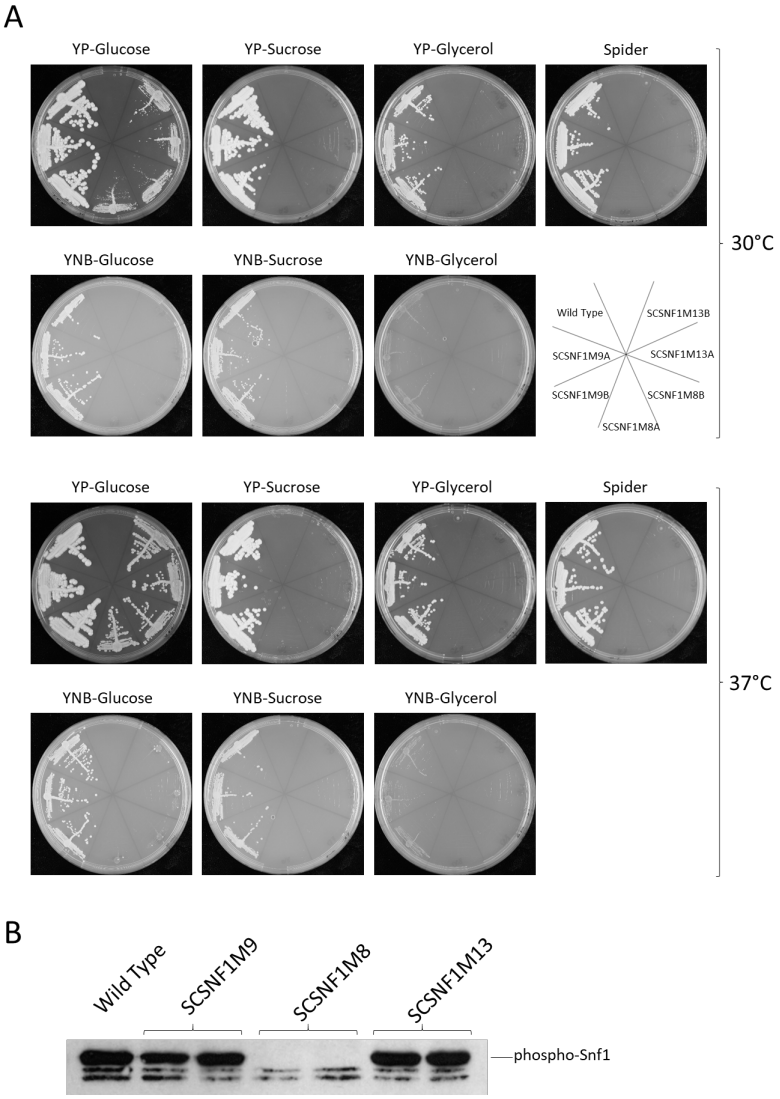

Figure 2.35: Snf1 catalytic activity is required for function. (A) The wild type, SCSNF1M9, SCSNF1M8, and SCSNF1M13 mutants were grown overnight in YPD before being diluted to an OD 600 of 2.0. 3µL were streaked on the shown media and grown for two days at 30° or 37°C. (B) Overnight cultures of the same strains were diluted in YPD and grown for one hour at 30°C before being washed and grown for an additional two hours at 30°C in the labeled medium before cell extracts were prepared. Equal amounts of protein were separated and probed with an antibody against phosphorylated Snf1-T208. The two smaller migrating bands are undefined protein which cross-reacts with the antibody (Ramírez-Zavala *et al.* 2017). For each mutant, two independently constructed strains are shown.

2.4.4 Generation of *snf1*Δ mutants through standard transformation

One drawback of the *snf1*Δ mutants generated through the above described inducible gene deletion is that it required additional genetic manipulation outside of the locus of interest; in this case, one copy of *ADH1* was deleted, and one copy of *SAP2* was replaced with the FLP-recombinase. In contrast, the standard gene deletion technique used in this work (described in section 4.10.1) affects only the locus of interest, avoiding any incidental effects of mutation at other loci. Thus it was desirable to generate *snf1*Δ mutants through this method as well for future investigation. An additional risk was that the ectopic *SNF1* allele integrated at the *ADH1* locus, which includes some of the 5' sequence which should encompass the promoter region of *SNF1*, lacks some regulatory elements or otherwise results in abnormal expression of *SNF1* which may allow for suppressor mutations to arise, facilitating excision of *SNF1*.

Thus, a renewed attempt was made to generate *snf1*Δ mutants through the standard methodology. The results described above show that SCSNF1M8 grows much better at 37°C, but also that longer incubation times are required for colonies to grow to a degree that they stand out from the background. Using this new knowledge, previously generated heterozygous *SNF1* mutants were transformed using the *SAT1*-flipper cassette flanked by 500bp regions corresponding with the region directly upstream and downstream of *SNF1* and incubated for three days at 37°C. Using these conditions, colonies grew; several candidates were selected from the population of small colonies and genetic analysis showed that the remaining copy of *SNF1* was successfully replaced by the *SAT1*-flipper cassette (Figure 2.36A). To avoid additional, unnecessary passaging of the strain which might lead to rise of suppressor mutations, the cassette was not recycled; these strains were named SCSNF1M21. Phenotypic comparison of SCSNF1M8 and SCSNF1M21, two differently generated *snf1*Δ mutants, showed identical growth in all conditions (Figure 2.36). This indicates that the mutants generated by inducible gene deletion did not contain suppressor mutations, and additionally strongly supported the assertion that *SNF1* in *C. albicans* is not, in fact, an essential gene.

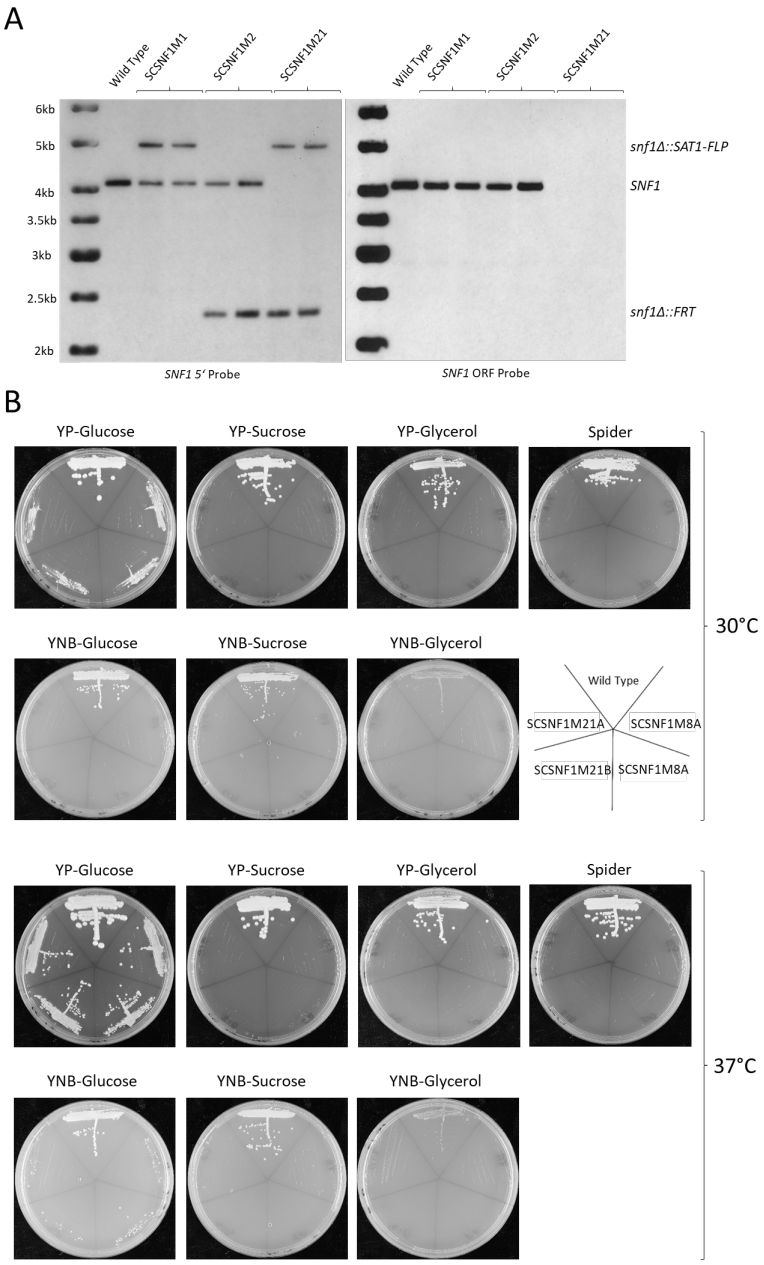

Figure 2.36: Deletion of *SNF1* via standard transformation. (A) SCSNF1M21 mutants are *snf1*Δ. EcoRI digested genomic DNA from the wild type, SCSNF1M1, SCSNF1M2, and SCSNFM21, mutants was hybridized with probes binding to the *SNF1* 5' sequence (left) or *SNF1* ORF (right). DNA size marker is shown on the left, and the genotype represented by bands is labeled on the right. (B) The wild type, SCSNF1M21 and SCSNF1M8 mutants were grown overnight in YPD before being diluted to an OD 600 of 2.0. 3µL were streaked on the shown media and grown for two days at 30° or 37°C. For each mutant, two independently constructed strains are shown.

3. Discussion

3.1 Regulation of Mig1 and Mig2 activity by the SNF1 pathway

3.1.1 Regulation of Mig1 in response to carbon source signaling

While the primary, intended goal of this study was to identify novel targets of SNF1 in *C. albicans*, Mig1 and Mig2 were also tempting targets for investigation. As described in greater detail in section 1.2.2, ScMig1 is perhaps the most noteworthy target of ScSNF1, and is the major transcriptional regulator of glucose repression. It is also directly phosphorylated by ScSNF1 at several locations which exhibit a conserved recognition motif. Mig1 in *C. albicans* entirely lacks this recognition motif (Figure 2.1). This led to some doubt as to whether it was phosphorylated by SNF1, or indeed at all in this organism. The ability of *mig1* deletion to partially restore growth of *snf4*Δ growth defects, most notably on rich media containing carbon sources other than glucose, confirmed that Mig1 is still functionally related to glucose repression. It remained an open question, however whether Mig1 still retained it's place as a target of SNF1. Two published phosphoproteomic investigations did not identify phosphorylated peptides belonging Mig1 (Beltrao *et al.* 2009; Willger *et al.* 2015), though both examined cells grown in media containing glucose, and as such Mig1 is not expected to be phosphorylated. Unpublished phosphoproteomic data from this lab in collaboration with the lab of Dr. Olaf Kniemeyer (Hans Knöll Institute, Jena, Germany) detected phosphorylation at Ser-281, Ser-358, and Ser-359, though detection of this phosphorylated residues was inconsistent across experimental replicates.

Initial experiments examining whether Mig1 was posttranslationally modified in response to carbon source did not identify modification, but surprisingly instead revealed that Mig1 protein levels are regulated by carbon source (Figure 2.5). This was striking because it diverges from the mode of regula-

tion of ScMig1, where instead Mig1 is shuttled out of the nucleus in response to the absence of glucose (De Vit *et al.* 1997). In fact, this mode of regulation much more resembled that of ScMig2, which is ubiquitinated in response to absence of glucose and subsequently degraded by the proteasome; this response is ultimately regulated by ScSNF1, but ScMig2 itself is apparently not a direct target of phosphorylation (Lim *et al.* 2011). Shortly after these results were produced, new evidence was published that supported the assertion that Mig1 is indeed a target of SNF1. In that work as well as others, Mig1 was shown to negatively regulate genes important for utilization of alternative carbon sources (Lagree *et al.* 2020; Murad *et al.* 2001; Cottier *et al.* 2017). Additionally, it showed that *SNF1* could be successfully deleted in mutants lacking *MIG1*, suggesting that the (here disproven) essentiality of *SNF1* was due to the lethality of hyperrepression of Mig1 targets. Furthermore, they too found that growing cells in the absence of glucose led to reduced Mig1 protein levels (Lagree *et al.* 2020). Interestingly, in certain conditions (Spider medium), they additionally observed a change in electrophoretic mobility of Mig1 suggestive of posttranslational modification.

To investigate this further, I supervised work which was undertaken by Sarah Weber during the course of her Bachelor's thesis (Weber 2020), in which she was able to show preliminary evidence that growth of cells in YP-Sucrose led to a carbon-source dependent change in mobility of Mig1 which was also dependent on the presence of *SNF4*. To follow up that work, such results were replicated in rich media containing glycerol (as was used in Lagree *et al.* 2020; Figure 2.7). This change in mobility was proven to be phosphorylation (Figure 2.6). Together these data alone and in conjunction with simultaneously published results present strong evidence that Mig1 is functionally conserved with ScMig1 and continues to act downstream of SNF1 to repress genes important for the utilization of alternative carbon sources, however the effects of SNF1-dependent phosphorylation differ. Rather than (or, potentially, in addition to) nuclear export, Mig1 protein levels are notably lowered. The underlying mechanism which leads to this effect has yet to be investigated. This reduction in protein levels may be due to degradation, as is the case for ScMig2, and may be triggered by phosphorylation. A second possibility is that Mig1 is inherently unstable and the reduced levels of protein are a result of reduced Mig1 translation, but it should be noted that Lagree *et al.* 2020 found that *MIG1* mRNA levels were unaffected by carbon source.

3.1.2 Regulation of Mig2 in response to carbon source signaling

The dominant repressor of glucose repressed genes in *S. cerevisiae* is ScMig1. However, an additional repressor, ScMig2, plays some largely redundant roles in this activity (Lutfiyya *et al.* 1998; Westholm *et al.* 2008). As mentioned above, Mig2 is indirectly regulated by ScSNF1 activity and degraded in response to growth on alternative carbon sources. Similar to Mig1, Mig2 is not well conserved with ScMig2 outside of its DNA-binding domain (Figure 2.2), and therefore may differ from its *S. cerevisiae* counterpart in function or regulation. The Bachelor's thesis of Weber 2020 showed the effect of *mig2* deletion on growth on alternative carbon sources in an *snf4*Δ mutant was largely identical to that of *mig1* deletion. In that work and here, deletion of both *MIG1* and *MIG2* was required for the largest improvement in growth (Figure 2.3). Additionally, while investigations of the transcriptional effect of Mig1 in *C. albicans* found that it regulate does some glucose-repressed genes, many were seemingly not affected by *mig1* deletion. Lagree *et al.* 2020 found that significant derepression similar to that seen in the wild type when grown on alternative carbon sources required that both *MIG1* and *MIG2* be deleted. Thus, interestingly, Mig2 plays a largely coequal role in glucose repression alongside Mig1 in *C. albicans*.

This greater degree of importance for Mig2 made investigation of the regulation of Mig2 activity more valuable. Lagree *et al.* 2020 were unsuccessful in detection of HA-tagged Mig2 protein. Here, Mig2-HA was detected. Unlike Mig1, Mig2 from cells grown in rich media is normally present in four electrophoretic forms (Figure 2.8). Shifting to growth on Spider medium, which lacks glucose, leads to a reduction in overall protein levels; additionally the largest forms become dominant. Phosphatase treatment showed that all but the smallest form are phosphoprotein (Figure 2.8A). In *snf4*Δ mutants, in which SNF1 is believed to be functional but at a vastly reduced degree, protein levels are reduced to a lesser degree in response to growth in Spider medium, and the nonphosphorylated form is dominant regardless of carbon source. One phosphoproteomic analysis of *C. albicans* found nine phosphorylated residues on Mig2, at Ser-91, Ser-92, Ser-94, Ser-110, Thr-111, Ser-113, Ser-132, Ser-135, and Ser-261 (Willger *et al.* 2015). Another found phosphorylation at three of those sites (Ser-94, Ser-113, and Ser-132; Beltrao *et al.* 2009). Phosphorylation of some or all of these sites could explain the various electrophoretic forms identified in this work, though this has not been experimentally proven. Nonetheless, Mig2 is indeed phosphorylated in *C. albicans* and the relative abundance of the different isoforms is dependent on carbon source, and this is dependent on SNF1 activity.

A simple explanation is that Mig2 protein levels are reduced in response to carbon source dependent hyperphosphorylation by activated SNF1. Much like the case of Mig1, it is unclear exactly what the reason for the reduced amount of protein is. The mechanism which leads to ScMig2 degradation may function similarly in *C. albicans*, but this raises questions regarding the purpose of direct phosphorylation of Mig2. It is possible that the two are in fact unrelated, or perhaps two separate mechanisms of regulation, where differential phosphorylation may affect DNA binding or subcellular localization. While many open questions regarding Mig2 remain, it is clear that this repressor plays a much greater role in glucose repression in *C. albicans* than it does in *S. cerevisiae*. Furthermore, this work has presented evidence that unlike ScMig2, is phosphorylated in an SNF1-dependent fashion, though much like in *S. cerevisiae*, Mig2 is ultimately regulated at the level of protein accumulation.

3.1.3 Mig1, Mig2, and cell wall integrity

Mutants in which SNF1 activity is presumed to be reduced, particularly those lacking *SAK1* or *SNF4*, exhibit hypersensitivity to chemicals which cause cell wall stress, indicative of reduced cell wall integrity (Noble *et al.* 2010; Mottola 2016; Ramírez-Zavala *et al.* 2017). A potential explanation for this is simply that carbohydrates are the major component of the cell wall (see section 1.3), and reduced carbohydrate metabolism results in an abnormal response to damage. Alternatively the SNF1 pathway may regulate proteins (either via phosphorylation or through transcriptional control) which are involved in cell wall construction or damage response. As targets of SNF1, the role of Mig1 and Mig2 in cell wall integrity were investigated (Figure 2.4). The results were somewhat surprising. In several of the tested conditions, the defects of an *snf4*Δ mutant were partially or fully suppressed by deletion of *MIG1* or both *MIG1* and *MIG2*.

This supported the hypothesis that cell wall integrity defects of SNF1 pathway mutants are due to metabolic deficiencies. However, deletion of *MIG1* actually exacerbated the hypersensitivity of the *snf4*Δ mutant to caspofungin, and the triple mutant (*snf4*Δ *mig1*Δ *mig2*Δ) was entirely unable to grow in the presence of caspofungin. The simplest explanation for these seemingly conflicting results is that both overexpression of certain Mig1/Mig2 target genes is detrimental to β-glucan synthesis, which is the process disrupted by caspofungin. Specific details notwithstanding, hyper-repression of metabolic genes by Mig1 and Mig2 seems to account for an appreciable degree of the cell wall defects of SNF1 pathway mutants, but does not completely explain it.

3.2 Generation of suppressors of *snf4*Δ

The task of identifying novel targets of a protein kinase is challenging. In the present work, two different approaches were utilized to search for elements which are downstream of SNF1. In one approach, microevolution was used as a tool to generate suppressor mutants which overcame a relatively minor growth defect in rich media. Microevolution in *Candida* spp. has been well documented *in vivo*, for example generating fluconazole resistant strains following treatment (reviewed in Morschhäuser 2016), but has also been achieved experimentally *in vitro*, for instance in generation of a hypervirulent strain of *C. glabrata* following prolonged coculture with murine macrophages (Brunke *et al.* 2014) or restoration of filamentation in a nonfilamentous *C. albicans* mutant via similar coculture (Wartenberg *et al.* 2014). Suppressor mutants generated from *snf4*Δ mutants showed disparate phenotypes (Figure 2.9) suggesting that distinct mutations had occurred.

Interestingly, Suppressor A exhibited hypersusceptibility to caffeine, but greater-than-wild type resistance to Congo red (as well as calcofluor white); these phenotypes were nearly identical to that of mutants lacking the protein kinase *SCH9* (Liu *et al.* 2010a, Ramírez-Zavala, unpublished data). Sequencing of *SCH9* in this mutant did not reveal any differences from the reference sequence. Sch9 is a downstream target of the Tor1 kinase (Kim *et al.* 2019) and interaction between the SNF1 and TOR pathways is well documented in *S. cerevisiae* (Bertram *et al.* 2002; Mayordomo *et al.* 2002; Orlova *et al.* 2006; Zhang *et al.* 2011). In *S. cerevisiae*, the transcription factor Hcm1 was shown to be negatively regulated by the TOR pathway and positively regulated by the SNF1 pathway, and also is important for normal response to nutrient starvation (Rodríguez-Colman *et al.* 2013). It stands to reason that one might expect disruption of the TOR pathway to result in the observed phenotypes of this suppressor mutant: slightly improved growth on alternative carbon sources, increased resistance to Congo red, and hypersusceptibility to caffeine.

Suppressors B and C exhibited identical phenotypes characterized by minor improvements in cell wall integrity but notably improved carbon source utilization (Figure 2.9). Suppressor B will be discussed in greater detail in the following sections because it contained a mutation within *SNF1* which conferred this phenotype. Because Suppressor C is phenotypically identical in tested conditions to this strain but has no mutations within *SNF1*, it is tempting to hypothesize that genetic alteration responsible affects a protein whose activity is dependent on SNF1 and whose loss of activity is largely responsible for the observed growth defects of the *snf4*Δ mutant. Under this hypothesis, the most likely candidates are *MIG1* and/or *MIG2*, though as

seen in Figures 2.3 and 2.4 the phenotype of an *snf4*Δ *mig1*Δ double mutant, and even an *snf4*Δ *mig1*Δ *mig2*Δ triple mutant does not quite match the growth of the Suppressor B or C strains. Additionally, sequencing of Suppressor C at the *MIG1* and *MIG2* loci did not reveal any differences from the reference sequence. This leaves the exciting possibility of a major as-of-yet undiscovered target of SNF1 which regulates, primarily, carbon source utilization, but also affects cell wall integrity.

3.2.1 Snf1$^{\Delta 311\text{-}316}$ is an Snf4-independent, active form of Snf1

The third mutant generated by microevolution of the *snf4*Δ mutant, Suppressor B, was unique in that it is defined by an *SNF*$^{\Delta 311\text{-}316}$ mutation in which 18 base pairs within the coding sequence of one allele *SNF1* were lost, resulting in a deletion of 6 amino acids (Figure 2.10). Numerous *SNF1* mutations which compensate for loss of *SNF4* have been identified in *S. cerevisiae*, including a variety of point mutations in the N-terminus and C-terminal truncation to remove the autoinhibitory domain (Celenza and Carlson 1989; Estruch *et al.* 1992; Leech *et al.* 2003; Jiang and Carlson 1996). The mutation identified here is unique in that it is located between the kinase and autoinhibitory domains. Because it does not directly affect the sites in which the kinase domain and autoinhibitory domain interface and phosphorylation at Thr-208 is unaffected (Figure 2.15), it seems likely that the underlying mechanism is that Snf1$^{\Delta 311\text{-}316}$ is locked in a partially active state where the autoinhibitory domain does not physically come into contact with the kinase domain, though more advanced structural investigations are required to test this hypothesis.

Phenotypically, *snf4*Δ mutants expressing *Snf1*$^{\Delta 311\text{-}316}$ resemble those expressing Snf1^{L181I} (Figures 2.11 through 2.15), which is homologous to ScSnf1^{L183I} which has been shown in that organism to confer Snf4-independence and in *C. albicans* to confer Sak1-independence (Leech *et al.* 2003; Ramírez-Zavala *et al.* 2017; Mottola 2016), but interestingly Snf1$^{\Delta 311\text{-}316}$ has a much more modest effect on the ability to filament in Spider medium in which glucose is the carbon source. The reason for this is unclear; one hypothesis is that Snf1^{L181I} is better able to associate with Kis2, or the targets of the Kis2-associated form of the complex, than Snf1$^{\Delta 311\text{-}316}$, because Kis2 plays a greater role in filamentous growth than Kis1, which itself is more important for utilization of alternative carbon sources and cell wall integrity (Ramírez-Zavala *et al.* 2017). This hypothesis is in line with the observation that Snf1$^{\Delta 311\text{-}316}$ still requires a β-subunit to elicit its function (Figure 2.16).

3.2.2 Snf1$^{\Delta 311\text{-}316}$ is preprogrammed

Perhaps the most striking aspect of the *SNF1*$^{\Delta 311\text{-}316}$ mutation is its genetic nature. In the wild type *SNF1* sequence there appears an eight nucleotide sequence (GCCAGATT) which is repeated, flanking an intervening ten nucleotide sequence. In the *SNF1*$^{\Delta 311\text{-}316}$ mutant, one repeat and the spacer are lost; the likeliest cause for this is recombination. This cis-strand recombination stands out from point mutations like those mentioned above because point mutations occur through random chance, while recombination is dependent on pre-existing sequence identity. Thus *SNF1* is encoded with the capability of generating a specific, active, Snf4-independent form of the protein. Repetitive sequences are extremely common in eukaryotic genomes, including that of *C. albicans*, often playing roles in modulation of gene expression (Biscotti *et al.* 2015; Freire-Benéitez *et al.* 2016).

More specifically, intragenic tandem repeats are also common. These repeats are hot spots for mutation, where repeats are gained or lost, altering protein function which may allow for rapid, reversible adaption to changing environmental conditions (Zhou *et al.* 2017; Wilkins *et al.* 2018). The repeat found in *SNF1* is not a tandem repeat, rather one with a spacer between it which is excised upon recombination. Because *C. albicans* is diploid, the excision is nonetheless reversible via recombination with the second allele; should selective pressure lead to both alleles converting to *SNF1*$^{\Delta 311\text{-}316}$, mating provides an opportunity to recover the wild type genotype. The theory that this mutation is a preprogrammed mechanism to rapidly adapt to the environment is challenged by the absence of evidence that Snf1$^{\Delta 311\text{-}316}$ provides an advantage over wild type Snf1.

In no tested conditions did otherwise wild type cells expressing the mutant grow better than the wild type or adapt to changing carbon source more quickly (Figure 2.17), though it may simply be that the conditions in which this is the case were not examined here. There also does not appear to be any detrimental effects of heterozygous expression of the mutant, which might encourage a return to the wild type after the particular stress in which it is advantageous is overcome, though a minor defect in cell wall integrity was observed when both alleles were replaced which may provide a degree of selective pressure to maintain one wild type allele. Despite these gaps in the understanding of this mutant, it remains true that Snf1$^{\Delta 311\text{-}316}$ represents an unusual situation where a gene is encoded with the ability to specifically alter its sequence to an active state which no longer depends on a secondary activator.

3.3 Czf1 is a regulator of cell wall integrity

A second, somewhat more targeted approach was also used in an attempt to identify SNF1 targets – screening a library of artificially activated zinc-cluster transcription factors (ZCFs). In *S. cerevisiae*, some ZCFs are known targets of ScSNF1, particularly ScCat8 and Sip4. As mentioned in section 1.2.2, experimental evidence suggested that Cat8 function in *C. albicans* has shifted away from glucose repression; this could suggest either that it is no longer a target of SNF1, or that SNF1 function has diversified. Sip4 lacks a clear homolog in *C. albicans*. As the largest family of transcription factors in *C. albicans*, there was clear potential for identifying SNF1 targets from this group. Screening *snf4*Δ mutants using pools of artificially activated ZCFs yielded only one which rescued one of the defects of this mutant – artificial activation of Czf1 restored resistance to cell wall stress.

This effect was not unique to the *snf4*Δ mutant – many additional kinase deletion mutants which exhibit varying degrees and patterns of susceptibility to different cell wall stress-inducing chemicals were also positively affected by artificial activation of Czf1 (Figures 2.23 and 2.24). This observation, plus the fact that Czf1 is phosphorylated (Figure 2.22, also five phosphorylated residues were reported in Willger *et al.* 2015) suggests the possibility that Czf1 is regulated via phosphorylation, though phosphorylation was detected even in rich media without cell wall stress and was not apparently affected by cell wall stress (Figure 2.22). Nor was it affected by deletion of any of the tested kinase mutants (Figures 2.22 and 2.25). It may be that several kinases can phosphorylate Czf1 and thus deletion of only one is insufficient to affect phosphorylation state, or perhaps that the responsible kinase was not among those tested; the mutants used here are not the only kinase mutants which exhibit cell wall defects (Blankenship *et al.* 2010; Eisman *et al.* 2006, unpublished results from Ramírez-Zavala). It is clear, however that many of the tested kinases in some way regulate Czf1 protein levels, which may be a mode of regulation of Czf1 – though protein levels were also unchanged in the wild type in response to cell wall stress.

3.3.1 Transcriptional regulation by Czf1

Czf1 lacks a homolog in *S. cerevisiae*, but past investigations in *C. albicans* have defined a role for it as a regulator of morphogenesis which acts opposite of Efg1 as an activator of filamentation in agar-embedded cells as well as promotes white-to-opaque switching (Brown *et al.* 1999; Vinces and Kumamoto 2007). Limited evidence did suggest a relationship between cell wall integrity and Czf1. Dhamgaye *et al.* 2012 found that *CZF1* was highly ex-

pressed in a fluconazole clinical isolate; that work found that *czf1*Δ mutants had increased susceptibilities to fluconazole (a result not found in this study and which a later work also did not find (Vasicek *et al.* 2014)) as well as terbinamyin and ansiomycin and increased resistance to Congo red (similar to results seen here), but did not regulate common drug resistance-associated genes. In that study, it was however shown that deletion of *CZF1* resulted in increased expression of the β-glucan synthase subunit *GSL1*. The results described here do not find this; rather, it seems that artificial activation of Czf1 has a minor activating effect on *GSL1*, if anything (Figure 2.26). This could contribute to the observed increase in resistance to cell wall stress in strains expressing that form of Czf1. If this opposite were true, that *czf1* deletion resulted in deficient *GSL1* expression, it would comfortably explain the hypersensitivity of *czf1*Δ mutants to caspofungin; this, however, was not the case.

One previous work has investigated the transcriptional role of Czf1 across the whole genome. Hernday *et al.* 2013 examined the transcriptome of white and opaque strains of the *czf1*Δ mutant in comparison to the wild type for each cell morphology. That work found a fairly limited set of only seven genes which were significantly differentially expressed dependent on Czf1. They hypothesized that Czf1 largely enacted its role in white-opaque switching via regulation of *EFG1* expression. The small number of differentially expressed genes in the deletion mutant contrasts with the 211 genes which were significantly activated by artificial activation of Czf1. Interestingly, the two experiments seem to conflict in some respects. For example, Hernday *et al.* 2013 found that *XOG1* expression was increased in the deletion mutant. Here it was shown that *XOG1* expression is increased by activation of Czf1. Interestingly, deletion of *XOG1*, which encodes an exoglucanase, results in increased susceptibility to drugs which target chitin and β-glucan synthesis (González *et al.* 1997). Additionally, very recent work has shown that deletion of *XOG1* also results in defective lactate-induced glucan masking, discussed in section 1.3, and deletion of *CZF1* has a similar effect (Childers *et al.* 2020). Taken together, these results connect Czf1 and modulation of the cell wall.

The RNA sequencing experiment conducted here also suggests other cell wall related roles for Czf1. All of the most highly enriched GO terms related somehow to the cell wall, including genes related to its construction. One class of genes which stood out were mannosyltransferases, several of which were activated, others repressed. Mutants deficient in mannosylation are known to be hypersusceptible to cell wall stress (Kapteyn *et al.* 2000; Hall *et al.* 2013). It may be that Czf1-regulated modulation of mannosylation is at least partially responsible for the restorative effect of Czf1 activation on cell

wall defective mutants. While fluorescence microscopy was unsuccessful in showing any change in mannan in the *snf4*Δ mutant nor in strains expressing artificially activated Czf1 (Figure 2.27), investigation at a much higher resolution using transmission electron microscopy revealed differences in the cell wall – it is possible that the amount of mannan is not notably affected, while the pattern or specific types of mannosylation differ. Interestingly, the dimensions of the inner or outer cell walls of kinase mutants which exhibited hypersusceptibility to cell wall stresses were not necessarily different from the wild type (indeed, in the *snf4*Δ mutant, neither differed), and in some cases one or both layers were thicker, in other cases thinner. The relationship between cell wall integrity is not directly correlated with the thickness of the cell wall.

Artificial activation of Czf1 also has diverse effects in different mutant backgrounds, also resulting in thicker or thinner inner or outer cell walls, not correlating with the ability of the mutant to improve resistance to cell wall stresses. Generally, however, activation of Czf1 had a marked impact on the outer cell wall, if not in length, at least in morphology. In nearly all mutant backgrounds, expression of artificially activated Czf1 resulted in a distinctly fibrous appearance, where individual (presumably mannan) fibrils were distinguishable, rather than a homogeneous dark band seen in other strains. It is important here to note that the method used to fix cells for this type of microscopy affects the appearance of the outer cell wall. Here, chemical fixation was used, which tends to result in shorter mannan fibrils in contrast with samples prepared by freezing methods (compare for example Böhm *et al.* 2016, which used chemical fixation, to Hall *et al.* 2013, where freezing was employed). Nonetheless, the methodology used here was sufficient for comparisons between similarly prepared strains, and differences in the outer cell wall were apparent. Thus Czf1 appears to regulate cell wall architecture, and particularly affects mannosylation of the cell wall.

3.4 *SNF1* is not an essential gene

One of the most unusual aspects of SNF1 in *C. albicans* has long been the apparent essentiality of the catalytic α-subunit Snf1. Sc*SNF1* is not an essential gene when cells are grown using glucose as the carbon source, but several published attempts to delete its *C. albicans* homolog have reported the inability to obtain null mutants (Petter *et al.* 1997; Enloe *et al.* 2000; Ramírez-Zavala *et al.* 2017). These attempts have employed diverse strategies. Petter *et al.* 1997 generated a heterozygous *SNF1* mutant using the recyclable *URA*-blaster method which relies on a uracil auxotrophic parental

strain and growth on uracil deficient (and by necessity minimal) medium followed by secondary selection for marker excision on media containing 5-fluoroorotic acid, which is toxic to uracil prototrophic cells. Four separate deletion cassettes were used in attempts to delete the remaining allele; all resulted in uracil prototrophic transformants which still expressed *SNF1*.

Enloe *et al.* 2000 described a single-transformation method to generate homozygous mutants and test for gene essentiality. Their approach also required selection on minimal media, starting with a parental strain which is auxotrophic for both arginine and uracil biosynthesis. There, the deletion cassette contains *ARG4* flanked by partial, nonfunctional fragments of *URA3*, which upon recombination with one another can excise *ARG4* and restore *URA3* functionality. Homozygous deletion relies on secondary recombination of the deletion cassette following the first transformation to replace the second allele; the rare spontaneous excision of *ARG4* in one allele therefore resulting in arginine and uracil prototrophic cells. In cases where the target gene is essential, and as was observed with *SNF1*, such doubly prototrophic strains exhibit trisomies and still express the gene of interest.

Ramírez-Zavala *et al.* 2017 used the recyclable *SAT1*-flipper cassette, which does not rely on auxotrophic parental strains, instead utilizing *SAT1*, which encodes for resistance to the drug nourseothricin. Transformants are selected on media containing nourseothricin. The deletion cassette is also flanked by FRT recombination sites and contains the *FLP*-recombinase gene under the control of an inducible promoter, allowing for excision and further usage of the same marker. Much like in the first published attempt, heterozygous mutants were viable, but no null mutants were identified following the second round of transformation.

Recently, Lagree *et al.* 2020 seemed to have solved the puzzle of *SNF1* essentiality. They found that deletion of *MIG1* allowed for *SNF1* to additionally be deleted. Thus it seemed that hyperrepression of some target or targets results in cell death. Therefore, Snf1 was required to be present unless Mig1 was absent. They speculated that a general repression of glucose transporters regulated by Mig1 was key to this. Prior to the publication of these results, the nature of *SNF1* essentiality was also investigated for this work. To this end, an inducible gene deletion approach was used, similar to that described in Michel *et al.* 2002, to investigate the phenotype of cells lacking *SNF1* just prior to death. Surprisingly, following induced excision of *SNF1*, cells remained viable as very small colonies which continued to grow following prolonged incubation (Figure 2.32). In fact, when plates were incubated at 37°C instead of the typical 30°C, the colonies grew nearly as well as the control strains which retained one allele of *SNF1*. Using this knowledge, the technique used in Ramírez-Zavala *et al.* 2017 was repeated with alterations

in temperature and incubation time for growth on selective media, and again null mutants were obtained.

In addition to the above described attempts to delete *SNF1*, Vyas *et al.* 2015 described additional evidence that suggested *SNF1* was essential. There, a *Candida* adapted CRISPR system was used to introduce a glucose repressible promoter in front of both alleles of *SNF1*, and as a result, transformants were apparently unable to grow on glucose. Interestingly, that experiment was conducted using the same growth conditions that were here shown to be optimal for identifying *snf1* null mutants; three days of incubation on rich medium at 37°C. This raises a question of why they did not observe growth when *SNF1* expression was repressed. Notably, even when grown in medium containing maltose, in which *SNF1* should be expressed, the strains grew fairly poorly; possibly *SNF1* expression even in this condition was below that of the wild type. One possibility is that the strain which was used in that work contained some additional mutation which resulted in a growth defect which exhibited a synthetic lethality with the glucose-induced repression of *SNF1*. This work also generated *SNF1* mutants in which kinase activity was abolished; surprisingly, in contrast to their experiment in*SNF1* essentiality, these strains grew fairly well at 37°C, and poorly at 30°C. Thus they concluded that Snf1 catalytic activity was not essential as it related to the overall viability of the cell. In contrast, here it has been shown that such kinase-dead mutants have an identical phenotype to the *snf1*Δ strains. This result is meaningful for two reasons. On one hand, it shows that Snf1 catalytic activity fully accounts for the role of SNF1 in growth. On the other hand, it provides an added layer of evidence that *SNF1* is not essential.

Though the possibility does exist that suppressor mutations have arisen which circumvent the essentiality of *SNF1*, the facts that the number of small colonies in the original inducible deletion experiment are comparable to the number of colonies from the control strains, and the reproducibility of the *snf1*Δ phenotype across two separate deletion techniques make this unlikely. Furthermore, the identical phenotype of *snf1*Δ mutants and those expressing catalytically inactive Snf1 suggests that the growth of the null mutants was not due to appearance of suppressor mutations. Additional experimentation also likely explains why the previous attempts were unsuccessful. Strains lacking *SNF1* grow extremely poorly on minimal media, to the point that a small number of transformant colonies are unlikely to be identified. For selection on nourseothricin, the incubation time/temperature typically used was insufficient for visible colonies to appear. The inducible gene deletion system used here is thus not only a useful approach for investigating truly essential genes, but a powerful tool for determining the essentiality of genes. Because the final excision of the gene of interest is highly efficient and does

not require specific conditions to select for null mutants, cells can be grown on any condition one may desire to find conditions where such a mutant is viable.

3.5 Conclusions

The original goal of this work was to characterize novel downstream elements of the SNF1 pathway in *C. albicans*. While this original goal was not met, new and interesting goals were formed and met during this process. The work presented here has uncovered unexpected results relating to signal transduction pathways which respond to various stresses. Mig1 and Mig2, known targets of ScSNF1, were shown to indeed be conserved targets. Surprisingly, both appear to be phosphorylated dependent on SNF1 activity in response to growth on alternative carbon sources – something that is not true of ScMig2. Furthermore, both appear to be regulated at the level of protein accumulation. This is the case for ScMig2, but not ScMig1, which is instead regulated by nuclear export/import. Thus even when a regulatory pathway is conserved, the fine details of the interaction between components of the pathway and the consequences of these interactions (in this case, phosphorylation by SNF1), have diverged.

In the search for novel targets of SNF1, an unusual mutation which rendered Snf1 independent from regulation by Snf4 was discovered. Rather than a point mutation or random insertion or deletion, the in-frame $SNF1^{\Delta 311\text{-}316}$ mutation occurred via recombination across a repeated segment of the *SNF1* coding sequence. This may be a preprogrammed event, a rapid-response option for responding to some (yet undetermined) stress in which such a mutation is advantageous. Other suppressor mutants were also identified, but their investigation is ongoing and may finally reveal novel targets of SNF1.

Screening a library of artificially activated ZCFs in an attempt to characterize one as a target of SNF1 instead uncovered a little-described role for Czf1 as a regulator of cell wall integrity which has yet to be tied to signaling pathways which normally regulate cell wall integrity. It appears to affect several aspects of cell wall structure, overall affecting the architecture and integrity of the cell wall. It was shown to be phosphorylated, but the purpose of this modification and the kinase or kinases responsible remain a mystery.

Finally, a long-standing puzzle has been solved: Why is SNF1 essential? In line with the other work presented here, the answer was in fact that the question was wrong. Using a nontraditional approach to gene deletion, indeed with the original goal of answering this question, null mutants were finally obtained. Further investigation uncovered the likely reasons why all

published (and perhaps some unpublished) attempts over the last several decades were unsuccessful in generating such knockouts. Taken together, the work presented here was unsuccessful in its goals; more importantly, however, it was successful in describing a multitude of discoveries which enrich the understanding of regulatory pathways within *C. albicans*.

4. Methods and Materials

4.1 Devices, solutions, and media

The devices, solutions, and media used in this study are listed in Tables 4.1 and 4.2.

Table 4.1: Devices used in this study.

Device	Manufacturer
30°C Incubator Model 400	Memmert
37°C Incubator Model B6200	Heraeus
APT.line KB (E3.1) Refrigerated Incubator	Binder
Biophotometer	Eppendorf
Cawomat 2000 IR Automatic Film Processor	CAWO Photochemisches Werk GmbH
Certomat BS-1 30°C Shaking Incubator	Sartorius
Coolpix E4500 Digital Camera	Nikon
D5300 HDSLR Digital Camera	Nikon
EasyjecT prima Eletroporator	Equibio
FastPrep®-24 Tissue and Cell Homogenizer	MP Biomedicals
Heraeus Fresco 21 Refrigerated Biofuge, Pico 21 Biofuge, Megafuge 1.0R	Thermo Scientific
Infinite® 200 PRO Microplate Reader	Tecan

Table 4.1: Devices used in this study.

Device	Manufacturer
InoLab pH Level 1 pH Meter	WTW
iX20 Gel Imager	Intas
AF 6000 LX Widefield Microscope System	Leica Microsystems
Mini-PROTEAN Tetra Cell Vertical Electrophoresis Chamber	Bio-Rad
Mixing Block MB-102 Heat Block	Bioer
OV2 Hybridization Oven	Biometra
peqSTAR X Thermocylcer	VWR Peqlab
PowerPac 300 Power Supply Unit	Bio-Rad
RC-5B Plus Superspeed Centrifuge	Sorvall
Replica Plater for 96-well plate	Sigma Aldrich
Stratalinker® 1800 UV Crosslinker	Stratagene
SMZ800N Stereomicroscope	Nikon
SpeedVac SC110 Centrifugal Evaporator	Savant
Sub Cell GT/Mini Sub Cell GT Horizontal Electrophoresis Chamber	Bio-Rad
TH15 37°C Shaking Incubator	Edmund Bühler, Johanna Otto GmbH
VacuGene XL Vacuum Blotting Unit and Pump	General Electric
Vortex Genie 2 Vortexer	Scientific Industries, Inc
Wise Stir MS-20A	wisd Laboratory Instruments

Table 4.2: Solutions and media used in this study.

Solution or Medium	Contents
Reagent (Northern Blot)	50g Blocking Reagent (Böhringer Mannheim), 1x P1 Buffer, pH 7.5 in 500mL water
Breaking Buffer (DNA Isolation)	100mM NaCl, 10mM Tris-Cl, 1mM EDTA, 2% TritonX-100, 1% SDS
Breaking Buffer (Protein Isolation)	1% SDS, 150mM NaCl, 100mM TEAB, 1 Tablet cOmplete Ultra Protease Inhibitor Cocktail (Roche), 1 Tablet PhosSTOP (Roche) in 10mL
CI (DNA Isolation)	Chloroform-Isoamyl Alcohol (24:1)
DEPC Water	0.1% (v/v) Diethylpyrocarbonate
Laemmli Buffer 2x	4% SDS, 20% glycerol, 10% β-mercaptoethanol, 0.004% bromphenol blue, 0.125 M Tris HCl, pH 6.8
LB+Ampicillin Medium	0.5% Yeast Extract, 1% Peptone, 0.5% NaCl (+1.5% Agar for plates) supplemented with 100µg/mL Ampicillin
Lysis Buffer (High-Purity DNA Isolation)	1M Sorbitol, 100mM pH5.8 NaCit, 50 mM pH8.0 EDTA (add before using: 2% β-mercaptoethanol, 500units/mL Lyticase)
P1 Buffer 10x	1M Maleic Acid, 1.5M NaCl, pH 7.5
P2 Buffer	1x Buffer P1, 1% Blocking Reagent (Böhringer Mannheim)
P3 Buffer	100mM Tris-Cl, 100mM NaCl, 50mM $MgCl_2$, pH 9.5
PCI (DNA Isolation)	Phenol-Chloroform-Isoamyl Alcohol (25:24:1)
Ponceau S Protein Stain	0.1% w/v Ponceau S, 5% Acetic Acid
Proteinase Buffer (High Purity DNA Isolation)	10mM pH7.5 Tris-HCl, 50mM pH8.0 EDTA, 0.5% SDS (add before using: 1mg/mL Proteinase K)
RP Buffer 5x	200mM 3-(N-morpholino)propanesulfonic acid, 50mM Sodium Acetate, 10mM EDTA, pH 7
Running Buffer (Northern Blot)	1x RP Buffer, 1% Formaldehyde in DEPC water
SDS Hybridization Buffer	50% Deionized Formamide, 5x SSPC, 2% Blocking Reagent, 0.1% N-Lauroylsarcosine, 7% SDS
SDS Running Buffer 10x	4M Tris, 2M Glycine, 1% SDS

Table 4.2: Solutions and media used in this study.

Solution or Medium	Contents
Serum agar	2% Agar, 10% Fetal Calf Serum
Solution A (Southern Blot)	0.25M Hydrochloric Acid
Solution B (Southern Blot)	1.5M NaCl, 0.5M NaOH
Solution C (Southern Blot)	1.5M NaCl, 0.5M Tris-Cl pH7.5
Spider Medium	1% Nutrient Broth, 1% Mannitol, 0.2% K_2HPO_4 (+1.35% Agar for plates)
SpiderD Medium	as above, with Mannitol replaced with 2% Glucose
SSC 20x	3M NaCl, 0.3M NaCit
SSPE 20x	3M NaCl, 0.2M NaH_2PO_4, 0.02M EDTA, pH 7.4
Stripping Solution	50% Deionized Formamide, 5% SDS, 50mM Tris-Cl, pH 7.5
TAE Buffer 1x	40mM Tris, 20mM Acetic Acid, 1mM EDTA
TBST	50mM Tris, 150mM NaCl, 0.1% Tween20, pH 7.6
TE-Buffer 10x	100mM Tris-Cl pH 7.5, 10mM EDTA pH 7.5
Transfer Buffer (Western Blot)	4M Tris, 2M Glycine, 0.2% SDS
Wash Buffer I (Northern Blot)	1x SSC, 0.1% SDS
Wash Buffer I (Southern Blot)	0.5% SSC 20x, 0.4% SDS, 6M Urea
Wash Buffer II (Northern Blot)	1x Buffer P1, 0.3% Tween 20
YCB-YE-BSA Medium	2.34% Yeast Carbon Base, 0.2% Yeast Extract, 0.4% Bovine Serum Albumin, pH 4
YNB Medium	0.67% Yeast Nitrogen Base with ammonium sulfate supplemented with 2% of either Glucose, Sucrose, Potassium Acetate, or Glycerol (+2% Agar for plates)

Table 4.2: Solutions and media used in this study.

Solution or Medium	Contents
YP Medium	1% Yeast Extract, 2% Peptone supplemented with 2% of either Glucose, Sucrose, Potassium Acetate, or Glycerol (+1.5% Agar for plates) and with additional chemicals at concentrations labeled in figures

4.2 Oligonucleotides

Oligonucleotides utilized in this work are described in Table 4.3. All oligonucleotides were purchased from Eurofins Genomics (Ebersberg, Germany).

Table 4.3: Oligonucleotides used in this study.

Oligonucleotide	Sequence (5' to 3')
ACT1 termrev	GCGGACATTTTATGATGGAATGAATGGG
ADH1 prom fwd	TGATAGAGACCCAATGCAAAGCC
ADH1 prom rev	GGCACGAGACGGAAACTCTTTAGG
ADH1 term1	AAGGTGCTGAACCAAACTGTGGTGA
ADH1 term2	GACAATCTTGATTGGGCATTTGATT
CZF1.01	GTCATTTTCCCGCAACATTAGATTAG
CZF1.05	GAGCTCCGCAGAACAACAGCAACA
CZF1HA fwd XhoI	ATATCTCGAGATGAGTTCAATACCCAATAT CAATTGG
CZF1HA rev	CCGGAACATCGTATGGGTATTTACTTCTGT ATTCAACAATACCTCTC
CZF1NB.01	CCTCTCGTCAATCACAACCACAACC
CZF1NB.02	GATTCTACCAAACTCGGCATGTTC
CZF1seq.01	TTTTCGTATCTGTTCACCCCA
CZF1seq.02	GTTAAAACACTTAACATAATACAAGAGTGG TG

Table 4.3: Oligonucleotides used in this study.

Oligonucleotide	Sequence (5' to 3')
CZF1seq.03	GCTGTTGTTGCTTGACTTGTTGC
CZF1seq.04	GCAACAATTGAAATTTTTATTTTCGATTAAC
GAL8	GTTATGAGGTTCGGACCGTTGC
GSL1 NB fwd 2	GAGCACCCAGATACTAGTTCTGTGG
GSL1 NB rev	GAAATATTGGTGGGACCACAAATAGTGC
HA ACT1 term rev	GGATTACGTTAAGGAGTGAAATTCTGG
MIG1.01	ATATGAGCTCCCACCATCAACCGAACC
MIG1.02	TGTACCGCGGTGCGACGTTGATTAACTTG
MIG1.03	ATATCTCGAGGATTTATAATTACTGGTGTTTTAATTTATAGATAG
MIG1.04	ATATGGGCCCGTTATTATTCACATTCGGATAGAAC
MIG1ETfwd	ATATGTCGACATGTCTATGTCCACACCTATGC
MIG1ETrev	ATATGGATCCTTAACTTAATAAATTGGTTAAACTCATTGGTTTAGC
MIG1HA fwd	ATATGAGCTCCTTCTTCATCGACTAATTTAGCTGG
MIG1HA rev	ATATGGATCCACTTAATAAATTGGTTAAACTCATTGGTTTAGC
MIG1seq.01	CCCCATCTTGAATTACCACGG
MIG1seq.03	CTACTTGAATACCATTCATATATCATGC
MIG1seq.05	CAACAACAGCAACAAACAAATATTGG
MIG1seq.06	CTTTCAGATGATGAACTTGTACC
MIG2.01	ATATGAGCTCCTTAATAACCTTTGCCAAGTCCCC
MIG2.02	ATATCCGCGGGGAGTGGTATGGTGATGGTTTTGG
MIG2.03	ATATCTCGAGGATACCTTATATACCTACTTGCC

Table 4.3: Oligonucleotides used in this study.

Oligonucleotide	Sequence (5' to 3')
MIG2.04	ATATGGGCCCAATGCTTATATGAGTGACAACG
MIG2seq.01	GCTGGTGTTGAAAGAGAGAGG
MNN45 NB fwd	ATGTCGCTCGTTAAATCAATAACATCG
MNN45 NB rev	ATGCTTTTCTTAAAGGTTTAACCATTTTTAAACC
NBHGT10.01	TGCCACACTTGGGTTTTCAC
NBHGT10.02	ATACCAACGGCAGCACCTTT
NBMAL2.01	AACCACACTTCGGTTGAGCA
NBMAL2.02	GCAATGAATGGTCGTCACCG
SAP2 P3	TTAACCAATGACATCAGAAATAGAAAGACGCC
SAP2 P4	CGCACGCGTGAATTATTGGTACTAGAAAGG
SCH9.01	ACTTGAGCTCCGACCATGAAGATGAGTG
SCH9.04	CAAGGGGCCCATAGAATATATACAACTATCAG
SCH9seq.01	GAAGGAGAAAAAGTAGGAACGG
SCH9seq.02	GGAGCTAAATATTCGGTGG
SCH9seq.03	GGGGTTGGAAGAATCATTGGG
SCH9seq.04	GGCCAAGTTTTCCAAGTTCG
SNF1.01	ATCCGAGCTCACACAAAAGACAAGAAC
SNF1.04	AAGTGGGCCCATTAAAATTGGTTGAATTTATTG
SNF1.05	AAGTCCGCGGATTAAAATTGGTTGAATTTATTG
SNF1.06	GTCAGAGCAAGCCCAAACTC
SNF1.09	GCCAGATTATTTGTTACCGCC
SNF1.10	GGCGGTAACAAATAATCTGGC
SNF1.12	ATATGAGCTCCCGAGTCCACACAAAAGACAAGAAC

Table 4.3: Oligonucleotides used in this study.

Oligonucleotide	Sequence (5' to 3')
SNF1.13	ATATCCGCGGGCAACACCAAAGCCATAGTAAAAATGATTAAC
SNF1d311-316.01	TATGCCAGATTTATCCAAAAACAAGAATAGCAAG
SNF1d311-316.02	GGATATCTGGCATATCTTGTTTAAACCATTCATC
SNF1d311-316.03	GGTTTAAACAAGATATGCCAGATTTATCCAAAAACAAGAATAGCAAG
SNF1d311-316.04	CTTGCTATTCTTGTTTTTGGATAAATCTGGCATATCTTGTTTAAACC
SNF1dC311.03	CTTACTTTATTTTAATCTGGCATATCTTGTTTAAACCATTCATC
SNF1dC311.04	GATATGCCAGATTAAAATAAAGTAAGTAAGTACTAGCTTAGATTGGATG
SNF1G51R.01	AGAATAAGACGGTATCAAATTCTCAAGACATT
SNF1-GFP.01	TCATGAGCTCAGCAATCGAAATCAAGTAATGAGATAT
SNF1in.04	ACGGTCATATCCCATCGTCACC
SNF1in-seq.01	GGCATCTTGTGGATCTCCT
SNF1in-seq.02	GGCAATACTCTACAGCAGC
SNF1K82R.03	GGCACAGGTCAAAAAGTTGCTTTGAGAATCATTAATCGTAAAACATTAGC
SNF1K82R.04	GCTAATGTTTTACGATTAATGATTCTCAAAGCAACTTTTTGACCTGTGCC

4.3 Plasmids

Plasmids utilized in this study are detailed in Table 4.4. All plasmids were propagated via expression in DH5α *E. coli*.

Table 4.4: Plasmids used in this study.

Plasmid	Description	Source
pMIG1M1	*SAT1*-Flipper cassette for *MIG1* deletion	Mottola et al, 2020, This study
PMIG2M1	*SAT1*-Flipper cassette for *MIG2* deletion	Mottola et al, 2020, This study
pMIG1H1	Cassette for expression of 3xHA tagged Mig1.	This study
pSNF1^{L181I}	Cassette containing the *SNF1*^{L181I} mutant allele	Ramírez-Zavala et al, 2017
pSNF1$^{\Delta 311\text{-}316}$	Cassette containing the *SNF1*$^{\Delta 311\text{-}316}$ mutant allele	Mottola and Morschhäuser, 2019, This study
pSNF1$^{\Delta C310}$	Cassette containing the *SNF1*$^{\Delta C310}$ mutant allele	Mottola and Morschhäuser, 2019, This study
pSNF1$^{\Delta C340}$	Cassette containing the *SNF1*$^{\Delta C340}$ mutant allele	Ramírez-Zavala et al, 2017
pSNF1^{K84R}	Cassette containing the *SNF1*^{K84R} mutant allele	Mottola et al, 2020, This study
pCZF1GAD1	Cassette for expression of *CZF1* fused with 3xHA and the *GAL4* activation domain from *S. cerevisiae,* under control of the *ADH1* promoter	Schillig and Morschhäuser, 2013
pUME6GAD1	Cassette for expression of *UME6* fused with 3xHA and the *GAL4* activation domain from *S. cerevisiae,* under control of the *ADH1* promoter	Schillig and Morschhäuser, 2013
pCZF1M2	*SAT1*-Flipper cassette for *CZF1* deletion	Mottola et al, submitted manuscript
pCZF1H1	Cassette for expression of 3xHA tagged Czf1.	Mottola et al, submitted manuscript
pCZF1K1	Complementation cassette for *CZF1*	This study
pCZF1E1	Cassette for expression of *CZF1* at the *ADH1* promoter	This study
pSNF1M1	*SAT1*-Flipper cassette for *SNF1* deletion	Ramírez-Zavala et al, 2017
pSNF1ex3	Cassette containing *SNF1* and *HygB* flanked by FRT sites and then by regions of the *ADH1* locus for integration at that site	Mottola et al, 2020
pSAP2FL1	Contains FLP recombinase under the control of the *SAP2* promoter	Mottola et al, 2020
pTET1-CZF1	Contains *CZF1,* used in construction of pCZF1E1	Ramírez-Zavala et al, 2008
pUPC2E1	Plasmid containing *UPC2* under control of the *ADH1* promoter, vector without *UPC2* was used to construct pCZF1E1	Schillig and Morschhäuser, 2013

4.4 *Candida albicans* strains

Candida albicans strains used in this study are described in Table 4.5. For all strains except suppressor strains, two mutants were constructed independently, labeled either A or B.

Table 4.5: Strains used in this study

Strain	Genotype	Reference
SC5314	Wild Type	Gillum et al, 1984
SCSNF4M4A/B	*snf4*Δ::*FRT*/*snf4*Δ::*FRT*	Ramirez-Zavala et al, 2017
SCΔ*snf4*MIG1M1A/B	*snf4*Δ::*FRT*/*snf4*Δ::*FRT*	Mottola et al, 2020, This study
	MIG1/*mig1*::*SAT1-FLP*	
SCΔ*snf4*MIG1M2A/B	*snf4*Δ::*FRT*/*snf4*Δ::*FRT*	Mottola et al, 2020, This study
	MIG1/*mig1*Δ::*FRT*	
SCΔ*snf4*MIG1M3A/B	*snf4*Δ::*FRT*/*snf4*Δ::*FRT*	Mottola et al, 2020, This study
	*mig1*Δ::*FRT*/*mig1*::*SAT1-FLP*	
SCΔ*snf4*MIG1M4A/B	*snf4*Δ::*FRT*/*snf4*Δ::*FRT*	Mottola et al, 2020, This study
	*mig1*Δ::*FRT*/*mig1*Δ::*FRT*	
SCΔ*snf4*Δ*mig1*MIG2M1A/B	*snf4*Δ::*FRT*/*snf4*Δ::*FRT*	Mottola et al, 2020, This study
	*mig1*Δ::*FRT*/*mig1*Δ::*FRT*	
	MIG2/mig2::*SAT1-FLP*	
SCΔ*snf4*Δ*mig1*MIG2M2A/B	*snf4*Δ::*FRT*/*snf4*Δ::*FRT*	Mottola et al, 2020, This study
	*mig1*Δ::*FRT*/*mig1*Δ::*FRT*	
	MIG2/*mig2*Δ::*FRT*	
SCΔ*snf4*Δ*mig1*MIG2M3A/B	*snf4*Δ::*FRT*/*snf4*Δ::*FRT*	Mottola et al, 2020, This study
	*mig1*Δ::*FRT*/*mig1*Δ::*FRT*	
	*mig2*Δ::*FRT*/mig2::*SAT1-FLP*	
SCΔ*snf4*Δ*mig1*MIG2M4A/B	*snf4*Δ::*FRT*/*snf4*Δ::*FRT*	Mottola et al, 2020, This study
	*mig1*Δ::*FRT*/*mig1*Δ::*FRT*	
	*mig2*Δ::*FRT*/*mig2*Δ::*FRT*	
SCMIG1M1A/B	*MIG1*/*mig1*::*SAT1-FLP*	This study
SCMIG1M2A/B	*MIG1*/*mig1*Δ::*FRT*	This study
SCMIG1M2H1A/B	*MIG1-3xHA-SAT1-FLP*/*mig1*Δ::*FRT*	This study
SCMIG1M2H2A/B	*MIG1-3xHA-FRT*/*mig1*Δ::*FRT*	This study
SCΔ*snf4*MIG1M2H1A/B	*snf4*Δ::*FRT*/*snf4*Δ::*FRT*	This study
	MIG1-3xHA-SAT1-FLP/*mig1*Δ::*FRT*	
SCΔ*snf4*MIG1M2H2A/B	*snf4*Δ::*FRT*/*snf4*Δ::*FRT*	This study
	MIG1-3xHA-FRT/*mig1*Δ::*FRT*	
SCMIG2M2H2A/B	*MIG2-3xHA-FRT*/*mig2*Δ::*FRT*	Weber 2020

Table 4.5: Strains used in this study

Strain	Genotype	Reference
SCΔ*snf4*MIG2M2H2A/B	*snf4*Δ::*FRT*/*snf4*Δ::*FRT*	Weber 2020
	MIG2-3xHA-FRT/*mig2*Δ::*FRT*	
SCΔ*snf4*SupA	*snf4*Δ::*FRT*/*snf4*Δ::*FRT*	This study
	unknown suppressor mutation	
SCΔ*snf4*SupB	*snf4*Δ::*FRT*/*snf4*Δ::*FRT*	Mottola and Morschhäuser 2019, This study
	SNF1/*SNF1*$^{\Delta 311\text{-}316}$	
SCΔ*snf4*SupC	*snf4*Δ::*FRT*/*snf4*Δ::*FRT*	Mottola and Morschhäuser 2019, This study
	unknown suppressor mutation	
SCΔ*snf4*SNF1$^{\mathrm{L181I}}$M1A/B	*snf4*Δ::*FRT*/*snf4*Δ::*FRT*	Mottola and Morschhäuser 2019, This study
	SNF1/*SNF1*^{L181I}-*SAT1-FLP*	
SCΔ*snf4*SNF1$^{\mathrm{L181I}}$M2A/B	*snf4*Δ::*FRT*/*snf4*Δ::*FRT*	Mottola and Morschhäuser 2019, This study
	SNF1/*SNF1*^{L181I}-*FRT*	
SCΔ*snf4*SNF1$^{\mathrm{L181I}}$M3A/B	*snf4*Δ::*FRT*/*snf4*Δ::*FRT*	Mottola and Morschhäuser 2019, This study
	SNF1^{L181I}-*FRT*/*SNF1*^{L181I}-*SAT1-FLP*	
SCΔ*snf4*SNF1$^{\mathrm{L181I}}$M4A/B	*snf4*Δ::*FRT*/*snf4*Δ::*FRT*	Mottola and Morschhäuser 2019, This study
	SNF1^{L181I}-*FRT*/*SNF1*^{L181I}-*FRT*	
SCΔ*snf4*SNF1$^{\Delta 311\text{-}316}$M1A/B	*snf4*Δ::*FRT*/*snf4*Δ::*FRT*	Mottola and Morschhäuser 2019, This study
	SNF1/*SNF1*$^{\Delta 311\text{-}316}$-*SAT1-FLP*	
SCΔ*snf4*SNF1$^{\Delta 311\text{-}316}$M2A/B	*snf4*Δ::*FRT*/*snf4*Δ::*FRT*	Mottola and Morschhäuser 2019, This study
	SNF1/*SNF1*$^{\Delta 311\text{-}316}$-*FRT*	
SCΔ*snf4*SNF1$^{\Delta 311\text{-}316}$M3A/B	*snf4*Δ::*FRT*/*snf4*Δ::*FRT*	Mottola and Morschhäuser 2019, This study
	SNF1$^{\Delta 311\text{-}316}$-*FRT*/*SNF1*$^{\Delta 311\text{-}316}$-*SAT1-FLP*	
SCΔ*snf4*SNF1$^{\Delta 311\text{-}316}$M4A/B	*snf4*Δ::*FRT*/*snf4*Δ::*FRT*	Mottola and Morschhäuser 2019, This study
	SNF1$^{\Delta 311\text{-}316}$-*FRT*/*SNF1*$^{\Delta 311\text{-}316}$-*FRT*	
SCΔ*snf4*SNF1$^{\Delta \mathrm{C310}}$M1A/B	*snf4*Δ::*FRT*/*snf4*Δ::*FRT*	Mottola and Morschhäuser 2019, This study
	SNF1/*SNF1*$^{\Delta C310}$-*SAT1-FLP*	
SCΔ*snf4*SNF1$^{\Delta \mathrm{C310}}$M2A/B	*snf4*Δ::*FRT*/*snf4*Δ::*FRT*	Mottola and Morschhäuser 2019, This study

Table 4.5: Strains used in this study

Strain	Genotype	Reference
	SNF1/SNF1$^{\Delta C310}$*-FRT*	
SCΔ*snf4*SNF1$^{\Delta C340}$M1A/B	*snf4*Δ::*FRT/snf4*Δ::*FRT*	Ramirez-Zavala et al, 2017
	SNF1/SNF1$^{\Delta C340}$*-SAT1-FLP*	
SCΔ*snf4 SNF1*/$^{\Delta C340}$M2A/B	*snf4*Δ::*FRT/snf4*Δ::*FRT*	Ramirez-Zavala et al, 2017
	SNF1/SNF1$^{\Delta C340}$*-FRT*	
SC3840M4A/B	*sak1*Δ::*FRT/sak1*Δ::*FRT*	Ramirez-Zavala et al, 2017
SCKIS1M4A/B	*kis1*Δ::*FRT/kis1*Δ::*FRT*	Ramirez-Zavala et al, 2017
SCΔ*kis1*SNF1$^{\Delta 311\text{-}316}$M1A/B	*kis1*Δ::*FRT/kis1*Δ::*FRT*	Mottola and Morschhäuser 2019, This study
	SNF1/SNF1$^{\Delta 311\text{-}316}$*-SAT1-FLP*	
SCΔ*kis1*SNF1$^{\Delta 311\text{-}316}$M2A/B	*kis1*Δ::*FRT/kis1*Δ::*FRT*	Mottola and Morschhäuser 2019, This study
	SNF1/SNF1$^{\Delta 311\text{-}316}$*-FRT*	
SCΔ*kis1*SNF1$^{\Delta 311\text{-}316}$M3A/B	*kis1*Δ::*FRT/kis1*Δ::*FRT*	Mottola and Morschhäuser 2019, This study
	SNF1$^{\Delta 311\text{-}316}$*-FRT/SNF1*$^{\Delta 311\text{-}316}$*-SAT1-FLP*	
SCΔ*kis1*SNF1$^{\Delta 311\text{-}316}$M4A/B	*kis1*Δ::*FRT/kis1*Δ::*FRT*	Mottola and Morschhäuser 2019, This study
	SNF1$^{\Delta 311\text{-}316}$*-FRT/SNF1*$^{\Delta 311\text{-}316}$*-FRT*	
SCSNF1$^{\Delta 311\text{-}316}$M1A/B	*SNF1/SNF1*$^{\Delta 311\text{-}316}$*-SAT1-FLP*	Mottola and Morschhäuser 2019, This study
SCSNF1$^{\Delta 311\text{-}316}$M2A/B	*SNF1/SNF1*$^{\Delta 311\text{-}316}$*-FRT*	Mottola and Morschhäuser 2019, This study
SCSNF1$^{\Delta 311\text{-}316}$M3A/B	*SNF1*$^{\Delta 311\text{-}316}$*-FRT/SNF1*$^{\Delta 311\text{-}316}$*-SAT1-FLP*	Mottola and Morschhäuser 2019, This study
SCSNF1$^{\Delta 311\text{-}316}$M4A/B	*SNF1*$^{\Delta 311\text{-}316}$*-FRT/SNF1*$^{\Delta 311\text{-}316}$*-FRT*	Mottola and Morschhäuser 2019, This study
SCΔ*snf4*CZF1GAD1A/B	*snf4*Δ::*FRT/snf4*Δ::*FRT*	Mottola and Morschhäuser 2019, This study
	ADH1/adh1::P$_{ADH1}$*-CZF1-GAL4AD-3xHA-SAT1*	
SCΔ*snf4*UME6GAD1A/B	*snf4*Δ::*FRT/snf4*Δ::*FRT*	This study
	ADH1/adh1::P$_{ADH1}$*-UME6-GAL4AD-3xHA-SAT1*	
SCΔ*snf4*CZF1E1A/B	*snf4*Δ::*FRT/snf4*Δ::*FRT*	This study
	ADH1/adh1::P$_{ADH1}$*-CZF1-SAT1*	
SCCZF1M1A/B	*CZF1/czf1*::*SAT1-FLP*	This study
SCCZF1M2A/B	*CZF1/czf1*Δ::*FRT*	This study
SCCZF1M3A/B	*czf1*Δ::*FRT/czf1*::*SAT1-FLP*	This study

Table 4.5: Strains used in this study

Strain	Genotype	Reference
SCCZF1M4A/B	*czf1*Δ::*FRT*/*czf1*Δ::*FRT*	This study
SCCZF1MK1A/B	*CZF1-SAT1-FLP*/*czf1*Δ::*FRT*	This study
SCCZF1MK2A/B	*CZF1-FRT*/*czf1*Δ::*FRT*	This study
SCCZF1E1A/B	*ADH1*/*adh1*::P*ADH1-CZF1-SAT1*	This study
SCCZF1GAD1A/B	*ADH1*/*adh1*::P*ADH1-CZF1-GAL4AD-3xHA-SAT1*	Schillig and Morschhäuser, 2013
SCCZF1H1A/B	*CZF1*/*CZF1-3xHA-SAT1*	This study
SCCLA4M4A/B	*cla4*Δ::*FRT*/*cla4*Δ::*FRT*	Ramírez-Zavala and Morschhäuser, unpublished
SCIRE1M4A/B	*ire1*Δ::*FRT*/*ire1*Δ::*FRT*	Ramírez-Zavala and Morschhäuser, unpublished
SCKIN2M4A/B	*kin2*Δ::*FRT*/*kin2*Δ::*FRT*	Ramírez-Zavala and Morschhäuser, unpublished
SCMCK1M4A/B	*mck1*Δ::*FRT*/*mck1*Δ::*FRT*	Ramírez-Zavala and Morschhäuser, unpublished
SCMKC1M4A/B	*mkc1*Δ::*FRT*/*mkc1*Δ::*FRT*	Ramírez-Zavala and Morschhäuser, unpublished
SCMKK2M4A/B	*mkk2*Δ::*FRT*/*mkk2*Δ::*FRT*	Ramírez-Zavala and Morschhäuser, unpublished
SCNIK1M4A/B	*nik1*Δ::*FRT*/*nik1*Δ::*FRT*	Ramírez-Zavala and Morschhäuser, unpublished
SCPAN3M4A/B	*pan3*Δ::*FRT*/*pan3*Δ::*FRT*	Ramírez-Zavala and Morschhäuser, unpublished
SCSSN3M4A/B	*ssn3*Δ::*FRT*/*ssn3*Δ::*FRT*	Ramírez-Zavala and Morschhäuser, unpublished
SCYCK2M4A/B	*yck2*Δ::*FRT*/*yck2*Δ::*FRT*	Ramírez-Zavala and Morschhäuser, unpublished
SCΔ*cla4*CZF1GAD1A/B	*cla4*Δ::*FRT*/*cla4*Δ::*FRT*	This study
	ADH1/*adh1*::P$_{ADH1}$-*CZF1-GAL4AD-3xHA-SAT1*	
SCΔ*ire1*CZF1GAD1A/B	*ire1*Δ::*FRT*/*ire1*Δ::*FRT*	This study
	ADH1/*adh1*::P$_{ADH1}$-*CZF1-GAL4AD-3xHA-SAT1*	
SCΔ*kin2*CZF1GAD1A/B	*kin2*Δ::*FRT*/*kin2*Δ::*FRT*	This study
	ADH1/*adh1*::P$_{ADH1}$-*CZF1-GAL4AD-3xHA-SAT1*	
SCΔ*mck1*CZF1GAD1A/B	*mck1*Δ::*FRT*/*mck1*Δ::*FRT*	This study
	ADH1/*adh1*::P$_{ADH1}$-*CZF1-GAL4AD-3xHA-SAT1*	
SCΔ*mkc1*CZF1GAD1A/B	*mkc1*Δ::*FRT*/*mkc1*Δ::*FRT*	This study
	ADH1/*adh1*::P$_{ADH1}$-*CZF1-GAL4AD-3xHA-SAT1*	
SCΔ*mkk2*CZF1GAD1A/B	*mkk2*Δ::*FRT*/*mkk2*Δ::*FRT*	This study
	ADH1/*adh1*::P$_{ADH1}$-*CZF1-GAL4AD-3xHA-SAT1*	
SCΔ*nik1*CZF1GAD1A/B	*nik1*Δ::*FRT*/*nik1*Δ::*FRT*	This study
	ADH1/*adh1*::P$_{ADH1}$-*CZF1-GAL4AD-3xHA-SAT1*	

Table 4.5: Strains used in this study

Strain	Genotype	Reference
SCΔ*pan3*CZF1GAD1A/B	*pan3*Δ::*FRT*/*pan3*Δ::*FRT*	This study
	ADH1/*adh1*::P_{ADH1}-*CZF1-GAL4AD-3xHA-SAT1*	
SCΔ*sak1*CZF1GAD1A/B	*sak1*Δ::*FRT*/*sak1*Δ::*FRT*	This study
	ADH1/*adh1*::P_{ADH1}-*CZF1-GAL4AD-3xHA-SAT1*	
SCΔ*ssn3*CZF1GAD1A/B	*ssn3*Δ::*FRT*/*ssn3*Δ::*FRT*	This study
	ADH1/*adh1*::P_{ADH1}-*CZF1-GAL4AD-3xHA-SAT1*	
SCΔ*yck2*CZF1GAD1A/B	*yck2*Δ::*FRT*/*yck2*Δ::*FRT*	This study
	ADH1/*adh1*::P_{ADH1}-*CZF1-GAL4AD-3xHA-SAT1*	
SCΔcla4CZF1H1A/B	*cla4*Δ::*FRT*/*cla4*Δ::*FRT*	This study
	CZF1/*CZF1-3xHA-SAT1*	
SCΔire1CZF1H1A/B	*ire1*Δ::*FRT*/*ire1*Δ::*FRT*	This study
	CZF1/*CZF1-3xHA-SAT1*	
SCΔkin2CZF1H1A/B	*kin2*Δ::*FRT*/*kin2*Δ::*FRT*	This study
	CZF1/*CZF1-3xHA-SAT1*	
SCΔmck1CZF1H1A/B	*mck1*Δ::*FRT*/*mck1*Δ::*FRT*	This study
	CZF1/*CZF1-3xHA-SAT1*	
SCΔmkc1CZF1H1A/B	*mkc1*Δ::*FRT*/*mkc1*Δ::*FRT*	This study
	CZF1/*CZF1-3xHA-SAT1*	
SCΔmkk2CZF1H1A/B	*mkk2*Δ::*FRT*/*mkk2*Δ::*FRT*	This study
	CZF1/*CZF1-3xHA-SAT1*	
SCΔnik1CZF1H1A/B	*nik1*Δ::*FRT*/*nik1*Δ::*FRT*	This study
	CZF1/*CZF1-3xHA-SAT1*	
SCΔpan3CZF1H1A/B	*pan3*Δ::*FRT*/*pan3*Δ::*FRT*	This study
	CZF1/*CZF1-3xHA-SAT1*	
SCΔssn3CZF1H1A/B	*ssn3*Δ::*FRT*/*ssn3*Δ::*FRT*	This study
	CZF1/*CZF1-3xHA-SAT1*	
SCΔyck2CZF1H1A/B	*yck2*Δ::*FRT*/*yck2*Δ::*FRT*	This study
	CZF1/*CZF1-3xHA-SAT1*	
SCSNF1M1A/B	*SNF1*/*snf1*::*SAT1-FLP*	Ramirez-Zavala et al, 2017
SCSNF1M2A/B	*SNF1*/*snf1*Δ::*FRT*	Ramirez-Zavala et al, 2017
SCSNF1M3A/B	*SNF1*/*snf1*Δ::*FRT*	Mottola et al, 2020
	ADH1/*adh1*::*FRT-SNF1-HygB-FRT*	
SCSNF1M4A/B	*snf1*Δ::*FRT*/snf1::*SAT1-FLP*	Mottola et al, 2020
	ADH1/*adh1*::*FRT-SNF1-HygB-FRT*	
SCSNF1M5A/B	*snf1*Δ::*FRT*/*snf1*Δ::*FRT*	Mottola et al, 2020
	ADH1/*adh1*::*FRT-SNF1-HygB-FRT*	
SCSNF1M6A/B	*snf1*Δ::*FRT*/*snf1*Δ::*FRT*	Mottola et al, 2020, This study
	ADH1/*adh1*::*FRT-SNF1-HygB-FRT*	
	SAP2/*sap2*::P_{SAP2}-*FLP-SAT1*	
SCSNF1M7A/B	*SNF1*/*snf1*Δ::*FRT*	Mottola et al, 2020, This study
	ADH1/*adh1*::*FRT-SNF1-HygB-FRT*	
	SAP2/*sap2*::P_{SAP2}-*FLP-SAT1*	

Table 4.5: Strains used in this study

Strain	Genotype	Reference
SCSNF1M8A/B	*snf1*Δ::*FRT*/*snf1*Δ::*FRT*	Mottola et al, 2020, This study
	ADH1/*adh1*::*FRT*	
	SAP2/*sap2*::P_{SAP2}-*FLP-SAT1*	
SCSNF1M9A/B	*SNF1*/*snf1*Δ::*FRT*	Mottola et al, 2020, This study
	ADH1/*adh1*::*FRT*	
	SAP2/*sap2*::P_{SAP2}-*FLP-SAT1*	
SCSNF1M10A/B	$SNF1^{K84R}$-*SAT1-FLP*/*snf1*Δ::*FRT*	Mottola et al, 2020, This study
	ADH1/*adh1*::*FRT-SNF1-HygB-FRT*	
SCSNF1M11A/B	$SNF1^{K84R}$-*FRT*/*snf1*Δ::*FRT*	Mottola et al, 2020, This study
	ADH1/*adh1*::*FRT-SNF1-HygB-FRT*	
SCSNF1M12A/B	$SNF1^{K84R}$-*FRT*/*snf1*Δ::*FRT*	Mottola et al, 2020, This study
	ADH1/*adh1*::*FRT-SNF1-HygB-FRT*	
	SAP2/*sap2*::P_{SAP2}-*FLP-SAT1*	
SCSNF1M13A/B	$SNF1^{K84R}$-*FRT*/*snf1*Δ::*FRT*	Mottola et al, 2020, This study
	ADH1/*adh1*::*FRT*	
	SAP2/*sap2*::P_{SAP2}-*FLP-SAT1*	
SCSNF1M21A/B	*snf1*Δ::*FRT*/snf1::*SAT1-FLP*	Mottola et al, 2020, This study

4.5 Growth of *E. coli* cultures

Plasmid-expressing *E. coli* was routinely grown overnight either on solid LB-agar plates or in liquid LB-medium, shaking at 200rpm. Growth on both solid and liquid medium was achieved at 37°C. Additionally, in order to select for plasmid-containing *E. coli*, media were typically supplemented with 100µg/mL Ampicillin. For long-term storage of strains, cells were frozen at -80°C in 17% glycerol.

4.6 Growth of *C. albicans* cultures

Typically, *C. albicans* was grown either overnight in liquid YPD medium shaking at 220rpm at 30°C, or for two-to-three days on solid YPD agar at 30°C. In order to select for transformants, agar plates were supplemented with 200µg/mL Nourseothricin. Following initial selection, plates and media were supplemented with 100µg/mL Nourseothricin to maintain a lower level

of selection. In order to induce excision of *FRT*-flanked regions of DNA, strains containing P_{SAP2}-*c*aFLP were grown overnight at 30°C in YCB-BSA medium. Strains were frozen for long-term storage at -80°C in 17% glycerol.

4.7 Construction of plasmids

Plasmids were constructed via restriction cloning. In short, fragments of DNA (typically, but not exclusively, including the pBluescript II KS(+) vector, *SAT1-Flipper* cassette (Reuss *et al.* 2004), and 500bp PCR fragments of DNA homologous to upstream or downstream regions of particular *C. albicans* genes with flanking restriction sites) were digested with various restriction enzymes, generating compatible sticky ends. Fragments were ligated overnight at 16°C with 100ng total DNA in 20µL total volume with T4 ligase, ATP, and ligase buffer (New England BioLabs). To maximize ligation efficiency, larger fragments and smaller fragments were combined in a molar ratio of 1:5. Competent DH5α *E. coli* was transformed with ligated plasmids by first mixing 10µL of ligation with 40µL thawed cells on ice. After 45 minutes of incubation, cells underwent heat shock at 42°C for one minute before being returned to ice. Soon after, 450µL LB-medium without ampicillin was added and cells were incubated, shaking at 37°C for one hour to allow for induction of the Amp^R gene. Following this incubation, cells were concentrated via centrifugation for one minute at 11,000rpm and removal of 400µL supernatant. Resuspended cells were plated on LB-agar supplemented with 100µg/mL ampicillin and grown overnight at 37°C. Plasmids were harvested from *E. coli* via the NucleoSpin Plasmid miniprep kit (Macherey-Nagel). Proper construction of plasmids was confirmed by both analytic restriction and sequencing.

4.8 Passaging and generation of suppressor mutants

In order to generate suppressors of the *snf4*Δ mutant, this strain was passaged daily in YPD at 30°C. After an initial preculture grown in 5mL YPD, 10mL of fresh medium was innoculated with 1µL of the preculture and grown for 24 hours. The following day, 1µL of this culture was transferred to 10mL of fresh medium and the process repeated. Additionally, an aliquot of the culture was frozen in 17% glycerol, and 100µL was plated on either YNB-Sucrose or YPD+Congo red (50µg/mL). Plates were incubated for three days at 30°C. Colonies that successfully grew on one of these media were streaked

on both YPD and additionally on the same medium they had been isolated on, in order to ensure the stability of the phenotype.

4.9 ZCF-GAD library screening for *snf4*Δ suppressors

In order to screen all 82 ZCF-GAD fusion proteins for the ability to suppress certain phenotypes of the *snf4*Δ mutant, plasmids containing expression cassettes were divided into nine pools (contents detailed in table 4.6). Plasmids in pools one through seven were digested with ApaI/SacII to excise expression cassettes. Pool eight was digested with KpnI/SacII, and pool nine was partially digested with KpnI/SacII. The *snf4*Δ mutant was transformed with each of the pools as described in section 4.10.1 and plated on YPD + 200µg/mL Nourseothricin. After two days of incubation at 30°C, colonies were washed off the plates and resuspended in 5mL water. 100µL of this suspension was spread on plates containing either YNB-Sucrose, YPD+Congo red (50µg/mL), or Spider agar. Plates were incubated for two days at 30°C. Colonies which were capable of growth on these media (and retained this growth ability after re-streaking on the same media) were further analysed to determine which specific fusion protein they expressed. Southern blots were performed as described in section 4.10.3 using probes specific to the 5' or 3' flanking regions of the *ADH1* locus, and strains which exhibited wild type *ADH1* were disregarded. Only one strain retained a suppressor phenotype and contained an altered *ADH1* allele. The identity of the fusion protein was determined by amplifying the sequence using the primers

Table 4.6: ZCF-GAD pools used for library screening

Pool 1	Pool 2	Pool 3	Pool 4	Pool 5	Pool 6	Pool 7	Pool 8	Pool 9
ARG81	*ARG83*	*LYS144*	*CTA7*	*FGR17*	*CWT1*	*CZF1*	*DAL81*	*HAL9*
CTF1	*ARO80*	*PPR1*	*FGR27*	*LYS142*	FCR1	*GAL4*	*LYS143*	*MRR2*
MRR1	*ASG1*	*SEF1*	*UGA3*	*SEF2*	*LYS14*	*UME7*	*ZCF7*	
ZCF13	*CAT8*	*UME6*	*ZCF1*	*STB5*	*SUC1*	*WOR2*	*ZCF26*	
ZCF16	*CTA4*	*TEA1*	*ZCF2*	*UPC2*	*UGA32*	*ZCF3*		
ZCF20	*LEU3*	*WAR1*	*ZCF9*	*ZCF11*	*UGA33*	*ZCF4*		
ZCF27	*PUT3*	*ZCF8*	*ZCF17*	*ZCF19*	*ZCF14*	*ZCF6*		
ZCF29	*RGT1*	*ZCF10*	*ZCF24*	*ZCF21*	*ZCF18*	*ZCF28*		
ZCF31	*ROB1*	*ZCF12*	*ZCF25*	*ZCF22*	*ZCF23*	orf19.2230		
orf19.1604	*ZCF5*	*ZNC1*	*ZCF32*	*ZCF39*	*ZFU2*			

prom_ADH1_fwd which binds in the *ADH1* promoter sequence, and GAL8, which binds in the *GAL4* activation domain. The size of the amplicon matched the expected size of *CZF1*-GAD, and sequencing confirmed the identity.

4.10 Genetic manipulation of *C. albicans*

The following methods were employed in order to transform *C. albicans* and validate success of these alterations.

4.10.1 Transformation of *C. albicans*

DNA fragments used to transform *C. albicans* were linearized by digestion of cassette-containing plasmids, separation on an agarose gel, and purification of the appropriate band.

Unless stated otherwise, all centrifugation steps occurred at 4°C, 4000rpm for 3 minutes. *C. albicans* strains chosen for transformation were first made electrocompetent. Five milliliters of YPD medium were inoculated with a single colony and grown as described in section 4.6. The following day, five microliters of this preculture was transferred to 50mL of fresh medium and grown again as described previously. The following morning, cells still in the logarithmic phase of growth were harvested via centrifugation at room temperature and resuspended in 100mM lithium acetate in TE buffer. This suspension was incubated for one hour at 30°C with shaking, followed by addition of 250µL 1M dithiothreitol and a further 30 minutes incubation.

Competent cells were washed by first adding 40mL cold, sterile water and centrifugation to remove the supernatant. A second wash of 25mL water and a third in 10mL cold 1M sorbitol followed. Finally, a concentrated cell suspension was achieved in sorbitol left in the tube after pouring off the supernatant. 40µL of cell suspension was mixed with 5µL of purified DNA in a chilled electroporation cuvette, which was subjected to electroporation at 1.8kV. One milliliter of YPD medium was added and transformed cells were incubated with shaking for 4 hours at 30°C to allow for expression of the *SAT1* resistance gene, before cells were plated on YPD agar supplemented with 200µg/mL and grown for two days at 30°C.

4.10.2 Isolation of chromosomal DNA

Genomic DNA was isolated from *C. albicans* strains for further analysis. All centrifugation steps were conducted at 13,000rpm for 5 minutes unless oth-

erwise specified. 1.5mL YPD medium were inoculated with a single colony of the strain of interest and grown as described in section 4.6. The following day, cells were transferred to 1.5mL locking tubes and pelleted via centrifugation for 2 minutes. Pellets were resuspended in 200µL TE buffer and 200µL Breaking Buffer, to which 200µL glass beads and 150µL PCI was added. Cells were then lysed by vortexing at high speed for 15 minutes. Samples were centrifuged and the aqueous layer was transferred to a new tube with 400µL ice-cold isopropanol, and nucleic acids were precipitated for at least 20 minutes at -20°C. Following precipitation, nucleic acids were pelleted by centrifugation, washed once in 70% ethanol, and dried in a centrifugal evaporator for 15 minutes to remove residual ethanol. Pellets were resuspended in 50µL water and stored at -20°C.

In some cases, it was necessary to quantify DNA. Therefore, the above procedure was modified in several ways. First, a greater culture volume (typically 5 or 10mL depending on the growth rate of particular strains) was necessary to achieve appropriate yield. Following the initial DNA precipitation, nucleic acids pellets were dissolved in 400µL TE buffer and 3µL of 10mg/mL RNase A was added to remove RNAs. The mixture was incubated for ten minutes at 37° before DNA was precipitated once again by addition of 1mL ice-cold ethanol and at least 20 minutes of storage at -20°C. From here, DNA was pelleted, and the protocol proceeded as described above with drying of the pellet.

4.10.3 Southern blot analysis

Following genetic modification of *C. albicans*, Southern blotting was used to ensure the correct modification was achieved and rule out incidental effects like tandem insertions. To this end, 6µL of genomic DNA (roughly 10µg) was digested with one or two restriction enzymes, with the goal of fragmenting the locus of interest into pieces generally between 1.5 and 10kb, with a pattern that differs dependent on genotype. Ideally, the pattern would also differentiate between alleles, but this was not always possible or deemed necessary. DNA was digested overnight at 37°C, then separated in a 1% agarose gel overnight at low voltage (typically around 36V). DNA was then transferred from the gel to a nylon membrane (GE Healthcare). To this end, the membrane was pretreated by first wetting with water then soaked in SSC 20x for five minutes. The membrane was then placed in a vacuum blotting unit, onto which the gel was laid and a vacuum of 50mbar was applied. The gel was covered with Solution A, a depurinating solution, for 20 minutes. Subsequently, it was replaced with Solution B, a denaturing solution, also for 20 minutes, and finally Solution C, a neutralizing solution, for 20 minutes.

After these treatments, the gel was covered with SSC 20x for a minimum of 1.5 hours, though longer times were routinely used to enhance transfer of large DNA fragments. Following transfer, the membrane was washed for 30 seconds in 0.4N NaOH, then for 30 seconds in 0.2M Tris-Cl pH7.5 to neutralize the membrane. Finally, DNA was covalently linked to the membrane by UV crosslinking.

The *ECL Enhanced Chemiluminescence Kit* (GE Healthcare) was used in order to detect specific fragments of DNA bound to the membrane. To prepare the membrane for probing, it was briefly washed in SSC 2x before being placed in a hybridization tube with 15mL ECL hybridization mix. The membrane was prehybridized in a rotisserie hybridization oven at 42°C for at least 30 minutes. During prehybridization, the probe was labeled. Probes were designed typically as 500nt PCR products complementary to regions directly up- or downstream of a gene of interest, though other probes such as internal gene probes were also used depending on purpose. Roughly 150ng of probe were mixed with diluted DNA ladder (New England BioLabs) in a total volume of 10µL. DNA was denatured at 100°C for five minutes then snap-cooled on ice to prevent renaturing. 10µL of both Labeling Reagent and glutaraldehyde (GE Healthcare) were added to the mixture, which was then incubated for 10 minutes at 37°C. Labeling Reagent contains horseradish peroxidase complexed with a positively charged polymer, causing close association with negatively charged DNA. In the presence of glutaraldehyde and 37°C, covalent bonding permanently associates the different components. Following this step, the labeled probe was added to the prehybridization mix and hybridization occurred overnight. The following day, the membrane was first washed twice in Wash Buffer I in the hybridization oven at 42°C for eight minutes each to remove unbound probe. Then, residual Wash Buffer I was removed by washing twice for five minutes at room temperature in SSC 2x. The membrane was then covered for one minute in a 1:1 mixture of Detection Reagents 1 and 2 (GE Healthcare). This mixture introduces hydrogen peroxide and luminol, which together with probe-bound horseradish peroxidase leads to oxidation of luminol and emission of light. To visualize, a blue-light sensitive film (GE Healthcare) was laid over the membrane and locked in a light-proof cassette to be exposed for between 5 and 45 minutes depending on strength of the probe. Finally, the film was developed, revealing bands corresponding with probe-bound DNA fragments, and analyzed.

4.10.4 Sanger sequencing

DNA (either in the form of plasmids or PCR products) was conducted by SeqLab (Göttingen, Germany). Samples were prepared in 15µL volume con-

taining 30pmol primer as well as about 1µg (plasmid) or 100ng (PCR product) of DNA.

4.11 Protein extraction and western immunoblot analysis

Expression of proteins of interest was investigated by preparation of cell extracts from *C. albicans* strains followed by western blot analysis. In some cases, cell extracts were additionally treated with phosphatase.

4.11.1 Preparation of cell extracts

In order to analyze protein levels, cell extracts were first produced. Five milli-liters of YPD or YNB-medium were inoculated with a single colony of the strain of interest and grown as described in section 4.6. The following day, 500µL was transferred into 50mL YPD or YNB-medium and grown for three hours, bringing cells to mid-logarithmic growth. In some cases, experiments required changing medium (for example to test the effect of addition of a stress agent or change nutrient availability). In these cases, following one hour of growth, cells were pelleted by centrifugation for five minutes, 4000rpm at room temperature, supernatant was removed, and the pellets were resuspended in new media. Cultures were then grown for a further two hours. Cells were then harvested by centrifugation for five minutes, 4000rpm, at 4°C and washed once in cold water. Cell pellets were optionally stored at -80°C or directly processed, beginning with resuspension in 500µL Breaking Buffer and transfer to 1.5mL locking tubes. 400µL acid-washed glass beads were added and cells were lysed using three 40 second pulses at 4M/s in a cell homogenizer, with one-minute intervals on ice to prevent overheating of samples. Cell homogenates were transferred to a new tube and centrifuged for 15 minutes, 13,000rpm at 4°C to pellet cell debris. Cleared cell lysate was transferred to new tubes and protein concentration was measured using the Bradford protein assay.

Occasionally, strains with particularly slow growth rates or inability to grow in certain media required modifications to this protocol. In particular, either higher culture volume (up to 2L) or longer growth times were required (up to total 5 hours). Cells were always harvested in mid-logarithmic growth.

4.11.2 Phosphatase treatment

In some cases, experiments required that cell extracts be treated with protein phosphatase. Because Breaking Buffer typically contains phosphatase inhibitors, these compounds were first removed by mixing 150µL cell extract with 250µL Breaking Buffer without phosphatase inhibitors and centrifuging for 15 minutes, 14,000g at 4°C in a centrifugal filter (Millipore). Concentrated cell extract was diluted back to 400µL with Breaking Buffer without phosphatase inhibitor and the process was repeated twice more, finally suspending the lysate in a total of 100µL. 39µL phosphatase inhibitor-free lysate was mixed with 5µL phosphatase buffer, 5µL 10mM manganese chloride, and 1µL lambda phosphatase (New England BioLabs). The reaction mixture was incubated for 30 minutes at 30°C, then phosphatase was heat inactivated by a 10 minute incubation at 65°C.

4.11.3 Western immunoblot analysis

Western blotting was used to compare protein levels, detect forms of a given protein with different molecular weights, or levels of phosphorylation, depending on experiment. Regardless of purpose, 10 or 20µg (when concentration was high enough to allow) of total protein was mixed with equal volume 2x Laemmli buffer and heated to 100°C for 5 minutes to fully denature protein. Samples were loaded onto a 9% SDS polyacrylamide gel and run for two hours at 100V. After electrophoresis, both the gel and a nitrocellulose membrane were equilibrated in cold transfer buffer for five minutes. Protein was then transferred to the membrane in a transfer cassette via electroblotting for one hour at 100V in cold transfer buffer. Following transfer, the membrane was stained for two minutes in Ponceau S and washed in water. If protein loading appeared equal, a photograph was taken, and the membrane was blocked for one hour in TBST with either 5% nonfat milk or 5% BSA (in the case where the epitope to be probed was phospho-Snf1) at room temperature. The membrane was then probed with 1:1,000 anti-phospho-AMPKα (Cell Signaling Technology, Inc.) or 1:250 horseradish peroxidase conjugated anti-HA (Invitrogen) overnight at 4°C. The next day, the membrane was washed four times, five minutes each, at room temperature in TBST. For anti-phospho-AMPKα probed membranes, horseradish peroxidase-conjugated anti-rabbit secondary antibody was diluted 1:10,000 into TBST+5% nonfat milk and applied to the membrane for one hour at room temperature before being washed again as previously described. Antibody-bound protein was visualized via enhanced chemiluminescence as described in section 4.10.3, with exposure times typically between 30 seconds

and 10 minutes.

4.12 RNA extraction and expression analysis

Expression of various transcripts of interest was investigated via northern blot analysis as well as reverse transcriptase followed by quantitative-PCR (RT-qPCR). Additionally, global expression was assayed via RNA sequencing.

4.12.1 RNA extraction

RNA was extracted from *C. albicans* cells for expression analysis. Cell pellets were obtained as described in section 4.11.1., with the modification that typically smaller culture volumes (10 or 20mL) were used. Cells were then processed using the *Quick*-RNA Fungal/Bacterial Miniprep Kit (Zymo Research) following the manufacturer's instructions, quantified via Nanodrop spectrophotometer, and stored at -80°C.

4.12.2 Northern blot analysis

Northern blotting was generally used to qualitatively compare expression of specific transcripts as well as visualize different transcript isoforms. All solutions were prepared with DEPC treated water. 10µg of RNA was mixed with 5x RNA loading buffer to a final concentration of 1x, loaded on a 1.2% RNA gel (1.2% agarose, 2% formaldehyde, 1x RP buffer), and separated at 80V for 1.5 hours. Following separation, equal loading of RNA was gauged by visualization of 28S and 18S RNA in a UV transilluminator, and a photograph was taken for documentation. If loading was equal, the gel was prepared for transfer by first washing twice in water, shaking for 15 minutes each, followed by two washes in 10x SSC, also for 15 minutes each. RNA was transferred to a nylon membrane (GE Healthcare) overnight via capillary action. To confirm successful and uniform transfer, RNA on the membrane was visualized in a UV transilluminator. If transfer was successful, RNA was covalently bound to the membrane using a UV crosslinker. To prepare for hybridization, the membrane was placed in a hybridization tube with 15mL hybridization solution (preheated at 65°C to dissolve precipitated SDS) and prehybridized for at least two hours in a rotisserie oven at 42°C. Probes were designed as PCR products typically spanning nearly all of the open reading frame of the gene of interest, utilizing dNTP mix containing digoxigenin-labeled deoxyuridine-triphosphate (Roche). Probes were denatured at 100°C

for five minutes, snap cooled on ice, and added to 15mL hybridization solution. After prehybridization, prehybridization solution was replaced with probe-containing hybridization solution. Hybridization occurred overnight.

The following day, the membrane was washed twice for 10 minutes in Wash Buffer I at room temperature to remove unbound probe. Then, residual was buffer was removed by washing once for five minutes in Wash Buffer II. The membrane was then blocked for 15 minutes at room temperature in 15mL P2 Buffer (1x Blocking Reagent, 1x P1 Buffer), followed by binding of alkaline phosphatase-conjugated anti-digoxigenin Fab fragments (Roche, diluted 1:10,000 in 15mL Buffer P2) for 30 minutes at room temperature. Unbound Fab fragments were washed off of the membrane in Wash Buffer II twice for five minutes each. In preparation for detection, the membrane was then bathed for five minutes in Buffer P3, then for five minutes in Buffer P3 with 10µL/mL CSPD, a chemiluminescent substrate for alkaline phosphatase. Luminescence was enhanced by incubation of the membrane for 10 minutes at 37°C and detected by film exposure, typically for two to ten minutes.

4.12.3 RNA sequencing

Triplicate overnight yeast cultures were diluted 10-2 in fresh YPD and grown for 3 hours at 30°C. Cells were harvested by centrifugation and washed once in water. Cells were broken using hot phenol and RNA was extracted using the RNeasy Mini Kit (Qiagen) according to the manufacturer's instructions. Samples were treated with TURBO DNase (Invitrogen) to remove any residual genomic DNA, and remaining RNA was cleaned by a second purification using the RNeasy Mini kit. Further steps to prepare for and conduct RNA sequencing were done by Eurofins Genomics (Konstanz, Germany). Such steps included purification of poly-A mRNA molecules, mRNA fragmentation, preparation of strand-specific cDNA libraries, adapter ligation, and Illumina (HiSeq 2500) sequencing (single reads, 1 x 50 base pair length). Between 35-48 million reads per sample were obtained as FASTQ files. Low quality reads were eliminated and adapter sequences trimmed using the Trimmomatic tool (v0.36)(Bolger *et al.* 2014) using default settings for single end reads. High quality reads were mapped to the reference genome (SC5314 Assembly 22) using STAR (v 2.6.1b)(Dobin *et al.* 2013). Read counts per ORF were extracted from the resulting BAM files using HTSeq (v 0.6.1)(Anders *et al.* 2015). Normalization and statistical comparisons of data were conducted using RStudio (v 1.1.456) with the DESeq2 package (v 1.14.1)(Love *et al.* 2014). Original data are available from the Gene Expression Omnibus (https://www.ncbi.nlm.nih.gov/geo/) using accession code GSE165091.

4.13 Growth and morphology assays

4.13.1 Growth assays on solid media

Spot assays were conducted to compare the ability of different *C. albicans* strains to grow in various conditions (e.g. available carbon source, stress agents, temperature, etc.). Five milliliters of YPD medium were inoculated with a single colony of strains of interest and grown as described in section 4.6. The following day, the optical densities of cultures were measured at 600nm (OD_{600}) with a biophotometer. In a 96-well plate, cultures were diluted to an OD_{600} of 2.0 and serially diluted 10-fold five times. Spots were plated on solid media of choice with a 48-pin replicator (transferring roughly 3µL) and plates were incubated at temperatures of interest for two-to-four days, at which points photographs were taken.

In some cases, an alternative approach was used to examine the ability to grow on alternative carbon sources. Overnight cultures were grown and diluted as described above, then 3µL of this suspension was streaked for single colonies on plates and incubated as described above.

Assays testing susceptibility to cell wall stress inducing agents were always conducted on YPD plates with or without (labeled "Control") the chemical of interest.

4.13.2 Growth curves

Growth curves were measured in order to quantify and compare doubling time of different strains. Five milliliters of YNB-medium were inoculated with a single colony of the strain of interest and grown as described in section 4.6. The following day, cells were washed once in water. OD_{600} was measured using a biophotometer and diluted to an OD_{600} of 1.0 in water. 20µl was transferred to 180µL YNB-medium containing different carbon sources in a 96-well plate. Plates were incubated for 60 hours in a plate reader (Tecan), shaking at 30°C. Every 10 minutes, OD_{600} was measured, and growth curves were created based on the averages of three independent replicates.

4.13.3 Colony morphology

In order to examine the morphology of individual colonies of different strains, 5mL of YPD medium were inoculated with a single colony of the strain of interest and grown as described in section 4.6. The following day, the culture was diluted by serial 10-fold dilution in water six times. 100µL of diluted

culture was plated with glass plating beads on solid media of interest and incubated 37° for seven days, at which point photographs of individual colonies were taken through a stereomicroscope. As a negative control (labeled "Control" on figures), strains were plated additionally on YPD and grown at 30°C.

4.14 Microscopy analyses

4.14.1 Fluorescent microscopy

In order to stain component of the cell wall and visualize them using fluorescence microscopy, overnight cultures were grown in 5ml YPD, then diluted 1:200 in YPD and grown for five hours at 30°C. Cells were washed twice in PBS, then resuspended in PBS+3.7% formaldehyde. After one hour of fixation at room temperature in the dark, cells were washed twice in 500mL PBS. 20uL of cells were transferred to 100uL 0.01% Calcofluor White or 100ug/mL Concanavalin A conjugated to Texas Red. After one hour staining, cells were visualized under a fluorescent microscope (Leica Microsystems).

4.14.2 Transmission electron microscopy

Single colonies grown on YPD for 2 days at 30°C were collected and fixed in fixation buffer (2.5% glutaraldehyde, 2% formaldehyde, 0.1M cacodylate pH 7,2) overnight at 4°C, followed by three washing steps in 50mM cacodylate buffer (pH 7.2). Cells were further fixed in 2% buffered osmium tetraoxide for 90-120 minutes, followed by three washing steps in. Cells were stained overnight with 0.5% uranyl acetate dihydrate for contrasting, and washed three times in water. Samples were dehydrated using increasing concentrations of ethanol followed by ethanol removal using propylene oxide. Cells were then embedded in epon at 60°C for 48 hours, ultrathin sections were cut using a microtome, and imaged using a JEOL JEM-1400 Flash transmission electron microscope (120kV) and a Matataki Flash digital camera. To determine the average thickness of the inner and outer cell wall, 10 representative cells were imaged and measured at 8 locations each using SightX TEM Imaging Viewer (v 2.1.13). Statistical comparisons were conducted and data plotted with GraphPad version 0.9, using one-way ANOVA, plus Dunnett's multiple comparison correction where appropriate.

References

Alonso-Monge, R. *et al.* (May 1999). "Role of the mitogen-activated protein kinase Hog1p in morphogenesis and virulence of *Candida albicans*." In: *Journal of bacteriology* 181 (10), pp. 3058–3068. ISSN: 0021-9193. DOI: 10.1128/JB.181.10.3058-3068.1999. ppublish.

Amodeo, G. A., Rudolph, M. J., and Tong, L. (Sept. 2007). "Crystal structure of the heterotrimer core of *Saccharomyces cerevisiae* AMPK homologue SNF1." In: *Nature* 449 (7161), pp. 492–495. ISSN: 1476-4687. DOI: 10.1038/nature06127. ppublish.

Anders, S., Pyl, P. T., and Huber, W. (2015). "HTSeq–a Python framework to work with high-throughput sequencing data". In: *Bioinformatics* 31 (2), pp. 166–169. ISSN: 1367-4811. DOI: 10.1093/bioinformatics/btu638.

Backhaus, K. *et al.* (Dec. 2013). "Mutations in SNF1 complex genes affect yeast cell wall strength." In: *European journal of cell biology* 92 (12), pp. 383–395. ISSN: 1618-1298. DOI: 10.1016/j.ejcb.2014.01.001. ppublish.

Ballou, E. R. *et al.* (Dec. 2016). "Lactate signalling regulates fungal β-glucan masking and immune evasion." In: *Nature microbiology* 2, p. 16238. ISSN: 2058-5276. DOI: 10.1038/nmicrobiol.2016.238. epublish.

Banerjee, M. *et al.* (Apr. 2008). "*UME6*, a novel filament-specific regulator of *Candida albicans* hyphal extension and virulence." In: *Molecular biology of the cell* 19 (4), pp. 1354–1365. ISSN: 1939-4586. DOI: 10.1091/mbc.E07-11-1110. ppublish.

Bastidas, R. J. *et al.* (Aug. 2008). "Signaling cascades as drug targets in model and pathogenic fungi." In: *Current opinion in investigational drugs (London, England : 2000)* 9 (8), pp. 856–864. ISSN: 1472-4472. ppublish.

Bates, S. *et al.* (Jan. 2006). "Outer chain N-glycans are required for cell wall integrity and virulence of *Candida albicans*." In: *The Journal of biological chemistry* 281 (1), pp. 90–98. ISSN: 0021-9258. DOI: 10.1074/jbc.M510360200. ppublish.

Beltrao, P. *et al.* (June 2009). "Evolution of phosphoregulation: comparison of phosphorylation patterns across yeast species." In: *PLoS biology* 7 (6), e1000134. ISSN: 1545-7885. DOI: 10.1371/journal.pbio.1000134. ppublish.

Bertram, P. G. *et al.* (Feb. 2002). "Convergence of TOR-nitrogen and Snf1-glucose signaling pathways onto Gln3." In: *Molecular and cellular biology* 22 (4), pp. 1246–1252. ISSN: 0270-7306. DOI: 10.1128/mcb.22.4.1246-1252.2002. ppublish.

Biscotti, M. A., Olmo, E., and Heslop-Harrison, J. S. P. (Sept. 2015). "Repetitive DNA in eukaryotic genomes." In: *Chromosome research* 23 (3), pp. 415–420. ISSN: 1573-6849. DOI: 10.1007/s10577-015-9499-z. ppublish.

Blankenship, J. R. *et al.* (Feb. 2010). "An extensive circuitry for cell wall regulation in *Candida albicans*." In: *PLoS pathogens* 6 (2), e1000752. ISSN: 1553-7374. DOI: 10.1371/journal.ppat.1000752. epublish.

Böhm, L., Muralidhara, P., and Pérez, J. C. (Apr. 2016). "A Candida albicans regulator of disseminated infection operates primarily as a repressor and governs cell surface remodeling." In: *Molecular microbiology* 100 (2), pp. 328–344. ISSN: 1365-2958. DOI: 10.1111/mmi.13320. ppublish.

Bolger, A. M., Lohse, M., and Usadel, B. (2014). "Trimmomatic: a flexible trimmer for Illumina sequence data". In: *Bioinformatics* 30, pp. 2114–2120. ISSN: 1460-2059. DOI: 10.1093/bioinformatics/btu170.

Bossche, H. V., Koymans, L., and Moereels, H. (1995). "P450 inhibitors of use in medical treatment: Focus on mechanisms of action". In: *Pharmacology & Therapeutics* 67, pp. 79–100. ISSN: 0163-7258. DOI: 10.1016/0163-7258(95)00011-5.

Bradford, L. L. and Ravel, J. (2017). "The Vaginal Mycobiome: A Contemporary Perspective On Fungi In Women's Health And Diseases." In: *Virulence* 8.3, pp. 342–351. ISSN: 2150-5608. DOI: 10.1080/21505594.2016.1237332.

Braun, K. A. *et al.* (July 2014). "Phosphoproteomic analysis identifies proteins involved in transcription-coupled mRNA decay as targets of Snf1 signaling." In: *Science signaling* 7 (333), ra64. ISSN: 1937-9145. DOI: 10.1126/scisignal.2005000. epublish.

Braun, P. C. and Calderone, R. A. (Mar. 1978). "Chitin synthesis in *Candida albicans*: comparison of yeast and hyphal forms." In: *Journal of bacteriology* 133 (3), pp. 1472–1477. ISSN: 0021-9193. DOI: 10.1128/JB.133.3.1472-1477.1978. ppublish.

Brown, D. H. *et al.* (Nov. 1999). "Filamentous growth of *Candida albicans* in response to physical environmental cues and its regulation by the unique *CZF1* gene." In: *Molecular microbiology* 34 (4), pp. 651–662. ISSN: 0950-382X. DOI: 10.1046/j.1365-2958.1999.01619.x. ppublish.

Brown, G. D. and Gordon, S. (Apr. 2005). "Immune recognition of fungal beta-glucans." In: *Cellular microbiology* 7 (4), pp. 471–479. ISSN: 1462-5814. DOI: 10.1111/j.1462-5822.2005.00505.x. ppublish.

Brown, G. D. *et al.* (Dec. 2012). "Hidden killers: human fungal infections." In: *Science translational medicine* 4 (165), 165rv13. ISSN: 1946-6242. DOI: 10.1126/scitranslmed.3004404. ppublish.

Brown, J. A. and Catley, B. J. (1992). "Monitoring polysaccharide synthesis in *Candida albicans*". In: *Carbohydrate Research* 227, pp. 195–202. ISSN: 0008-6215. DOI: 10.1016/0008-6215(92)85071-7.

Brown, V., Sabina, J., and Johnston, M. (2009). "Specialized Sugar Sensing in Diverse Fungi". In: *Current Biology* 19.5, pp. 436–441. ISSN: 0960-9822. DOI: 10.1016/j.cub.2009.01.056.

Brown, V., Sexton, J. A., and Johnston, M. (2006). "A Glucose Sensor in *Candida albicans*". In: *Eukaryotic Cell* 5.10, pp. 1726–1737. ISSN: 1535-9778. DOI: 10.1128/ec.00186-06.

Brunke, S. *et al.* (Oct. 2014). "One small step for a yeast - microevolution within macrophages renders *Candida glabrata* hypervirulent due to a single point mutation." In: *PLoS pathogens* 10 (10), e1004478. ISSN: 1553-7374. DOI: 10.1371/journal.ppat.1004478. epublish.

Bruno, V. M. *et al.* (Mar. 2006). "Control of the C. albicans cell wall damage response by transcriptional regulator Cas5." In: *PLoS pathogens* 2 (3), e21. ISSN: 1553-7374. DOI: 10.1371/journal.ppat.0020021. ppublish.

Bulawa, C. E. *et al.* (Nov. 1995). "Attenuated virulence of chitin-deficient mutants of *Candida albicans*." In: *Proceedings of the National Academy of Sciences of the United States of America* 92 (23), pp. 10570–10574. ISSN: 0027-8424. DOI: 10.1073/pnas.92.23.10570. ppublish.

Calvez, T. L. *et al.* (2009). "Fungal Diversity In Deep-sea Hydrothermal Ecosystems". In: *Applied And Environmental Microbiology* 75.20, pp. 6415–6421. ISSN: 0099-2240. DOI: 10.1128/aem.00653-09.

Cantero, P. D. and Ernst, J. F. (May 2011). "Damage to the glycoshield activates PMT-directed O-mannosylation via the Msb2-Cek1 pathway in *Candida albicans*." In: *Molecular microbiology* 80 (3), pp. 715–725. ISSN: 1365-2958. DOI: 10.1111/j.1365-2958.2011.07604.x. ppublish.

Carling, D. *et al.* (1989). "Purification and characterization of the AMP-activated protein kinase. Copurification of acetyl-CoA carboxylase kinase and 3-hydroxy-3-methylglutaryl-CoA reductase kinase activities". In: *European journal of biochemistry* 186 (1-2), pp. 129–136. ISSN: 0014-2956. DOI: 10.1111/j.1432-1033.1989.tb15186.x.

Carlson, M., Osmond, B. C., and Botstein, D. (1981). "Mutants of yeast defective in sucrose utilization." In: *Genetics* 98 (1), pp. 25–40. ISSN: 0016-6731.

Celenza, J. L. and Carlson, M. (1989). "Mutational analysis of the *Saccharomyces cerevisiae* SNF1 protein kinase and evidence for functional interaction with the SNF4 protein." In: *Molecular and cellular biology* 9 (11), pp. 5034–5044. ISSN: 0270-7306. DOI: 10.1128/mcb.9.11.5034.

— (1986). "A yeast gene that is essential for release from glucose repression encodes a protein kinase". In: *Science* 233.4769, pp. 1175–1180. DOI: 10.1126/science.3526554.

Chaffin, W. L. *et al.* (Mar. 1998). "Cell wall and secreted proteins of *Candida albicans*: identification, function, and expression." In: *Microbiology and molecular biology reviews : MMBR* 62 (1), pp. 130–180. ISSN: 1092-2172. ppublish.

Chandrashekarappa, D. G., McCartney, R. R., and Schmidt, M. C. (Dec. 2011). "Subunit and domain requirements for adenylate-mediated protection of Snf1 kinase activation loop from dephosphorylation." In: *The Journal of biological chemistry* 286 (52), pp. 44532–44541. ISSN: 1083-351X. DOI: 10.1074/jbc.M111.315895. ppublish.

Chen, T. *et al.* (Jan. 2019a). "Exposure of *Candida albicans* β (1,3)-glucan is promoted by activation of the Cek1 pathway." In: *PLoS genetics* 15 (1), e1007892. ISSN: 1553-7404. DOI: 10.1371/journal.pgen.1007892. epublish.

Chen, T. *et al.* (Sept. 2019b). "Lrg1 Regulates β (1,3)-Glucan Masking in *Candida albicans* through the Cek1 MAP Kinase Pathway." In: *mBio* 10 (5). ISSN: 2150-7511. DOI: 10.1128/mBio.01767-19. epublish.

Childers, D. S. *et al.* (Apr. 2016). "The Rewiring of Ubiquitination Targets in a Pathogenic Yeast Promotes Metabolic Flexibility, Host Colonization and Virulence." In: *PLoS pathogens* 12 (4), e1005566. ISSN: 1553-7374. DOI: 10.1371/journal.ppat.1005566. epublish.

Childers, D. S. *et al.* (July 2020). "Epitope Shaving Promotes Fungal Immune Evasion." In: *mBio* 11 (4). ISSN: 2150-7511. DOI: 10.1128/mBio.00984-20. epublish.

Cohen, P. (Apr. 2002). "Protein kinases–the major drug targets of the twenty-first century?" In: *Nature reviews. Drug discovery* 1 (4), pp. 309–

315. ISSN: 1474-1776. DOI: 10.1038/nrd773. ppublish.

Cortegiani, A. *et al.* (2018). "Epidemiology, clinical characteristics, resistance, and treatment of infections by *Candida auris*". In: *Journal of Intensive Care* 6. ISSN: 2052-0492. DOI: 10.1186/s40560-018-0342-4.

Corvey, C. *et al.* (July 2005). "Carbon Source-dependent assembly of the Snf1p kinase complex in *Candida albicans*." In: *The Journal of biological chemistry* 280 (27), pp. 25323–25330. ISSN: 0021-9258. DOI: 10.1074/jbc.M503719200. ppublish.

Cottier, F. *et al.* (Oct. 2015). "MIG1 Regulates Resistance of *Candida albicans* against the Fungistatic Effect of Weak Organic Acids." In: *Eukaryotic cell* 14 (10), pp. 1054–1061. ISSN: 1535-9786. DOI: 10.1128/EC.00129-15. ppublish.

Cottier, F. *et al.* (Nov. 2017). "The Transcriptional Response of *Candida albicans* to Weak Organic Acids, Carbon Source, and *MIG1* Inactivation Unveils a Role for *HGT16* in Mediating the Fungistatic Effect of Acetic Acid." In: *G3 (Bethesda, Md.)* 7 (11), pp. 3597–3604. ISSN: 2160-1836. DOI: 10.1534/g3.117.300238. epublish.

Cottier, F. *et al.* (Oct. 2019). "Remasking of *Candida albicans* β-Glucan in Response to Environmental pH Is Regulated by Quorum Sensing." In: *mBio* 10 (5). ISSN: 2150-7511. DOI: 10.1128/mBio.02347-19. epublish.

Crute, B. E. *et al.* (Dec. 1998). "Functional domains of the alpha1 catalytic subunit of the AMP-activated protein kinase." In: *The Journal of biological chemistry* 273 (52), pp. 35347–35354. ISSN: 0021-9258. DOI: 10.1074/jbc.273.52.35347. ppublish.

Cullen, P. J. and Sprague, G. F. (Dec. 2000). "Glucose depletion causes haploid invasive growth in yeast." In: *Proceedings of the National Academy of Sciences of the United States of America* 97 (25), pp. 13619–13624. ISSN: 0027-8424. DOI: 10.1073/pnas.240345197. ppublish.

Dalal, C. K. *et al.* (Sept. 2016). "Transcriptional rewiring over evolutionary timescales changes quantitative and qualitative properties of gene expression." In: *eLife* 5. ISSN: 2050-084X. DOI: 10.7554/eLife.18981. epublish.

Dale, S. *et al.* (Mar. 1995). "Similar substrate recognition motifs for mammalian AMP-activated protein kinase, higher plant HMG-CoA reductase kinase-A, yeast SNF1, and mammalian calmodulin-dependent protein kinase I." In: *FEBS letters* 361 (2-3), pp. 191–195. ISSN: 0014-5793. DOI: 10.1016/0014-5793(95)00172-6. ppublish.

Davis, S. E. *et al.* (Oct. 2014). "Masking of β(1-3)-glucan in the cell wall of *Candida albicans* from detection by innate immune cells depends on phosphatidylserine." In: *Infection and immunity* 82 (10), pp. 4405–4413. ISSN: 1098-5522. DOI: 10.1128/IAI.01612-14. ppublish.

De Vit, M. J., Waddle, J. A., and Johnston, M. (Aug. 1997). "Regulated nuclear translocation of the Mig1 glucose repressor." In: *Molecular biology of the cell* 8, pp. 1603–1618. ISSN: 1059-1524. DOI: 10.1091/mbc.8.8.1603. ppublish.

Delgado-Silva, Y. *et al.* (2014). "Participation of *Candida albicans* transcription factor RLM1 in cell wall biogenesis and virulence." In: *PloS one* 9 (1), e86270. ISSN: 1932-6203. DOI: 10.1371/journal.pone.0086270. epublish.

Dennehy, K. M. and Brown, G. D. (Aug. 2007). "The role of the beta-glucan receptor Dectin-1 in control of fungal infection." In: *Journal of leukocyte biology* 82 (2), pp. 253–258. ISSN: 0741-5400. DOI: 10.1189/jlb.1206753. ppublish.

DeVit, M. J. and Johnston, M. (Nov. 1999). "The nuclear exportin Msn5 is required for nuclear export of the Mig1 glucose repressor of *Saccharomyces cerevisiae*." In: *Current biology : CB* 9, pp. 1231–1241. ISSN: 0960-9822. DOI: 10.1016/s0960-9822(99)80503-x. ppublish.

Dhamgaye, S. *et al.* (Aug. 2012). "RNA sequencing revealed novel actors of the acquisition of drug resistance in *Candida albicans*." In: *BMC genomics* 13, p. 396. ISSN: 1471-2164. DOI: 10.1186/1471-2164-13-396. epublish.

Dichtl, K., Samantaray, S., and Wagener, J. (Sept. 2016). "Cell wall integrity signalling in human pathogenic fungi." In: *Cellular microbiology* 18 (9), pp. 1228–1238. ISSN: 1462-5822. DOI: 10.1111/cmi.12612. ppublish.

Dobin, A. *et al.* (2013). "STAR: ultrafast universal RNA-seq aligner". In: *Bioinformatics* 29 (1), pp. 15–21. ISSN: 1367-4811. DOI: 10.1093/bioinformatics/bts635.

Douglas, C. M. *et al.* (Nov. 1997). "Identification of the FKS1 gene of *Candida albicans* as the essential target of 1,3-beta-D-glucan synthase inhibitors." In: *Antimicrobial agents and chemotherapy* 41 (11), pp. 2471–2479. ISSN: 0066-4804. DOI: 10.1128/AAC.41.11.2471. ppublish.

Dudley, A. M. *et al.* (2005). "A global view of pleiotropy and phenotypically derived gene function in yeast." In: *Molecular systems biology* 1, p. 2005.0001. ISSN: 1744-4292. DOI: 10.1038/msb4100004. ppublish.

Eisman, B. *et al.* (Feb. 2006). "The Cek1 and Hog1 mitogen-activated protein kinases play complementary roles in cell wall biogenesis and chlamydospore formation in the fungal pathogen *Candida albicans*." In: *Eukaryotic cell* 5 (2), pp. 347–358. ISSN: 1535-9778. DOI: 10.1128/EC.5.2.347-358.2006. ppublish.

Enloe, B., Diamond, A., and Mitchell, A. P. (Oct. 2000). "A single-transformation gene function test in diploid *Candida albicans*." In: *Journal of bacteriology* 182 (20), pp. 5730–5736. ISSN:

0021-9193. DOI: 10.1128/jb.182.20.5730-5736.2000. ppublish.

Estruch, F. *et al.* (Nov. 1992). "N-terminal mutations modulate yeast SNF1 protein kinase function." In: *Genetics* 132 (3), pp. 639–650. ISSN: 0016-6731. ppublish.

Fan, J., Chaturvedi, V., and Shen, S.-H. (2002). "Identification and Phylogenetic Analysis of a Glucose Transporter Gene Family from the Human Pathogenic Yeast *Candida albicans*". In: *Journal of Molecular Evolution* 55.3, pp. 336–346. ISSN: 0022-2844. DOI: 10.1007/s00239-002-2330-4.

Ferguson, B. A. *et al.* (2003). "Coarse-scale Population Structure Of Pathogenic Armillaria Species In A Mixed-conifer Forest In The Blue Mountains Of Northeast Oregon". In: *Canadian Journal Of Forest Research* 33.4, pp. 612–623. ISSN: 0045-5067. DOI: 10.1139/x03-065.

Ferguson, F. M. and Gray, N. S. (May 2018). "Kinase inhibitors: the road ahead." In: *Nature reviews. Drug discovery* 17 (5), pp. 353–377. ISSN: 1474-1784. DOI: 10.1038/nrd.2018.21. ppublish.

Fernández-García, P. *et al.* (2012). "Phosphorylation of yeast hexokinase 2 regulates its nucleocytoplasmic shuttling." In: *The Journal of biological chemistry* 287 (50), pp. 42151–42164. ISSN: 1083-351X. DOI: 10.1074/jbc.M112.401679. ppublish.

Fleming, A. (1980). "On The Antibacterial Action Of Cultures Of A Penicillium, With Special Reference To Their Use In The Isolation Of B. Influenzae". In: *Clinical Infectious Diseases* 2.1, pp. 129–139. ISSN: 1058-4838. DOI: 10.1093/clinids/2.1.129.

Flick, K. M. *et al.* (2003). "Grr1-dependent Inactivation of Mth1 Mediates Glucose-induced Dissociation of Rgt1 from HXT Gene Promoters". In: *Molecular Biology of the Cell* 14.8, pp. 3230–3241. ISSN: 1059-1524. DOI: 10.1091/mbc.e03-03-0135.

Floudas, D. *et al.* (2012). "The Paleozoic Origin Of Enzymatic Lignin Decomposition Reconstructed From 31 Fungal Genomes." In: *Science* 336.6089, pp. 1715–1719. ISSN: 1095-9203. DOI: 10.1126/science.1221748.

Fonzi, W. A. (Nov. 1999). "PHR1 and PHR2 of *Candida albicans* encode putative glycosidases required for proper cross-linking of beta-1,3- and beta-1,6-glucans." In: *Journal of bacteriology* 181 (22), pp. 7070–7079. ISSN: 0021-9193. DOI: 10.1128/JB.181.22.7070-7079.1999. ppublish.

Freire-Benéitez, V. *et al.* (Mar. 2016). "*Candida albicans* repetitive elements display epigenetic diversity and plasticity." In: *Scientific reports* 6, p. 22989. ISSN: 2045-2322. DOI: 10.1038/srep22989. epublish.

Galán-Díez, M. *et al.* (Apr. 2010). "*Candida albicans* beta-glucan exposure is controlled by the fungal CEK1-mediated mitogen-activated protein kinase pathway that modulates immune responses triggered through dectin-1." In: *Infection and immunity* 78 (4), pp. 1426–1436. ISSN: 1098-5522. DOI: 10.1128/IAI.00989-09. ppublish.

Gancedo, J. M. (1992). "Carbon catabolite repression in yeast". In: *European Journal of Biochemistry* 206, pp. 297–313. ISSN: 0014-2956. DOI: 10.1111/j.1432-1033.1992.tb16928.x.

García, R. *et al.* (Sept. 2015). "Genomic profiling of fungal cell wall-interfering compounds: identification of a common gene signature." In: *BMC genomics* 16, p. 683. ISSN: 1471-2164. DOI: 10.1186/s12864-015-1879-4. epublish.

Goffeau, A. *et al.* (1996). "Life With 6000 Genes". In: *Science* 274.5287, pp. 546–567. ISSN: 0036-8075. DOI: 10.1126/science.274.5287.546.

González, M. M. *et al.* (Sept. 1997). "Phenotypic characterization of a *Candida albicans* strain deficient in its major exoglucanase." In: *Microbiology (Reading, England)* 143 (Pt 9), pp. 3023–3032. ISSN: 1350-0872. DOI: 10.1099/00221287-143-9-3023. ppublish.

Gordee, R. S. *et al.* (1988). "Anti-Candida Activity and Toxicology of LY121019, a Novel Semisynthetic Polypeptide Antifungal Antibiotic". In: *Annals of the New York Academy of Sciences* 544, pp. 294–309. ISSN: 0077-8923. DOI: 10.1111/j.1749-6632.1988.tb40415.x.

Gow, N. A. R. and Hube, B. (Aug. 2012). "Importance of the *Candida albicans* cell wall during commensalism and infection." In: *Current opinion in microbiology* 15 (4), pp. 406–412. ISSN: 1879-0364. DOI: 10.1016/j.mib.2012.04.005. ppublish.

Gray, K. C. *et al.* (Feb. 2012). "Amphotericin primarily kills yeast by simply binding ergosterol." In: *PNAS* 109 (7), pp. 2234–2239. ISSN: 1091-6490. DOI: 10.1073/pnas.1117280109. ppublish.

Hall, R. A. *et al.* (2013). "The Mnn2 mannosyltransferase family modulates mannoprotein fibril length, immune recognition and virulence of *Candida albicans*." In: *PLoS pathogens* 9 (4), e1003276. ISSN: 1553-7374. DOI: 10.1371/journal.ppat.1003276. ppublish.

Hallen-Adams, H. E. and Suhr, M. J. (2017). "Fungi In The Healthy Human Gastrointestinal Tract." In: *Virulence* 8.3, pp. 352–358. ISSN: 2150-5608. DOI: 10.1080/21505594.2016.1247140. Ppublis.

Hasim, S. *et al.* (Jan. 2017). "β-(1,3)-Glucan Unmasking in Some *Candida albicans* Mutants Correlates with Increases in Cell Wall Surface Roughness and Decreases in Cell Wall Elasticity." In: *Infection and immunity* 85 (1). ISSN: 1098-5522. DOI: 10.1128/IAI.00601-16. epublish.

Havlickova, B., Czaika, V. A., and Friedrich, M. (2008). "Epidemiological Trends In Skin Mycoses Worldwide." In: *Mycoses* 51, pp. 2–15.

ISSN: 1439-0507. DOI: 10.1111/j.1439-0507.2008.01606.x.

Hawksworth, D. L. and Lücking, R. (2017). "Fungal Diversity Revisited: 2.2 To 3.8 Million Species." In: *Microbiology Spectrum* 5, pp. 79–95. ISSN: 2165-0497. DOI: 10.1128/microbiolspec.FUNK-0052-2016.

Hedges, D., Proft, M., and Entian, K. D. (Apr. 1995). "CAT8, a new zinc cluster-encoding gene necessary for derepression of gluconeogenic enzymes in the yeast *Saccharomyces cerevisiae*." In: *Molecular and cellular biology* 15 (4), pp. 1915–1922. ISSN: 0270-7306. DOI: 10.1128/mcb.15.4.1915. ppublish.

Heinisch, J. J. *et al.* (Apr. 2010). "Measurement of the mechanical behavior of yeast membrane sensors using single-molecule atomic force microscopy." In: *Nature protocols* 5 (4), pp. 670–677. ISSN: 1750-2799. DOI: 10.1038/nprot.2010.19. ppublish.

Heredia, M. Y. *et al.* (July 2020). "An expanded cell wall damage signaling network is comprised of the transcription factors Rlm1 and Sko1 in *Candida albicans*." In: *PLoS genetics* 16 (7), e1008908. ISSN: 1553-7404. DOI: 10.1371/journal.pgen.1008908. epublish.

Hernday, A. D. *et al.* (Oct. 2013). "Structure of the transcriptional network controlling white-opaque switching in *Candida albicans*." In: *Molecular microbiology* 90 (1), pp. 22–35. ISSN: 1365-2958. DOI: 10.1111/mmi.12329. ppublish.

Homann, O. R. *et al.* (Dec. 2009). "A phenotypic profile of the *Candida albicans* regulatory network." In: *PLoS genetics* 5 (12), e1000783. ISSN: 1553-7404. DOI: 10.1371/journal.pgen.1000783. ppublish.

Hong, S. P. and Carlson, M. (2007). "Regulation of Snf1 Protein Kinase in Response to Environmental Stress". In: *J Biol Chem* 282.23, pp. 16838–16845. DOI: 10.1074/jbc.M700146200.

Hong, S. P. *et al.* (2003). "Activation of yeast Snf1 and mammalian AMP-activated protein kinase by upstream kinases". In: *Proc Natl Acad Sci U S A* 100.15, pp. 8839–8843. DOI: 10.1073/pnas.1533136100.

Hsu, H. E. *et al.* (2015). "Feedback Control of Snf1 Protein and Its Phosphorylation Is Necessary for Adaptation to Environmental Stress". In: *J Biol Chem* 290.27, pp. 16786–16796. DOI: 10.1074/jbc.M115.639443.

Hyde, K. D. *et al.* (2019). "The Amazing Potential Of Fungi: 50 Ways We Can Exploit Fungi Industrially". In: *Fungal Diversity* 97.1, pp. 1–136. ISSN: 1878-9129. DOI: 10.1007/s13225-019-00430-9.

Jiang, R. and Carlson, M. (Dec. 1996). "Glucose regulates protein interactions within the yeast SNF1 protein kinase complex." In: *Genes & development* 10 (24), pp. 3105–3115. ISSN: 0890-9369. DOI: 10.1101/gad.10.24.3105. ppublish.

Jiao, R. *et al.* (June 2015). "The SNF1 Kinase Ubiquitin-associated Domain Restrains Its Activation, Activity, and the Yeast Life Span." In: *The Journal of biological chemistry* 290 (25), pp. 15393–15404. ISSN: 1083-351X. DOI: 10.1074/jbc.M115.647032. ppublish.

Jo, J.-h., Kennedy, E. A., and Kong, H. H. (2017). "Topographical And Physiological Differences Of The Skin Mycobiome In Health And Disease." In: *Virulence* 8.3, pp. 324–333. ISSN: 2150-5608. DOI: 10.1080/21505594.2016.1249093.

Johnston, M., Flick, J. S., and Pexton, T. (June 1994). "Multiple mechanisms provide rapid and stringent glucose repression of GAL gene expression in *Saccharomyces cerevisiae*." In: *Molecular and cellular biology* 14, pp. 3834–3841. ISSN: 0270-7306. DOI: 10.1128/mcb.14.6.3834. ppublish.

Jung, U. S. *et al.* (Nov. 2002). "Regulation of the yeast Rlm1 transcription factor by the Mpk1 cell wall integrity MAP kinase." In: *Molecular microbiology* 46 (3), pp. 781–789. ISSN: 0950-382X. DOI: 10.1046/j.1365-2958.2002.03198.x. ppublish.

Kamada, Y. *et al.* (Apr. 1996). "Activation of yeast protein kinase C by Rho1 GTPase." In: *The Journal of biological chemistry* 271 (16), pp. 9193–9196. ISSN: 0021-9258. DOI: 10.1074/jbc.271.16.9193. ppublish.

Kaniak, A. *et al.* (2004). "Regulatory Network Connecting Two Glucose Signal Transduction Pathways in *Saccharomyces cerevisiae*". In: *Eukaryotic Cell* 3.1, pp. 221–231. ISSN: 1535-9778. DOI: 10.1128/ec.3.1.221-231.2004.

Kapitzky, L. *et al.* (Dec. 2010). "Cross-species chemogenomic profiling reveals evolutionarily conserved drug mode of action." In: *Molecular systems biology* 6, p. 451. ISSN: 1744-4292. DOI: 10.1038/msb.2010.107. ppublish.

Kapteyn, J. C. *et al.* (Feb. 2000). "The cell wall architecture of *Candida albicans* wild-type cells and cell wall-defective mutants." In: *Molecular microbiology* 35 (3), pp. 601–611. ISSN: 0950-382X. DOI: 10.1046/j.1365-2958.2000.01729.x. ppublish.

Kardos, N. and Demain, A. L. (2011). "Penicillin: The Medicine With The Greatest Impact On Therapeutic Outcomes". In: *Applied Microbiology And Biotechnology* 92.4, pp. 677–687. ISSN: 0175-7598. DOI: 10.1007/s00253-011-3587-6.

Kim, S. W. *et al.* (Sept. 2019). "Cross-talk between Tor1 and Sch9 regulates hyphae-specific genes or ribosomal protein genes in a mutually exclusive manner in *Candida albicans*." In: *Molecular microbiology* 112 (3), pp. 1041–1057. ISSN: 1365-2958. DOI: 10.1111/mmi.14346. ppublish.

Klis, F. M., Groot, P. de, and Hellingwerf, K. (2001). "Molecular organization of the cell wall of *Candida albicans*." In: *Medical mycology* 39 Suppl 1, pp. 1–8. ISSN: 1369-3786. ppublish.

Kuchin, S., Treich, I., and Carlson, M. (July 2000). "A regulatory shortcut between the Snf1 protein kinase and RNA polymerase II holoenzyme." In: *Proceedings of the National Academy of Sciences of the United States of America* 97 (14), pp. 7916–7920. ISSN: 0027-8424. DOI: 10.1073/pnas.140109897. ppublish.

Kuchin, S., Vyas, V. K., and Carlson, M. (June 2002). "Snf1 protein kinase and the repressors Nrg1 and Nrg2 regulate FLO11, haploid invasive growth, and diploid pseudohyphal differentiation." In: *Molecular and cellular biology* 22 (12), pp. 3994–4000. ISSN: 0270-7306. DOI: 10.1128/mcb.22.12.3994-4000.2002. ppublish.

Lagree, K. *et al.* (Jan. 2020). "Roles of *Candida albicans* Mig1 and Mig2 in glucose repression, pathogenicity traits, and SNF1 essentiality." In: *PLoS genetics* 16 (1), e1008582. ISSN: 1553-7404. DOI: 10.1371/journal.pgen.1008582. epublish.

Lakshmanan, J., Mosley, A. L., and Özcan, S. (2003). "Repression of transcription by Rgt1 in the absence of glucose requires Std1 and Mth1". In: *Current Genetics* 44.1, pp. 19–25. ISSN: 0172-8083. DOI: 10.1007/s00294-003-0423-2.

Leech, A. *et al.* (Apr. 2003). "Isolation of mutations in the catalytic domain of the snf1 kinase that render its activity independent of the snf4 subunit." In: *Eukaryotic cell* 2 (2), pp. 265–273. ISSN: 1535-9778. DOI: 10.1128/ec.2.2.265-273.2003. ppublish.

Lenardon, M. D. *et al.* (2009). "Dissection of the *Candida albicans* class I chitin synthase promoters". In: *Molecular Genetics and Genomics* 281. ISSN: 1617-4615. DOI: 10.1007/s00438-009-0423-0.

Lesage, P., Yang, X., and Carlson, M. (May 1996). "Yeast SNF1 protein kinase interacts with SIP4, a C6 zinc cluster transcriptional activator: a new role for SNF1 in the glucose response." In: *Molecular and cellular biology* 16 (5), pp. 1921–1928. ISSN: 0270-7306. DOI: 10.1128/mcb.16.5.1921. ppublish.

Levin, D. E. (Dec. 2011). "Regulation of cell wall biogenesis in *Saccharomyces cerevisiae*: the cell wall integrity signaling pathway." In: *Genetics* 189 (4), pp. 1145–1175. ISSN: 1943-2631. DOI: 10.1534/genetics.111.128264. ppublish.

Li, R. *et al.* (2015). "*Candida albicans* Cek1 mitogen-activated protein kinase signaling enhances fungicidal activity of salivary histatin 5." In: *Antimicrobial agents and chemotherapy* 59 (6), pp. 3460–3468. ISSN: 1098-6596. DOI: 10.1128/AAC.00214-15. ppublish.

Liang, S.-H. and Bennett, R. J. (Dec. 2019). "The Impact of Gene Dosage and Heterozygosity on The Diploid Pathobiont *Candida albicans*". In: *Journal of fungi (Basel, Switzerland)* 6 (1). ISSN: 2309-608X. DOI: 10.3390/jof6010010. epublish.

Lim, M. K. *et al.* (May 2011). "Galactose induction of the GAL1 gene requires conditional degradation of the Mig2 repressor." In: *The Biochemical journal* 435 (3), pp. 641–649. ISSN: 1470-8728. DOI: 10.1042/BJ20102034. ppublish.

Liu, W. *et al.* (June 2010a). "The protein kinase CaSch9p is required for the cell growth, filamentation and virulence in the human fungal pathogen *Candida albicans*." In: *FEMS yeast research* 10 (4), pp. 462–470. ISSN: 1567-1364. DOI: 10.1111/j.1567-1364.2010.00617.x. ppublish.

Liu, Y., Xu, X., and Kuo, M.-H. (Jan. 2010b). "Snf1p regulates Gcn5p transcriptional activity by antagonizing Spt3p." In: *Genetics* 184 (1), pp. 91–105. ISSN: 1943-2631. DOI: 10.1534/genetics.109.110957. ppublish.

Lo, W. S. and Dranginis, A. M. (Jan. 1998). "The cell surface flocculin Flo11 is required for pseudohyphae formation and invasion by *Saccharomyces cerevisiae*." In: *Molecular biology of the cell* 9 (1), pp. 161–171. ISSN: 1059-1524. DOI: 10.1091/mbc.9.1.161. ppublish.

Lo, W. S. *et al.* (Aug. 2001). "Snf1–a histone kinase that works in concert with the histone acetyltransferase Gcn5 to regulate transcription." In: *Science (New York, N.Y.)* 293 (5532), pp. 1142–1146. ISSN: 0036-8075. DOI: 10.1126/science.1062322. ppublish.

Love, M. I., Huber, W., and Anders, S. (2014). "Moderated estimation of fold change and dispersion for RNA-seq data with DESeq2". In: *Genome biology* 15 (12), p. 550. ISSN: 1474-760X. DOI: 10.1186/s13059-014-0550-8.

Lutfiyya, L. L. *et al.* (Dec. 1998). "Characterization of three related glucose repressors and genes they regulate in *Saccharomyces cerevisiae*." In: *Genetics* 150 (4), pp. 1377–1391. ISSN: 0016-6731. ppublish.

Martchenko, M. *et al.* (June 2007). "Transcriptional rewiring of fungal galactose-metabolism circuitry." In: *Current biology : CB* 17 (12), pp. 1007–1013. ISSN: 0960-9822. DOI: 10.1016/j.cub.2007.05.017. ppublish.

Mayer, F. V. *et al.* (Nov. 2011). "ADP regulates SNF1, the *Saccharomyces cerevisiae* homolog of AMP-activated protein kinase." In: *Cell metabolism* 14 (5), pp. 707–714. ISSN: 1932-7420. DOI: 10.1016/j.cmet.2011.09.009. ppublish.

Mayordomo, I., Estruch, F., and Sanz, P. (Sept. 2002). "Convergence of the target of rapamycin and the Snf1 protein kinase pathways in the regulation of the subcellular localization of Msn2, a transcriptional activator of STRE (Stress Response Element)-regulated genes." In: *The Journal of biological chemistry* 277 (38), pp. 35650–35656. ISSN: 0021-9258. DOI: 10.1074/jbc.M204198200. ppublish.

Mazur, P. *et al.* (Oct. 1995). "Differential expression and function of two homologous subunits of yeast 1,3-beta-D-glucan synthase." In: *Molecu-*

lar and cellular biology 15 (10), pp. 5671–5681. ISSN: 0270-7306. DOI: 10.1128/mcb.15.10.5671. ppublish.

Mcgovern, P. E. *et al.* (2004). "Fermented Beverages Of Pre- And Proto-historic China". In: *Proceedings Of The National Academy Of Sciences* 101.51, pp. 17593–17598. ISSN: 0027-8424. DOI: 10.1073/pnas.0407921102.

Mesa-Arango, A. C., Scorzoni, L., and Zaragoza, O. (2012). "It Only Takes One To Do Many Jobs: Amphotericin B As Antifungal And Immunomodulatory Drug". In: *Frontiers In Microbiology* 3. ISSN: 1664-302X. DOI: 10.3389/fmicb.2012.00286.

Michel, S. *et al.* (Oct. 2002). "Generation of conditional lethal *Candida albicans* mutants by inducible deletion of essential genes." In: *Molecular microbiology* 46 (1), pp. 269–280. ISSN: 0950-382X. DOI: 10.1046/j.1365-2958.2002.03167.x. ppublish.

Mora-Montes, H. M. *et al.* (Apr. 2010). "A multifunctional mannosyltransferase family in *Candida albicans* determines cell wall mannan structure and host-fungus interactions." In: *The Journal of biological chemistry* 285 (16), pp. 12087–12095. ISSN: 1083-351X. DOI: 10.1074/jbc.M109.081513. ppublish.

Moreno, I. *et al.* (Feb. 2010). "Dosage-dependent roles of the Cwt1 transcription factor for cell wall architecture, morphogenesis, drug sensitivity and virulence in *Candida albicans*." In: *Yeast (Chichester, England)* 27 (2), pp. 77–87. ISSN: 1097-0061. DOI: 10.1002/yea.1733. ppublish.

Moriya, H. and Johnston, M. (2004). "Glucose sensing and signaling in *Saccharomyces cerevisiae* through the Rgt2 glucose sensor and casein kinase I". In: *Proceedings of the National Academy of Sciences* 101.6, pp. 1572–1577. ISSN: 0027-8424. DOI: 10.1073/pnas.0305901101.

Morschhäuser, J. (Mar. 2016). "The development of fluconazole resistance in *Candida albicans* - an example of microevolution of a fungal pathogen." In: *Journal of microbiology (Seoul, Korea)* 54 (3), pp. 192–201. ISSN: 1976-3794. DOI: 10.1007/s12275-016-5628-4. ppublish.

Mottola, A. (2016). "Functional Analysis of the Snf1 Activating Kinase Sak1 in *Candida albicans*". Master's Thesis. University of Würzburg.

Mowat, A. M. (2003). "Anatomical Basis Of Tolerance And Immunity To Intestinal Antigens." In: *Nature Reviews. Immunology* 3.4, pp. 331–341. ISSN: 1474-1733. DOI: 10.1038/nri1057.

Munro, C. A. *et al.* (Mar. 2001). "Chs1 of *Candida albicans* is an essential chitin synthase required for synthesis of the septum and for cell integrity." In: *Molecular microbiology* 39 (5), pp. 1414–1426. ISSN: 0950-382X. DOI: 10.1046/j.1365-2958.2001.02347.x. ppublish.

Munro, C. A. *et al.* (Jan. 2005). "Mnt1p and Mnt2p of *Candida albicans* are partially redundant alpha-1,2-mannosyltransferases that participate in O-linked mannosylation and are required for adhesion and virulence." In: *The Journal of biological chemistry* 280 (2), pp. 1051–1060. ISSN: 0021-9258. DOI: 10.1074/jbc.M411413200. ppublish.

Munro, C. A. *et al.* (Mar. 2007). "The PKC, HOG and Ca2+ signalling pathways co-ordinately regulate chitin synthesis in *Candida albicans*." In: *Molecular microbiology* 63 (5), pp. 1399–1413. ISSN: 0950-382X. DOI: 10.1111/j.1365-2958.2007.05588.x. ppublish.

Murad, A. M. *et al.* (Nov. 2001). "Transcript profiling in *Candida albicans* reveals new cellular functions for the transcriptional repressors CaTup1, CaMig1 and CaNrg1." In: *Molecular microbiology* 42 (4), pp. 981–993. ISSN: 0950-382X. DOI: 10.1046/j.1365-2958.2001.02713.x. ppublish.

Nath, N., McCartney, R. R., and Schmidt, M. C. (2003). "Yeast Pak1 kinase associates with and activates Snf1". In: *Mol Cell Biol* 23.11, pp. 3909–3917. DOI: 10.1128/mcb.23.11.3909-3917.2003.

Nather, K. and Munro, C. A. (Aug. 2008). "Generating cell surface diversity in *Candida albicans* and other fungal pathogens." In: *FEMS microbiology letters* 285 (2), pp. 137–145. ISSN: 0378-1097. DOI: 10.1111/j.1574-6968.2008.01263.x. ppublish.

Nayak, V. *et al.* (2006). "Structure and Dimerization of the Kinase Domain from Yeast Snf1, a Member of the Snf1/AMPK Protein Family". In: *Structure* 14.3, pp. 477–85. ISSN: 0969-2126 (Print) 0969-2126 (Linking). DOI: 10.1016/j.str.2005.12.008.

Nehlin, J. O., Carlberg, M., and Ronne, H. (Nov. 1991). "Control of yeast GAL genes by MIG1 repressor: a transcriptional cascade in the glucose response." In: *The EMBO journal* 10, pp. 3373–3377. ISSN: 0261-4189. ppublish.

Noble, S. M. *et al.* (July 2010). "Systematic screens of a *Candida albicans* homozygous deletion library decouple morphogenetic switching and pathogenicity." In: *Nature genetics* 42 (7), pp. 590–598. ISSN: 1546-1718. DOI: 10.1038/ng.605. ppublish.

Nocedal, I. and Johnson, A. D. (2015). "How Transcription Networks Evolve and Produce Biological Novelty." In: *Cold Spring Harbor symposia on quantitative biology* 80, pp. 265–274. ISSN: 1943-4456. DOI: 10.1101/sqb.2015.80.027557. ppublish.

Orlova, M., Barrett, L., and Kuchin, S. (Oct. 2008). "Detection of endogenous Snf1 and its activation state: application to Saccharomyces and Candida species." In: *Yeast (Chichester, England)* 25 (10), pp. 745–754. ISSN: 1097-0061. DOI: 10.1002/yea.1628. ppublish.

Orlova, M. *et al.* (Nov. 2006). "Nitrogen availability and TOR regulate the Snf1 protein kinase in *Saccharomyces cerevisiae*." In: *Eukaryotic*

cell 5 (11), pp. 1831–1837. ISSN: 1535-9778. DOI: 10.1128/EC.00110-06. ppublish.

Ozaki, K. *et al.* (May 1996). "Rom1p and Rom2p are GDP/GTP exchange proteins (GEPs) for the Rho1p small GTP binding protein in *Saccharomyces cerevisiae*." In: *The EMBO journal* 15 (9), pp. 2196–2207. ISSN: 0261-4189. ppublish.

Özcan, S., Leong, T., and Johnston, M. (1996a). "Rgt1p of *Saccharomyces cerevisiae*, a key regulator of glucose-induced genes, is both an activator and a repressor of transcription." In: *Molecular and Cellular Biology* 16.11, pp. 6419–6426. ISSN: 0270-7306. DOI: 10.1128/mcb.16.11.6419.

Özcan, S. *et al.* (1996b). "Two glucose transporters in *Saccharomyces cerevisiae* are glucose sensors that generate a signal for induction of gene expression." In: *Proceedings of the National Academy of Sciences* 93.22, pp. 12428–12432. ISSN: 0027-8424. DOI: 10.1073/pnas.93.22.12428.

Papamichos-Chronakis, M., Gligoris, T., and Tzamarias, D. (Apr. 2004). "The Snf1 kinase controls glucose repression in yeast by modulating interactions between the Mig1 repressor and the Cyc8-Tup1 co-repressor." In: *EMBO reports* 5, pp. 368–372. ISSN: 1469-221X. DOI: 10.1038/sj.embor.7400120. ppublish.

Pappas, P. G. *et al.* (2015). "Clinical Practice Guideline for the Management of Candidiasis: 2016 Update by the Infectious Diseases Society of America". In: *Clinical Infectious Diseases*, Pages e1–e50. ISSN: 1058-4838. DOI: 10.1093/cid/civ933.

Pappas, P. G. *et al.* (2018). "Invasive Candidiasis." In: *Nature Reviews. Disease Primers* 4.1, p. 18026. ISSN: 2056-676X. DOI: 10.1038/nrdp.2018.26. Epublis.

Pasula, S., Jouandot, D., and Kim, J.-H. (2007). "Biochemical evidence for glucose-independent induction of HXT expression in *Saccharomyces cerevisiae*". In: *FEBS Letters* 581.17, pp. 3230–3234. ISSN: 0014-5793. DOI: 10.1016/j.febslet.2007.06.013.

Petter, R., Chang, Y. C., and Kwon-Chung, K. J. (Dec. 1997). "A gene homologous to *Saccharomyces cerevisiae* SNF1 appears to be essential for the viability of *Candida albicans*." In: *Infection and immunity* 65 (12), pp. 4909–4917. ISSN: 0019-9567. DOI: 10.1128/IAI.65.12.4909-4917.1997. ppublish.

Pfaller, M. A., Pappas, P. G., and Wingard, J. R. (2006). "Invasive Fungal Pathogens: Current Epidemiological Trends". In: *Clinical Infectious Diseases* 43.Supplement 1, S3–s14. DOI: 10.1086/504490.

Pfaller, M. A. *et al.* (2019). "Twenty Years of the SENTRY Antifungal Surveillance Program: Results for Candida Species From 1997–2016". In: *Open Forum Infectious Diseases* 6, S79–S94. ISSN: 2328-8957. DOI: 10.1093/ofid/ofy358.

Philip, B. and Levin, D. E. (Jan. 2001). "Wsc1 and Mid2 are cell surface sensors for cell wall integrity signaling that act through Rom2, a guanine nucleotide exchange factor for Rho1." In: *Molecular and cellular biology* 21 (1), pp. 271–280. ISSN: 0270-7306. DOI: 10.1128/MCB.21.1.271-280.2001. ppublish.

Pradhan, A. *et al.* (Nov. 2018). "Hypoxia Promotes Immune Evasion by Triggering β-Glucan Masking on the *Candida albicans* Cell Surface via Mitochondrial and cAMP-Protein Kinase A Signaling." In: *mBio* 9 (6). ISSN: 2150-7511. DOI: 10.1128/mBio.01318-18. epublish.

Pradhan, A. *et al.* (Nov. 2019). "Non-canonical signalling mediates changes in fungal cell wall PAMPs that drive immune evasion." In: *Nature communications* 10 (1), p. 5315. ISSN: 2041-1723. DOI: 10.1038/s41467-019-13298-9. epublish.

Prill, S. K.-H. *et al.* (Jan. 2005). "PMT family of *Candida albicans*: five protein mannosyltransferase isoforms affect growth, morphogenesis and antifungal resistance." In: *Molecular microbiology* 55 (2), pp. 546–560. ISSN: 0950-382X. DOI: 10.1111/j.1365-2958.2004.04401.x. ppublish.

Qin, J. *et al.* (2010). "A Human Gut Microbial Gene Catalogue Established By Metagenomic Sequencing." In: *Nature* 464.7285, pp. 59–65. ISSN: 1476-4687. DOI: 10.1038/nature08821.

Ram, A. F. J. and Klis, F. M. (2006). "Identification of fungal cell wall mutants using susceptibility assays based on Calcofluor white and Congo red." In: *Nature protocols* 1 (5), pp. 2253–2256. ISSN: 1750-2799. DOI: 10.1038/nprot.2006.397. ppublish.

Ramírez, M. A. and Lorenz, M. C. (Oct. 2009). "The transcription factor homolog CTF1 regulates beta-oxidation in *Candida albicans*." In: *Eukaryotic cell* 8 (10), pp. 1604–1614. ISSN: 1535-9786. DOI: 10.1128/EC.00206-09. ppublish.

Ramírez-Zavala, B. *et al.* (2008). "Environmental induction of white-opaque switching in *Candida albicans*." In: *PLoS pathogens* 4 (6), e1000089. ISSN: 1553-7374. DOI: 10.1371/journal.ppat.1000089. epublish.

Ramírez-Zavala, B. *et al.* (June 2017). "The Snf1-activating kinase Sak1 is a key regulator of metabolic adaptation and in vivo fitness of *Candida albicans*." In: *Molecular microbiology* 104 (6), pp. 989–1007. ISSN: 1365-2958. DOI: 10.1111/mmi.13674. ppublish.

Randez-Gil, F. *et al.* (May 1997). "Glucose derepression of gluconeogenic enzymes in *Saccharomyces cerevisiae* correlates with phosphorylation of the gene activator Cat8p." In: *Molecular and cellular biology* 17 (5), pp. 2502–2510. ISSN: 0270-7306. DOI: 10.1128/mcb.17.5.2502. ppublish.

Remy, W. *et al.* (1994). "Four Hundred-million-year-old Vesicular Arbuscular Mycorrhizae." In: *Proceedings Of The National Academy Of Sciences* 91.25, pp. 11841–11843. ISSN: 0027-8424. DOI: 10.1073/pnas.91.25.11841.

Reuss, O. *et al.* (2004). "The Sat1 Flipper, An Optimized Tool For Gene Disruption In Candida Albicans." In: *Gene* 341, pp. 119–127. ISSN: 0378-1119. DOI: 10.1016/j.gene.2004.06.021.

Rodríguez-Colman, M. J. *et al.* (Aug. 2013). "The FOX transcription factor Hcm1 regulates oxidative metabolism in response to early nutrient limitation in yeast. Role of Snf1 and Tor1/Sch9 kinases." In: *Biochimica et biophysica acta* 1833 (8), pp. 2004–2015. ISSN: 0006-3002. DOI: 10.1016/j.bbamcr.2013.02.015. ppublish.

Román, E. *et al.* (July 2016). "The Cek1-mediated MAP kinase pathway regulates exposure of α-1,2 and β-1,2-mannosides in the cell wall of *Candida albicans* modulating immune recognition." In: *Virulence* 7 (5), pp. 558–577. ISSN: 2150-5608. DOI: 10.1080/21505594.2016.1163458. ppublish.

Romani, L. (2011). "Immunity To Fungal Infections." In: *Nature Reviews. Immunology* 11.4, pp. 275–288. ISSN: 1474-1741. DOI: 10.1038/nri2939.

Rubenstein, E. M. *et al.* (Jan. 2008). "Access denied: Snf1 activation loop phosphorylation is controlled by availability of the phosphorylated threonine 210 to the PP1 phosphatase." In: *The Journal of biological chemistry* 283 (1), pp. 222–230. ISSN: 0021-9258. DOI: 10.1074/jbc.M707957200.

Ruiz, A., Xu, X., and Carlson, M. (Apr. 2011). "Roles of two protein phosphatases, Reg1-Glc7 and Sit4, and glycogen synthesis in regulation of SNF1 protein kinase." In: *Proceedings of the National Academy of Sciences of the United States of America* 108 (16), pp. 6349–6354. ISSN: 1091-6490. DOI: 10.1073/pnas.1102758108.

— (Oct. 2013). "Ptc1 protein phosphatase 2C contributes to glucose regulation of SNF1/AMP-activated protein kinase (AMPK) in *Saccharomyces cerevisiae*." In: *The Journal of biological chemistry* 288 (43), pp. 31052–31058. ISSN: 1083-351X. DOI: 10.1074/jbc.M113.503763.

Ruiz-Herrera, J. *et al.* (Jan. 2006). "Molecular organization of the cell wall of *Candida albicans* and its relation to pathogenicity." In: *FEMS yeast research* 6 (1), pp. 14–29. ISSN: 1567-1356. DOI: 10.1111/j.1567-1364.2005.00017.x. ppublish.

Sabire Özcan, J. D. and Johnston, M. (1998). "Glucose sensing and signaling by two glucose receptors in the yeast *Saccharomyces cerevisiae*". In: *The EMBO Journal* 17.9, pp. 2566–2573. ISSN: 1460-2075. DOI: 10.1093/emboj/17.9.2566.

Sandai, D. *et al.* (Dec. 2012). "The evolutionary rewiring of ubiquitination targets has reprogrammed the regulation of carbon assimilation in the pathogenic yeast *Candida albicans*." In: *mBio* 3 (6). ISSN: 2150-7511. DOI: 10.1128/mBio.00495-12. epublish.

Sanz, P. *et al.* (2000). "Regulatory Interactions between the Reg1-Glc7 Protein Phosphatase and the Snf1 Protein Kinase". In: *Molecular and Cellular Biology* 20.4, pp. 1321–1328. DOI: 10.1128/mcb.20.4.1321-1328.2000.

Sawistowska-Schröder, E. T., Kerridge, D., and Perry, H. (1984). "Echinocandin inhibition of 1,3-β-D-glucan synthase from *Candida albicans*". In: *FEBS Letters* 173, pp. 134–138. ISSN: 0014-5793. DOI: 10.1016/0014-5793(84)81032-7.

Schillig, R. and Morschhäuser, J. (Sept. 2013). "Analysis of a fungus-specific transcription factor family, the *Candida albicans* zinc cluster proteins, by artificial activation." In: *Molecular microbiology* 89 (5), pp. 1003–1017. ISSN: 1365-2958. DOI: 10.1111/mmi.12327. ppublish.

Schmidt, M. C. and McCartney, R. R. (Sept. 2000). "β-subunits of Snf1 kinase are required for kinase function and substrate definition." In: *The EMBO journal* 19 (18), pp. 4936–4943. ISSN: 0261-4189. DOI: 10.1093/emboj/19.18.4936. ppublish.

Schüller, H. J. and Entian, K. D. (Mar. 1991). "Extragenic suppressors of yeast glucose derepression mutants leading to constitutive synthesis of several glucose-repressible enzymes." In: *Journal of bacteriology* 173, pp. 2045–2052. ISSN: 0021-9193. DOI: 10.1128/jb.173.6.2045-2052.1991. ppublish.

Seed, P. C. (2015). "The Human Mycobiome". In: *Cold Spring Harbor Perspectives In Medicine* 5.5, A019810–a019810. ISSN: 2157-1422. DOI: 10.1101/cshperspect.a019810.

Sexton, J. A., Brown, V., and Johnston, M. (2007). "Regulation of sugar transport and metabolism by the *Candida albicans* Rgt1 transcriptional repressor". In: *Yeast* 24.10, pp. 847–860. ISSN: 0749-503X. DOI: 10.1002/yea.1514.

Shashkova, S. *et al.* (Aug. 2017). "The yeast Mig1 transcriptional repressor is dephosphorylated by glucose-dependent and -independent mechanisms." In: *FEMS microbiology letters* 364 (14). ISSN: 1574-6968. DOI: 10.1093/femsle/fnx133. ppublish.

Sherrington, S. L. *et al.* (May 2017). "Adaptation of *Candida albicans* to environmental pH induces cell wall remodelling and enhances innate immune recognition." In: *PLoS pathogens* 13 (5), e1006403. ISSN: 1553-7374. DOI: 10.1371/journal.ppat.1006403. epublish.

Sievers, F. *et al.* (Oct. 2011). "Fast, scalable generation of high-quality protein multiple sequence alignments using Clustal Omega." In: *Molecular systems biology* 7, p. 539. ISSN: 1744-4292. DOI: 10.1038/msb.2011.75. epublish.

Simpson-Lavy, K. J. and Johnston, M. (Oct. 2013). "SUMOylation regulates the SNF1 protein kinase." In: *Proceedings of the National Academy of Sciences of the United States of America* 110 (43), pp. 17432–17437. ISSN: 1091-6490. DOI: 10.1073/pnas.1304839110. ppublish.

Smith, F. C. *et al.* (June 1999). "The SNF1 kinase complex from *Saccharomyces cerevisiae* phosphorylates the transcriptional repressor protein Mig1p in vitro at four sites within or near regulatory domain 1." In: *FEBS letters* 453, pp. 219–223. ISSN: 0014-5793. DOI: 10.1016/s0014-5793(99)00725-5. ppublish.

Sobel, J. D. (2007). "Vulvovaginal Candidosis". In: *The Lancet* 369.9577, pp. 1961–1971. ISSN: 0140-6736. DOI: 10.1016/S0140-6736(07)60917-9.

Sohn, K. *et al.* (Jan. 2003). "EFG1 is a major regulator of cell wall dynamics in *Candida albicans* as revealed by DNA microarrays." In: *Molecular microbiology* 47 (1), pp. 89–102. ISSN: 0950-382X. DOI: 10.1046/j.1365-2958.2003.03300.x. ppublish.

Spellberg, B. *et al.* (2005). "Mice With Disseminated Candidiasis Die Of Progressive Sepsis." In: *The Journal Of Infectious Diseases* 192.2, pp. 336–343. ISSN: 0022-1899. DOI: 10.1086/430952.

Sutherland, C. M. *et al.* (2003). "Elm1p Is One of Three Upstream Kinases for the *Saccharomyces cerevisiae* SNF1 Complex". In: *Current Biology* 13.15, pp. 1299–1305. ISSN: 0960-9822. DOI: 10.1016/S0960-9822(03)00459-7.

Tachibana, C. *et al.* (Mar. 2005). "Combined global localization analysis and transcriptome data identify genes that are directly coregulated by Adr1 and Cat8." In: *Molecular and cellular biology* 25, pp. 2138–2146. ISSN: 0270-7306. DOI: 10.1128/MCB.25.6.2138-2146.2005. ppublish.

Tebung, W. A. *et al.* (July 2016). "Rewiring of the Ppr1 Zinc Cluster Transcription Factor from Purine Catabolism to Pyrimidine Biogenesis in the Saccharomycetaceae." In: *Current biology : CB* 26 (13), pp. 1677–1687. ISSN: 1879-0445. DOI: 10.1016/j.cub.2016.04.064. ppublish.

Tebung, W. A. *et al.* (2017). "Put3 Positively Regulates Proline Utilization in *Candida albicans*". In: *mSphere* 2 (6). ISSN: 2379-5042. DOI: 10.1128/mSphere.00354-17. epublish.

Tedersoo, L. *et al.* (2014). "Fungal Biogeography. Global Diversity And Geography Of Soil Fungi." In: *Science* 346.6213, p. 1256688. ISSN: 1095-9203. DOI: 10.1126/science.1256688.

Treitel, M. A. and Carlson, M. (Apr. 1995). "Repression by SSN6-TUP1 is directed by MIG1, a repressor/activator protein." In: *Proceedings of the National Academy of Sciences of the United States of America* 92, pp. 3132–3136. ISSN: 0027-8424. DOI: 10.1073/pnas.92.8.3132. ppublish.

Treitel, M. A., Kuchin, S., and Carlson, M. (Nov. 1998). "Snf1 protein kinase regulates phosphorylation of the Mig1 repressor in *Saccharomyces cerevisiae*." In: *Molecular and cellular biology* 18, pp. 6273–6280. ISSN: 0270-7306. DOI: 10.1128/mcb.18.11.6273. ppublish.

Trivedi, N. B. *et al.* (1986). "Bakers' Yeast". In: *Critical Reviews In Biotechnology* 4.1, pp. 75–109. ISSN: 0738-8551. DOI: 10.3109/07388558609150791.

Tu, J. and Carlson, M. (Oct. 1994). "The GLC7 type 1 protein phosphatase is required for glucose repression in *Saccharomyces cerevisiae*." In: *Molecular and cellular biology* 14 (10), pp. 6789–6796. ISSN: 0270-7306. DOI: 10.1128/mcb.14.10.6789. ppublish.

— (1995). "REG1 binds to protein phosphatase type 1 and regulates glucose repression in *Saccharomyces cerevisiae*." In: *The EMBO journal* 14 (23), pp. 5939–5946. ISSN: 0261-4189. ppublish.

Tzamarias, D. and Struhl, K. (Apr. 1995). "Distinct TPR motifs of Cyc8 are involved in recruiting the Cyc8-Tup1 corepressor complex to differentially regulated promoters." In: *Genes & development* 9, pp. 821–831. ISSN: 0890-9369. DOI: 10.1101/gad.9.7.821. ppublish.

Vallier, L. G. and Carlson, M. (May 1994). "Synergistic release from glucose repression by mig1 and ssn mutations in *Saccharomyces cerevisiae*." In: *Genetics* 137, pp. 49–54. ISSN: 0016-6731. ppublish.

Van Ende, M., Wijnants, S., and Van Dijck, P. (2019). "Sugar Sensing and Signaling in *Candida albicans* and Candida glabrata". In: *Frontiers in microbiology* 10, p. 99. ISSN: 1664-302X. DOI: 10.3389/fmicb.2019.00099.

Varela, J. A. *et al.* (2019). "Origin Of Lactose Fermentation In *Kluyveromyces lactis* By Interspecies Transfer Of A Neofunctionalized Gene Cluster During Domestication". In: *SSRN Electronic Journal*. ISSN: 1556-5068. DOI: 10.2139/ssrn.3441908.

Vasicek, E. M. *et al.* (Nov. 2014). "Disruption of the transcriptional regulator Cas5 results in enhanced killing of Candida albicans by Fluconazole." In: *Antimicrobial agents and chemotherapy* 58 (11), pp. 6807–6818. ISSN: 1098-6596. DOI: 10.1128/AAC.00064-14. ppublish.

Vincent, O. and Carlson, M. (Dec. 1998). "Sip4, a Snf1 kinase-dependent transcriptional activator, binds to the carbon source-responsive element of gluconeogenic genes." In: *The EMBO journal* 17 (23), pp. 7002–7008. ISSN: 0261-4189. DOI: 10.1093/emboj/17.23.7002. ppublish.

— (Dec. 1999). "Gal83 mediates the interaction of the Snf1 kinase complex with the transcription activator Sip4." In: *The EMBO journal* 18 (23), pp. 6672–6681. ISSN: 0261-4189. DOI: 10.1093/emboj/18.23.6672. ppublish.

Vincent, O. *et al.* (May 2001). "Subcellular localization of the Snf1 kinase is regulated by specific β subunits and a novel glucose signaling

mechanism." In: *Genes & development* 15 (9), pp. 1104–1114. ISSN: 0890-9369. DOI: 10.1101/gad.879301. ppublish.

Vinces, M. D., Haas, C., and Kumamoto, C. A. (May 2006). "Expression of the *Candida albicans* morphogenesis regulator gene *CZF1* and its regulation by Efg1p and Czf1p." In: *Eukaryotic cell* 5 (5), pp. 825–835. ISSN: 1535-9778. DOI: 10.1128/EC.5.5.825-835.2006. ppublish.

Vinces, M. D. and Kumamoto, C. A. (Sept. 2007). "The morphogenetic regulator Czf1p is a DNA-binding protein that regulates white opaque switching in *Candida albicans*." In: *Microbiology (Reading, England)* 153 (Pt 9), pp. 2877–2884. ISSN: 1350-0872. DOI: 10.1099/mic.0.2007/005983-0. ppublish.

Vyas, V. K., Kuchin, S., and Carlson, M. (June 2001). "Interaction of the repressors Nrg1 and Nrg2 with the Snf1 protein kinase in *Saccharomyces cerevisiae*." In: *Genetics* 158 (2), pp. 563–572. ISSN: 0016-6731. ppublish.

Vyas, V. K., Barrasa, M. I., and Fink, G. R. (2015). "A *Candida albicans* CRISPR system permits genetic engineering of essential genes and gene families." In: *Science advances* 1 (3), e1500248. ISSN: 2375-2548. DOI: 10.1126/sciadv.1500248. ppublish.

Vyas, V. K. *et al.* (Feb. 2003). "Snf1 kinases with different beta-subunit isoforms play distinct roles in regulating haploid invasive growth." In: *Molecular and cellular biology* 23 (4), pp. 1341–1348. ISSN: 0270-7306. DOI: 10.1128/mcb.23.4.1341-1348.2003. ppublish.

Waldorf, A. R. and Polak, A. (1983). "Mechanisms Of Action Of 5-fluorocytosine." In: *Antimicrobial Agents And Chemotherapy* 23.1, pp. 79–85. ISSN: 0066-4804. DOI: 10.1128/aac.23.1.79.

Wartenberg, A. *et al.* (Dec. 2014). "Microevolution of *Candida albicans* in macrophages restores filamentation in a nonfilamentous mutant." In: *PLoS genetics* 10 (12), e1004824. ISSN: 1553-7404. DOI: 10.1371/journal.pgen.1004824. epublish.

Watamoto, T. *et al.* (Sept. 2011). "Transcriptional regulation of drug-resistance genes in *Candida albicans* biofilms in response to antifungals." In: *Journal of medical microbiology* 60 (Pt 9), pp. 1241–1247. ISSN: 1473-5644. DOI: 10.1099/jmm.0.030692-0. ppublish.

Waterhouse, A. M. *et al.* (May 2009). "Jalview Version 2–a multiple sequence alignment editor and analysis workbench." In: *Bioinformatics (Oxford, England)* 25 (9), pp. 1189–1191. ISSN: 1367-4811. DOI: 10.1093/bioinformatics/btp033. ppublish.

Watson, P. F. *et al.* (1989). "Defective sterol C5-6 desaturation and azole resistance: A new hypothesis for the mode of action of azole antifungals". In: *Biochemical and Biophysical Research Communications* 164.3, pp. 1170–1175. ISSN: 0006-291X. DOI: 10.1016/0006-291x(89)91792-0.

Weber, S. (2020). "Investigation of the Glucose Repression Pathway in *Candida albicans*". Bachelor's Thesis. University of Würzburg.

Westholm, J. O. *et al.* (Dec. 2008). "Combinatorial control of gene expression by the three yeast repressors Mig1, Mig2 and Mig3." In: *BMC genomics* 9, p. 601. ISSN: 1471-2164. DOI: 10.1186/1471-2164-9-601. epublish.

Wheeler, M. l. *et al.* (2016). "Immunological Consequences Of Intestinal Fungal Dysbiosis". In: *Cell Host & Microbe* 19.6, pp. 865–873. ISSN: 1931-3128. DOI: 10.1016/j.chom.2016.05.003.

Wheeler, R. T. and Fink, G. R. (Apr. 2006). "A drug-sensitive genetic network masks fungi from the immune system." In: *PLoS pathogens* 2 (4), e35. ISSN: 1553-7374. DOI: 10.1371/journal.ppat.0020035. ppublish.

Wieczorke, R. *et al.* (1999). "Concurrent knock-out of at least 20 transporter genes is required to block uptake of hexoses in Saccharomyces cerevisiaes". In: *FEBS Letters* 464.3, pp. 123–128. ISSN: 0014-5793. DOI: 10.1016/s0014-5793(99)01698-1.

Wilkins, M., Zhang, N., and Schmid, J. (June 2018). "Biological roles of protein-coding tandem repeats in the yeast *Candida albicans*". In: *Journal of fungi (Basel, Switzerland)* 4 (3). ISSN: 2309-608X. DOI: 10.3390/jof4030078. epublish.

Willger, S. D. *et al.* (May 2015). "Analysis of the *Candida albicans* Phosphoproteome." In: *Eukaryotic cell* 14 (5), pp. 474–485. ISSN: 1535-9786. DOI: 10.1128/EC.00011-15. ppublish.

Wilson, J. B. *et al.* (2012). "Plant Species Richness: The World Records". In: *Journal Of Vegetation Science* 23.4. Ed. by M. Palmer, pp. 796–802. ISSN: 1100-9233. DOI: 10.1111/j.1654-1103.2012.01400.x.

Wilson, M. A. *et al.* (Aug. 2011). "Ubp8 and SAGA regulate Snf1 AMP kinase activity." In: *Molecular and cellular biology* 31 (15), pp. 3126–3135. ISSN: 1098-5549. DOI: 10.1128/MCB.01350-10. ppublish.

Wilson, W. A., Hawley, S. A., and Hardie, D. G. (1996). "Glucose repression/derepression in budding yeast: SNF1 protein kinase is activated by phosphorylation under derepressing conditions, and this correlates with a high AMP:ATP ratio". In: *Current Biology* 6.11, pp. 1426–1434. ISSN: 0960-9822. DOI: 10.1016/S0960-9822(96)00747-6.

Woods, A. *et al.* (July 1994). "Yeast SNF1 is functionally related to mammalian AMP-activated protein kinase and regulates acetyl-CoA carboxylase in vivo." In: *The Journal of biological chemistry* 269 (30), pp. 19509–19515. ISSN: 0021-9258. ppublish.

Xie, J. L. *et al.* (Sept. 2017). "The *Candida albicans* transcription factor Cas5 couples stress responses, drug resistance and cell cycle regula-

tion." In: *Nature communications* 8 (1), p. 499. ISSN: 2041-1723. DOI: 10.1038/s41467-017-00547-y. epublish.

Xiong, K. *et al.* (Nov. 2020). "Efg1 and Cas5 Orchestrate Cell Wall Damage Response to Caspofungin in *Candida albicans*". In: *Antimicrobial agents and chemotherapy*. ISSN: 1098-6596. DOI: 10.1128/AAC.01584-20. aheadofprint.

Yang, X., Hubbard, E. J., and Carlson, M. (July 1992). "A protein kinase substrate identified by the two-hybrid system." In: *Science (New York, N.Y.)* 257 (5070), pp. 680–682. ISSN: 0036-8075. DOI: 10.1126/science.1496382. ppublish.

Yang, X., Jiang, R., and Carlson, M. (Dec. 1994). "A family of proteins containing a conserved domain that mediates interaction with the yeast SNF1 protein kinase complex." In: *The EMBO journal* 13 (24), pp. 5878–5886. ISSN: 0261-4189. ppublish.

Yapar, N. (2014). "Epidemiology And Risk Factors For Invasive Candidiasis". In: *Therapeutics And Clinical Risk Management*, p. 95. ISSN: 1178-203X. DOI: 10.2147/tcrm.s40160.

Young, E. T. *et al.* (July 2003). "Multiple pathways are co-regulated by the protein kinase Snf1 and the transcription factors Adr1 and Cat8." In: *The Journal of biological chemistry* 278 (28), pp. 26146–26158. ISSN: 0021-9258. DOI: 10.1074/jbc.M301981200. ppublish.

Young, E. T. *et al.* (Aug. 2012). "The AMP-activated protein kinase Snf1 regulates transcription factor binding, RNA polymerase II activity, and mRNA stability of glucose-repressed genes in *Saccharomyces cerevisiae*." In: *The Journal of biological chemistry* 287 (34), pp. 29021–29034. ISSN: 1083-351X. DOI: 10.1074/jbc.M112.380147. ppublish.

Zaragoza, O., Rodríguez, C., and Gancedo, C. (Jan. 2000). "Isolation of the MIG1 gene from *Candida albicans* and effects of its disruption on catabolite repression." In: *Journal of bacteriology* 182 (2), pp. 320–326. ISSN: 0021-9193. DOI: 10.1128/jb.182.2.320-326.2000. ppublish.

Zhang, J. *et al.* (Nov. 2011). "Mapping the interaction of Snf1 with TORC1 in *Saccharomyces cerevisiae*." In: *Molecular systems biology* 7, p. 545. ISSN: 1744-4292. DOI: 10.1038/msb.2011.80. epublish.

Zhou, Z. *et al.* (2017). "Highly mutable tandem DNA repeats generate a cell wall protein variant more frequent in disease-causing *Candida albicans* isolates than in commensal isolates." In: *PloS one* 12 (6), e0180246. ISSN: 1932-6203. DOI: 10.1371/journal.pone.0180246. epublish.

Zimmermann, F. K. *et al.* (1977). "Genetics of carbon catabolite repression in Saccharomycess cerevisiae: genes involved in the derepression process." In: *Molecular & general genetics : MGG* 151.1 (1), pp. 95–103. ISSN: 0026-8925. DOI: 10.1007/BF00446918.

Supplementary Material

Table 4.7: List of genes significantly (p<.01) differentially expressed when Czf1 is artificially activated in the wild type.

log2 Fold Change	Fold Change	Identifiers		
10.81	1791.76	C1_13080W	OP4	orf19.4934
9.86	930.33	C4_05580C		orf19.1239
9.70	833.29	C5_00540C	AGA1	orf19.935
8.65	401.39	CR_04440C	RBR1	orf19.535
8.05	265.23	CR_06670W	CFL11	orf19.701
7.84	228.95	C2_03350W	PGA17	orf19.893
7.83	227.28	C4_03520C	RBT1	orf19.1327
7.56	189.33	C5_01380W	CFL5	orf19.1930
7.23	149.65	C1_02520W	SCW4	orf19.2941
7.09	136.57	C2_09800C		orf19.1370
7.08	135.76	C2_09130C	IFF6	orf19.4072
6.70	103.94	C2_02230C		orf19.1541
6.60	96.84	C7_03560W		orf19.6688
6.46	88.19	C3_00600W	IFF11	orf19.5399
6.38	83.16	C5_02080C	HSP12	orf19.3160
6.29	78.40	C1_13100W		orf19.4936.1
6.19	73.01	C5_02110W		orf19.4216
6.07	67.31	CR_02920C	AQY1	orf19.2849
6.03	65.39	C1_05890W		orf19.2460
6.01	64.52	C2_05180W	WH11	orf19.3548.1
5.99	63.41	C1_06370C	PBR1	orf19.6274
5.89	59.44	C5_04250W	MRV8	orf19.3908
5.85	57.48	C3_03980C		orf19.2812
5.66	50.41	C4_06820C	CZF1	orf19.3127
5.60	48.52	C2_08890W		orf19.217
5.49	45.08	C2_00750W		orf19.2049
5.48	44.66	C1_07040C		orf19.6200
5.45	43.71	C4_02660W		orf19.2734
5.44	43.31	C2_09820W		orf19.1368
5.35	40.82	CR_08510W	PGA13	orf19.6420
5.34	40.58	C1_02070W	HSP31	orf19.3664
5.31	39.80	C5_02460C	ECM331	orf19.4255
5.24	37.73	CR_02280W	PGA23	orf19.3740
5.12	34.79	C2_06630C		orf19.36.1

Table 4.7 continued from previous page

log2 Fold Change	Fold Change	Identifiers		
5.11	34.57	C3_06660C		orf19.7455
5.08	33.89	C4_06320C		orf19.2905
5.05	33.22	C1_05140W	BRG1	orf19.4056
5.04	32.97	C6_04620C	NAG4	orf19.2160
5.01	32.29	C3_05630W	GTT1	orf19.6998
4.96	31.14	CR_03450W	HXT5	orf19.4384
4.96	31.07	C6_00810C		orf19.3643
4.91	30.02	CR_03580C		orf19.4384.1
4.81	28.13	C1_10170W		orf19.4886
4.73	26.50	C4_03570W	HWP1	orf19.1321
4.70	26.05	C6_02890C	HPD1	orf19.5565
4.67	25.47	C2_09220W	DDR48	orf19.4082
4.65	25.06	C4_01070W	HGT17	orf19.4682
4.65	25.03	C1_06280C	UME6	orf19.1822
4.59	24.15	C6_00470C	FET99	orf19.4212
4.39	21.01	C4_04470W	SAP10	orf19.3839
4.37	20.66	C2_00760C		orf19.2048
4.36	20.58	CR_02750C	PGA34	orf19.2833
4.35	20.32	C2_08640C	PST2	orf19.3612
4.15	17.79	C5_04140W		orf19.3897
4.15	17.76	C1_04500W	ICL1	orf19.6844
4.14	17.62	C2_02220C		orf19.1539
4.12	17.37	C3_04730C		orf19.5933
4.06	16.67	C5_04470C		orf19.3932
4.03	16.33	CR_08990C	SLP3	orf19.7296
3.94	15.30	CR_09140C		orf19.7310
3.89	14.84	C4_00130W	RBT5	orf19.5636
3.87	14.58	C5_04480C		orf19.3932.1
3.84	14.29	C1_11200W		orf19.2296
3.76	13.57	C6_01990W	PLB1	orf19.689
3.76	13.53	C5_00100C		orf19.5686
3.73	13.30	C5_00870C	GIT4	orf19.1980
3.71	13.10	C2_07720C		orf19.2210
3.65	12.59	C6_02830W	MNN45	orf19.5557
3.65	12.53	C5_01360W	CFL4	orf19.1932
3.64	12.48	C2_10150W		orf19.1766
3.63	12.42	C4_03000C		orf19.2691
3.63	12.41	C2_06590C	GIT1	orf19.34
3.63	12.41	CR_04220C		orf19.510
3.60	12.14	C1_11270W		orf19.675
3.58	11.93	C3_02800W	ADH4	orf19.271
3.51	11.36	C1_08790W	TPO3	orf19.4737
3.50	11.34	C4_00120W	PGA7	orf19.5635
3.48	11.14	C2_02600C	FGR22	orf19.1586
3.46	10.98	CR_08890C	ASR2	orf19.7284
3.45	10.95	C1_07580C	PRY1	orf19.2787
3.45	10.94	C1_05520W		orf19.413
3.44	10.87	C3_01900C		orf19.1656
3.39	10.46	CR_02020C	OPT1	orf19.2602

Table 4.7 continued from previous page

log2 Fold Change	Fold Change	Identifiers		
3.38	10.44	C5_00140C		orf19.5683
3.38	10.43	C3_00220W	HGT19	orf19.5447
3.38	10.40	C1_02990C	XOG1	orf19.2990
3.37	10.35	C2_09530W	EAP1	orf19.1401
3.36	10.30	C1_08940C	MSN4	orf19.4752
3.36	10.29	C1_06610C	HAK1	orf19.6249
3.32	9.99	C4_03470C	ECE1	orf19.3374
3.32	9.96	C1_04940C		orf19.750
3.30	9.85	CR_03890W	WOR3	orf19.467
3.23	9.36	C5_03050C	PGA58	orf19.4334
3.21	9.25	C1_08530W		orf19.398
3.12	8.67	C6_02100W		orf19.3499
3.10	8.57	C4_02030W	RFX2	orf19.4590
3.09	8.53	C4_04190C		orf19.1430
3.08	8.46	C4_06620C		orf19.2870
3.08	8.45	C3_03460C		orf19.344
3.06	8.31	C3_04580C	STP1	orf19.5917
3.04	8.21	C3_03450C	BMT7	orf19.342
3.04	8.21	C2_06990W		orf19.2253
3.02	8.13	C7_00870W		orf19.7029
3.00	7.98	C3_07160W	PGA32	orf19.6784
2.99	7.94	C2_08340C		orf19.1349
2.97	7.83	CR_01470W	CSP37	orf19.2531
2.96	7.79	C1_08230C	PLB5	orf19.5102
2.96	7.76	C1_01510W		orf19.3337
2.96	7.76	C4_04770C	MNN22	orf19.3803
2.92	7.54	C4_05900C		orf19.1277
2.90	7.47	C1_00310W		orf19.6077
2.89	7.42	C7_00660W	GAC1	orf19.7053
2.88	7.37	C1_11490C	BTA1	orf19.1171
2.87	7.30	C1_06340W		orf19.6277
2.84	7.18	C3_02870C		orf19.278
2.83	7.13	C4_04790W	FAV1	orf19.3801
2.81	6.99	C1_10740C	ASR1	orf19.2344
2.80	6.97	C4_04080C	PGA31	orf19.5302
2.79	6.93	C1_04010C		orf19.4476
2.79	6.90	C1_05920W		orf19.2457
2.79	6.90	C7_01170C		orf19.6899
2.77	6.83	C4_03710C		orf19.1307
2.76	6.78	C1_10110W		orf19.4880
2.75	6.73	C1_11660W	GAD1	orf19.1153
2.75	6.73	C6_00080C		orf19.6329
2.75	6.71	C7_00280W	HGT12	orf19.7094
2.75	6.71	C2_07630C		orf19.1862
2.74	6.68	C1_09690W	MLS1	orf19.4833
2.73	6.62	C1_07430W	PHO100	orf19.4424
2.72	6.59	C5_04400W	RNY11	orf19.3926
2.71	6.53	C1_02110C	HGT2	orf19.3668
2.67	6.35	C3_05580C	GAP2	orf19.6993

Table 4.7 continued from previous page

log2 Fold Change	Fold Change	Identifiers		
2.66	6.32	C6_00860W	GPX1	orf19.87
2.64	6.24	C3_02610C	GLX3	orf19.251
2.62	6.16	C6_00730W		orf19.3655
2.62	6.15	C3_05450C		orf19.6983
2.61	6.11	C3_01370C	PGA44	orf19.1714
2.58	6.00	C1_12010C	KIP4	orf19.5265
2.57	5.94	C2_05860C		orf19.5210
2.54	5.82	CR_00310C		orf19.7502
2.54	5.80	C2_05810W		orf19.5204
2.53	5.78	C5_03430W		orf19.2638
2.49	5.64	C4_04840C	AGP3	orf19.3795
2.48	5.58	C5_01450W	PRC2	orf19.4135
2.45	5.47	C7_03290C	RBR3	orf19.5124
2.43	5.40	C5_03510C		orf19.6660
2.42	5.35	C1_01740W	CTN1	orf19.4551
2.41	5.33	C7_00770W		orf19.7042
2.41	5.31	C2_02570W		orf19.1582
2.41	5.31	C2_05640W		orf19.6874
2.40	5.28	C7_00930W	GPH1	orf19.7021
2.38	5.22	C1_11670W		orf19.1152
2.38	5.21	C6_00960W	CAN1	orf19.97
2.38	5.21	C3_00320W	RHR2	orf19.5437
2.37	5.17	C4_01100C	AGP2	orf19.4679
2.36	5.13	C1_00220W	PHR2	orf19.6081
2.34	5.07	CR_10790W	MAL2	orf19.7668
2.33	5.04	C2_09590C		orf19.1395
2.31	4.95	C1_00780C	HGC1	orf19.6028
2.30	4.94	C5_03610W	HEX1	orf19.6673
2.30	4.92	C1_01930W		orf19.4530.1
2.29	4.88	C1_07030C	RBT4	orf19.6202
2.28	4.87	CR_02880W		orf19.2846
2.28	4.86	CR_04420C	RBR2	orf19.532
2.27	4.83	CR_07480W		orf19.6117
2.26	4.80	C7_00630C		orf19.7056
2.25	4.77	C2_07570W	RNR22	orf19.1868
2.25	4.75	C1_02730W		orf19.2962
2.25	4.74	C1_03870C		orf19.4459
2.25	4.74	C3_06320W	ALS7	orf19.7400
2.24	4.74	C3_03500W	SKN2	orf19.348
2.24	4.74	C5_01830C	HAL9	orf19.3190
2.24	4.73	C4_04860W		orf19.3793
2.24	4.71	CR_10200W		orf19.7596
2.23	4.68	C6_00070C	PGA25	orf19.6336
2.22	4.67	C1_11700C	MRF1	orf19.1149
2.22	4.64	C4_01850C	PDC12	orf19.4608
2.21	4.62	C2_07230C	ZCF10	orf19.2280
2.21	4.62	C1_02250W	CWH8	orf19.3682
2.21	4.62	C2_04470W	ADH3	orf19.4505
2.21	4.61	C1_14060W		orf19.7214

Table 4.7 continued from previous page

log2 Fold Change	Fold Change	Identifiers		
2.19	4.55	C4_03430W	MOH1	orf19.3369
2.17	4.49	C4_02900C	CRH11	orf19.2706
2.16	4.47	C6_00250W		orf19.1183
2.15	4.45	C4_00080C		orf19.376
2.15	4.44	C1_07990C		orf19.5070
2.13	4.37	C2_02390W		orf19.1562
2.12	4.35	C4_03100W	RBT7	orf19.2681
2.11	4.31	C4_02330C		orf19.2770
2.09	4.27	C4_02620C		orf19.2737
2.09	4.26	C3_00360W		orf19.5431
2.09	4.25	CR_05380C	YCP4	orf19.5286
2.09	4.25	CR_02130W	ECM4	orf19.2613
2.09	4.24	C4_05140C	GDB1	orf19.744
2.08	4.23	C7_00170W	VPS70	orf19.7106
2.08	4.22	C1_14360C	WSC4	orf19.7251
2.07	4.21	C7_03140W		orf19.5141
2.07	4.21	C4_06340W	AGO1	orf19.2903
2.07	4.20	C5_04830W	SFL2	orf19.3969
2.06	4.16	C2_03120W	AMO1	orf19.5784
2.06	4.16	C2_09420W		orf19.1600
2.06	4.16	C3_07730W	WOR4	orf19.6713
2.05	4.15	C2_08100W		orf19.2175
2.05	4.14	C5_04130C	CHT2	orf19.3895
2.04	4.12	C6_00940C		orf19.95
2.03	4.08	C6_03170C	MDR1	orf19.5604
2.03	4.07	C4_05560C	ARO9	orf19.1237
2.01	4.03	C1_09180W	LYS143	orf19.4776
2.01	4.02	CR_05750W		orf19.6637
2.01	4.02	C2_02980C	DLD1	orf19.5805
2.00	4.00	CR_02400W	PHO112	orf19.3727
2.00	3.99	C4_06990W	MNN46	orf19.3110
1.99	3.98	C2_06460W	RTA3	orf19.23
1.99	3.98	C6_01450C		orf19.3439
1.99	3.96	C7_03480W		orf19.6705
1.98	3.96	C2_03520C	ADAEC	orf19.868
1.98	3.95	C4_04030W	JEN2	orf19.5307
1.98	3.95	C3_04200W	AFP99	orf19.5862
1.97	3.93	CR_02640W	RFG1	orf19.2823
1.97	3.92	C2_10650W		orf19.5342.2
1.97	3.92	CR_10840C	XYL2	orf19.7676
1.97	3.91	C2_00770W		orf19.2047
1.96	3.89	C1_00270W		orf19.6079
1.95	3.87	CR_05540C		orf19.5848
1.93	3.82	C2_01010W	HGT8	orf19.2021
1.91	3.75	C4_01860C		orf19.4607
1.90	3.73	C6_02670C	WSC2	orf19.5537
1.88	3.69	C4_05780C	CFL2	orf19.1264
1.88	3.68	C5_00880C	GIT3	orf19.1979
1.88	3.68	C7_02810W	PRX1	orf19.5180

Table 4.7 continued from previous page

log2 Fold Change	Fold Change	Identifiers		
1.88	3.68	CR_05990C	SFL1	orf19.454
1.88	3.67	CR_06030C		orf19.3852
1.87	3.66	C2_01780W	MSB2	orf19.1490
1.87	3.64	C1_11280W		orf19.674
1.86	3.63	C2_10020C		orf19.1780
1.86	3.63	CR_04820W		orf19.6311
1.85	3.60	C1_03820W	PDR16	orf19.1027
1.84	3.58	C2_08050C	SIT1	orf19.2179
1.84	3.57	C1_08330C	ADH2	orf19.5113
1.84	3.57	C4_04250W		orf19.1424
1.83	3.55	CR_02070C	ADH5	orf19.2608
1.82	3.52	C6_04410C		orf19.2124
1.81	3.51	CR_03040C	HGT18	orf19.2425
1.79	3.47	C1_00290W	POL93	orf19.6078
1.79	3.46	C6_04400W		orf19.2123
1.79	3.45	C4_04380C		orf19.1409.2
1.78	3.45	C1_13430C		orf19.4970
1.78	3.44	CR_10770W		orf19.7666
1.78	3.44	CR_09210W	SUC1	orf19.7319
1.78	3.42	C5_05390C	PGA4	orf19.4035
1.78	3.42	C1_10350C		orf19.4906
1.77	3.41	C4_02740W		orf19.2724
1.77	3.40	C4_05130C	ALD6	orf19.742
1.76	3.38	C5_03490C		orf19.6658
1.76	3.38	CR_07060C	CRZ2	orf19.2356
1.76	3.38	CR_01900C	HNM3	orf19.2587
1.75	3.37	C3_03230C		orf19.321
1.75	3.37	C1_05840W	PRN1	orf19.2467
1.75	3.36	C1_05440C		orf19.419
1.74	3.33	C3_04190W		orf19.5861.1
1.73	3.33	C7_01070C		orf19.7006
1.73	3.31	C1_10580C		orf19.1830
1.72	3.30	CR_00170W	ZCF38	orf19.7518
1.72	3.28	CR_07730W	HGT14	orf19.2633
1.71	3.27	CR_10340W	PTP3	orf19.7610
1.71	3.27	C3_05990C		orf19.7380
1.70	3.26	C6_02090C		orf19.3501
1.70	3.24	C2_07440C		orf19.1887
1.70	3.24	C1_08900W		orf19.4749
1.70	3.24	C3_07560W	TCC1	orf19.6734
1.69	3.23	C1_05200C		orf19.446
1.69	3.23	C2_05660W	PNG2	orf19.6877
1.69	3.23	C3_03410C		orf19.338
1.68	3.20	C5_00230C		orf19.972
1.67	3.19	C5_05450C	MUM2	orf19.4044
1.67	3.19	CR_10780C	IAH1	orf19.7667
1.67	3.18	C4_05610C		orf19.1246
1.67	3.18	CR_02210W		orf19.3751
1.66	3.17	C2_04050C	DCK1	orf19.815

Table 4.7 continued from previous page

log2 Fold Change	Fold Change	Identifiers		
1.66	3.17	C4_00200C	MET15	orf19.5645
1.66	3.17	C7_03220C	ZCF29	orf19.5133
1.66	3.15	C2_09010W	STB3	orf19.203
1.65	3.14	C1_04350C		orf19.5203
1.65	3.14	CR_00180C	CHT1	orf19.7517
1.65	3.14	C7_00290C	HGT13	orf19.7093
1.65	3.14	C1_14290C	MDG1	orf19.7239
1.65	3.14	C3_05320W		orf19.6968
1.65	3.14	C2_00080C	FAV3	orf19.1914
1.64	3.12	C3_02630C		orf19.254
1.64	3.11	C1_06920C		orf19.6219
1.64	3.11	C1_11680C		orf19.1150.1
1.63	3.10	C1_06940C	ATC1	orf19.6214
1.63	3.10	C3_01020W		orf19.2506
1.63	3.10	C2_00660C	SOD4	orf19.2062
1.62	3.08	C1_09080C	PGA6	orf19.4765
1.62	3.08	C1_00150C	RIM8	orf19.6091
1.62	3.07	C1_08310W	OPY2	orf19.5110
1.62	3.06	C1_01710W		orf19.3360
1.61	3.05	C1_10500W		orf19.993
1.60	3.02	C2_03320W	CHK1	orf19.896
1.59	3.02	C4_02180C	ZCF26	orf19.4573
1.59	3.01	CR_10860C	CTA26	orf19.7680
1.59	3.01	C5_00390C		orf19.951
1.59	3.00	C4_03460C		orf19.3373
1.57	2.97	C4_04660C		orf19.3815
1.57	2.96	C5_02240W	PTH2	orf19.4231
1.57	2.96	C2_09460C		orf19.1604
1.56	2.95	C1_05900W		orf19.2459
1.56	2.94	C2_05330C		orf19.3563
1.55	2.93	C6_02490C		orf19.5518
1.55	2.93	C1_14300C	NCR1	orf19.7242
1.54	2.90	C3_07670W		orf19.6720
1.54	2.90	C6_03050C		orf19.5587
1.53	2.89	C4_07120C	MSH2	orf19.3093
1.53	2.89	C6_04600W	DAC1	orf19.2157
1.53	2.88	CR_03710C		orf19.4370
1.53	2.88	C2_00740C		orf19.2050
1.52	2.87	C3_04550C	CMK1	orf19.5911
1.52	2.86	C4_00840W		orf19.4711
1.51	2.85	C7_02420C		orf19.6469
1.51	2.84	C1_03430W		orf19.3043
1.51	2.84	CR_00200W	PCK1	orf19.7514
1.51	2.84	C7_00090C	CSA1	orf19.7114
1.50	2.83	C3_01130C		orf19.2515
1.50	2.83	C4_03620C	CDR3	orf19.1313
1.50	2.83	C6_00240C		orf19.1182
1.50	2.82	C7_00230W		orf19.7100
1.49	2.82	C7_00430W		orf19.7077

Table 4.7 continued from previous page

log2 Fold Change	Fold Change	Identifiers		
1.49	2.82	C7_03230C		orf19.5132
1.49	2.81	C1_11590W	PLD1	orf19.1161
1.49	2.81	CR_03810W	PRP13	orf19.4379
1.49	2.81	C1_01830C	UBC8	orf19.4540
1.49	2.81	C1_02700C		orf19.2959.1
1.49	2.80	C2_03110W		orf19.5785
1.49	2.80	CR_07160C		orf19.733
1.49	2.80	C7_01620C	KCH1	orf19.6563
1.48	2.79	CR_00090C		orf19.7531
1.48	2.78	CR_01730W	IFU5	orf19.2568
1.47	2.78	C2_07750W	RHO2	orf19.2204.2
1.47	2.77	C1_07650W		orf19.2779
1.47	2.77	C1_13480W	HSP70	orf19.4980
1.47	2.77	CR_10020C		orf19.7578
1.46	2.76	C1_13470W	KNS1	orf19.4979
1.46	2.76	C2_03020C		orf19.5799
1.46	2.76	C7_02430C		orf19.6465
1.46	2.75	CR_09120C	TUB1	orf19.7308
1.46	2.75	CR_07150W	GLK1	orf19.734
1.46	2.75	C5_03810C		orf19.1113
1.46	2.75	CR_00060C		orf19.7538
1.46	2.75	C5_00070W	CDC11	orf19.5691
1.46	2.74	C4_03340C		orf19.1438
1.46	2.74	CR_00050W	INO2	orf19.7539
1.45	2.73	C4_03070W	PGA54	orf19.2685
1.45	2.73	C1_04140W	IFD6	orf19.1048
1.44	2.72	C1_14030W		orf19.7210
1.44	2.71	C5_04280C	GLN3	orf19.3912
1.44	2.71	C1_03320C	EHD3	orf19.3029
1.44	2.71	C7_01940C		orf19.6527
1.44	2.71	C1_03150C		orf19.3007.2
1.43	2.70	C1_09160W	AOX1	orf19.4774
1.43	2.70	C5_05440C		orf19.4043
1.43	2.69	C1_14440C	GDI1	orf19.7261
1.43	2.69	C7_04280C		orf19.7140
1.43	2.69	C3_07810C	SEC61	orf19.6176
1.43	2.69	CR_07890W	EFG1	orf19.610
1.43	2.69	C1_09170W	CTA8	orf19.4775
1.42	2.68	C3_03870C	SAP9	orf19.6928
1.42	2.67	C4_00420C		orf19.5671
1.42	2.67	C1_00060W	TUP1	orf19.6109
1.41	2.67	C5_02860C	GRP2	orf19.4309
1.41	2.66	C4_04530C	PHR1	orf19.3829
1.41	2.66	C4_00110C	FRP1	orf19.5634
1.40	2.64	C1_07370C	CPH1	orf19.4433
1.40	2.64	C3_01550C	TOS1	orf19.1690
1.40	2.64	C1_01290C		orf19.3318
1.40	2.63	C3_01510W		orf19.1698
1.40	2.63	C1_01360C		orf19.3325

Table 4.7 continued from previous page

log2 Fold Change	Fold Change	Identifiers		
1.40	2.63	C4_04710W	GYP1	orf19.3811
1.39	2.63	C2_00140W	NDT80	orf19.2119
1.39	2.62	C3_04000C	CTN3	orf19.2809
1.39	2.62	C1_04680W	PIL1	orf19.778
1.39	2.62	CR_06140W		orf19.3869
1.39	2.62	CR_03790C	KRE1	orf19.4377
1.39	2.62	C4_01220C		orf19.4668
1.39	2.61	C3_00850C		orf19.6160
1.39	2.61	C4_04320W	FRE10	orf19.1415
1.38	2.61	C2_06320W		orf19.5495
1.38	2.61	C4_00440C	OPT7	orf19.5673
1.38	2.61	CR_07440W	ACE2	orf19.6124
1.38	2.61	C3_07330W		orf19.6758
1.38	2.61	C3_03610W	FUR4	orf19.360
1.38	2.60	C4_04370C	VAC7	orf19.1409
1.37	2.59	C7_01560C	NUP	orf19.6570
1.37	2.59	C3_04530C	TEC1	orf19.5908
1.37	2.59	C2_06870C	PST1	orf19.2241
1.37	2.59	C6_00210W		orf19.1180
1.37	2.59	C1_08320W	TKL1	orf19.5112
1.37	2.58	C5_00730W	HYR3	orf19.575
1.37	2.58	CR_05610C	SRR1	orf19.5843
1.36	2.57	CR_05390W	PST3	orf19.5285
1.36	2.57	C3_07950C	SRB1	orf19.6190
1.36	2.57	CR_06440C	BCR1	orf19.723
1.36	2.56	C1_09060C		orf19.4763
1.36	2.56	C2_07730W	YVC1	orf19.2209
1.36	2.56	C4_04580W	ZDS1	orf19.3823
1.36	2.56	C6_00930C		orf19.94
1.35	2.56	C1_10090C		orf19.4878
1.35	2.55	C5_03930C		orf19.3219
1.35	2.55	CR_03620C		orf19.4380.1
1.35	2.55	C5_04260W		orf19.3910
1.35	2.55	C4_04460C		orf19.3840
1.35	2.54	CR_02240C	OPT2	orf19.3746
1.35	2.54	C1_13670W	OSM2	orf19.5005
1.35	2.54	C7_02040C	CUP9	orf19.6514
1.35	2.54	C4_06130W		orf19.4715
1.34	2.54	C2_02410W		orf19.1564
1.34	2.54	C2_07760W		orf19.2204
1.34	2.53	C4_04010W		orf19.5311
1.34	2.53	C4_07050W	YDC1	orf19.3104
1.34	2.53	C6_00110C		orf19.6326
1.33	2.52	C2_00100C	PGA52	orf19.1911
1.33	2.52	C5_04870W		orf19.3973
1.33	2.52	C4_05300W	XKS1	orf19.1290
1.33	2.52	C7_00410C		orf19.7079
1.33	2.51	C4_02340W		orf19.2769
1.33	2.51	C1_03380W	TPS2	orf19.3038

Table 4.7 continued from previous page

log2 Fold Change	Fold Change	Identifiers		
1.32	2.50	C1_00390W	ENA2	orf19.6070
1.32	2.50	C4_05350W		orf19.1793
1.32	2.50	C2_00260C	MUQ1	orf19.2107
1.32	2.50	C1_10240C		orf19.4894
1.32	2.49	CR_06590C	RGS2	orf19.695
1.32	2.49	CR_08670C		orf19.6443
1.31	2.49	C6_01720C	SUR7	orf19.3414
1.31	2.48	C3_03900C	HTB1	orf19.6925
1.31	2.48	C2_10420W	FGR6-4	orf19.3490
1.31	2.48	CR_02040W	PRK1	orf19.2605
1.31	2.47	C3_06670C		orf19.7456
1.31	2.47	C6_03790C	HGT10	orf19.5753
1.31	2.47	C2_08980C	PGA55	orf19.207
1.30	2.46	C1_10420C		orf19.4912
1.30	2.46	C1_07810C		orf19.5051
1.30	2.46	C4_07220C		orf19.3080
1.30	2.46	C3_03640W	DAL9	orf19.6956
1.30	2.46	C2_03360W		orf19.891
1.29	2.45	C6_00230W		orf19.1181
1.29	2.45	CR_06260W		orf19.3878
1.29	2.45	CR_08710W		orf19.6448
1.29	2.45	C6_04140C		orf19.4553
1.29	2.45	C1_03290W	NGG1	orf19.3023
1.29	2.44	C2_10690W	TPS3	orf19.5348
1.29	2.44	C1_08180C		orf19.5095
1.28	2.44	C2_02940W	MET1	orf19.5811
1.28	2.43	C4_05080C		orf19.3769
1.28	2.43	C6_00280W	CPH2	orf19.1187
1.27	2.41	CR_10800C		orf19.7670
1.27	2.41	CR_01770C		orf19.2574
1.27	2.41	C1_09320C		orf19.4792
1.27	2.41	C1_03270W		orf19.3021
1.26	2.40	C3_00930W	ATO2	orf19.2496
1.26	2.40	C1_11610C		orf19.1159
1.26	2.40	C2_03440W	PGA33	orf19.876
1.26	2.40	CR_00070W	BNR1	orf19.7537
1.26	2.39	C6_03180C		orf19.5605
1.26	2.39	CR_08960C	MPS1	orf19.7293
1.26	2.39	CR_04130C	EAF7	orf19.497
1.26	2.39	C1_13880C		orf19.5026
1.26	2.39	C1_07010W		orf19.6205
1.26	2.39	C7_00320C	PMR1	orf19.7089
1.25	2.38	C2_10570W	SGS1	orf19.5335
1.25	2.38	C2_10630W		orf19.5342
1.25	2.38	CR_00260W	KIN2	orf19.7510
1.24	2.37	C1_11720W		orf19.1146
1.24	2.37	C1_03100W		orf19.3003
1.24	2.36	C2_01640W	SLA1	orf19.1474
1.24	2.36	C1_12960C	BNI1	orf19.4927

Table 4.7 continued from previous page

log2 Fold Change	Fold Change	Identifiers		
1.24	2.36	C6_00350W	PKH3	orf19.1196
1.24	2.36	C2_09950W	FCY21	orf19.1357
1.24	2.36	C5_00930C	TFS1	orf19.1974
1.24	2.36	C4_04420W	FGR3	orf19.3845
1.23	2.35	CR_07170W		orf19.732
1.23	2.35	C4_00020W	VMA6	orf19.364
1.23	2.35	CR_04640W	DIT1	orf19.1741
1.23	2.35	C2_09630C		orf19.1391
1.23	2.35	C1_09000W		orf19.4756
1.23	2.34	C2_08130W	ARA1	orf19.2172
1.23	2.34	C4_02940W	ABP1	orf19.2699
1.23	2.34	C4_02390W	PGA62	orf19.2765
1.23	2.34	C1_03400W		orf19.3041
1.23	2.34	CR_07070C	ALS3	orf19.1816
1.22	2.33	C1_01400C		orf19.3329
1.22	2.33	C3_06470W	AAF1	orf19.7436
1.22	2.33	C2_07930C	VRP1	orf19.2190
1.22	2.33	C4_06250C	SEC3	orf19.2911
1.22	2.33	C2_01930C		orf19.1505
1.21	2.32	C5_01240W	AUR1	orf19.1945
1.21	2.32	C3_00400C		orf19.5426
1.21	2.32	C2_00120C	EMC9	orf19.1907
1.21	2.32	C2_10860C		orf19.5369
1.21	2.32	C5_04560C	CUP1	orf19.3940.1
1.21	2.31	C1_11540C	CTA3	orf19.1166
1.21	2.31	CR_03920C	TPO4	orf19.473
1.21	2.31	C2_10590W	GAL4	orf19.5338
1.21	2.31	C5_03570W		orf19.6668
1.21	2.31	C6_04430W	CST5	orf19.2127
1.20	2.30	C1_07520C	IST2	orf19.2792
1.20	2.30	C5_00150C		orf19.5682
1.20	2.30	C1_06930W	PGA63	orf19.6217
1.20	2.30	CR_00150C	POT1	orf19.7520
1.20	2.30	C7_01100C		orf19.6896
1.20	2.30	C6_01690W	ACF2	orf19.3417
1.20	2.29	C3_07340W	GCY1	orf19.6757
1.20	2.29	C2_10670W		orf19.5345
1.20	2.29	C3_05270C	HGT5	orf19.6005
1.20	2.29	C4_00400W	MNR2	orf19.5667
1.20	2.29	C1_07120W	GAP4	orf19.4456
1.19	2.29	CR_01420W		orf19.2528
1.19	2.28	C3_05970C	HAL3	orf19.7378
1.19	2.28	C7_02750W	FGR6-1	orf19.5191
1.19	2.28	CR_08470W		orf19.6416
1.19	2.28	C3_03850C	SOL1	orf19.6930
1.19	2.28	CR_00910W		orf19.3264.1
1.19	2.28	C3_03210W		orf19.320
1.19	2.28	C1_00140W	KEL1	orf19.6092
1.19	2.28	C1_01890C		orf19.4534

Table 4.7 continued from previous page

log2 Fold Change	Fold Change	Identifiers		
1.19	2.28	C6_00710W		orf19.3658
1.19	2.27	C4_04000W	MET4	orf19.5312
1.18	2.27	C3_00810C	FOX2	orf19.1288
1.18	2.27	C2_06070W	FAA2-1	orf19.4114
1.18	2.27	CR_03700C		orf19.4369
1.18	2.27	C1_07540C	BBC1	orf19.2791
1.18	2.27	C3_07460W		orf19.6742
1.18	2.27	C1_11930W		orf19.5274
1.18	2.27	CR_02800C		orf19.2838
1.18	2.27	C7_00080C	SAC7	orf19.7115
1.18	2.26	CR_08860W	PDK2	orf19.7281
1.18	2.26	C1_02960C		orf19.2987
1.17	2.26	C2_07390C		orf19.1893
1.17	2.25	C3_00890C		orf19.6166
1.17	2.25	C4_07230C	VID21	orf19.3077
1.17	2.25	C3_04320W	VAM3	orf19.5875
1.17	2.25	CR_05570C	RNR3	orf19.5845
1.17	2.25	CR_02460W		orf19.3720
1.17	2.25	C6_03620C		orf19.5730
1.17	2.25	C3_05810C	SKN1	orf19.7362
1.17	2.24	C5_01970C	CDC24	orf19.3174
1.16	2.24	C7_01960W		orf19.6525
1.16	2.24	C4_04050C	RHD3	orf19.5305
1.16	2.24	C1_08270C	MED15	orf19.5105
1.16	2.24	CR_09180W	CDG1	orf19.7314
1.16	2.24	C2_09100C		orf19.4068
1.16	2.24	C1_11350C	TOS4	orf19.668
1.16	2.23	C2_10840W	RDH54	orf19.5367
1.16	2.23	C1_11730W		orf19.1144
1.16	2.23	C3_04770C	ZCF32	orf19.5940
1.16	2.23	CR_07560W	RGD3	orf19.729.1
1.15	2.22	C1_08540C		orf19.399
1.15	2.22	C7_02200W	WHI3	orf19.6494
1.15	2.22	CR_05920C	MHP1	orf19.6621
1.15	2.22	C2_08140C	PHM7	orf19.2170
1.15	2.22	C1_00550W	CIS2	orf19.6053
1.15	2.22	CR_03850W	HGT3	orf19.4356
1.15	2.22	CR_01210C	HSE1	orf19.3233
1.15	2.21	C2_01880C	ZCF6	orf19.1497
1.15	2.21	C1_11210C	HAP43	orf19.681
1.14	2.21	C5_04510W	GDE1	orf19.3936
1.14	2.21	C5_02840C	HSL1	orf19.4308
1.14	2.20	C2_08450W		orf19.3635
1.14	2.20	C1_12140W		orf19.5250
1.14	2.20	C7_01430C		orf19.6586
1.13	2.19	CR_08030C	FGR32	orf19.593
1.13	2.19	CR_04120C		orf19.496
1.13	2.19	C4_06480C	CEK1	orf19.2886
1.13	2.19	C2_03640W	UGA11	orf19.854

Table 4.7 continued from previous page

log2 Fold Change	Fold Change	Identifiers		
1.13	2.19	C6_04040C	RVS167	orf19.1220
1.13	2.18	CR_10230W		orf19.7598
1.13	2.18	C5_04600C	GRR1	orf19.3944
1.13	2.18	C6_00410C	SRO77	orf19.1203
1.12	2.18	C1_06600W		orf19.6250
1.12	2.18	C3_07820W		orf19.6177
1.12	2.18	C2_09580W	AGE2	orf19.1396
1.12	2.18	C6_03990C		orf19.5775
1.12	2.18	C2_00060C		orf19.1917
1.12	2.18	CR_07250C		orf19.6143
1.12	2.17	CR_04480C	LAP3	orf19.539
1.12	2.17	C4_07130W		orf19.3091
1.12	2.17	C1_05760C	PGA26	orf19.2475
1.12	2.17	C4_06540W	MNN4	orf19.2881
1.12	2.17	C1_05910W	SIP5	orf19.2458
1.11	2.16	C1_11140W		orf19.2302
1.11	2.16	C1_10010C	SWE1	orf19.4867
1.11	2.16	C6_00590W	SLY41	orf19.4199
1.11	2.16	C2_00180C		orf19.2114
1.11	2.15	C6_00260W		orf19.1185
1.11	2.15	CR_09440C		orf19.7341
1.11	2.15	C2_03790C	ASR3	orf19.842
1.10	2.15	C1_10140C		orf19.4883
1.10	2.15	C6_00670W	CDC14	orf19.4192
1.10	2.15	C1_01390C	HOT1	orf19.3328
1.10	2.15	CR_02190C	SEF1	orf19.3753
1.10	2.15	CR_07960C	TRK1	orf19.600
1.10	2.14	C6_02420W		orf19.3483
1.09	2.13	C2_01540W		orf19.1461
1.09	2.13	C4_06770W		orf19.3132
1.09	2.13	C6_04570W	NAG6	orf19.2151
1.08	2.12	C1_00230C	BFA1	orf19.6080
1.08	2.12	CR_09340W		orf19.7329
1.08	2.12	C3_07100C		orf19.6790
1.08	2.11	C3_01360C	IRO1	orf19.1715
1.08	2.11	C2_10030C	MP65	orf19.1779
1.08	2.11	C2_01980C	SRD1	orf19.1510
1.07	2.10	C5_01350W		orf19.1933
1.07	2.09	C4_05590W		orf19.1240
1.07	2.09	C3_00100W		orf19.5465
1.07	2.09	C1_00570C		orf19.6049
1.07	2.09	C6_02780C	MIF2	orf19.5551
1.07	2.09	C4_00030C		orf19.366
1.06	2.09	C3_07360W	DLD2	orf19.6755
1.06	2.09	CR_09860W	YTA6	orf19.7558
1.06	2.09	C1_12410C	PKH2	orf19.5224
1.06	2.09	C3_01890C		orf19.1658
1.05	2.07	C7_04180W	FAA2-3	orf19.7156
1.05	2.07	C1_13810W		orf19.5019

Table 4.7 continued from previous page

log2 Fold Change	Fold Change	Identifiers		
1.05	2.07	C4_04170C	AXL2	orf19.5292
1.04	2.06	C1_01210W		orf19.3309
1.04	2.06	C2_06890C		orf19.2244
1.04	2.06	C7_00970C	YOX1	orf19.7017
1.04	2.06	C7_00260C		orf19.7096
1.04	2.06	C3_05780C	CRZ1	orf19.7359
1.04	2.05	CR_06070W		orf19.3859
1.04	2.05	C3_04640W	ZCF31	orf19.5924
1.04	2.05	C6_02640C		orf19.5534
1.03	2.05	C2_08080C	IFM3	orf19.2176
1.03	2.05	C2_07390C		orf19.1893
1.03	2.04	C5_00380W		orf19.952
1.03	2.04	C4_06190C	MPH1	orf19.2919
1.02	2.03	C6_00890W		orf19.90
1.02	2.03	C3_03660W	IRS4	orf19.6953
1.02	2.03	C5_00330C		orf19.956
1.02	2.03	C3_00030C		orf19.5469
1.01	2.01	C7_04110W	ENV7	orf19.7164
1.01	2.01	C2_09620W		orf19.1392
1.01	2.01	C5_03170C		orf19.4349
1.01	2.01	C2_09270C	SGT1	orf19.4089
1.01	2.01	C3_02640C	ZCF1	orf19.255
1.01	2.01	C2_05260W	BUD14	orf19.3555
1.01	2.01	C2_02490C		orf19.1573
1.00	2.00	C5_00220W	ROT2	orf19.974
1.00	2.00	CR_06040W		orf19.3854
1.00	2.00	C4_04560C		orf19.3826
1.00	2.00	CR_03220C		orf19.2401
0.99	1.99	C4_00190W		orf19.5644
0.99	1.98	C6_03100W	SHE3	orf19.5595
0.97	1.96	C2_08320C		orf19.1351
0.97	1.96	C1_04480C	TUS1	orf19.6842
0.97	1.95	CR_00190W	NGS1	orf19.7516
0.97	1.95	C6_04550C		orf19.2149
0.96	1.95	C1_02370C		orf19.3694
0.95	1.94	C4_01320C	OPT6	orf19.4655
0.95	1.94	C1_13740W	KAR9	orf19.5011
0.95	1.94	C3_04260W		orf19.5869
0.95	1.93	CR_08450C		orf19.6414
0.95	1.93	C4_01420W		orf19.4643
0.95	1.93	C3_05910W	ZCF35	orf19.7371
0.94	1.92	C2_04200W	TBF1	orf19.801
0.94	1.92	C7_03180C	HHO1	orf19.5137.1
0.94	1.92	CR_04870C		orf19.6306
0.94	1.91	C1_10680C		orf19.1840
0.93	1.91	C1_10280C		orf19.4898
0.93	1.91	C4_05530W	FGR6-10	orf19.1234
0.92	1.90	C1_04700C		orf19.775
0.92	1.89	C5_00890C	GIT2	orf19.1978

Table 4.7 continued from previous page

log2 Fold Change	Fold Change	Identifiers		
0.91	1.88	C4_02320C	SOD1	orf19.2770.1
0.90	1.87	C5_01470C		orf19.4142
0.88	1.84	C3_01250W	PMC1	orf19.1727
0.84	1.79	C1_13870W	MET3	orf19.5025
-0.85	0.56	C5_00650C	THR1	orf19.923
-0.89	0.54	C2_01030W		orf19.2019
-0.89	0.54	C4_06670W		orf19.3142
-0.90	0.54	C2_07260C	DQD1	orf19.2283
-0.90	0.54	CR_07710W	ARO2	orf19.1986
-0.90	0.53	CR_10400W		orf19.7617
-0.90	0.53	C4_05850C		orf19.1272
-0.90	0.53	CR_04810W	RPS3	orf19.6312
-0.91	0.53	C7_01570C		orf19.6569
-0.91	0.53	CR_06960W		orf19.2369
-0.92	0.53	C1_10450W	GLY1	orf19.986
-0.92	0.53	C7_00300W		orf19.7092
-0.92	0.53	C6_01970C	RPL25	orf19.687.1
-0.92	0.53	C2_00600C		orf19.2067
-0.92	0.53	C5_05130C		orf19.4005
-0.93	0.53	C1_10700C	NIT3	orf19.2351
-0.93	0.52	C5_04720C		orf19.3957
-0.94	0.52	C4_03750C		orf19.1303
-0.95	0.52	C4_05750C	LEA1	orf19.1260
-0.95	0.52	C3_01090W		orf19.2511.2
-0.96	0.51	C4_03700W		orf19.1308
-0.96	0.51	C3_04620C		orf19.5920
-0.96	0.51	C2_08040C	RPS10	orf19.2179.2
-0.96	0.51	C1_05180C		orf19.446.2
-0.96	0.51	C1_07400C		orf19.4428
-0.97	0.51	CR_04500C		orf19.541
-0.97	0.51	C5_01980C		orf19.3173
-0.97	0.51	C1_07890C	ADE5,7	orf19.5061
-0.97	0.51	C2_01230W		orf19.2001
-0.97	0.51	C7_03000C		orf19.5161
-0.98	0.51	C1_00510W		orf19.6057
-0.98	0.51	C2_04460W	LYS22	orf19.4506
-0.98	0.51	C3_03310C		orf19.331
-0.98	0.51	CR_06150C	ADE13	orf19.3870
-0.98	0.51	C2_02690W	SER2	orf19.5838
-0.98	0.51	C5_00620W		orf19.927
-0.98	0.51	CR_01560W		orf19.2542
-0.98	0.51	C4_03900C	RAM1	orf19.5046
-0.99	0.50	C4_01520C	RPL20B	orf19.4632
-0.99	0.50	CR_00930W	ATO10	orf19.3263
-0.99	0.50	CR_09240C		orf19.7322
-0.99	0.50	C4_03250C	RHD2	orf19.2668
-0.99	0.50	C2_02900W		orf19.5814
-1.00	0.50	C3_02210C		orf19.1624
-1.00	0.50	C2_05410W		orf19.3572.3

Table 4.7 continued from previous page

log2 Fold Change	Fold Change	Identifiers		
-1.00	0.50	CR_06330C		orf19.3887
-1.00	0.50	C2_10140W		orf19.1767
-1.00	0.50	C1_13720W		orf19.5009
-1.00	0.50	C6_03120W	POL5	orf19.5597
-1.00	0.50	C4_02670W		orf19.2733
-1.00	0.50	C7_03990C		orf19.7182
-1.00	0.50	C3_07690C		orf19.6718
-1.00	0.50	C6_03730C		orf19.5747
-1.00	0.50	CR_03160W		orf19.2408
-1.01	0.50	C2_10340W	HEM4	orf19.1744
-1.01	0.50	C1_07200W	YMC1	orf19.4447
-1.01	0.50	C1_01060W	MBF1	orf19.3294
-1.01	0.50	C6_04240W		orf19.1082
-1.01	0.50	C2_06970W	AAH1	orf19.2251
-1.01	0.50	C1_11650W	EGD1	orf19.1154
-1.02	0.49	C1_01820C		orf19.4542
-1.02	0.49	C1_09620C		orf19.4825
-1.02	0.49	C7_02680W	TOM22	orf19.3696
-1.02	0.49	C6_03760C	SHM2	orf19.5750
-1.03	0.49	C3_05940C		orf19.7375
-1.03	0.49	C5_02160W	SST2	orf19.4222
-1.03	0.49	CR_05890C		orf19.6625
-1.03	0.49	C5_03850W		orf19.1109
-1.03	0.49	C1_00700W		orf19.6035
-1.03	0.49	C5_04530W		orf19.3938
-1.04	0.49	C6_03910C		orf19.5767
-1.04	0.49	C1_06540C		orf19.6259
-1.04	0.49	C6_01980C		orf19.688
-1.04	0.49	C7_01350C		orf19.6916
-1.04	0.49	C1_07500C	LHP1	orf19.2795
-1.04	0.49	CR_00900W	TRM1	orf19.3265
-1.04	0.49	C1_11160C		orf19.2299
-1.04	0.49	C1_08050W		orf19.5077
-1.04	0.48	C4_02880C		orf19.2708
-1.04	0.48	C2_04960C		orf19.3528
-1.05	0.48	C4_04160W		orf19.5293
-1.05	0.48	C5_04960W		orf19.3984
-1.05	0.48	C1_00500C	GLO1	orf19.6058
-1.05	0.48	C2_05000C	MRPL10	orf19.3532
-1.05	0.48	C6_00620W	FCA1	orf19.4195.1
-1.05	0.48	C2_00880W		orf19.2036
-1.05	0.48	C3_01850W		orf19.1662
-1.05	0.48	C1_13070C	FAD3	orf19.4933
-1.05	0.48	CR_02950C		orf19.2852
-1.06	0.48	C1_01600W	MRP20	orf19.3350
-1.06	0.48	C4_05650W		orf19.1250
-1.06	0.48	C2_01430W	APT1	orf19.1448
-1.06	0.48	C3_02470C	RPL9B	orf19.236
-1.06	0.48	C1_13520C	MCU1	orf19.4983

Table 4.7 continued from previous page

log2 Fold Change	Fold Change	Identifiers		
-1.06	0.48	C2_05450C	MDJ2	orf19.3574
-1.06	0.48	C5_00550C		orf19.934
-1.06	0.48	C7_02480W		orf19.6461
-1.06	0.48	C2_07300C	RPA12	orf19.2287
-1.06	0.48	C4_03720C		orf19.1306
-1.06	0.48	C4_01200C	AAT22	orf19.4669
-1.07	0.48	C1_04880C	MRPL37	orf19.755
-1.07	0.48	C3_06530W		orf19.7442
-1.07	0.48	CR_04360C	NHP2	orf19.526
-1.07	0.48	C3_02040C		orf19.1642
-1.07	0.48	C1_06070W		orf19.2438
-1.07	0.48	C7_01020C		orf19.7012
-1.07	0.48	C7_02660C		orf19.3698
-1.07	0.48	CR_01550C		orf19.2541
-1.07	0.48	C7_01220W	GCN3	orf19.6904
-1.07	0.48	C1_12540W		orf19.3762
-1.08	0.47	C7_01420W	GIR2	orf19.6587
-1.08	0.47	C6_04300W		orf19.1087
-1.08	0.47	C6_01290C	QDR3	orf19.136
-1.08	0.47	CR_06530W		orf19.713
-1.08	0.47	C3_03390C	YAH1	orf19.336
-1.08	0.47	CR_06980W		orf19.2367
-1.09	0.47	C5_03480C		orf19.6656
-1.09	0.47	C1_04970W		orf19.51
-1.09	0.47	C1_04370C		orf19.5201
-1.09	0.47	C1_01150C		orf19.3303
-1.09	0.47	C4_03730C		orf19.1305
-1.09	0.47	C5_00320W		orf19.961.2
-1.09	0.47	C4_04810C		orf19.3798
-1.09	0.47	C4_00700C		orf19.4172
-1.10	0.47	CR_08520C		orf19.6419.1
-1.10	0.47	C3_06800C		orf19.6822
-1.10	0.47	CR_04530W	FUM11	orf19.543
-1.10	0.47	C3_06540C		orf19.7443
-1.10	0.47	C3_00340W		orf19.5433
-1.10	0.47	C4_03780C		orf19.1300
-1.10	0.47	C1_00340W	HBR1	orf19.6074
-1.10	0.47	C5_04880C	PUT2	orf19.3974
-1.11	0.46	C2_09660W		orf19.1388
-1.11	0.46	C3_06740W		orf19.6829
-1.11	0.46	C6_01860C	HCH1	orf19.3396
-1.11	0.46	C5_03110C		orf19.4340.1
-1.12	0.46	C5_02070C		orf19.3161
-1.12	0.46	C1_12760W		orf19.6346
-1.12	0.46	C1_08470W		orf19.392
-1.12	0.46	C3_01080W	MRPL33	orf19.2511.1
-1.12	0.46	C5_05140W		orf19.4006
-1.12	0.46	C2_02310W		orf19.1549
-1.12	0.46	C2_02710C		orf19.5835

Table 4.7 continued from previous page

log2 Fold Change	Fold Change	Identifiers		
-1.13	0.46	CR_03570C	YVH1	orf19.4401
-1.13	0.46	C1_08710W		orf19.4730
-1.13	0.46	C4_00740W		orf19.4168
-1.13	0.46	C2_01580W	REX2	orf19.1466
-1.13	0.46	C1_14090W		orf19.7215.3
-1.13	0.46	C4_01490W	NIP1	orf19.4635
-1.14	0.45	C1_06800W		orf19.6230
-1.14	0.45	C5_02790C	GAP1	orf19.4304
-1.14	0.45	C1_03720C		orf19.1037
-1.14	0.45	C2_02540W		orf19.1578
-1.15	0.45	C5_02410C		orf19.4250
-1.15	0.45	C1_05990C		orf19.2446
-1.15	0.45	CR_02520W	RPC19	orf19.172
-1.15	0.45	C2_09060C	ASN1	orf19.198
-1.15	0.45	C1_12310C	CSI2	orf19.5232
-1.15	0.45	C7_02120C		orf19.6503
-1.15	0.45	C6_02460C		orf19.5515
-1.15	0.45	CR_07030C		orf19.2362
-1.16	0.45	C1_01580W		orf19.3348
-1.16	0.45	C1_03650C	MRPL27	orf19.3064
-1.16	0.45	C2_02160W	SAM37	orf19.1532
-1.16	0.45	C4_05320W	LYS1	orf19.1789.1
-1.16	0.45	C2_02270C		orf19.1545
-1.16	0.45	C5_05250C		orf19.4018
-1.16	0.45	C2_04810W	HIS3	orf19.183
-1.17	0.45	C3_05900W		orf19.7370
-1.17	0.44	C2_02740C	HPT1	orf19.5832
-1.17	0.44	C1_10080W		orf19.4875
-1.17	0.44	CR_00680W	BUD22	orf19.3287
-1.17	0.44	C1_11100W		orf19.2306
-1.17	0.44	C1_09930W		orf19.4861
-1.17	0.44	C5_03860W	HAM1	orf19.1108
-1.18	0.44	C7_03680W		orf19.6703
-1.18	0.44	C1_10780C	HNT1	orf19.2341
-1.18	0.44	CR_06120W	RPL7	orf19.3867
-1.18	0.44	C1_03840W		orf19.1026.1
-1.18	0.44	C4_00660W		orf19.4176
-1.19	0.44	C2_07800W		orf19.2201
-1.19	0.44	C2_01830W	PRP39	orf19.1492
-1.19	0.44	CR_02890C		orf19.2847
-1.19	0.44	C7_03700C	ENP1	orf19.5507
-1.20	0.44	C1_05800C		orf19.2472
-1.20	0.44	C1_11880W		orf19.5279
-1.20	0.44	C4_05020W	IMG2	orf19.3777
-1.20	0.44	C5_02990W		orf19.4324
-1.20	0.43	C2_01180W	COX17	orf19.2006.1
-1.20	0.43	CR_10120C		orf19.7588
-1.21	0.43	C4_04100C	ECM1	orf19.5299
-1.21	0.43	C2_01510C		orf19.1458

Table 4.7 continued from previous page

log2 Fold Change	Fold Change	Identifiers		
-1.21	0.43	C2_05960C		orf19.5216
-1.22	0.43	C1_05060W	REI1	orf19.59
-1.22	0.43	C3_06950W		orf19.6805
-1.22	0.43	CR_09950C	SIK1	orf19.7569
-1.22	0.43	C3_00950C		orf19.2499
-1.22	0.43	C7_01210C		orf19.6903
-1.23	0.43	C2_07900W	GDH2	orf19.2192
-1.23	0.43	C2_06520C		orf19.28
-1.23	0.43	C1_07570C		orf19.2788
-1.24	0.42	C5_00850C		orf19.588
-1.24	0.42	C1_04710C		orf19.773
-1.25	0.42	CR_02330C	KAR4	orf19.3736
-1.25	0.42	C2_10270W	PUS7	orf19.1753
-1.25	0.42	C5_00450C	IFG3	orf19.944
-1.25	0.42	C1_06380C		orf19.6273
-1.25	0.42	C7_03790W	MRP7	orf19.7203
-1.25	0.42	C1_13680C	GCV3	orf19.5006
-1.25	0.42	C2_07430C		orf19.1888
-1.26	0.42	CR_06970C		orf19.2368
-1.27	0.42	C2_05750W		orf19.6886
-1.27	0.42	C1_07710C	ADE4	orf19.1233
-1.28	0.41	C3_07570C		orf19.6732
-1.28	0.41	C3_04270C	CTP1	orf19.5870
-1.28	0.41	C1_11990W		orf19.5267
-1.29	0.41	C1_07790C		orf19.5049
-1.30	0.41	C1_14130W	FTR1	orf19.7219
-1.30	0.41	CR_05480W		orf19.3518
-1.31	0.40	C3_02510C	SAP8	orf19.242
-1.32	0.40	C3_06590W	LYS9	orf19.7448
-1.32	0.40	C3_06600C		orf19.7449
-1.32	0.40	C3_06760W		orf19.6828
-1.33	0.40	C3_04660C	ARG11	orf19.5926
-1.34	0.40	C4_05730W		orf19.1258
-1.34	0.40	C1_03620C		orf19.3061.1
-1.34	0.39	CR_03660C		orf19.4365
-1.34	0.39	CR_02060W		orf19.2607
-1.35	0.39	CR_00380W		orf19.7495
-1.35	0.39	C4_02050W	HGH1	orf19.4587
-1.35	0.39	CR_05430W	CSP1	orf19.3512
-1.35	0.39	C2_05230C	RPF2	orf19.3553
-1.37	0.39	C6_01430C	FRP6	orf19.3441
-1.37	0.39	C5_04030W		orf19.1287
-1.38	0.38	C2_01570W		orf19.1465
-1.40	0.38	C4_05310W		orf19.1789
-1.40	0.38	CR_03280W	IFR2	orf19.2396
-1.40	0.38	C2_06040C		orf19.4116
-1.44	0.37	C7_03820C		orf19.7200
-1.47	0.36	C3_01040C	PRM9	orf19.2508
-1.49	0.36	C4_01170C	BMT9	orf19.4673

Table 4.7 continued from previous page

log2 Fold Change	Fold Change	Identifiers		
-1.49	0.36	C6_03610W	FGR17	orf19.5729
-1.54	0.34	C3_04170W		orf19.5860
-1.57	0.34	CR_03270W		orf19.2397
-1.58	0.33	C2_03370W	THI20	orf19.889
-1.59	0.33	C1_02130C	GAL1	orf19.3670
-1.60	0.33	CR_06660W	SEO1	orf19.700
-1.60	0.33	C6_01420C		orf19.3442
-1.62	0.33	C6_02500C	GCV1	orf19.5519
-1.62	0.32	CR_08700C	ARF1	orf19.6447
-1.64	0.32	C2_06340W	EFH1	orf19.5498
-1.66	0.32	C4_03770W		orf19.1301
-1.67	0.32	C5_00710W	IFF8	orf19.570
-1.73	0.30	C2_10180W	IFR1	orf19.1763
-1.81	0.28	C7_02910W	ENA21	orf19.5170
-1.83	0.28	C5_03910C		orf19.1105
-1.83	0.28	C3_01970C		orf19.1651
-1.85	0.28	C3_03040W	AIP2	orf19.300
-1.85	0.28	C4_00750C		orf19.4167
-1.86	0.27	C2_05250C	AAT1	orf19.3554
-1.90	0.27	C4_05770C	CFL1	orf19.1263
-2.03	0.25	C1_10150W	WOR1	orf19.4884
-2.08	0.24	C6_04190C		orf19.1075
-2.08	0.24	C1_02600W	SNO1	orf19.2948
-2.09	0.23	C1_05710C	UGA4	orf19.2479
-2.12	0.23	C1_11630C	FUS1	orf19.1156
-2.31	0.20	C4_03760W		orf19.1302
-2.35	0.20	C2_06930C		orf19.2247
-2.40	0.19	CR_06860C	ARO10	orf19.1847
-2.52	0.17	CR_07810W	YHB5	orf19.3710
-2.52	0.17	C6_01510W	OYE23	orf19.3433
-2.53	0.17	C1_02590C	SNZ1	orf19.2947
-2.55	0.17	C2_01630W		orf19.1473
-2.65	0.16	C1_12000C		orf19.5266
-2.76	0.15	C1_08170C	BUL1	orf19.5094
-2.93	0.13	C6_03320W		orf19.5620
-2.97	0.13	CR_07800W	SAP2	orf19.3708
-3.31	0.10	C3_01050C		orf19.2509
-3.44	0.09	C3_05610W	MNN14	orf19.6996
-5.66	0.02	C6_00440C	FET34	orf19.4215

Gene Ontology Term	Frequency	Background frequency	Corrected P-value	Gene(s) annotated to the term
biological process involved in interspecies interaction between organisms	29 out of 211 genes, 13.7%	325 out of 6473 background genes, 5.0%	0.00027	PHR2, HGC1, XOG1, ICL1, BRG1, UME6, RBT4, PHO100, WH11, PST2, EAP1, RHR2, IFF11, ALS7, PGA7, RFX2, ECE1, RBT1, HWP1, SAP10, HEX1, SFL2, PLB1, MDR1, NAG4, CSP37, PHO112, YCP4, CFL11
carbohydrate metabolic process	20 out of 211 genes, 9.5%	197 out of 6473 background genes, 3.0%	0.00258	PHR2, SCW4, XOG1, ICL1, MLS1, C1_14060W_A, C2_10150W_A, RHR2, SKN2, C4_02620C_A, CRH11, MNN22, GDB1, HEX1, CHT2, MNN45, GAC1, GPH1, PHO112, MAL2
cellular carbohydrate metabolic process	14 out of 211 genes, 6.6%	105 out of 6473 background genes, 1.6%	0.00317	PHR2, XOG1, ICL1, MLS1, C1_14060W_A, RHR2, SKN2, MNN22, GDB1, MNN45, GAC1, GPH1, PHO112, MAL2
biological adhesion	12 out of 211 genes, 5.7%	94 out of 6473 background genes, 1.5%	0.02288	XOG1, PBR1, EAP1, RHR2, C3_02870C_A, ALS7, RBT5, RFX2, HWP1, SAP10, C5_02110W_A, SFL2
cell adhesion	10 out of 211 genes, 4.7%	67 out of 6473 background genes, 1.0%	0.02564	XOG1, PBR1, EAP1, RHR2, C3_02870C_A, ALS7, RBT5, HWP1, C5_02110W_A, SFL2
cellular polysaccharide metabolic process	9 out of 211 genes, 4.3%	56 out of 6473 background genes, 0.9%	0.03362	PHR2, XOG1, C1_14060W_A, SKN2, MNN22, GDB1, MNN45, GAC1, GPH1
single-species submerged biofilm formation	14 out of 211 genes, 6.6%	129 out of 6473 background genes, 2.0%	0.03379	HGC1, XOG1, BRG1, PBR1, WH11, EAP1, RHR2, ALS7, PGA7, RBT5, ECE1, HWP1, CZF1, AQY1
biofilm formation	15 out of 211 genes, 7.1%	146 out of 6473 background genes, 2.3%	0.03523	HGC1, XOG1, BRG1, PBR1, WH11, EAP1, RHR2, ALS7, PGA7, RBT5, ECE1, HWP1, CZF1, MRV8, AQY1
aggregation of unicellular organisms	15 out of 211 genes, 7.1%	146 out of 6473 background genes, 2.3%	0.03523	HGC1, XOG1, BRG1, PBR1, WH11, EAP1, RHR2, ALS7, PGA7, RBT5, ECE1, HWP1, CZF1, MRV8, AQY1
cell aggregation	15 out of 211 genes, 7.1%	146 out of 6473 background genes, 2.3%	0.03523	HGC1, XOG1, BRG1, PBR1, WH11, EAP1, RHR2, ALS7, PGA7, RBT5, ECE1, HWP1, CZF1, MRV8, AQY1
polysaccharide metabolic process	9 out of 211 genes, 4.3%	57 out of 6473 background genes, 0.9%	0.03881	PHR2, XOG1, C1_14060W_A, SKN2, MNN22, GDB1, MNN45, GAC1, GPH1
submerged biofilm formation	14 out of 211 genes, 6.6%	132 out of 6473 background genes, 2.0%	0.0435	HGC1, XOG1, BRG1, PBR1, WH11, EAP1, RHR2, ALS7, PGA7, RBT5, ECE1, HWP1, CZF1, AQY1
single-species biofilm formation on inanimate substrate	13 out of 211 genes, 6.2%	117 out of 6473 background genes, 1.8%	0.04825	HGC1, XOG1, BRG1, PBR1, WH11, EAP1, RHR2, PGA7, RBT5, ECE1, HWP1, CZF1, AQY1
glucan metabolic process	7 out of 211 genes, 3.3%	35 out of 6473 background genes, 0.5%	0.05248	PHR2, XOG1, C1_14060W_A, SKN2, GDB1, GAC1, GPH1
cellular glucan metabolic process	7 out of 211 genes, 3.3%	35 out of 6473 background genes, 0.5%	0.05248	PHR2, XOG1, C1_14060W_A, SKN2, GDB1, GAC1, GPH1
single-species biofilm formation	14 out of 211 genes, 6.6%	135 out of 6473 background genes, 2.1%	0.05556	HGC1, XOG1, BRG1, PBR1, WH11, EAP1, RHR2, ALS7, PGA7, RBT5, ECE1, HWP1, CZF1, AQY1

Figure 4.1: Significantly enriched gene ontology terms related to cellular processes of genes whose expression is significantly ($p<0.01$) increased by at least fourfold when Czf1 is artificially activated in the wild type. Terms mapped using the Candida Genome Database GO Term Finder (http://candidagenome.org/cgi-bin/GO/goTermFinder)

Gene Ontology Term	Frequency	Background frequency	Corrected P-value	Gene(s) annotated to the term
hydrolase activity, hydrolyzing O-glycosyl compounds	9 out of 211 genes, 4.3%	43 out of 6473 background genes, 0.7%	0.0009	PHR2, SCW4, XOG1, C1_14060W_A, CRH11, GDB1, HEX1, CHT2, MAL2
hydrolase activity, acting on glycosyl bonds	9 out of 211 genes, 4.3%	53 out of 6473 background genes, 0.8%	0.00535	PHR2, SCW4, XOG1, C1_14060W_A, CRH11, GDB1, HEX1, CHT2, MAL2
sugar transmembrane transporter activity	6 out of 211 genes, 2.8%	25 out of 6473 background genes, 0.4%	0.01412	HGT2, HGT19, HGT17, NAG4, HGT12, HXT5
carbohydrate transmembrane transporter activity	6 out of 211 genes, 2.8%	26 out of 6473 background genes, 0.4%	0.01786	HGT2, HGT19, HGT17, NAG4, HGT12, HXT5
monosaccharide transmembrane transporter activity	5 out of 211 genes, 2.4%	22 out of 6473 background genes, 0.3%	0.07047	HGT2, HGT19, HGT17, NAG4, HGT12
cell adhesion molecule binding	3 out of 211 genes, 1.4%	6 out of 6473 background genes, 0.1%	0.0762	XOG1, EAP1, HWP1

Figure 4.2: Significantly enriched gene ontology terms related to cellular function of genes whose expression is significantly ($p<0.01$) increased by at least fourfold when Czf1 is artificially activated in the wild type. Terms mapped using the Candida Genome Database GO Term Finder (http://candidagenome.org/cgi-bin/GO/goTermFinder)

Gene Ontology Term	Frequency	Background frequency	Corrected P-value	Gene(s) annotated to the term
cell surface	34 out of 211 genes, 16.1%	200 out of 6473 background genes, 3.1%	5.52E-14	PHR2, XOG1, RBT4, PHO100, PLB5, PGA17, IFF6, DDR48, EAP1, IFF11, PGA44, ALS7, PGA32, PGA7, RBT5, CRH11, RBT1, HWP1, PGA31, SAP10, ECM331, PGA58, CHT2, PGA25, FET99, GPH1, RBR3, CSP37, PGA23, PHO112, PGA34, RBR2, RBR1, PGA13
cell wall	27 out of 211 genes, 12.8%	163 out of 6473 background genes, 2.5%	1.38E-10	PHR2, XOG1, PLB5, WH11, PST2, IFF6, DDR48, EAP1, IFF11, GLX3, ALS7, RBT5, CRH11, ECE1, RBT1, HWP1, PGA31, SAP10, HSP12, C5_02110W_A, ECM331, CHT2, GPH1, RBR3, CSP37, RBR2, PGA13
fungal-type cell wall	27 out of 211 genes, 12.8%	163 out of 6473 background genes, 2.5%	1.38E-10	PHR2, XOG1, PLB5, WH11, PST2, IFF6, DDR48, EAP1, IFF11, GLX3, ALS7, RBT5, CRH11, ECE1, RBT1, HWP1, PGA31, SAP10, HSP12, C5_02110W_A, ECM331, CHT2, GPH1, RBR3, CSP37, RBR2, PGA13
external encapsulating structure	28 out of 211 genes, 13.3%	219 out of 6473 background genes, 3.4%	3.10E-08	PHR2, XOG1, PLB5, WH11, C2_07630C_A, PST2, IFF6, DDR48, EAP1, IFF11, GLX3, ALS7, RBT5, CRH11, ECE1, RBT1, HWP1, PGA31, SAP10, HSP12, C5_02110W_A, ECM331, CHT2, GPH1, RBR3, CSP37, RBR2, PGA13
hyphal cell wall	14 out of 211 genes, 6.6%	69 out of 6473 background genes, 1.1%	2.99E-06	PHR2, PLB5, WH11, PST2, DDR48, GLX3, CRH11, ECE1, RBT1, HWP1, HSP12, C5_02110W_A, GPH1, CSP37
intrinsic component of plasma membrane	12 out of 211 genes, 5.7%	65 out of 6473 background genes, 1.0%	8.78E-05	PHR2, HGT2, EAP1, HGT19, GAP2, HGT17, AGP2, CRH11, SAP10, MDR1, HGT12, OPT1
extracellular region	20 out of 211 genes, 9.5%	177 out of 6473 background genes, 2.7%	9.52E-05	PHR2, XOG1, RBT4, PHO100, PRY1, PLB5, OP4, IFF11, RBT5, CRH11, RBT7, ECE1, RBT1, SAP10, HEX1, CHT2, RNY11, PLB1, PHO112, MAL2
cell periphery	46 out of 211 genes, 21.8%	762 out of 6473 background genes, 11.8%	0.00178	PHR2, HGT2, XOG1, PLB5, TPO3, C2_00750W_A, WH11, GIT1, C2_07630C_A, PST2, IFF6, DDR48, EAP1, HGT19, IFF11, GLX3, GAP2, ALS7, RBT5, HGT17, AGP2, CRH11, ECE1, RBT1, HWP1, PGA31, SAP10, CFL4, CFL5, HSP12, C5_02110W_A, ECM331, CHT2, FET99, CAN1, MDR1, HGT12, GPH1, RBR3, CSP37, OPT1, AQY1, RBR2, YCP4, PGA13, SLP3
integral component of plasma membrane	8 out of 211 genes, 3.8%	43 out of 6473 background genes, 0.7%	0.00574	HGT2, HGT19, GAP2, HGT17, AGP2, MDR1, HGT12, OPT1
yeast-form cell wall	9 out of 211 genes, 4.3%	56 out of 6473 background genes, 0.9%	0.00665	PHR2, WH11, GLX3, RBT5, CRH11, PGA31, HSP12, C5_02110W_A, CHT2
cell wall-bounded periplasmic space	3 out of 211 genes, 1.4%	6 out of 6473 background genes, 0.1%	0.06033	PHO100, HEX1, PHO112

Figure 4.3: Significantly enriched gene ontology terms related to cellular compartment of genes whose expression is significantly ($p<0.01$) increased by at least fourfold when Czf1 is artificially activated in the wild type. Terms mapped using the Candida Genome Database GO Term Finder (http://candidagenome.org/cgi-bin/GO/goTermFinder)

Acknowledgments

There are so many that I owe thanks to for parts both small and large in my life these past several years while I have worked towards this achievement. The first naturally is my primary supervisor, Prof. Dr. Joachim Morschhäuser. I thank him for the opportunity to continue and expand upon the work I accomplished during my master's thesis, for imparting to me so much of his expertise and deep knowledge of the *C. albicans* field, and helping me grow as a scientist. My work would not have been as productive as it was without his scientific insights as well as the excellent genetic tools previously developed in his lab. I also thank my second supervisor, Dr. J. Christian Pérez, who has known me as a scientist for nearly as long as Prof. Dr. Morschhäuser, and during that time has enriched my work through valuable scientific discussions, and who I hope forgives me for thinking that he was a postdoc when we first met. As well, I thank Prof. Dr. Bernhard Hube, my third supervisor, for sharing his insight, suggestions, and criticisms during our meetings to strengthen my work.

Thanks go also to the current and former members of the Morschhäuser lab that shaped my time working there: Dr. Bernardo Ramírez-Zavala for supervising me during my master's thesis and sharing his vast knowledge of the *Candida* field and lab techniques, Christina Popp, Kim Setiawan and Dr. Irene Hampe for scientific discussions, Sonja Schwanfelder, Ines Krüger, Sabrina Schneider, and Julia Haubenreißer for assisting me with my work and making sure the lab ran smoothly, and also my own students Sarah Weber and Erika Gorte for teaching me how to teach them. Additionally, I want to thank the former and current members of the Pérez lab in general for their friendship and scientific discussions, and in particular Dr. Valentina del Olmo Toledo and Philipp Reuter-Weißenberger for their assistance in my RNA sequencing analysis.

I also want to acknowledge the friends I made while completing this work. First, Elisa Venturini and Gianluca Prezza, who I met practically as soon as I arrived in Germany and have become some of my closest friends. Also, Gianluca Matera, Dr. Sergio Moreno-Velasquez, Fabian Imdahl, Jens Ade,

and honorary band manager Dr. Marie Eckstein, my fellow members of the unofficial institute band, Los Candidos. Furthermore, I want to acknowledge even more friends, including Sarah Wilkins, Manuela Fuchs, Falk Ponath, Dr. Daniel Ryan, Shuba Varshini, and Gohar Mädler. It would take several pages to list all of the friends and colleagues who have positively impacted my work and made the last several years so enjoyable, so I ask for forgiveness to those who I didn't explicitly name here – you know that I appreciate your friendship. I also want to thank my family for their support, as always. I know it isn't easy for them seeing me only a few weeks a year, and I thank them for their understanding. I also want to particularly thank my Uncle, Robert Mottola, for taking the time to read through and comment on this work to give me a viewpoint from someone outside of the field.

Finally, I must also thank the organizations that made this work possible. I thank the Graduate School of Life Sciences at the University of Würzburg for granting me a Fellowship and organizing useful courses, and the CRC/Transregio 124 (FungiNet) for further funding following the end of the fellowship as well as organizing valuable symposia and meetings.